Genetic and functional characterization of antimicrobial secondary metabolites produced by *Burkholderia* species

By

© 2020
Jennifer R. Klaus

M.S., Fort Hays State University, 2014
B.S., Fort Hays State University, 2011

Submitted to the graduate degree program in the Department of Molecular Biosciences and the Graduate Faculty of the University of Kansas in partial fulfillment of the requirements for the degree of Doctor of Philosophy.

_____
Chairperson – Dr. Josie Chandler

_____
Dr. Susan Egan

_____
Dr. Lynn Hancock

_____
Dr. P. Scott Hefty

_____
Dr. Lena Hileman

Date Defended: 11 June 2020

The dissertation committee for Jennifer R. Klaus certifies that this is the approved version of the following dissertation:

Genetic and functional characterization of antimicrobial secondary metabolites produced by *Burkholderia* species

_____
Chairperson – Dr. Josie Chandler

Date Approved: 11 June 2020

Abstract:

Within the bacterial genus *Burkholderia*, the *Bptm* group is made up of three closely related species: *Burkholderia pseudomallei, B. thailandensis,* and *B. mallei*. This group contains both pathogenic and non-pathogenic species each with distinctly different lifestyles. *B. mallei* is a host-adapted equine pathogen, *B. thailandensis* is a non-pathogenic soil saprophyte, and *B. pseudomallei* is an opportunistic human pathogen that causes the disease melioidosis, which can be fatal up to 40% of the time. The *Bptm* species possess many conserved biosynthetic gene clusters coding for secondary metabolites. The conservation of secondary metabolites across this group affords opportunities to learn how these metabolites are useful among each member's diverse biological niches. Secondary metabolites can be underappreciated contributors to bacterial fitness and also have roles in pathogenicity: the regulation and chemical biology of two examples, malleilactone and methylated hydroxy-alkylquinolones (HMAQs), encoded by the *mal* and *hmq* operons, respectively, are the focus of this work.

Herein, we characterize *B. pseudomallei* malleilactone and show that it is important for virulence in nematode hosts, as well as cytotoxic to eukaryotic cells and some Gram-positive bacteria. Studies on its regulation revealed that malleilactone can be induced by treatment with various antibiotics, notably by the antibiotic trimethoprim via the activator MalR, and that a global secondary metabolite regulator ScmR, which is activated by acyl-homoserine lactone-dependent quorum sensing, strongly suppresses malleilactone production in later growth stages, likely by blocking its activation by MalR.

Further contained within this work are the novel findings that efflux is important for malleilactone export and for mitigating malleilactone self-toxicity. We show that the *B. pseudomallei* BpeEF-OprC efflux pump system, encoded adjacent to the *mal* gene cluster, exports endogenous malleilactone into the extracellular environment. Notably, our results show that BpeEF-OprC protects *mal*-expressing cells from self-toxic effects of *mal* biosynthesis, especially under oxidative stress and in conditions where the recently-described malleicyprol-family malleilactone isomers, which were recently reported in *B.*

thailandensis to have increased toxicity relative to malleilactone, are likely favored. We demonstrate that BpeT and BpeS, known regulators of the *bpeEF-oprC* operon, also play minor roles in *mal* cluster regulation. Additionally, studies within reveal that the *mal* genes are strongly upregulated under iron starvation conditions, in which we see that malleilactone provides a fitness benefit to wild-type cells, though in a siderophore-dependent manner. Our *B. pseudomallei*-purified malleilactone can bind to ferric iron. Taken all together, these findings all point to a notable and previously under-characterized contribution of malleilactone to *B. pseudomallei* fitness in situations of iron limitation. The new evidence from this dissertation suggests that malleilactone promotes fitness under stress, including growth-inhibiting antibiotics, host immune responses, and nutrient (iron) limitation, and that *B. pseudomallei* possesses an innate *mal* resistance mechanism.

Regarding the HMAQ-family compounds, a transposon mutant screen performed by collaborators helped to identify HMAQs as *B. thailandensis*-produced antimicrobial compounds. Our results demonstrate using both liquid and plate co-culture assays that HMAQs are important for *B. thailandensis* to compete with another soil species, *Bacillus subtilis*. We also show that previously-uncharacterized HmqL catalyzes the formation of *N*-oxide derivatives of HMAQs in *B. thailandensis*, which have further increased antimicrobial potency against *B. subtilis*.

Altogether, in this work we provide new insights into the biology of *B. thailandensis* and *B. pseudomallei* malleilactone and HMAQ secondary metabolites and their roles in survival in the host and in polymicrobial soil communities, and information that could be important for developing new therapeutics to treat melioidosis and other diseases.

Acknowledgements:

I begin with gratitude to the University of Kansas and the Department of Molecular Biosciences for the opportunity to pursue my PhD. The collegial connections I formed with faculty, staff, and fellow students within the MB department, with the many undergraduate students I taught, and as a member and officer of the MB graduate student organization all strengthened my resolve and led to brighter days. I'm thankful for the strong and versatile science technique training, feedback, and educator guidance that I received from my many interactions with my committee members Dr. Susan Egan, Dr. Scott Hefty, and Dr. Lynn Hancock, and thanks, Dr. Lena Hileman, for backing me up (twice!) on my committee.

During my time at KU, I worked on collaborative projects with Dr. Mario Rivera (LSU), Dr. Cory Berkland, Dr. Mohammad Seyedsayamdost (Princeton), Dr. Brian Ackley, Dr. Eric Déziel (INRS, Québec), Dr. Ajai Dandekar (UW Seattle), and many of the talented students and staff in their labs. These collaborations gave me chances to explore new techniques and appreciate a diversity of perspectives and approaches, as well as to foster professional relationships and grow my network.

I am especially glad for my opportunity to work alongside, to be mentored by, and to earn my PhD with Dr. Josie Chandler. Your kindness, encouragement, scientific zeal, and approachability made it so easy to communicate with you about everything from in-depth chemistry papers that we both struggled to grasp at first, to how to make my seminar slides flow better, to our impressions of the newest Star Wars film that we saw as a lab group. Thank you for generously providing me with a well-stocked scientific process toolkit and with ample opportunities to grow and flourish both in your lab and beyond at so many meetings and conferences over the years all around the U.S., Canada, and even Germany. Thank you for fostering a laboratory environment that was rich in learning opportunities and constructive feedback and where I always felt heard and appreciated. My labmates Kara, Patricia, Jakki, Saida, Rhea, Pratik, Lennel, Vaughn, Brielle, Sam, Cheyenne, Kade, and Alicia were a joy to work with every day, and I want to give

a special thanks to Kyle, Tiffany, Wyatt, Natalie, and Tony, as it was an honor for me to have the opportunity to mentor you and work closely with you on research in the Chandler lab.

I am so, so grateful for my husband David, my parents Randy and Debbie Pfannenstiel, my in-laws Deb and Don Klaus and Susan and Tim Peterson, and for all of my family for loving and supporting me in countless ways on this long, arduous, chaotic science adventure as a graduate student. They offered timely temporary reprieves from the daily grind and plentiful encouragement in both good and bad times that were instrumental in my success. My master's advisor Dr. Rob Channell also deserves a lot of credit for laying the groundwork and preparing me to be a successful PhD graduate-level scientist. We don't get far in life without friends (particularly on an academic journey like this), and I'm ever thankful for and blessed by the camaraderie, solidarity, drinks with, and support of so many of mine, especially my fellow MB grad students Taybor, Matt, Victoria, Aaron, Sonia, and Mahekta.

Table of Contents:

Abstract iii

Acknowledgements v

Chapter 1: Introduction 1
Introduction to *Burkholderia* and the *Bptm* group species 1
Melioidosis: disease progression and therapeutic approaches 4
B. pseudomallei and *B. mallei* pathogenesis mechanisms 6
Overview of secondary metabolites produced by the *Bptm* group 7
Malleilactone 8
Hydroxy-methyl-alkylquinolines 13
Dissertation overview 16
References 19

Chapter 2: Malleilactone is a *Burkholderia pseudomallei* virulence factor regulated by antibiotics and quorum sensing **27**
Abstract 28
Introduction 30
Materials & Methods 32
Results 40
The *B. pseudomallei mal* genes code for malleilactone biosynthesis 40
Antibiotic activation of the *B. pseudomallei mal* genes 42
Malleilactone cytotoxicity and *B. pseudomallei* virulence 43
Induction of the *mal* genes relies on MalR and sufficient *malR* expression 45
Malleilactone production is repressed by *N*-3-hydroxy-octanoyl homoserine lactone and *N*-3-hydroxy-decanoyl homoserine lactone 47
Malleilactone production is repressed by a quorum sensing-activated regulator, ScmR 49
Discussion 52
Supporting information 55
References 64

Chapter 3: *Burkholderia thailandensis* methylated hydroxy-alkylquinolines: biosynthesis and antimicrobial activity in co-cultures **68**
Abstract 69
Introduction 71
Materials & Methods 73
Results 80
Antimicrobial activity of *B. thailandensis* bactobolin-null mutants 80
Identification and isolation of antimicrobial-deficient transposon mutants 82
Identification and activities of *hmq* gene products 83
Biosynthesis and antimicrobial activity of HMAQ-NO 85
Antimicrobial activities of structurally related hydroxy-alkylquinolines 87
HMAQ-NO promotes competition in liquid co-cultures 87
HMAQ biosynthesis in *B. ambifaria* 89
Discussion 91
Supporting information 93
References 98

Chapter 4: Efflux pumps alleviate self-toxicity of the *Burkholderia pseudomallei* cytotoxin malleilactone **103**
Abstract 104
Introduction 105
Materials & Methods 108
Results 112
Efflux pumps increase resistance to purified malleilactone in *E. coli* 112
The *B. pseudomallei* BpeEF-OprC pump exports malleilactone from the cell 113
The malleilactone biosynthetic products cause self-poisoning in the absence of BpeEF-OprC 116
Examination of regulatory networks of the *bpeEF-oprC* and *mal* gen clusters 118
Discussion 121
References 126

Chapter 5: The potential role of the cytotoxic polyketide malleilactone in *Burkholderia pseudomallei* iron acquisition **132**
Abstract 133
Introduction 134
Materials & Methods 137
Results 142
Regulation of the *mal* gene cluster during iron starvation 142
Purified malleilactone can coordinate with iron 146
Malleilactone deficiency results in poorer low-iron growth in a siderophore-dependent manner 147
Discussion 149
References 152

Chapter 6: Discussion **157**
Summary of findings 157
Discussion and significance 158
Future directions 161
References 165

Chapter 1: Introduction to *Burkholderia* species and secondary metabolites

The "Malleilactone" and "Hydroxy-methyl-alkylquinolones" sections of this chapter are adapted from the manuscript:

Jennifer R. Klaus*, Pratik Koirala*, Pauline Coulon*, Eric Déziel, Mohammad R. Seyedsayamdost, Josephine R. Chandler. Review Article: Studies of *Burkholderia pseudomallei-thailandensis-mallei* to understand the ecology and evolution of secondary metabolites. (*in preparation for submission to Journal of Industrial Microbiology and Biotechnology*, *equal contributions by JRK, PK, PC)

Introduction to *Burkholderia* and the *Bptm* group species

The Gram-negative genus *Burkholderia* contains a diverse collection of at least 120 species of Beta-Proteobacteria with varied ecologies, as per the DSMZ collection curated by the Leibniz Institute. Most of the *Burkholderia* species are known to have comparatively large genome sizes of at least 7 million base pairs, and they contain two circular chromosomes. The environmentally-widespread *B. cepacia* complex (Bcc) strains, a >20-member consortium/group consisting of *B. cepacia, B. cenocepacia, B. vietnamiensis, B. multivorans, B. ambifaria* and others, are pathogens that are often associated with infections in the lungs of cystic fibrosis patients (1-3). Many other *Burkholderia* species are plant pathogens or nonpathogenic soil-dwelling saprophytes often with high tolerance of acidic soils (4). Others of these are opportunistic human pathogens such as *B. oklahomensis* (5). Certain strains of *Burkholderia* species have potential roles in bioremediation and in the biocontrol of plant pathogens (6). The focus of this body of work is on the *Bptm* group, consisting of *B. pseudomallei, B. thailandensis,* and *B. mallei.* This group of *Burkholderia* species is of particular research interest due to strong evolutionary relatedness

despite their divergent ecological and biological niches, their genetic tractability and ease of culturing and laboratory manipulation, and their pathogenic relevance to both large draft animals and to humans.

B. pseudomallei is an opportunistic human pathogen that is commonly found in soils and waters in semi-tropical regions such as northern Australia and northeastern Asia, especially in Thailand and Vietnam (7, 8). This species was originally identified in 1912 (9), and has been previously known as *Malleomyces pseudomallei* through the 1960s (10) and more recently as *Pseudomonas pseudomallei* (11) before being reclassified within the *Burkholderia* genus in the early 1990s (12). Infections caused by *B. pseudomallei* all fall under the term melioidosis, formerly known as Whitmore's disease after one of the scientists who first identified it, and they can have a fatality rate as high as 40% (13). Helicopter pilots and soldiers who fought in the Vietnam War often became infected after inhaling circulating dust, and in some cases the manifestations of the infection did not occur for many years after the exposure (14, 15), earning it the nickname "the Vietnam time bomb" as propagated in late 1960s news articles and a 1967 TIME magazine article. The disease conditions and treatments of melioidosis will be explored in more detail in the next section.

B. thailandensis was originally isolated from rice fields in Thailand (16, 17). It is a soil saprophyte that is also widely found in tropical soils and waters in northeast Asia and northern Australia. *B. thailandensis* is not known to be pathogenic toward humans and requires a much higher infectious dose than *B. pseudomallei* in animal challenge studies (18). It is a very close relative of *B. pseudomallei* and as such, it has often been used to more safely and easily study aspects of virulence in lieu of utilizing the pathogenic strain in research laboratories (19).

B. mallei is an animal pathogen that is thought to have evolved from a host-adapted *B. pseudomallei* strain. It has a smaller genome size by 1-1.5 million base pairs than the other two members of the *Bptm* group (20), suggestive of reductive evolution due likely to its host-restricted nature; it has not been isolated outside of a host in any free-living environmental reservoir. *B. mallei* causes the highly contagious disease glanders (also historically known as malleus, equinia, and farcy) in horses, mules, and donkeys, commonly manifesting as respiratory disease and also as slow-healing skin abscesses that can

result in death by sepsis (21-23). Descriptions of this bacterial ailment of animals under its various names have been around for centuries, and records of the symptoms it causes in horses have been found among writings of ancient Greeks and Romans (21, 24). *B. mallei* was deployed as a bioweapon that was used by the Axis powers against the draft animals of the Allied powers during World War I (25). Like *B. pseudomallei, B. mallei* is also intrinsically resistant to many types of antimicrobials (26, 27). *B. mallei* can cause human infections, though these tend to be rare but severe and sometimes fatal. Many of the more recent human infections have been the result of research-related laboratory accidents (24, 28).

Due to their innate antibiotic resistance, potent infectivity, and potential for bioweaponization, *B. mallei* and *B. pseudomallei* are listed as biosafety level 3 (BSL3) organisms and tier-1 select agents by the USDA and the CDC (https://www.selectagents.gov/SelectAgentsandToxinsList.html). Because their study has been restricted to BSL3 facilities until more recently, *B. thailandensis* has served as a surrogate study organism due to its lack of human pathogenicity and high degree of genetic relatedness to the other two species. Multiple BSL2-safe strains of both *B. mallei* and *B. pseudomallei* have been developed that have a variety of strongly attenuating mutations, which earned them exclusion from the government select agent lists (29-32). These three species have proved valuable laboratory models for multiple areas of study, including quorum sensing, secretion systems, and biofilm development, because of how closely related they are to one another genetically despite ecologically and environmentally varied lifestyles. This group offers researchers an important look at how the genetically-conserved features can benefit bacteria in free-living populations (in *B. thailandensis*), within a host (in *B. mallei*), and perhaps in aid in the transition between the two lifestyles (in *B. pseudomallei*, capable of both) (33), and also at how the genetically-unique features within this group have helped each species adapt to its particular lifestyle niche.

Melioidosis: disease progression and therapeutic approaches

Estimates from 2016 suggest that as many as ~89,000 cases of melioidosis occur annually worldwide (13), and infections can be fatal up to 40% of the time, depending on the nature and severity of the infection and on the quality and availability of medical treatment in the area. Humans can become infected with *B. pseudomallei* through consumption of, inhalation of, or open-skin exposure to contaminated water or soil, especially during the heavy rainy seasons in the regions of Australia and southeast Asia where it naturally occurs. Farmers and workers who spend time in agricultural fields and rice paddies are especially at risk (34), as are individuals with diabetes, renal failure, chronic pulmonary disease, and alcoholism (35, 36).

The *B. pseudomallei* incubation period ranges from 1 to 21 days (37). Many incidences of disease are acute cases with symptoms over a few weeks to months, though some are chronic with symptoms lasting for multiple months. Additionally, many cases of recurrent melioidosis due to reinfection and relapse have been documented (37-42). Melioidosis cases can present with a wide variety of symptoms (43, 44), due perhaps in part to variability in virulence factor expression by *B. pseudomallei* (45) and the multiple infection and entry routes. This makes it difficult for clinicians and doctors to specifically diagnose, especially outside of regions where infections commonly occur. As determined by multiple studies, over half of individuals present with a pneumonia-like severe deep lung infection, especially following inhalation (46, 47). As a result of ingestion or percutaneous inoculation, bacteremia can occur at rates as high as 40% of cases and cause septicemia and dissemination to multiple organs, and septic shock can be as prevalent as 20% of cases (23, 43). Percutaneous inoculation and ingestion can also cause localized skin abscesses and mucosal abscesses of the gastrointestinal tract, including the liver, spleen and prostate (23, 43). Melioidosis can affect the musculoskeletal system as well as manifest with neurological involvement (48-51) in the form of flaccid paralysis, brainstem signs, and central nervous system infection.

Melioidosis cases often do not fully resolve without extensive antimicrobial treatment lasting for a few to many months. This treatment is usually administered in two separate phases: the acute, intensive phase of intravenous antibiotics over 1-2 weeks to suppress the initial infection, and the eradication phase of oral antimicrobial therapy over the following 3-6 months to prevent relapse. Intravenous ceftazidime (a cephalosporin) or a carbapenem like imipenem or meropenem treatment is commonly used for the acute 10-14-day phase, which is more complex and longer in duration for more advanced pneumonia patients (52). A combination of the bacterial folate pathway inhibitors trimethoprim and sulfamethoxazole, called co-trimoxazole, without other drugs has been found effective since at least the 1970s (11) and this has become the standard oral eradication phase treatment (35). Doxycycline, chloramphenicol, and kanamycin are among drugs that were previously used more commonly either separately or in various combinations but have been dropped in favor of co-trimoxazole only (23, 53). A combination of the beta-lactam amoxicillin and clavulanic acid, called co-amoxiclav, is utilized for treatments in pregnant women, in those with sulfonamide allergies, and as a second-line alternative therapy for patients who do not respond as well to other drugs (46, 54). Chronic conditions and those with multiple or severe co-morbidities require stronger and longer treatments (43). Some *B. pseudomallei* resistance to many of these antibiotics singly has been noted in various strains, through fortunately, resistance to the combination therapy co-trimoxazole is still quite rare (55-58).

Especially because of the biothreat potential, future development of additional treatment options includes attempts to optimize the effectiveness of current antibiotics and attempts to design an effective vaccine. Research efforts are focused on both novel sources of anti-*Burkholderia* compounds as well as next-generation members of antibiotic compound families that show promise or currently work against *B. pseudomallei* (43, 54). Attempts have been made in each of subunit, outer-membrane vesicle, plasmid-based DNA, killed whole-cell, and live attenuated vaccines types (35, 46), with sterile immunity only sometimes reported and protection conferred being quite condition-dependent in animals (59). Thus, melioidosis vaccine studies have not progressed beyond animal challenge models into humans so far.

B. pseudomallei and *B. mallei* pathogenesis mechanisms

B. pseudomallei is a facultative intracellular pathogen (60) that is known to invade, multiply, and persist in both non-phagocytic cells as well as phagocytic cells such as macrophages during infections. Much has been experimentally demonstrated regarding the major steps in *B. pseudomallei* pathogenesis (35). *B. pseudomallei* adheres to eukaryotic cells, induces its endocytosis, and then it escapes the endocytic vacuole into the cytoplasm, where it replicates (46, 61). Intracellular bacterial cells utilize actin-based motility, spreading to neighboring cells via membrane fusion and causing the formation of multinucleated giant cells (46, 61). Further, *B. pseudomallei* can suppress the activation and the antimicrobial free radical nitric oxide production of macrophages, and it is also able to avoid autophagic attack to ensure its intra-host survival (61).

Much remains to be understood about the full arsenal of virulence factors possessed by the human pathogens *B. mallei* and *B. pseudomallei,* though much early research attention has been given to those factors that are well-known across other groups of pathogenic bacteria, such as the presence of a capsule, production of toxins and biofilms, and the use of secretion systems such as type 3 (T3SS) and type 6 (T6SS). A number of laboratory animal infection model systems for studying the pathogenesis of these strains are well-established, and they continue to be improved upon. *Caenorhabditis elegans* nematodes, various species of amoebae, and a variety of small mammalian models (mice, rats, hamsters) with multiple challenge methodologies (intranasal, intraperitoneal, and more recently, intubation-mediated intratracheal (IMIT) (62) deliveries) have all been used to analyze *Burkholderia* infections. T3SS, a needle-like apparatus that facilitates bacterial infection of eukaryotic cells through the secretion of effector proteins, has been shown to contribute strongly to overall survival of *B. pseudomallei* as well as to dissemination from the lung following direct lung inoculation via IMIT in mice (63). The influence of less well conserved virulence factors, such as the lesser known ‘small’ virulence factors (64, 65) are also becoming better understood. For example, the *Burkholderia* lethal factor 1 toxin, a previously

undescribed small protein, has been shown to bind to and inhibit the helicase activity of eukaryotic translation initiation factor eIF4A (66).

Plenty of virulence contributors are not as well studied, historically in large part because of the difficulties associated with working with BSL3-level pathogens. *B. thailandensis* has served as a surrogate, but there are obvious limitations to how applicable and translatable virulence studies in a non-pathogen are to its pathogenic relative strains. However, comparisons of them have revealed likely pathogenicity components; for example, *B. thailandensis* lacks the *wcb* capsular polysaccharide genes that contribute to *B. pseudomallei* virulence (67). One BSL2-safe strain of *B. pseudomallei,* JW270, is deficient for the *wcb* capsule-encoding operon, which renders it significantly attenuated in an acute murine respiratory infection model and thus eligible for exclusion from the select agent list (29). Another BSL2-safe strain, *B. pseudomallei* Bp82, is an adenine and thiamine auxotrophic mutant that is also severely attenuated in Syrian hamsters and immunocompromised mice (30).

Overview of secondary metabolites produced by the *Bptm* group

These *Burkholderia* species also have many gene clusters coding for biosynthesis of secondary metabolites. In all, over 20 biosynthetic gene clusters have been identified in the *Bptm* group that encode secondary metabolites (summarized in (64, 68)). While some are unique to just one or two members of the *Bptm* group, some of those are conserved across the whole group. This could suggest that there are one or more functional roles of the conserved metabolite products that contribute to survival of the bacteria across diverse environments, such as complex community environmental competition, nutrient limitations, or within a host. Two examples that will be discussed in this work are malleilactone and methylated hydroxy-alkylquinolones. Other recent examples include the antimicrobial bactobolins (for a review, see (69)) and thailandamides (70, 71). The products of at least 13 of those gene clusters have been characterized (72-74). Of those, many remain poorly understood in terms of their biology and their particular benefit to bacterial producers.

Understanding more about the functions of small molecules and secondary metabolite products could give insight into the conditions under which they are most helpful to the producing bacteria (or conditions when they are harmful), improving our understanding of diverse bacterial biology. If these factors are important for virulence or survival of pathogenic producing bacteria, such products could be targeted for therapeutic anti-infectives or anti-virulence treatments in a more pathogen-specific manner. Additionally, secondary metabolite study could expand our existing knowledge of small-molecule biochemistry. Some of the molecules could additionally serve as lead compounds or scaffolds to be modified for alternative medicinal or therapeutic purposes.

Studies of small molecules can be technically challenging, as they are not often very abundantly expressed in standard laboratory culturing conditions. Purification difficulties are often experienced too. Genetic overexpression approaches and specialized culture conditions have been utilized to overcome some of these obstacles (74-76). Thus, understanding the regulation of such "cryptic" biosynthetic gene clusters provides useful knowledge both toward advancing research applications and toward appreciating how and when they might become activated (or suppressed) in biologically-relevant or natural conditions. We believe that despite the experimental challenges related to their study, this *Burkholderia* group, and especially *B. pseudomallei*, is a great set of model species by which to further understand the biology of secondary metabolites because of the abundance and diversity of encoded secondary metabolite and small-molecule biosynthetic gene clusters and the availability and suitability of lab animal infection models that mimic the human condition melioidosis.

Malleilactone

Over the past decade, interest has grown in the secondary metabolite malleilactone (also known as burkholderic acid) (**Fig. 1.1-C**), the product of genes encoded in the *mal* (*bur*) biosynthetic cluster. The *mal* cluster consists of *malA* through *malM* thought to be organized in an operon, along with the divergently transcribed upstream gene *malR*. These genes are highly conserved (77), sharing at least 80%

identity among the *Bptm* group, though the genes *malAa* and *malBb* are absent in *B. thailandensis* (**Fig. 1.1-A**). Additionally, this operon is present in *B. oklahomensis,* a close relative of *B. pseudomallei* that was isolated from a patient in Oklahoma (5). Because the *mal* cluster has been evolutionarily conserved across this clade of species with divergent ecologies and environmental niches (host-restricted pathogen *B. mallei,* soil-dwelling opportunistic pathogens *B. pseudomallei* and *B. oklahomensis*, and saprophytic non-pathogen *B. thailandensis*), it offers a unique opportunity to learn about how secondary metabolites might provide fitness advantages to bacteria living diverse lifestyles.

The current understanding of *mal* biosynthesis occurs as follows in *B. thailandensis*. Authors of (77) suggest that based on specific domains found in *malA*- and *malF*-encoded polyketide synthases, a condensation of two separate polyketide chains (one from the C-16 methyl through the C-6a carbonyl, and the other from the C-1 methyl through the C-4/C-5 olefin carbons) gives rise to malleilactone. Briefly, they propose that MalA forms the latter chain from propionic acid and a hydroxymalonyl extender, further supported by the presence of a FkbH homolog (MalH) which would catalyze the linkage of the two polyketide chains. They propose that MalF forms the former chain by elongating a caprylic starter, first by incorporation of a methylmalonyl extender and second, of a non-reduced malonyl extender. Finally, they propose that the chains are joined by condensation-domain-catalyzed ester bond formation by MalF and that the furan lactone ring cyclization is mediated by the MalF reductase domain. Largely corroborating these findings independently, the authors of (78) additionally used stable isotope labeling to demonstrate that acetate units likely form the carbon skeleton of the C-16 to C-6a chain and that its propionyl moiety likely originates from methionine. Because of high *mal* cluster conservation, biosynthesis is thought to occur similarly in *B. mallei* and *B. pseudomallei*.

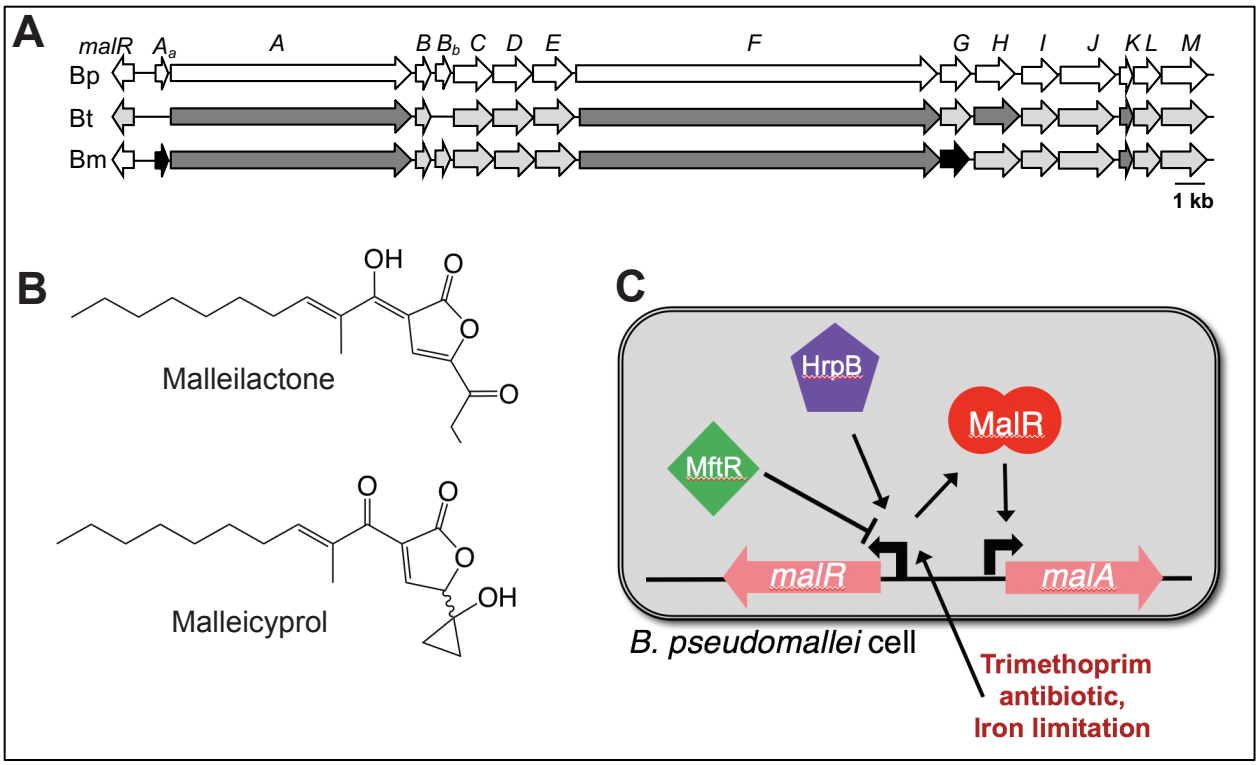

Figure 1.1. Malleilactone. (A) The *mal* gene cluster from *B. pseudomallei* (Bp), *B. thailandensis* (Bt) and *B. mallei* (Bm). Shading indicates % identity to the *B. pseudomallei* protein sequences. White, 100%; light gray, 90-99%; dark gray, 80-89%; black <80%. Lowercase letters indicate genes that are present in *B. pseudomallei* and *B. mallei* but missing in *B. thailandensis.* (B) Structure of malleilactone and malleicyprol. It is thought that malleicyprol degrades to form malleilactone. (C) Model of *mal* gene regulation. Regulation occurs at the promoter of the first *mal* gene *(malA*) by the transcriptional activator MalR, encoded upstream of *malA.* Expression of *malR* is influenced by the urate-responsive repressor MftR, the host-responsive activator HrpB, trimethoprim antibiotics, and conditions of iron limitation.

Functionally, *malA* and *malF* contribute to *B. thailandensis* pathogenesis in co-cultures with the soil nematode *Caenorhabditis elegans* and the social amoeba *Dictyostelium discoidium* (77). When exposed to wild-type *B. thailandensis, C. elegans* become lethargic, and like *D. discoidium,* they also become reproduction-deficient, which is suggestive of some type of bacterial toxicity effect(s). These phenotypes are notably alleviated in *mal* mutants (77). The role of malleilactone in virulence was also observed in two high-throughput screens in mice that used *B. pseudomallei* transposon mutant libraries, one large ~20,000 mutant large library from which pools were inoculated into mice (62) and one that used smaller libraries of ~100 mutants per mouse to test ~1,250 total mutants (79). From the larger library, multiple insertional-disruption *mal* gene mutants were 3-7-fold reduced in the mouse lung compared with the input

population (62). From the smaller library, a *malA* disruption mutant was 3-fold reduced in the lung but ~40-fold reduced in the spleen (79). Together, these studies suggest that the *mal* genes might play a role in infection dissemination to different organs in a mouse. Additionally, purified *B. thailandensis* malleilactone has low-micromolar cytotoxicity against MCF7 human breast cancer cells (77) as well as antimicrobial activity against *Staphylococcus aureus* and *Bacillus subtilis* (2-20 μg/mL). Thus, the product(s) of the malleilactone biosynthesis pathway appear to be important *in vivo* for pathogenesis, as well as cytotoxic to eukaryotic cells and also antimicrobial to some Gram-positive bacteria.

Like other secondary metabolites, malleilactone production is very low or absent in standard laboratory conditions (75, 77, 78, 80). Replacement of the native *mal* cluster promoter with an inducible one was necessary for its early characterization (77, 78). Seyedsayamdost et al. (75) used a small-molecule screen in search of elicitors of this 'silent' biosynthetic gene cluster in *B. thailandensis*. It was shown that sublethal concentrations of some antibiotics can promote *mal* expression (75). This antibiotic induction of the *mal* genes in *B. thailandensis* has since been confirmed (76, 80). Both trimethoprim and another folate biosynthesis pathway inhibitor, sulfamethoxazole, induce most strongly, and a DNA crosslinker (mitomycin C) drug also causes moderate *mal* induction. Of note, trimethoprim and sulfamethoxazole are widely used to treat melioidosis caused by *B. pseudomallei* infections in humans, though it remains unclear what, if any, biological significance this has *in vivo*.

There is a positive *mal* regulator, MalR, that is encoded upstream of the *mal* gene cluster. MalR belongs to the LuxR-family of quorum sensing (QS) signal-responsive transcriptional activators. LuxR-family receptors typically activate gene expression upon binding to QS signals, which are acyl-homoserine lactones (AHLs) produced by LuxI-family signal synthases (for reviews, see (81, 82)). MalR is termed an orphan LuxR because it lacks a cognate LuxI-family signal synthase. Despite being a classical LuxR-family protein, work in heterologous *E. coli* models showed that *B. thailandensis* MalR is non-responsive to the three native AHL signals produced in *B. thailandensis* and *B. pseudomallei* (80). MalR is important for the induction of the *B. thailandensis mal* genes by treatment with the antibiotic trimethoprim, which increases *malR* expression (80). These results could suggest that malleilactone is

produced to enhance *Burkholderia* survival in response to certain antibiotics encountered during competition with other species.

The contributions of malleilactone during infections of *C. elegans*, *D. discoidium*, and mice suggest that it is likely upregulated somehow during host colonization. While direct links have yet to be experimentally demonstrated *in vivo*, at least three other malleilactone regulation mechanisms could be important in hosts. First, overexpressing the AraC-family transcriptional regulator HrpB increases *malR* transcription (83) and strongly activates malleilactone production in a MalR-dependent manner (Chandler lab, *B. pseudomallei* unpublished results, see **Fig. 5.1** in Chapter V). HrpB regulates the T3SS virulence gene cluster in the plant pathogen *Ralstonia solanacearum* in response to plant cell contact (84), and while highly related orthologs of both exist in the *Bptm* group, the small body of evidence testing this directly remains inconclusive as to whether HrpB functions similarly in these *Burkholderias* in response to host cues (83). Second, the MarR-family transcriptional regulator MftR was shown in *B. thailandensis* to de-repress *malR* and thus promote *mal* gene transcription and malleilactone production upon encountering and binding to its inducer urate (74, 85, 86), which is commonly produced by host xanthine oxidoreductase as part of the host's antimicrobial response (for a review, see (87)). Third, microarray (88) analyses of *B. pseudomallei* grown in iron-depleted media revealed that *malR* is upregulated relative to iron-replete conditions. Mechanistically, this low-iron regulation is yet to be fully understood, though there is a putative binding site for the iron-responsive regulator Fur occurring upstream of *malR* (Chandler lab, *B. pseudomallei* unpublished observation). These latter results support the idea that malleilactone has a role in acquiring iron during conditions of iron starvation, an idea that is explored further in Chapter 5 of this work. Altogether, the current body of evidence regarding the functions and regulation (**Fig. 1.1-B**) of the *mal* biosynthetic gene cluster products suggests that malleilactone likely has some role in promoting the fitness of producer cells under stress, including growth-inhibiting antibiotics, host immune responses, and nutrient (iron) limitation.

Hydroxy-methyl-alkylquinolines

Several bacteria are known to produce alkylated quinoline antibiotics, which are involved in bacterial and fungal competition, virulence, iron acquisition, and cell-cell signaling, among other things (90-97). *B. thailandensis* and *B. pseudomallei* both produce alkylated quinolones, specifically the 4-hydroxy-3-methyl-alkylquinolone (HMAQ) molecules. HMAQs are biosynthesized from the products of the *hmqABCDEFG* genes (**Fig. 1.2-A**). These genes are present in 98% of *B. pseudomallei* and 79% of *B. thailandensis* strains (98). It is noteworthy that the *hmq* gene cluster is entirely absent in *B. mallei*. Interestingly, the cluster is only present in 36% of sequenced *Burkholderia cepacia* complex (Bcc) strains (98), and thus is more highly conserved in *B. pseudomallei* and *B. thailandensis* than Bcc members. The *hmq* genes share high similarity to the *pqsABCDE* genes involved in biosynthesis of the 4-hydroxy-2-alkylquinolones (HAQ) in *Pseudomonas aeruginosa* (98, 99). Among the *P. aeruginosa* HAQs are 2-heptyl-4(1*H*)-quinolone (HHQ) and the *Pseudomonas* quinolone signal 2-heptyl-3-hydroxy-4(1*H*)-quinolone (PQS) (98, 99). The *P. aeruginosa pqs* cluster differs from the *Burkholderia hmq* cluster in several important ways. First, the two *Burkholderia* species uniquely code for HmqF, which adds a double bond to the methyl alkylquinolone alkyl chain (100), and HmqG, which adds the methyl group on the quinolone cycle (99). Second, the *hmq* locus is missing a *pqsH* homolog, which is responsible for synthesis of PQS. Thus, the *Burkholderias* do not biosynthesize a structural equivalent of PQS. PQS is a quorum-sensing signal that is detected by the PQS receptor PqsR (97). Accordingly, there is also no homolog of PqsR encoded in the *Burkholderia* genomes.

Despite these key differences, many other aspects of the *Burkholderia* HMAQ biosynthesis and the *P. aeruginosa* HAQ biosynthesis are largely similar (**Fig. 1.2-B**, (98, 99)). Anthranilic acid is the precursor of both HMAQ and HAQ biosynthesis. Anthranilic acid is synthesized from tryptophan via the KynBUA and PhnAB pathways in *Burkholderia* and *Pseudomonas*, respectively, and/or from chorismic acid via the TrpEG pathway. From anthranilic acid, HmqA/PqsA synthesizes anthraniloyl-CoA, and then HmqD/PqsD transfers malonyl-CoA and acetyl-CoA to anthraniloyl-CoA to form 2-

aminobenzoylacetate-CoA. Next, the putative 2-aminobenzoylacetyl-CoA thioesterase HmqE/PqsE could be used to remove the CoA from 2-aminobenzoylacetyl-CoA to yield 2-aminobenzoylacetate. In *Burkholderia,* 2-aminobenzoylacetate is thought to be methylated by HmqG (99). In both *Pseudomonas* and *Burkholderia,* PqsBC/HmqBC modifies the unmethylated or methylated 2-aminobenzoylacetate, respectively, by incorporating fatty acid-derived alkyl groups. This final step makes the HAQs or HMAQs, respectively. In *P. aeruginosa,* HAQs can be converted to the quorum-sensing molecule PQS by PqsH (101) or to an *N*-oxide form by PqsL (102). A PqsL homolog, HmqL, in *Burkholderia* is proposed to similarly convert HMAQs to *N*-oxide derivatives (99). Interestingly, within the *Burkholderia* genus, *B. pseudomallei* and *B. thailandensis* are the only two species that encode *hmqL* (99). It is unclear why other *Burkholderias* do not encode *hmqL.*

Interestingly, while *B. thailandensis* and *B. pseudomallei* mainly produce unsaturated C_9 congeners (HMAQ-C_9:2' and HMAQNO-C_9:2'), the Bcc species produce both HMAQ-C_7 and -C_9 congeners that can be either unsaturated or saturated (99, 103). The C_9 congeners could be synthesized from decanoic acid while octanoic acid could be used to synthesize C_7 congeners as it is in *P. aeruginosa* (100, 104). These differences could alter the degree of activity in different bacteria, which has been observed with synthetic HMAQs in laboratory experiments (105). It is likely that changes in the alkyl group length or substitution might change the specific target site or ability to penetrate different types of bacterial cells. Different HAQs have been shown to have distinct targets and can have synergistic activities against other bacteria (106). Thus, producing several molecular species with different alkyl side chains could provide some advantages during competition with other species in soil. It is also possible the HMAQs have other important functions in soil bacteria which remain unstudied. Future research efforts are needed to determine how *Burkholderia* species could use a variety of HMAQs in niche protection and to uncover the therapeutic potential of HMAQs and their derivatives, which will be facilitated through recent advances in whole synthesis of the HMAQs (105).

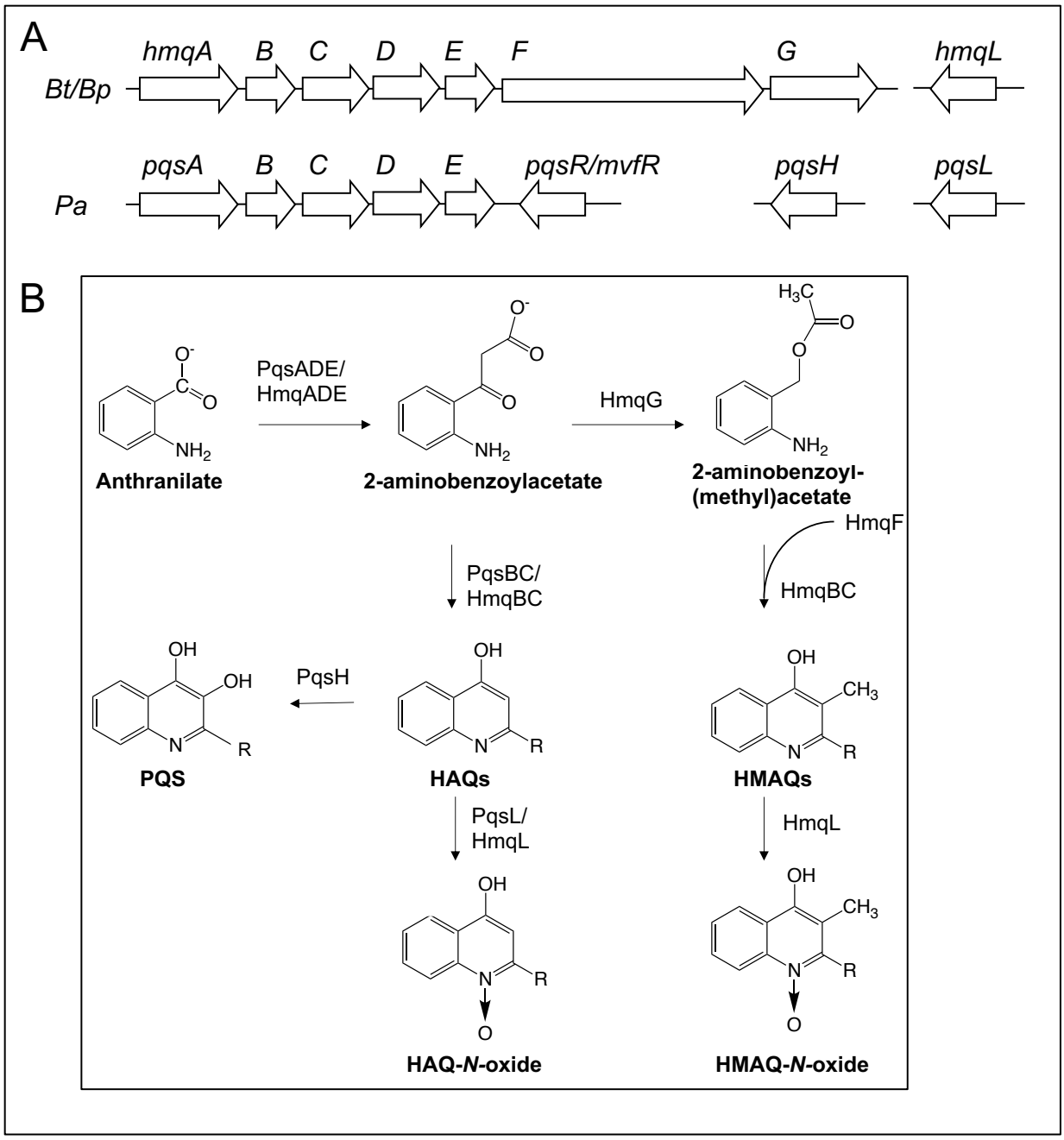

Figure 1.2. Hydroxy-alkylquinolines. (A) The *hmq* gene cluster in *B. thailandensis* (Bt) and *B. pseudomallei* (Bp) and the homologous *pqs* gene cluster in *P. aeruginosa* (Pa). (B) Biosynthesis of alkylquinolones by *hmq* gene products in *B. thailandensis/B. pseudomallei* and by *pqs* gene products in *P. aeruginosa.* The specific steps are described in the text.

Dissertation overview

The scope of this body of work involves understanding more about the regulation and biological functions of antimicrobial secondary metabolites produced by members of the *Bptm* group, namely, the products made by the malleilactone biosynthesis genes in *B. pseudomallei* and the 4-hydroxy-3-methyl-quinolones (HMAQs) produced by *B. thailandensis.* In the case of the virulence factor malleilactone, learning more about the chemical biology of these molecules, how they are regulated, and under what conditions they best function can provide insights that can be translated into therapeutic anti-infectives against *B. pseudomallei* infections. Regarding HMAQs, our discoveries set the stage for understanding how these molecules contribute to survival of these bacteria in soil environment and for future work to understand the therapeutic potential of the HMAQ family of molecules.

Chapter 2 describes some of the earliest characterizations of malleilactone in the pathogenic strain *B. pseudomallei,* including a protocol for purifying malleilactone, its cytotoxic activity against eukaryotic and bacterial cells, and molecular chemical analysis and characterization demonstrating that it is the same compound produced by nonpathogenic *B. thailandensis.* I show that malleilactone contributes to *B. pseudomallei* virulence in the soil nematode *C. elegans* and that its production can be promoted by treatment with various antibiotics, notably by the antibiotic trimethoprim though the activator MalR. Further, I show using a heterologous *E. coli* system that despite high homology to AHL signal-responsive LuxR proteins, MalR is non-responsive to the three native AHL signals produced in *B. pseudomallei*. However, malleilactone production was increased in *B. pseudomallei* deficient in AHL signaling, suggestive of AHL quorum sensing suppression. I show that the global secondary metabolite regulator ScmR is quorum-sensing activated at high cell densities and is responsible for strong repression of malleilactone in late stationary phase, likely by disallowing the activity of the MalR positive regulator.

Chapter 3 describes the results of a transposon library screen for genes important for the killing of *Bacillus subtilis* by *B. thailandensis* in a plate-based co-culture assay, which showed the *hmq* operon contributes to the antimicrobial activity of *B. thailandensis*. We and collaborators used analytical

chemistry to characterize *hmq*-encoded HMAQ-family compounds and we demonstrated that they are notable contributors to enhanced *B. thailandensis* competitiveness against *B. subtilis* in both plate-based and liquid co-culture assays. Further, this transposon screen revealed the influence of an accessory putative monooxygenase gene that we named *hmqL* on the formation of *N*-oxide derivatives of HMAQs, which are also potent antimicrobials against *B. subtilis* and other Gram-positive species. Heterologous expression of *hmqL* in the species *Burkholderia ambifaria,* which lacks a similar accessory homolog, enabled it to produce HMAQ-*N*-oxides when it previously did not, further evidence we use to demonstrate the role of HmqL in the biosynthesis of HMAQ-family derivative antimicrobial compounds.

Chapter 4 describes our findings that efflux is important for mitigating malleilactone self-toxicity. We showed that efflux plays an important role in *Escherichia coli* resistance to purified malleilactone, and we identified a specific efflux pump system (BpeEF-OprC) that is important for *B. pseudomallei* to survive endogenous malleilactone production. The *bpeE-bpeF-oprC* RND-family multidrug efflux pump-encoding operon is genetically adjacent to the *mal* biosynthetic gene cluster. Our results demonstrated that, when active, the BpeEF-OprC pump exports malleilactone into the extracellular environment. Notably, I showed that this efflux pump is important for protecting *mal* cluster-expressing cells from self-toxic effects of *mal* biosynthesis, especially under paraquat-induced oxidative stress and in conditions where the recently-described malleicyprol-family malleilactone isomers (**Fig. 1.1-C**), which were recently reported in *B. thailandensis* to have increased toxicity relative to malleilactone, are likely favored. I show that known regulators of the *bpeEF-oprC* operon, BpeT and BpeS, also play small roles in *mal* cluster regulation, and that there is some but not perfect overlap between the set of antimicrobials that can induce *mal* gene cluster expression and that are also drug substrates for BpeEF-OprC.

Chapter 5 describes my work on characterizing the strong increase of malleilactone gene cluster expression under conditions of iron starvation relative to iron supplemented growth media, wherein known *mal* gene regulators are examined for regulatory influence under iron starvation. I showed that malleilactone provides a fitness benefit to wild-type cells under iron starvation, but in a manner that is dependent upon the presence of genes encoding known *B. pseudomallei* siderophores. We also showed,

with the help of collaborators, that purified malleilactone can bind to ferric iron, a finding that further points to a notable and previously under-characterized contribution of malleilactone to *B. pseudomallei* fitness in situations of iron limitations.

Altogether, results described in this work provide new insights into the functions of *B. thailandensis/B. pseudomallei* secondary metabolites malleilactone and HMAQs. These results reveal new biology about these bacteria, mechanisms of survival in the host and in polymicrobial soil communities, and information that could be important for developing new therapeutics to treat melioidosis and other diseases.

REFERENCES:

1. Mahenthiralingam E, Coenye T, Chung JW, Speert DP, Govan JR, Taylor P, Vandamme P. 2000. Diagnostically and experimentally useful panel of strains from the *Burkholderia cepacia* complex. J Clin Microbiol 38:910-3.

2. Mahenthiralingam E, Urban TA, Goldberg JB. 2005. The multifarious, multireplicon *Burkholderia cepacia* complex. Nat Rev Microbiol 3:144-56.

3. Scoffone VC, Chiarelli LR, Trespidi G, Mentasti M, Riccardi G, Buroni S. 2017. *Burkholderia cenocepacia* Infections in Cystic Fibrosis Patients: Drug Resistance and Therapeutic Approaches. Front Microbiol 8:1592.

4. Stopnisek N, Bodenhausen N, Frey B, Fierer N, Eberl L, Weisskopf L. 2014. Genus-wide acid tolerance accounts for the biogeographical distribution of soil *Burkholderia* populations. Environ Microbiol 16:1503-12.

5. Glass MB, Steigerwalt AG, Jordan JG, Wilkins PP, Gee JE. 2006. *Burkholderia oklahomensis* sp. nov., a *Burkholderia pseudomallei*-like species formerly known as the Oklahoma strain of *Pseudomonas pseudomallei*. Int J Syst Evol Microbiol 56:2171-6.

6. Eberl L, Vandamme P. 2016. Members of the genus *Burkholderia*: good and bad guys. F1000Res 5.

7. Wuthiekanun V SM, Dance DAB, White NJ. 1995. The isolation of *Pseudomonas pseudomallei* from soil in Northeastern Thailand. Transactions of the Royal Society of Tropical Medicine and Hygiene 89:41-43.

8. Cheng AC, Currie BJ. 2005. Melioidosis: epidemiology, pathophysiology, and management. Clin Microbiol Rev 18:383-416.

9. Whitmore A, Krishnaswami CS. 1912. An Account of the Discovery of a Hitherto Undescribed Infective Disease Occurring Among the Population of Rangoon. The Indian Medical Gazette:262-267.

10. Dannenberg AM, Jr., Scott EM. 1958. Melioidosis: pathogenesis and immunity in mice and hamsters. I. Studies with virulent strains of *Malleomyces pseudomallei*. J Exp Med 107:153-66.

11. Fuller PB, Fisk DE, Byrd RB, Griggs GA, Smith MR. 1978. Treatment of pulmonary melioidosis with combination of trimethoprim and sulfamethoxazole. Chest 74:222-4.

12. Yabuuchi E, Kosako Y, Oyaizu H, Yano I, Hotta H, Hashimoto Y, Ezaki T, Arakawa M. 1992. Proposal of *Burkholderia* gen. nov. and transfer of seven species of the genus *Pseudomonas* homology group II to the new genus, with the type species *Burkholderia cepacia* (Palleroni and Holmes 1981) comb. nov. Microbiol Immunol 36:1251-75.

13. Limmathurotsakul D, Golding N, Dance DAB, Messina JP, Pigott DM, Moyes CL, Rolim DB, Bertherat E, Day NPJ, Peacock SJ, Hay SI. 2016. Predicted global distribution of *Burkholderia pseudomallei* and burden of melioidosis. Nature Microbiology 1.

14. Trinh TT, Nguyen LDN, Nguyen TV, Tran CX, Le AV, Nguyen HV, Assig K, Lichtenegger S, Wagner GE, Do CD, Steinmetz I. 2018. Melioidosis in Vietnam: Recently Improved Recognition but still an Uncertain Disease Burden after Almost a Century of Reporting. Trop Med Infect Dis 3.

15. Howe C, Sampath A, Spotnitz M. 1971. The Pseudomallei Group: A Review. The Journal of Infectious Diseases 124:598-606.

16. Brett PJ, DeShazer D, Woods DE. 1998. *Burkholderia thailandensis* sp. nov., a *Burkholderia pseudomallei*-like species. Int J Syst Bacteriol 48 Pt 1:317-20.

17. Brett PJ, Deshazer D, Woods DE. 1997. Characterization of *Burkholderia pseudomallei* and *Burkholderia pseudomallei*-like strains. Epidemiol Infect 118:137-48.

18. Smith MD, Angus BJ, Wuthiekanun V, White NJ. 1997. Arabinose assimilation defines a nonvirulent biotype of *Burkholderia pseudomallei*. Infection and immunity 65:4319-4321.

19. Haraga A, West TE, Brittnacher MJ, Skerrett SJ, Miller SI. 2008. *Burkholderia thailandensis* as a model system for the study of the virulence-associated type III secretion system of *Burkholderia pseudomallei*. Infect Immun 76:5402-11.

20. Holden MT, Titball RW, Peacock SJ, Cerdeno-Tarraga AM, Atkins T, Crossman LC, Pitt T, Churcher C, Mungall K, Bentley SD, Sebaihia M, Thomson NR, Bason N, Beacham IR, Brooks K, Brown KA, Brown NF, Challis GL, Cherevach I, Chillingworth T, Cronin A, Crossett B, Davis P, DeShazer D, Feltwell T, Fraser A, Hance Z, Hauser H, Holroyd S, Jagels K, Keith KE, Maddison M, Moule S, Price C, Quail MA, Rabbinowitsch E, Rutherford K, Sanders M, Simmonds M, Songsivilai S, Stevens K, Tumapa S, Vesaratchavest M, Whitehead S, Yeats C, Barrell BG, Oyston PC, Parkhill J. 2004. Genomic plasticity of the causative agent of melioidosis, *Burkholderia pseudomallei*. Proc Natl Acad Sci U S A 101:14240-5.

21. Wilkinson L. 1981. Glanders: medicine and veterinary medicine in common pursuit of a contagious disease. Med Hist 25:363-84.

22. Khan I, Wieler LH, Melzer F, Elschner MC, Muhammad G, Ali S, Sprague LD, Neubauer H, Saqib M. 2013. Glanders in animals: a review on epidemiology, clinical presentation, diagnosis and countermeasures. Transbound Emerg Dis 60:204-21.

23. Currie BJ. 2014. *Burkholderia pseudomallei* and *Burkholderia mallei*: Melioidosis and Glanders. Mandell, Douglas, and Bennett's Principles and Practice of Infectious Diseases 2:2541-2551.e2.

24. Van Zandt KE, Greer MT, Gelhaus HC. 2013. Glanders: an overview of infection in humans. Orphanet J Rare Dis 8:131.

25. Wheelis M. 1998. First shots fired in biological warfare. Nature 395:213.

26. Thibault FM, Hernandez E, Vidal DR, Girardet M, Cavallo JD. 2004. Antibiotic susceptibility of 65 isolates of *Burkholderia pseudomallei* and *Burkholderia mallei* to 35 antimicrobial agents. J Antimicrob Chemother 54:1134-8.

27. Schweizer HP, Peacock SJ. 2008. Antimicrobial drug-selection markers for *Burkholderia pseudomallei* and *B. mallei*. Emerg Infect Dis 14:1689-92.

28. Srinivasan A, Kraus CN, DeShazer D, Becker PM, Dick JD, Spacek L, Bartlett JG, Byrne WR, Thomas DL. 2001. Glanders in a military research microbiologist. N Engl J Med 345:256-8.

29. Warawa JM, Long D, Rosenke R, Gardner D, Gherardini FC. 2009. Role for the *Burkholderia pseudomallei* capsular polysaccharide encoded by the *wcb* operon in acute disseminated melioidosis. Infect Immun 77:5252-61.

30. Propst KL, Mima T, Choi KH, Dow SW, Schweizer HP. 2010. A *Burkholderia pseudomallei* Δ*purM* mutant is avirulent in immunocompetent and immunodeficient animals: candidate strain for exclusion from select-agent lists. Infect Immun 78:3136-43.

31. Norris MH, Propst KL, Kang Y, Dow SW, Schweizer HP, Hoang TT. 2011. The *Burkholderia pseudomallei* Δ*asd* mutant exhibits attenuated intracellular infectivity and imparts protection against acute inhalation melioidosis in mice. Infect Immun 79:4010-8.

32. Gutierrez MG, Warawa JM. 2016. Attenuation of a select agent-excluded *Burkholderia pseudomallei* capsule mutant in hamsters. Acta Trop 157:68-72.

33. French CT, Bulterys PL, Woodward CL, Tatters AO, Ng KR, Miller JF. 2020. Virulence from the rhizosphere: ecology and evolution of *Burkholderia pseudomallei*-complex species. Curr Opin Microbiol 54:18-32.

34. Chaowagul W, White NJ, Dance DAB, Wattanagoon Y, Naigowit P, Davis TME, Looareesuwan S, Pitakwatchara N. 1989. Melioidosis: A Major Cause of Community-Acquired Septicemia in Northeastern Thailand. The Journal of Infectious Diseases 159:890-899.

35. Wiersinga WJ, Currie BJ, Peacock SJ. 2012. Melioidosis. N Engl J Med 367:1035-44.

36. Currie BJ, Ward L, Cheng AC. 2010. The epidemiology and clinical spectrum of melioidosis: 540 cases from the 20 year Darwin prospective study. PLoS Negl Trop Dis 4:e900.

37. Currie BJ, Fisher DA, Anstey NM, Jacups SP. 2000. Melioidosis: acute and chronic disease, relapse and re-activation. Transactions of the Royal Society of Tropical Medicine and Hygiene 94:301-304.

38. Limmathurotsakul D, Chaowagul W, Chierakul W, Stepniewska K, Maharjan B, Wuthiekanun V, White NJ, Day NP, Peacock SJ. 2006. Risk factors for recurrent melioidosis in northeast Thailand. Clin Infect Dis 43:979-86.

39. Limmathurotsakul D, Chaowagul W, Chantratita N, Wuthiekanun V, Biaklang M, Tumapa S, White NJ, Day NP, Peacock SJ. 2008. A simple scoring system to differentiate between relapse and re-infection in patients with recurrent melioidosis. PLoS Negl Trop Dis 2:e327.

40. Maharjan B, Chantratita N, Vesaratchavest M, Cheng A, Wuthiekanun V, Chierakul W, Chaowagul W, Day NP, Peacock SJ. 2005. Recurrent melioidosis in patients in northeast Thailand is frequently due to reinfection rather than relapse. J Clin Microbiol 43:6032-4.

41. Chaowagul W, Suputtamongkol Y, Dance D, Rajchanuvong A, Pattaraarechachai J, White NJ. 1993. Relapse in Melioidosis: Incidence and Risk Factors. Journal of Infectious Diseases 168:1181-1185.

42. Limmathurotsakul D, Chaowagul W, Day NP, Peacock SJ. 2009. Patterns of organ involvement in recurrent melioidosis. Am J Trop Med Hyg 81:335-7.

43. Currie BJ. 2015. Melioidosis: evolving concepts in epidemiology, pathogenesis, and treatment. Semin Respir Crit Care Med 36:111-25.

44. Amorn L, Somchai B. 1989. Melioidosis: Review and Update. Reviews of Infectious Diseases 11:413-425.

45. Sarovich DS, Price EP, Webb JR, Ward LM, Voutsinos MY, Tuanyok A, Mayo M, Kaestli M, Currie BJ. 2014. Variable virulence factors in *Burkholderia pseudomallei* (melioidosis) associated with human disease. PLoS One 9:e91682.

46. Gassiep I, Armstrong M, Norton R. 2020. Human Melioidosis. Clin Microbiol Rev 33.

47. Kingsley PV, Leader M, Nagodawithana NS, Tipre M, Sathiakumar N. 2016. Melioidosis in Malaysia: A Review of Case Reports. PLoS Negl Trop Dis 10:e0005182.

48. Kung CT, Li CJ, Ko SF, Lee CH. 2013. A melioidosis patient presenting with brainstem signs in the emergency department. J Emerg Med 44:e9-12.

49. Andersen EW, Mackay MT, Ryan MM. 2016. Neurologic Melioidosis: Case Report of a Rare Cause of Acute Flaccid Paralysis. J Pediatr 170:319-21.

50. Nandasiri S, Wimalaratna H, Manjula M, Corea E. 2012. Transverse myelitis secondary to melioidosis: a case report. BMC Infect Dis 12:232.

51. Woods ML, 2nd, Currie BJ, Howard DM, Tierney A, Watson A, Anstey NM, Philpott J, Asche V, Withnall K. 1992. Neurological melioidosis: seven cases from the Northern Territory of Australia. Clin Infect Dis 15:163-9.

52. Inglis TJ. 2010. The Treatment of Melioidosis. Pharmaceuticals (Basel) 3:1296-1303.

53. Fisher DA, Harris PNA. 2014. Melioidosis: refining management of a tropical time bomb. The Lancet 383:762-764.

54. Dance D. 2014. Treatment and prophylaxis of melioidosis. Int J Antimicrob Agents 43:310-8.

55. Ahmad N, Hashim R, Mohd Noor A. 2013. The In Vitro Antibiotic Susceptibility of Malaysian Isolates of *Burkholderia pseudomallei*. Int J Microbiol 2013:121845.

56. Dance DA, Davong V, Soeng S, Phetsouvanh R, Newton PN, Turner P. 2014. Trimethoprim/sulfamethoxazole resistance in *Burkholderia pseudomallei*. Int J Antimicrob Agents 44:368-9.

57. Saiprom N, Amornchai P, Wuthiekanun V, Day NP, Limmathurotsakul D, Peacock SJ, Chantratita N. 2015. Trimethoprim/sulfamethoxazole resistance in clinical isolates of *Burkholderia pseudomallei* from Thailand. Int J Antimicrob Agents 45:557-9.

58. Chantratita N, Rholl DA, Sim B, Wuthiekanun V, Limmathurotsakul D, Amornchai P, Thanwisai A, Chua HH, Ooi WF, Holden MT, Day NP, Tan P, Schweizer HP, Peacock SJ. 2011. Antimicrobial resistance to ceftazidime involving loss of penicillin-binding protein 3 in *Burkholderia pseudomallei*. Proc Natl Acad Sci U S A 108:17165-70.

59. Peacock SJ, Limmathurotsakul D, Lubell Y, Koh GC, White LJ, Day NP, Titball RW. 2012. Melioidosis vaccines: a systematic review and appraisal of the potential to exploit biodefense vaccines for public health purposes. PLoS Negl Trop Dis 6:e1488.

60. Pruksachartvuthi S, Aswapokee N, Thankerngpol K. 1990. Survival of *Pseudomonas pseudomallei* in human phagocytes. J Med Microbiol 31:109-14.

61. Allwood EM, Devenish RJ, Prescott M, Adler B, Boyce JD. 2011. Strategies for Intracellular Survival of *Burkholderia pseudomallei*. Front Microbiol 2:170.

62. Gutierrez MG, Yoder-Himes DR, Warawa JM. 2015. Comprehensive identification of virulence factors required for respiratory melioidosis using Tn-seq mutagenesis. Front Cell Infect Microbiol 5:78.

63. Gutierrez MG, Pfeffer TL, Warawa JM. 2015. Type 3 secretion system cluster 3 is a critical virulence determinant for lung-specific melioidosis. PLoS Negl Trop Dis 9:e3441.

64. Biggins JB, Kang HS, Ternei MA, DeShazer D, Brady SF. 2014. The chemical arsenal of *Burkholderia pseudomallei* is essential for pathogenicity. J Am Chem Soc 136:9484-90.

65. Stone JK, DeShazer D, Brett PJ, Burtnick MN. 2014. Melioidosis: molecular aspects of pathogenesis. Expert Rev Anti Infect Ther 12:1487-99.

66. Cruz-Migoni A, Hautbergue GM, Artymiuk PJ, Baker PJ, Bokori-Brown M, Chang CT, Dickman MJ, Essex-Lopresti A, Harding SV, Mahadi NM, Marshall LE, Mobbs GW, Mohamed R, Nathan S, Ngugi SA, Ong C, Ooi WF, Partridge LJ, Phillips HL, Raih MF, Ruzheinikov S, Sarkar-Tyson M, Sedelnikova SE, Smither SJ, Tan P, Titball RW, Wilson SA, Rice DW. 2011. A *Burkholderia pseudomallei* toxin inhibits helicase activity of translation factor eIF4A. Science 334:821-4.

67. Reckseidler SL, DeShazer D, Sokol PA, Woods DE. 2001. Detection of bacterial virulence genes by subtractive hybridization: identification of capsular polysaccharide of *Burkholderia pseudomallei* as a major virulence determinant. Infect Immun 69:34-44.

68. Kunakom S, Eustaquio AS. 2019. Burkholderia as a Source of Natural Products. J Nat Prod 82:2018-2037.

69. Greenberg EP, Chandler JR, Seyedsayamdost MR. 2020. The Chemistry and Biology of Bactobolin: A 10-Year Collaboration with Natural Product Chemist Extraordinaire Jon Clardy. J Nat Prod doi:10.1021/acs.jnatprod.9b01237.

70. Ishida K, Lincke T, Behnken S, Hertweck C. 2010. Induced biosynthesis of cryptic polyketide metabolites in a *Burkholderia thailandensis* quorum sensing mutant. J Am Chem Soc 132:13966-8.

71. Ishida K, Lincke T, Hertweck C. 2012. Assembly and absolute configuration of short-lived polyketides from *Burkholderia thailandensis*. Angew Chem Int Ed Engl 51:5470-4.

72. Thapa SS, Grove A. 2019. Do Global Regulators Hold the Key to Production of Bacterial Secondary Metabolites? Antibiotics (Basel) 8.

73. Liu X, Cheng YQ. 2014. Genome-guided discovery of diverse natural products from Burkholderia sp. J Ind Microbiol Biotechnol 41:275-84.

74. Gupta A, Bedre R, Thapa SS, Sabrin A, Wang G, Dassanayake M, Grove A. 2017. Global Awakening of Cryptic Biosynthetic Gene Clusters in *Burkholderia thailandensis*. ACS Chem Biol 12:3012-3021.

75. Seyedsayamdost MR. 2014. High-throughput platform for the discovery of elicitors of silent bacterial gene clusters. Proc Natl Acad Sci U S A 111:7266-71.

76. Okada BK, Wu Y, Mao D, Bushin LB, Seyedsayamdost MR. 2016. Mapping the Trimethoprim-Induced Secondary Metabolome of *Burkholderia thailandensis*. ACS Chem Biol 11:2124-30.

77. Biggins JB, Ternei MA, Brady SF. 2012. Malleilactone, a polyketide synthase-derived virulence factor encoded by the cryptic secondary metabolome of *Burkholderia pseudomallei* group pathogens. J Am Chem Soc 134:13192-5.

78. Franke J, Ishida K, Hertweck C. 2012. Genomics-driven discovery of burkholderic acid, a noncanonical, cryptic polyketide from human pathogenic *Burkholderia* species. Angew Chem Int Ed Engl 51:11611-5.

79. Moule MG, Spink N, Willcocks S, Lim J, Guerra-Assuncao JA, Cia F, Champion OL, Senior NJ, Atkins HS, Clark T, Bancroft GJ, Cuccui J, Wren BW. 2015. Characterization of New Virulence Factors Involved in the Intracellular Growth and Survival of *Burkholderia pseudomallei*. Infect Immun 84:701-10.

80. Truong TT, Seyedsayamdost M, Greenberg EP, Chandler JR. 2015. A *Burkholderia thailandensis* Acyl-Homoserine Lactone-Independent Orphan LuxR Homolog That Activates Production of the Cytotoxin Malleilactone. J Bacteriol 197:3456-62.

81. Abisado RG, Benomar S, Klaus JR, Dandekar AA, Chandler JR. 2018. Bacterial Quorum Sensing and Microbial Community Interactions. MBio 9.

82. Waters CM, Bassler BL. 2005. Quorum sensing: cell-to-cell communication in bacteria. Annu Rev Cell Dev Biol 21:319-46.

83. Lipscomb L, Schell MA. 2011. Elucidation of the regulon and *cis*-acting regulatory element of HrpB, the AraC-type regulator of a plant pathogen-like type III secretion system in *Burkholderia pseudomallei*. J Bacteriol 193:1991-2001.

84. Marenda M, Brito B, Callard D, Genin S, Barberis P, Boucher C, Arlat M. 1998. PrhA controls a novel regulatory pathway required for the specific induction of *Ralstonia solanacearum hrp* genes in the presence of plant cells. Mol Microbiol 27:437-53.

85. Grove A. 2010. Urate-responsive MarR homologs from Burkholderia. Mol Biosyst 6:2133-42.

86. Gupta A, Grove A. 2014. Ligand-binding pocket bridges DNA-binding and dimerization domains of the urate-responsive MarR homologue MftR from *Burkholderia thailandensis*. Biochemistry 53:4368-80.

87. Martin HM, Hancock JT, Salisbury V, Harrison R. 2004. Role of xanthine oxidoreductase as an antimicrobial agent. Infect Immun 72:4933-9.

88. Tuanyok A, Kim HS, Nierman WC, Yu Y, Dunbar J, Moore RA, Baker P, Tom M, Ling JM, Woods DE. 2005. Genome-wide expression analysis of iron regulation in *Burkholderia pseudomallei* and *Burkholderia mallei* using DNA microarrays. FEMS Microbiol Lett 252:327-35.

89. Ooi WF, Ong C, Nandi T, Kreisberg JF, Chua HH, Sun G, Chen Y, Mueller C, Conejero L, Eshaghi M, Ang RM, Liu J, Sobral BW, Korbsrisate S, Gan YH, Titball RW, Bancroft GJ, Valade E, Tan P. 2013. The condition-dependent transcriptional landscape of *Burkholderia pseudomallei*. PLoS Genet 9:e1003795.

90. Reen FJ, McGlacken GP, O'Gara F. 2018. The expanding horizon of alkyl quinolone signalling and communication in polycellular interactomes. FEMS Microbiol Lett 365.

91. Kilani-Feki O, Culioli G, Ortalo-Magne A, Zouari N, Blache Y, Jaoua S. 2011. Environmental *Burkholderia cepacia* strain Cs5 acting by two analogous alkyl-quinolones and a didecyl-phthalate against a broad spectrum of phytopathogens fungi. Curr Microbiol 62:1490-5.

92. Kilani-Feki O, Zouari I, Culioli G, Ortalo-Magne A, Zouari N, Blache Y, Jaoua S. 2012. Correlation between synthesis variation of 2-alkylquinolones and the antifungal activity of a *Burkholderia cepacia* strain collection. World J Microbiol Biotechnol 28:275-81.

93. Mahenthiralingam E, Song L, Sass A, White J, Wilmot C, Marchbank A, Boaisha O, Paine J, Knight D, Challis GL. 2011. Enacyloxins are products of an unusual hybrid modular polyketide synthase encoded by a cryptic *Burkholderia ambifaria* Genomic Island. Chem Biol 18:665-77.

94. Mori T, Yamashita T, Furihata K, Nagai K, Suzuki K, Hayakawa Y, Shin-Ya K. 2007. Burkholone, a new cytotoxic antibiotic against IGF-I dependent cells from *Burkholderia* sp. J Antibiot (Tokyo) 60:713-6.

95. Li D, Oku N, Hasada A, Shimizu M, Igarashi Y. 2018. Two new 2-alkylquinolones, inhibitory to the fish skin ulcer pathogen *Tenacibaculum maritimum*, produced by a rhizobacterium of the genus *Burkholderia* sp. Beilstein J Org Chem 14:1446-1451.

96. Deziel E, Lepine F, Milot S, He J, Mindrinos MN, Tompkins RG, Rahme LG. 2004. Analysis of *Pseudomonas aeruginosa* 4-hydroxy-2-alkylquinolines (HAQs) reveals a role for 4-hydroxy-2-heptylquinoline in cell-to-cell communication. Proc Natl Acad Sci U S A 101:1339-44.

97. Diggle SP, Matthijs S, Wright VJ, Fletcher MP, Chhabra SR, Lamont IL, Kong X, Hider RC, Cornelis P, Camara M, Williams P. 2007. The *Pseudomonas aeruginosa* 4-quinolone signal molecules HHQ and PQS play multifunctional roles in quorum sensing and iron entrapment. Chem Biol 14:87-96.

98. Coulon PML, Groleau MC, Deziel E. 2019. Potential of the *Burkholderia cepacia* Complex to Produce 4-Hydroxy-3-Methyl-2-Alkyquinolines. Front Cell Infect Microbiol 9:33.

99. Vial L, Lepine F, Milot S, Groleau MC, Dekimpe V, Woods DE, Deziel E. 2008. *Burkholderia pseudomallei*, *B. thailandensis*, and *B. ambifaria* produce 4-hydroxy-2-alkylquinoline analogues with a methyl group at the 3 position that is required for quorum-sensing regulation. J Bacteriol 190:5339-52.

100. Agarwal A, Kahyaoglu C, Hansen DB. 2012. Characterization of HmqF, a protein involved in the biosynthesis of unsaturated quinolones produced by *Burkholderia thailandensis*. Biochemistry 51:1648-57.

101. Schertzer JW, Brown SA, Whiteley M. 2010. Oxygen levels rapidly modulate *Pseudomonas aeruginosa* social behaviours via substrate limitation of PqsH. Mol Microbiol 77:1527-38.

102. Drees SL, Ernst S, Belviso BD, Jagmann N, Hennecke U, Fetzner S. 2018. PqsL uses reduced flavin to produce 2-hydroxylaminobenzoylacetate, a preferred PqsBC substrate in alkyl quinolone biosynthesis in *Pseudomonas aeruginosa*. J Biol Chem 293:9345-9357.

103. Diggle SP, Lumjiaktase P, Dipilato F, Winzer K, Kunakorn M, Barrett DA, Chhabra SR, Camara M, Williams P. 2006. Functional genetic analysis reveals a 2-Alkyl-4-quinolone signaling system in the human pathogen *Burkholderia pseudomallei* and related bacteria. Chem Biol 13:701-10.

104. Dulcey CE, Dekimpe V, Fauvelle DA, Milot S, Groleau MC, Doucet N, Rahme LG, Lepine F, Deziel E. 2013. The end of an old hypothesis: the *Pseudomonas* signaling molecules 4-hydroxy-2-alkylquinolines derive from fatty acids, not 3-ketofatty acids. Chem Biol 20:1481-91.

105. Piochon M, Coulon PML, Caulet A, Groleau M-C, Déziel E, Gauthier C. 2020. Synthesis and Antimicrobial Activity of *Burkholderia*-Related 4-Hydroxy-3-Methyl-2-Alkenylquinolones (HMAQs) and Their N-Oxide Counterparts doi:10.26434/chemrxiv.11859144.v1.

106. Wu Y, Seyedsayamdost MR. 2017. Synergy and Target Promiscuity Drive Structural Divergence in Bacterial Alkylquinolone Biosynthesis. Cell Chem Biol 24:1437-1444 e3.

Chapter 2: Malleilactone is a *Burkholderia pseudomallei* virulence factor regulated by antibiotics and quorum sensing

This chapter is written as per:

***Jennifer R. Klaus**,* Jacqueline Deay, Benjamin Neuenswander, Wyatt Hursh, Zhe Gao, Tiffany Bouddhara, Todd D. Williams, Justin Douglas, Kyle Monize, Patricia Martins, Charlotte Majerczyk, Mohammad R. Seyedsayamdost, Blake R. Peterson, Mario Rivera, and Josephine R. Chandler. Malleilactone is a *Burkholderia pseudomallei* virulence factor regulated by antibiotics and quorum sensing 2018. Journal of Bacteriology 200(14): e00008-18.

COLLABORATIONS AND WORKLOAD ALLOCATIONS:

Jennifer R. Klaus (with some assistance from Patricia Martins, Kyle Monize, and Tiffany Bouddhara) did the cloning and genetic manipulations. Jennifer R. Klaus performed transcriptional reporter assays (*lacZ* and *lux*), droplet digital PCR assays, and *C. elegans* infection experiments. Jacqueline Deay, Jennifer R. Klaus, and Wyatt Hursh optimized and performed sample preparation for UV/Vis and mass spectrometry (MS) analysis. Benjamin Neuenswander performed UV-Vis/MS analyses and assisted Jennifer R. Klaus in data interpretation. Benjamin Neuenswander purified malleilactone. Todd D. Williams performed tandem MS/MS analysis. Justin Douglas performed NMR analysis. Zhe Gao (mentored by Blake R. Peterson) performed eukaryotic cell line cytotoxicity assays. Tiffany Bouddhara and Josephine R. Chandler performed bacterial strain minimum inhibitory concentration assays. Mohammad R. Seyedsayamdost, Charlotte Majerczyk, and Mario Rivera provided some early conceptual project discussions and experimental design input. Jennifer R. Klaus and Josephine R. Chandler managed project conceptualization and experimental design and wrote the manuscript.

ABSTRACT

Burkholderia pseudomallei, the causative agent of melioidosis, encodes almost a dozen predicted polyketide (PK) biosynthetic gene clusters. Many of these are regulated by LuxR-I-type acyl-homoserine (AHL) quorum-sensing systems. One of the PK gene clusters, the *mal* gene cluster, is conserved in the close relative *Burkholderia thailandensis.* The *B. thailandensis mal* genes code for the cytotoxin malleilactone and are regulated by a genetically linked LuxR-type transcription factor, MalR. Although AHLs typically interact with LuxR-type proteins to modulate gene transcription, the *B. thailandensis* MalR does not appear to be an AHL receptor. Here, we characterize the *mal* genes and MalR in *B. pseudomallei*. We use chemical analyses to demonstrate that the *B. pseudomallei mal* genes code for malleilactone. Our results show MalR and the *mal* genes contribute to the ability of *B. pseudomallei* to kill *Caenorhabditis elegans*. In *B. thailandensis,* antibiotics like trimethoprim can activate MalR by driving transcription of the *mal* genes, and we demonstrate some of the same antibiotics induce expression of *B. pseudomallei malR.* We also demonstrate *B. pseudomallei* MalR does not respond to AHLs directly. Our results suggest MalR is indirectly repressed by AHLs, possibly through a repressor, ScmR. We further show that malleilactone is a *B. pseudomallei* virulence factor and provide the foundation for understanding how malleilactone contributes to the pathology of melioidosis infections.

IMPORTANCE

Many bacterially-produced polyketides are cytotoxic to mammalian cells and potentially important contributors to pathogenesis during infection. We are interested in the polyketide gene clusters encoded by *Burkholderia pseudomallei,* which causes the often-fatal human disease melioidosis. Using knowledge gained by studies in the close relative, *Burkholderia thailandensis,* we show that one of the *B. pseudomallei* polyketide biosynthetic clusters produces a cytotoxic polyketide, malleilactone. Malleilactone contributes to *B. pseudomallei* virulence in a *Caenorhabditis elegans* infection model and is regulated by an orphan LuxR family quorum-sensing transcription factor, MalR. Our studies demonstrate that malleilactone biosynthesis or MalR could be new targets for developing therapeutics to treat melioidosis.

INTRODUCTION

Burkholderia pseudomallei is the causative agent of melioidosis, an often fatal and difficult to treat condition estimated to be responsible for ~90,000 deaths worldwide per year (about 40% of total infections) (1). Despite the severity and worldwide incidence of melioidosis, the basic biology and pathogenesis mechanisms of this species remain relatively poorly understood, in part because of the difficulty of handling it in the laboratory. Because *B. pseudomallei* poses a high risk to national security and public health, it is considered a tier 1 select agent and as such, requires biosafety level 3 (BSL3) safety conditions for handling. Due to this restriction, much knowledge of *B. pseudomallei* stems from studies conducted on a close relative, *Burkholderia thailandensis,* which is safe for handling in BSL2 laboratory conditions. *B. thailandensis* and *B. pseudomallei* have a high degree of genetic relatedness and share about 85% of their genes. Speciation is due to differences in some metabolic capabilities, species-specific genes (including virulence genes in *B. pseudomallei*), and four large-scale (>10 kb) genomic inversions (2, 3). In addition to *B. thailandensis,* two *B. pseudomallei* attenuated strains were recently excluded from select agent regulations (4, 5), and thus can be used in BSL2 laboratory conditions. These strains provide new opportunities to study *B. pseudomallei* directly.

We are interested in understanding the pathogenic mechanisms of *B. pseudomallei,* particularly those mediated by small-molecule toxins, which are emerging as an important contributor to *B. pseudomallei* virulence in mammalian infections (6, 7). A substantial portion of the *B. pseudomallei* genome is dedicated to polyketide (PK) and nonribosomal peptide (NRP) secondary metabolism, with almost a dozen predicted PK/NRP gene clusters (6). Some of these gene clusters are also present in *B. thailandensis*, which has been used as a surrogate in some cases (8-10). Some of the clusters have been studied directly in *B. pseudomallei,* particularly those that are not shared in *B. thailandensis* (6, 7, 11-13). In many cases, no polyketide products, or very low concentrations, are synthesized in standard laboratory conditions, making them difficult to identify and study. In some cases, the products can be generated

using a genetic approach of synthetically inducing transcription of the biosynthetic genes (6, 8, 14). In others, specific laboratory conditions can trigger production (9, 15).

Many predicted secondary metabolite gene clusters in *B. pseudomallei* are regulated by acyl-homoserine lactone (AHL) quorum sensing (16, 17). These systems typically involve *luxI-luxR* gene pairs coding for signal synthase and receptor proteins, respectively. In some cases, *luxR* genes are not linked to any *luxI,* and these are called orphans or solos (18, 19). Many LuxR orphans are AHL responsive; however, at least some appear to be signal independent (20, 21). In *B. pseudomallei,* there are three LuxR-LuxI signaling systems, BpsR1-I1, BpsR2-I2, and BpsR3-I3. There are also two orphans, MalR (also called BpsR4) and BpsR5. MalR in *B. thailandensis* has been shown to control production of malleilactone (20), the product of a PK/NRP gene cluster and a cytotoxin that contributes to *B. thailandensis* virulence in nematodes (8). At least in *B. thailandensis,* MalR appears to be an unusual LuxR orphan, in that it is not a receptor for AHLs (20).

In this study, we focus on the malleilactone (*mal)* biosynthetic genes in *B. pseudomallei,* and specifically on the product and regulation of the *mal* cluster. The protein products of the *mal* biosynthetic genes and *malR* share ~80% identity in *B. thailandensis* and *B. pseudomallei.* The *mal* genes are silent in *B. thailandensis* under standard laboratory conditions. Expression of the *mal* cluster seems to be induced by certain antibiotics, including several used to treat melioidosis infections. Induction is through increased expression of *malR.* Here, we use knowledge gained from studies of the *B. thailandensis mal* genes to guide studies in *B. pseudomallei.* We demonstrate that the product of the *B. pseudomallei* genes is also malleilactone and that malleilactone contributes to *B. pseudomallei* virulence, as it does in *B. thailandensis.* The results of this work provide new information on small-molecule biosynthesis and regulation in *B. pseudomallei* and the biology of this understudied pathogen.

MATERIALS & METHODS

Bacterial strains, culture conditions, and reagents.

All bacterial strains, plasmids, and primers used in this study are listed in **Tables S2.3-5** in the supporting information. We used *B. pseudomallei* strain Bp82 (4), a select agent-excluded Δ*purM* derivative of the fully virulent strain 1026b. Bp82 is an adenine and thiamine auxotroph. We refer to Bp82 as wild-type *B. pseudomallei*. We used *E. coli* strains DH5α and DH10B (Invitrogen) for genetic manipulations and strain BW27783 (36), which constitutively expresses the arabinose transporter, for recombinant *E. coli* experiments. Bacteria were grown in Luria-Bertani (LB) broth (10 g tryptone, 5 g yeast extract, and 5 g NaCl per liter) supplemented with 50 mM morpholinepropanesulfonic acid (MOPS) where indicated, or M9 minimal medium supplemented with 0.4% glucose and 10 mM *para*-chloro-phenylalanine (*p*-Cl-Phe, Sigma) for *B. pseudomallei* counterselection during mutant construction. All *B. pseudomallei* growth media were supplemented with 1.6 mM adenine hemisulfate and 0.005% thiamine HCl, with the exception of LB agar plates, which were not supplemented. All growth was at 37˚C with shaking at 250 rpm, with the exception of *C. elegans* infection assays, which were at 20˚C (see below). Acyl-homoserine lactones were purchased from Sigma-Aldrich and Cayman Chemicals, stored in ethyl acetate acidified with 0.1mL per liter glacial acetic acid, and added to empty culture tubes and dried down prior to addition of bacterial cultures. When appropriate, the following antibiotics were used (per mL): 15 μg (*E. coli*) and 100 μg (*B. pseudomallei*) gentamicin, 100 μg ampicillin (*E. coli*), 50 μg (*E. coli*) and 1 mg (*B. pseudomallei*) kanamycin, and 25 μg (*E. coli*) and 2 mg (*B. pseudomallei*) zeocin. We added 1 mM isopropyl-β-D-thiogalactopyranoside (IPTG) as indicated.

We assayed β-galactosidase activity by using a Tropix Galacto-Light Plus chemiluminescence kit according to the manufacturer's protocol (Applied Biosystems, Foster City, CA). In all cases, β-galactosidase activity is reported as light units relative to the optical density at 600 nm (OD_{600}). Genomic DNA, PCR and DNA fragments, and plasmid DNA were purified by using a Puregene Core A kit,

plasmid purification mini-prep kit, or PCR cleanup/gel extraction kits (Qiagen or IBI–MidSci) according to the manufacturer's protocol.

Genetic manipulations.

Unmarked, in-frame deletions of *malR, malF,* and *scmR* were constructed using previously described methods (37). Briefly, DNA fragments containing ~500 to 1,000 bp DNA flanking each gene were generated by PCR or DNA synthesis (Genscript, New Jersey) and fused together creating an unmarked, nonpolar deletion of each gene with incorporated HindIII and XbaI sites. These fragments were digested with HindIII and XbaI and cloned into HindIII-, XbaI-digested pEX18Km-*pheS*, which was transformed into Bp82 by electroporation. Merodiploids were selected on LB agar containing kanamycin, and deletion mutants were counterselected on M9 agar with *p*-Cl-Phe. Mutant strains were verified by testing for kanamycin sensitivity and by PCR-amplifying the deletion region and sequencing the PCR product. The pUC18miniTn7T derivatives were introduced by electroporation into *B. pseudomallei* strains with the helper plasmid pTNS3, as previously described (38). We used PCR to verify insertion into the *attn7* site near *glmS3,* as previously described (38).

For recombinant *malR* expression in *E. coli*, *malR* was amplified from genomic DNA isolated from *B. pseudomallei* Bp82 by using primers that incorporated restriction sites (EcoRI and XmaI) into the product. The amplicon was cut with EcoRI and XmaI and ligated to EcoRI-, XmaI-digested pJN105 to make pJN105 P_{BAD}-*malR*. To generate a *lacZ* fusion to the *malA* promoter for recombinant *E. coli* experiments, the region upstream of *B. pseudomallei malA* extending from positions -1 to -476 with respect to the translational start site was synthesized (Genscript, New Jersey), with restriction sites (NcoI and HindIII) incorporated into the product. The G-block was digested with NcoI and HindIII and ligated to NcoI- and HindIII-digested pQF50 to make pQF50 P*malA-lacZ*.-To make the P*lac-malR* expression cassette, we first constructed the IPTG-inducible expression vector pUC18-mini-Tn7T-Km-P*lac* by digesting the kanamycin (Km) resistance gene from pUC18-mini-Tn7T-Km-FRT (38) with SalI and NsiI and using this fragment to replace the trimethoprim (Tp) resistance gene in SalI-NsiI-digested pUC18-

min-Tn7T-LAC-Tp (20) to make pUC18-mini-Tn7T-LAC-Km. We then cloned *malR* into this vector by PCR-amplifying *malR* from the Bp82 genome using primers that incorporated restriction sites (SacI and HindIII) into the product. The amplicon was cut with SacI and HindIII and ligated into SacI- and HindIII-digested pUC18-mini-Tn7T-Km-P*lac* to generate pUC18-mini-Tn7T-Km-P*lac-malR*. The P*lac-scmR* expression cassette was made by introducing an EcoRI-HindIII-cut *scmR* PCR-generated amplicon to the EcoRI-HindIII-cut pUC18-mini-Tn7T-Km P*lac-malR*. To make the pUC18-mini-Tn7T-Zeo-P*malA-lux* reporter plasmid, the *B. pseudomallei malA* promoter region from bp -1 to -1244 with respect to the translational start site was amplified from Bp82 genomic DNA using primers that incorporated BamHI and PstI. The fragment was digested with BamHI and PstI and then ligated into BamHI- and PstI-digested plasmid pCM53 (promoterless *lux* reporter plasmid) (39). To make the pUC18-mini-Tn7T-Zeo-P*malA-lacZ* reporter plasmid, we first constructed a pUC18-mini-Tn7T-Zeo-P*malA*-GFP intermediate plasmid. This was done by PCR-amplifying the GFP gene from pUC18-mini-Tn7T-Kan-GFP (40) and incorporating restriction sites PstI and SpeI, PCR-amplifying the promoter and open reading frame of the zeocin resistance gene (*ble*) from pUC18-mini-Tn7T-Zeo-P*malA-lux* and incorporating restriction sites SpeI and StuI, and ligating both of those fragments into PstI- and StuI-digested pUC18-mini-Tn7T-Zeo-P*malA-lux* (releasing the *luxCDABE* cassette and the *ble* gene). Then, the *lacZ* gene was subcloned from the pUC18-mini-Tn7T-Gm-*lacZ* plasmid (41) by digesting with AseI, treating with Klenow (New England BioLabs) to blunt-end the fragment, then digestion with PstI. The *lacZ* was ligated to pUC18-mini-Tn7T-Zeo-P*malA*-GFP plasmid digested with SpeI, Klenow-treated, then digested with PstI (to remove the GFP gene) to generate pUC18-mini-Tn7T-Zeo-P*malA-lacZ*. In all cases, constructs generated using PCR were verified by sequencing.

HR-LC-MS measurements.

For measuring malleilactone in *B. pseudomallei* cultures, samples were prepared by diluting stationary-phase *B. pseudomallei* cultures to an OD_{600} of 0.05 into 50 mL LB-MOPS in a 250-mL flask, and growing cultures 24 h with 250 rpm shaking at 37°C. *B. pseudomallei* growth media was

supplemented with adenine and thiamine, and where indicated, cultures were also supplemented with trimethoprim at 4.5 μg/mL, IPTG at 1 mM or synthetic AHLs at 5 μM each. Each culture was extracted with an equivalent volume of ethyl acetate, and the organic phase was collected using a separatory funnel. The organic phase was then dried down under nitrogen air and suspended in 300 μL dimethyl sulfoxide (DMSO) plus 1300 μL acetonitrile. Subsequent dilutions in acetonitrile were then performed as needed. Injections of 2 μL each were made on an Acquity ultraperformance liquid chromatography (UPLC) system (Waters) with a wash of 500 μL acetonitrile and 800 μL of water/methanol (1:1) between each injection. The UPLC was coupled to a photodiode array detector and an LCT Premier TOF mass spectrometer (Waters), and the system was fitted with an Acquity C_{18} ethylene bridged hybrid (BEH) column (2.1 x 50 mm, 1.7 μm; Waters). The chromatography was developed using an aqueous mobile phase with NH_4OH at pH 9.8 and an organic phase of acetonitrile increased by gradient of 5% to 99% over 2.7 min and then held at 99% acetonitrile for 0.4 min; flow rate was 0.6 mL per min. Relative malleilactone was reported as the growth-adjusted total area under the 370 nm peak corresponding with malleilactone (the λ_{max} of malleilactone is 373 nm). In all cases, fragments were monitored using mass spectrometry to validate the molecular weight of malleilactone in the expected peak.

Mass spectral data were collected by negative ion electrospray from 100 to 1,100 *m/z* with capillary set to 2,500 V, desolvation gas set to 300°C, and cone set to 35 V. Relative malleilactone was reported using the peak area at 370 nm, the λ_{max} of malleilactone. For LC-MS/MS experiments, negative ion electrospray spectra were acquired on a Waters Qtof Premier (Waters/Micromass, Manchester, UK) mass spectrometer operated in v mode at a resolution of 10,000. Spectra were acquired over the mass range 50 to 1,000 u, accumulating data for 3 seconds per cycle. MS/MS spectra were simultaneously collected using collision-induced dissociation (CID), using a MS1 quadropole set to transmit the precursor mass (*m/z* 305.1), with a selection window of 4 u. The collision energy was ramped from 15 to 45 eV per acquisition cycle to obtain a distribution of fragments from low to high mass. Product ions in the CID spectra ranged from the same mass to 2 mmu, and the relative abundances of CID fragments ranged from the same to better than 5%.

B. pseudomallei malleilactone purification and analysis.

Samples for malleilactone purification were grown and ethyl acetate extracted as described for mass spectrometry analysis, except growth was in 650 mL media with 4.5 µg/mL trimethoprim in 2.8-liter flasks, and the dried ethyl acetate extract was reconstituted in 10 mL acetonitrile. For comparison, *B. thailandensis* cultures were grown similarly except with 15 µg/mL trimethoprim and no adenine or thiamine added to the growth media. For malleilactone purification, two separate rounds of chromatography were performed on a Waters autopurification system equipped with a Waters 996 photodiode array (PDA), a 2525 binary pump, a 2767 sample manager, a Waters ZQ single quad mass spectrometer, and a Waters XBridge C_{18} column (5 µm, 19 by 150 mm). For the first round of chromatography, injections of 1,200 µL each were made using an aqueous mobile phase with NH_4OH at pH 9.8 and an organic phase of acetonitrile which increased by gradient from 25% to 45% over 4 min, followed by a hold at 100% for 2 min; the flow rate was 20 µL/min. The fractions were pooled and evaporated using a Genevac instrument at 35°C, and the residue was reconstituted in 10 mL of acetonitrile. For the second round of chromatography, injections of 1200 µL each were made using an aqueous mobile phase with 20 mM NH_4HCOO at pH 7.0, and an organic mobile phase of acetonitrile with a gradient of 35% to 55% over 4 min followed by a hold at 100% for 2 min. Fractions were triggered by UV at 370 nm and mass at 305 *m/z* with a mass spectrometer set to negative ionization, with the capillary at 2.9 kV, the source at 100°C, and the cone at 50 V. Final fractions were pooled and evaporated under a stream of N_2 gas and stored dry at -20˚C. For NMR characterization, purified malleilactone was dissolved in $CDCl_3$ (Cambridge Isotopes) and transferred to a 5-mm tube (Wilmad-LabGlass)**.** All NMR spectra were acquired on a 500 MHz AVIII spectrometer (Bruker) equipped with a cryogenically cooled broadband observe probe. Data was processed and visualized using Topspin (Bruker) and MestReNova (Mestrelabs) software.

Malleilactone susceptibility experiments.

The MICs of malleilactone against bacterial pathogens were determined using a protocol adapted from the 2003 guidelines of the Clinical and Laboratory Standards Institute (CLSI, formerly NCCLS), using the microtiter MIC method. Inocula for each test organism were prepared by suspending a colony from an LB agar plate into tryptic soy broth and growing for 3 to 5 h at 37°C with shaking, then adjusting the culture turbidity in phosphate-buffered saline (PBS) to the equivalent of a 1.0 McFarland standard (3×10^8 CFU/mL). These cell suspensions were used as inocula for microtiter MIC assays. Inocula (2.5 µL), which each corresponded to $1x10^6$ cells, was added to 100 µL wells each containing malleilactone diluted in cation-adjusted Mueller-Hinton II broth, and these were incubated with shaking for 24 h at 37°C. The MIC was defined as the lowest concentration of malleilactone (in µg/mL) in which bacterial growth in the well was not measurable by determining the turbidity at 600 nm (A_{600}) on a 96-well plate reader.

Malleilactone cytotoxicity experiments.

The minimum concentration causing 50% loss of viability (IC_{50}) of malleilactone against cultured A549 and Jurkat cells was measured using propidium iodide staining and flow cytometry (42). Briefly, A549 cells (ATCC CCL-185) were cultured in Dulbecco's modified Eagle medium (DMEM) (D6429; Sigma). Jurkat cells (ATCC TIB-152) were cultured in RPMI-1640 medium (R8758; Sigma). Media was supplemented with fetal bovine serum (FBS; 10%), penicillin (100 units/mL), and streptomycin (100 µg/mL). Cells were maintained in a humidified 5% CO_2 incubator at 37°C. A 96-well microtiter plate was seeded with 8,000 cells in 200 µL medium per well and grown at 37°C for 16 h. Cells were then treated with fresh medium containing concentrations of malleilactone ranging from 10^{-12} to 10^{-4} M. After incubation at 37˚C for 48 h, adherent A459 cells were washed with phosphate-buffered saline (pH 7.4) and suspended by treatment with trypsin-EDTA solution (50 µL) for 10 min at 37˚C, followed by addition of propidium iodide (3 µM final concentration) in complete medium (100 µL). For Jurkat cells in suspension, propidium iodide (2 µL, 3 µM final concentration) was added directly to the medium. Viable

cells were quantified by light scattering and exclusion of propidium iodide using a CytoFLEX flow cytometer. The data from 3 replicates were used to generate a dose-responsive curve. These curves were fitted by nonlinear regression with an inhibitor vs. response variable-slope 4-parameter model (GraphPad Prism 7) to determine the concentration that causes 50% loss of viability (IC_{50}) values.

C. elegans infections.

To assess the contributions of MalR and malleilactone genes in *B. pseudomallei* virulence, we used a *Caenorhabditis elegans* infection model using the N2 Bristol wild-type *C. elegans* strain. *C. elegans* were cultured at 20˚C on solid nematode growth medium (NGM; 3 g NaCl, 2.5 g Bacto peptone, 17 g Bacto agar, 5 μg cholesterol, 1 mM [each] $CaCl_2$ and $MgSO_4$, and 1 mM KPO_4 buffer [pH 6.0] per liter), and the *E. coli* strain OP50 was used as the *C. elegans* food source. When *C. elegans* were cultured on *B. pseudomallei* strains, 3.2 mM adenine and 0.010% thiamine were added to the NGM plates. For infection assays, overnight cultures of *B. pseudomallei* or the *E. coli* OP50 food source were diluted to an OD_{600} of 0.1, and 30-40 μl were spread onto the center of the NGM plates and the plates were incubated overnight at 37˚C. Plates were acclimated to room temperature for ~1 h prior to seeding the plates with *C. elegans (*10 late larval [L4]-staged worms per plate). Survival of the worms was monitored every 24 h until all worms were dead or until generation of new offspring prevented survival counts (in the case of *E. coli*). Of note, in every case, few to no deaths of OP50-fed worm were observed, and very few offspring were ever generated by worms that were fed *B. pseudomallei*.

Droplet digital PCR.

RNA was harvested from *B. pseudomallei* cells at the indicated durations or optical densities using methods described previously (43). Droplet digital PCR was performed on a QX200 droplet digital PCR (ddPCR) (Bio-Rad) system using EvaGreen Supermix. Each reaction contained 0.25 to 0.5 ng of cDNA template, 900 nM each primer, and 10 μl EvaGreen Supermix in a 20-μl final volume. After generating 40 μl of oil droplets, 40 rounds of PCR were conducted using the following cycling conditions: 95˚C for 30

sec, 58˚C for 30 sec, and 68˚C for 30 sec. Absolute transcript levels were determined using QuantaSoft software (Bio-Rad). In all cases, a no-template control reaction was performed, which contained no detectable transcripts. The *rpoD* RNA polymerase sigma factor gene was used as a reference gene unless otherwise noted, and the results are reported as the calculated transcript amount of a given gene per calculated *rpoD* transcript.

Transcription reporter assays.

To assess MalR activation of *malA* in *B. pseudomallei*, we used a *B. pseudomallei* strain with either a P*malA-lacZ* or a P*malA-luxCDABE* fusion cassette introduced to the neutral *glmS3* site in the chromosome (see **Table S2.3** in supporting information). Logarithmic-phase cultures were diluted to an OD_{600} of 0.05 in LB broth supplemented with antibiotics at the concentrations indicated. Reporter activity was determined by measuring β-galactosidase activity as described above or by direct luminescence measurements on a BioTek Synergy 2 plate reader. In all cases, β-galactosidase or luminescence activity is reported as light units relative to the optical density at 600 nm (OD_{600}).

RESULTS

The *B. pseudomallei mal* genes code for malleilactone biosynthesis.

The *B. thailandensis* malleilactone (*mal*) biosynthetic genes are encoded in an ~35 kb region that is also present in *B. pseudomallei* and *B. mallei* (**Fig. 2.1-A**). The predicted proteins encoded by this cluster share ~80 to 90% amino acid identity in all three species. The genomic organization of this region is also well conserved, with the exception of two genes coding for hypothetical proteins ($MalA_a$ and $MalB_b$), which are found in *B. pseudomallei* and *B. mallei* but not in *B. thailandensis.* The product of the *mal* genes in *B. thailandensis* is malleilactone. Based on the sequence conservation among these three species, we predicted that the *B. pseudomallei mal* gene product might be similar or identical to malleilactone. To test this prediction, we deleted the *B. pseudomallei malF* gene that is required for *B. thailandensis* malleilactone production (8). We compared the secondary metabolic profile of the *B. pseudomallei malF* mutant with that of the parental wild-type strain (Bp82) using a high-resolution liquid chromatography-mass spectrometry approach (HR-LC-MS). In the *B. pseudomallei* Bp82 culture, we observed a relatively small peak corresponding to the molecular weight of *B. thailandensis* malleilactone that was absent in *malF* mutant cultures (**Fig. 2.1-B**).

Under standard conditions, *B. pseudomallei* produced limited quantities of the presumed malleilactone product, which precluded further studies to characterize the structure of this compound. In *B. thailandensis,* malleilactone production is triggered by subinhibitory concentrations (below the MIC) of the antibiotic trimethoprim (15, 20). Thus, we grew *B. pseudomallei* cells with 4.5 μg/mL trimethoprim, a concentration that slowed growth by about 25%. Cells grown with this trimethoprim concentration produced ~5-fold-higher titers of the presumed malleilactone compound than did untreated cells (**Fig. 2.1-B**). Thus, we used trimethoprim as an inducer to generate sufficient quantities for further characterization. We initially characterized the product using a tandem HR-MS (HR-MS/MS) approach. The HR-MS/MS fragmentation pattern of the *B. pseudomallei* malleilactone-like product was consistent with that of *B. thailandensis* malleilactone (**Fig. 2.1-C;** see also **Fig. S2.1** in the supporting information).

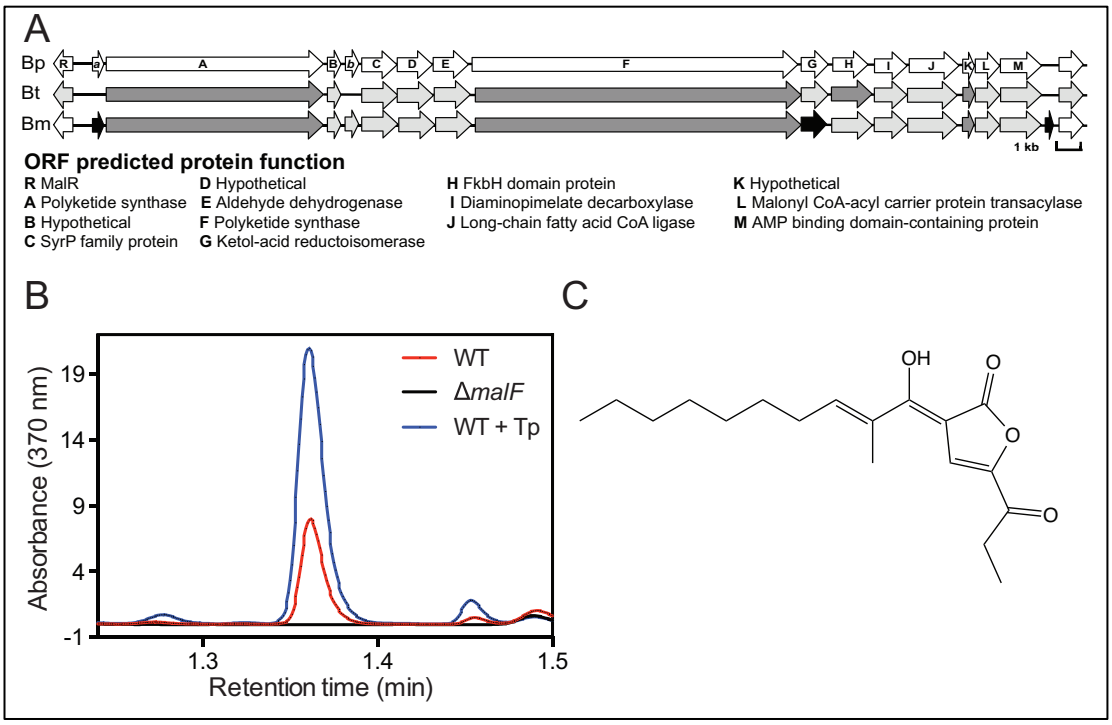

Figure 2.1. The *B. pseudomallei mal* genes code for production of malleilactone. (A) The *mal* gene cluster from *B. pseudomallei* (Bp), *B. thailandensis* (Bt) and *B. mallei* (Bm) with predicted function of each encoded protein. Shading indicates percent identity to the *B. pseudomallei* protein sequences. White, 100%; light gray, 90 to 99%; dark gray, 80 to 89%; black <80%. (B) Production of a malleilactone-like product in *B. pseudomallei* cultures. Levels of malleilactone production in the wild type (WT), Δ*malF* strain, and WT grown with 4.5 μg/mL trimethoprim are shown. (C) Proposed *B. pseudomallei* malleilactone structure consistent with liquid chromatography-mass spectrometry (LC-MS)/MS and nuclear magnetic resonance (NMR) results.

We also purified the product and conducted structural analysis by nuclear magnetic resonance spectroscopy (NMR). We used a purification procedure similar to that reported previously for *B. thailandensis* (20), with an important modification. We found that compound stability during and after purification was significantly improved by using a neutral pH in the mobile-phase buffer during secondary purification (pH 6.5) (see Materials and Methods). Our NMR data agreed well with those published for *B.* thailandensis-produced malleilactone (8, 14) (see **Fig. S2.2 and Table S2.2** in the supporting information). Together, our results demonstrate that the product of the *B. pseudomallei mal* genes is malleilactone, and that malleilactone production is enhanced during growth with trimethoprim.

Antibiotic activation of the *B. pseudomallei mal* genes.

Trimethoprim is an inhibitor of the tetrahydrofolate biosynthesis pathway. Several antibiotics with other cellular targets also induce *B. thailandensis mal* gene expression, including fluoroquinolone DNA gyrase inhibitors and the cell wall biosynthesis inhibitors piperacillin and ceftazidime (15). These antibiotics activate *mal* gene expression at concentrations that slow growth. However, slowed growth is not sufficient to induce the *mal* cluster, as some antibiotics such as the ribosome inhibitor kanamycin do not induce *B. thailandensis mal* gene expression. We were interested in identifying which antibiotics can induce expression of the *mal* genes in *B. pseudomallei.* To identify *mal*-inducing antibiotics, we constructed a reporter strain by fusing a promoterless *lacZ* gene to the promoter of *malA*, the first gene in the *mal* gene cluster, and introducing this reporter into the *glmS3* site in the *B. pseudomallei* genome. We tested a variety of antibiotics at sublethal but growth-slowing concentrations. Our results show that trimethoprim induces the P*malA-lacZ* reporter (**Table 2.1**), consistent with our mass spectrometry results (**Fig. 2.1-B**). *B. pseudomallei mal* genes were also induced by antibiotics other than trimethoprim, such as sulfamethoxazole (inhibits the tetrahydrofolate biosynthetic pathway, similarly to trimethoprim), and, to a lesser extent, ciprofloxacin (a fluoroquinolone), ceftazidime, and piperacillin. It is of note that trimethoprim, sulfamethoxazole, and ceftazidime are clinically used to treat melioidosis, although it is unclear whether this finding has any importance *in vivo*. Three antibiotics, namely, kanamycin, polymyxin B (an outer membrane-integrity disruptor), and imipenim (a β-lactam), did not activate expression of the *mal* genes.

Because some antibiotics trigger induction of oxidative stress response pathways through production of reactive oxygen species (22), we wondered if induction of oxidative stress could lead to activation of *mal* gene expression. Thus, we tested whether paraquat (1,1'-dimethyl-4,4'-bipyridinium dichloride), which induces oxidative stress through the production of superoxide, can induce *mal* gene expression. We tested paraquat at concentrations that slow growth, and our results showed that paraquat did not induce the *mal* gene cluster, consistent with the idea that *mal* gene expression is not induced by oxidative stress. Instead, our results suggest that a variety of antibiotics with different cellular targets can induce

expression of the *B. pseudomallei mal* biosynthetic genes. Some of the same antibiotics also induce the *B. thailandensis mal* genes, suggesting a similar mechanism of antibiotic-dependent *mal* gene regulation in both species.

Table 1. Ability of antibiotics to activate P*malA-lacZ* in *B. pseudomallei*

Growth inhibitor (μg/mL)[a]	Antibiotic mechanism	Relative P*malA-lacZ* activity[b]
None	-	1
Trimethoprim (15)	THF pathway inhibitor[c]	10.7 (0.4)
Sulfamethoxazole (500)	THF pathway inhibitor	10.5 (3.1)
Ceftazidime (1.75)	cell wall synthesis inhibitor	4.9 (0.7)
Piperacillin (10)	cell wall synthesis inhibitor	4.7 (1.1)
Ciprofloxacin (1)	DNA gyrase inhibitor	4.1 (0.8)
Imipenem (1.7)	cell wall synthesis inhibitor	1.8 (0.2)
Polymyxin B (600-700)	membrane permeabilization	1.4 (0.1)
Kanamycin (150)	30S ribosome inhibitor	0.9 (0.1)
Paraquat [500-700 nM][d]	reactive oxygen stress	1.3 (0.1)

[a]The concentration of antibiotic used is indicated in parentheses, and in each case this concentration resulted in about 50 to 70% reduction of growth yield as determined by the optical density at 600 nm (OD_{600}) measured at the time of β-galactosidase measurement, compared with an identically-grown untreated culture.
[b]Growth-adjusted β-galactosidase activity is given relative to the untreated control. β-galactosidase activity and optical density at 600 nm (OD_{600}) were determined after 24 h. Values are the mean of at least three independent experiments with the statistical range of the median indicated in parentheses.
[c]THF, tetrahydrofolate reductase.
[d]Paraquat generates oxidative stress through superoxide production.

Malleilactone cytotoxicity and *B. pseudomallei* virulence.

Previously, malleilactone was shown to be cytotoxic to several bacteria and to mammalian cells (8). Thus, we assessed the toxicity of our malleilactone preparation. We tested the concentration of malleilactone required to cause a 50% decrease in the viability of cultured human A549 bronchial epithelial cells and human Jurkat T lymphocyte cells after 48 h in culture (IC_{50}). The IC_{50} of malleilactone was found to be 7.4 μg/mL (24 μM) for the A549 cell line and 2.5 μg/mL (8 μM) for the Jurkat cell line (**Fig. S2.3** in the supporting information). This IC_{50} is comparable with those previously reported for malleilactone against other mammalian cells (8). We also determined the minimum inhibitory concentration (MIC) of malleilactone against several bacterial species. Malleilactone was cytotoxic to some Gram-positive bacterial species, including *Staphylococcus aureus*, at concentrations ranging from 5 to 20 μg/mL (18 to 70 μM) (**Table S2.1** in the supporting information).

The cytotoxicity of malleilactone suggests that it might function as a virulence factor in *B. pseudomallei.* We used a *Caenorhabditis elegans* infection model to test whether malleilactone contributes to *B. pseudomallei* virulence. Previous studies indicate that *B. pseudomallei* rapidly kills *C. elegans* through production of several secreted toxins, although only one has been identified (11, 23-26). Toxins also appear to be a significant contributor to *B. pseudomallei* pathogenicity in mammalian infections (6, 7). We tested virulence of our *malF* biosynthesis mutant and a strain with a deletion in *malR*. MalR is an orphan LuxR and is encoded adjacent to the *mal* biosynthesis genes. The *B. thailandensis* MalR is important for *C. elegans* infections (8) and has been shown to be a *mal* gene regulator (20) (**Fig. 2.1-A**). For our virulence assays, we placed *C. elegans* on a lawn of *B. pseudomallei* cells on nematode growth medium supplemented with adenine and thiamine and monitored worm survival daily. Under these conditions, the attenuated *B. pseudomallei* Bp82 strain was able to kill *C. elegans* within about 3 days (**Fig. 2.2**). *C. elegans* worms on Bp82 lawns also showed slowed movement and were reproduction deficient, as they produced fewer eggs than identically treated nematodes that were fed nonpathogenic *Escherichia coli*. Thus, similar to findings for virulent *B. pseudomallei* strains (23, 25,

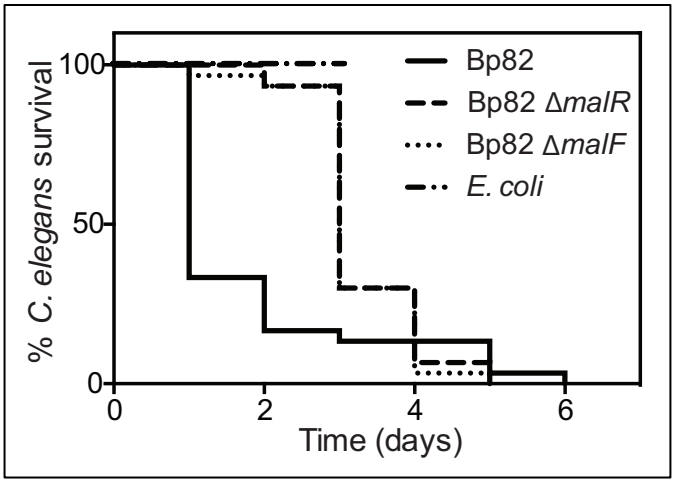

Figure 2.2. Malleilactone contributes to *B. pseudomallei* killing of *C. elegans.* Death of *C. elegans* over time when placed on a lawn of *B. pseudomallei* Bp82 WT, Bp82 Δ*malF*, or Bp82 Δ*malR*, or *E. coli* OP50 cells. In the case of *E. coli,* generation of new offspring prevented survival counts after day 3. Results are from one experiment with 30 worms on each strain, but they are representative of similar experiments done on separate days. The data were plotted using GraphPad Prism software, which generated survival fraction calculations (Kaplan-Meier limit method) and analyzed the data (log rank Mantel-Cox test). By this analysis, the median survival of each mutant is statistically different from the Bp82 parent (median survival is 3 days for Δ*malF* and Δ*malR* strains and 1 day for WT; $P < 0.0001$).

26), our results demonstrate that Bp82 was able to kill *C. elegans* in the presence of adenine and thiamine in the growth medium. Compared with Bp82, the *malF* and *malR* mutants were slower to kill *C. elegans* under identical growth conditions (**Fig. 2.2**). These results support the notion that malleilactone production and the putative regulator MalR are important for *B. pseudomallei* virulence.

Induction of the *mal* genes relies on MalR and sufficient *malR* expression.

MalR appears to be a key *mal* gene regulator in *B. thailandensis,* and our *C. elegans* infection results indicate that MalR is also important in *B. pseudomallei*. To test whether *B. pseudomallei* MalR regulates the *mal* genes*,* we introduced a short-half-life P*malA-luxCDABE* reporter into the neutral *glmS3* site in the genome of our *malR* mutant and the Bp82 parent and monitored reporter induction in each strain grown with or without trimethoprim. Not surprisingly, we observed little to no P*malA-luxCDABE* reporter induction in either strain grown without trimethoprim (**Fig. 2.3**) At 15 μg/mL (a concentration that reduced the growth yield by 50% at 24 h), trimethoprim activated the Bp82 reporter by about 6-fold, with maximal induction at 8-10 h (**Fig. 2.3**). However, there was no trimethoprim-dependent reporter induction in *malR* mutant cells, showing that MalR is important for trimethoprim activation of *mal* gene transcription. In *B. thailandensis,* MalR is not activated by trimethoprim directly, but rather the antibiotic

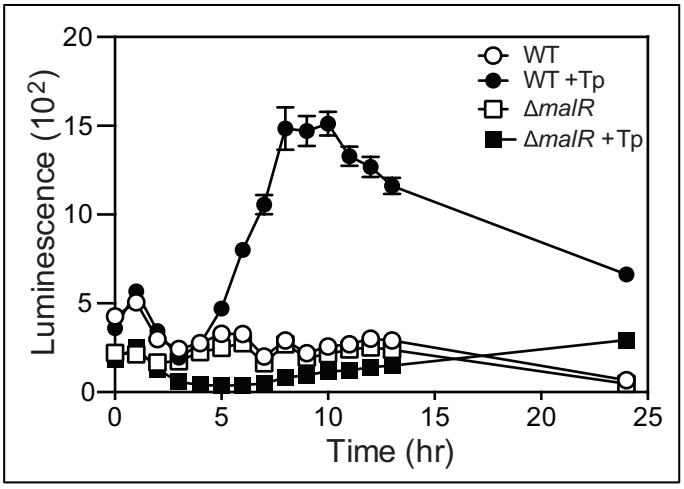

Figure 2.3. MalR is required for trimethoprim-dependent expression of *malA* in *B. pseudomallei.* Shown is the growth-adjusted activity of a P*malA-luxBCABE* chromosomal reporter in the *malR* mutant or its isogenic parent, Bp82 WT, grown with 15 μg/mL trimethoprim (Tp) or without trimethoprim. Results are the means and standard errors from three independent experiments.

increases MalR activity by driving *malR* transcription. We tested whether trimethoprim similarly increases *B. pseudomallei malR* transcription using quantitative droplet digital PCR. Our results show that trimethoprim increases *B. pseudomallei malR* transcription 4-fold (**Fig. S2.4** in the supporting information), consistent with the idea that trimethoprim activates *B. pseudomallei* MalR indirectly by driving *malR* transcription.

Our results suggest that MalR activity correlates with the level of *malR* expression. We sought to more directly test this hypothesis. We constructed an isopropyl-β-D-thiogalactopyranoside (IPTG)-inducible *malR* expression cassette by fusing *malR* to the P*lac* promoter and moved this cassette into the neutral *glmS3* site in the genome of our *malR* mutant. We measured malleilactone production in this P*lac-malR*-containing strain and also in the *malR* mutant and Bp82 parent strains containing the empty P*lac* cassette (**Fig. 2.4**). Consistent with our previous results (**Fig. 2.1-B and Fig. 2.2**), malleilactone was relatively low in the P*lac*-labeled Bp82 and even lower in the *malR* mutant. However, the *malR* mutant containing P*lac-malR* had malleilactone levels that exceeded that produced by Bp82 by more than 7-fold ($P < 0.015$). Thus, *malR* expression is sufficient to induce malleilactone production to high levels, even in the absence of trimethoprim.

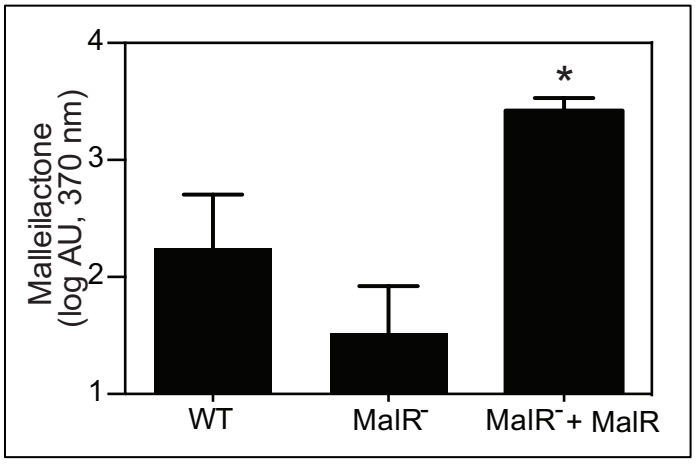

Figure 2.4. Expression of *lac* promoter-controlled *malR* is sufficient for malleilactone production in *B. pseudomallei.* Cells were grown with isopropyl-β-D-thiogalactopyranoside (IPTG) to induce *malR* expression, and cultures were collected at stationary phase (24 h), extracted with ethyl acetate, and assessed for relative malleilactone, as described in the Materials and Methods. Data shown are the growth-adjusted peak areas corresponding with malleilactone at 370 nm (the malleilactone λ_{max}). WT, Bp82 with the P*lac* cassette; MalR$^-$, Bp82 Δ*malR* with the P*lac* cassette; MalR$^-$ + MalR, Bp82 Δ*malR* with the P*lac-malR* cassette. All cultures were grown with 1 mM IPTG. Results are the means and standard errors from three independent experiments. *, statistical significance by *t* test ($P < 0.015$) compared with both WT and MalR$^-$.

Malleilactone production is repressed by *N*-3-hydroxy-octanoyl homoserine lactone and *N*-3-hydroxy-decanoyl homoserine lactone.

Results with *B. thailandensis* indicate that MalR is not a typical LuxR family protein, in that it is not an AHL receptor. Previous studies with recombinant *E. coli* showed that *B. thailandensis* MalR activation of the *malA* promoter is not influenced, either positively or negatively, by AHLs (20). MalR proteins in *B. pseudomallei* and *B. thailandensis* differ by only 5 amino acids. Some of these changes could possibly affect the ability of MalR to respond to AHLs. Thus, we engineered plasmids to test *B. pseudomallei* MalR activity in recombinant *E. coli*. We used a plasmid with an arabinose-inducible *B. pseudomallei malR* and another plasmid containing a 1,000-bp fragment containing the *B. pseudomallei malA* promoter (from positions -1 to -1000 with respect to the predicted MalA translational start site) fused to a promoterless *lacZ* gene. In *E. coli, lacZ* activation required arabinose induction of *B. pseudomallei* MalR and was not influenced by any of the AHLs tested (**Fig. S2.5** in the supporting information), including the *B. pseudomallei* AHLs *N*-octanoyl homoserine lactone (C8-HSL), *N*-3-hydroxy-octanoyl homoserine lactone (3OHC8-HSL) and N-3-hydroxy-decanoyl homoserine lactone (3OHC10-HSL).

Our results indicate that *B. pseudomallei* MalR does not interact with AHLs directly. However, activation of the *mal* genes might be regulated by AHLs through other indirect mechanisms. To test this possibility, we used a *B. pseudomallei* mutant with deletions in all three of the AHL synthases (*bpsI1, bpsI2,* and *bpsI3*). We compared malleilactone produced by this strain with that of wild type. In our experiments, the AHL mutant showed ~10-fold higher malleilactone than the Bp82 parent (**Fig. 2.5-A**). Malleilactone levels were restored to wild-type levels by exogenously adding all three of the *B. pseudomallei*-produced AHLs to the growth medium (5 μM each). When added individually, 3OHC8-HSL, and to a lesser extent 3OHC10-HSL, repressed malleilactone production, but C8-HSL did not.

How does quorum sensing repress malleilactone production? Based on our previous results, MalR is a likely candidate for indirect regulation by AHLs. In support of this idea, introducing a *malR* deletion to the AHL synthase mutant reduced malleilactone to almost undetectable levels (**Fig. 2.5-A**). We

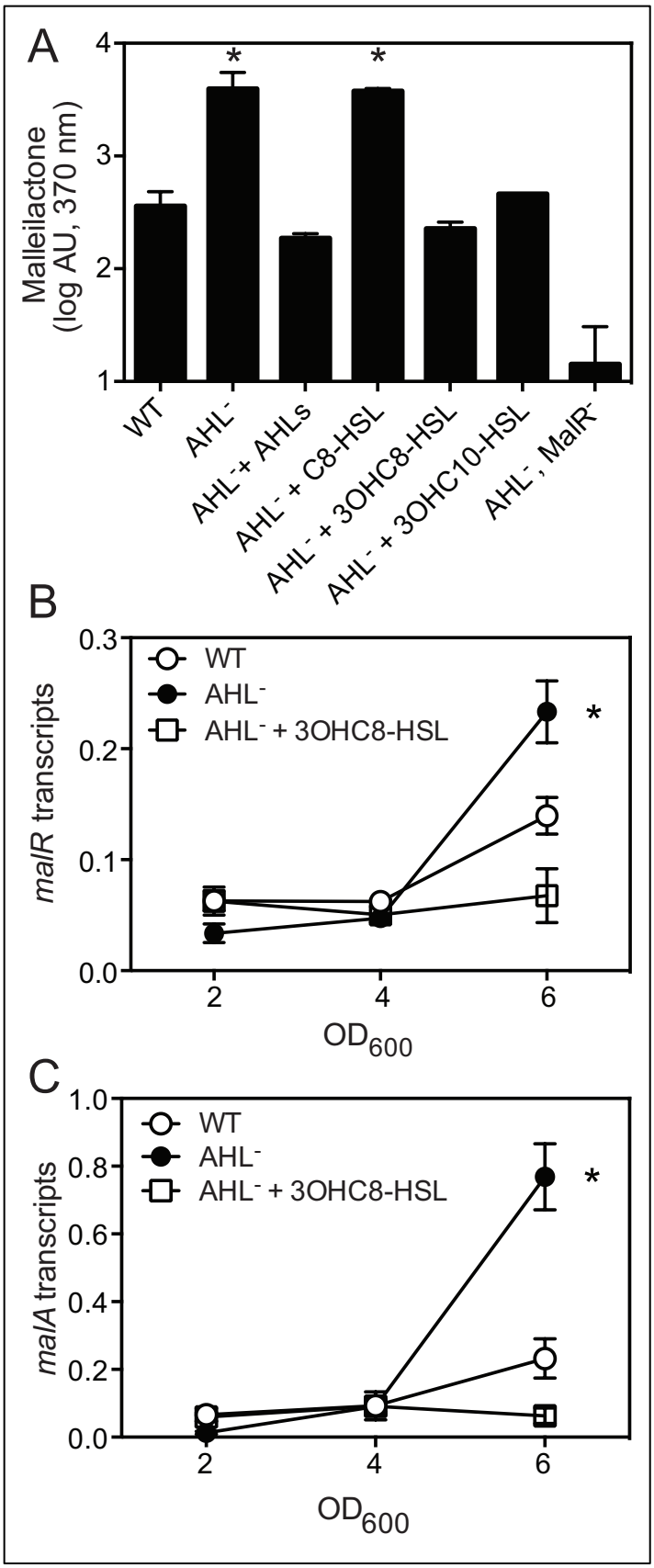

Figure 2.5. AHL-dependent regulation of malleilactone biosynthesis. (A) Cells were collected during stationary phase (24 h), extracted with ethyl acetate, and assessed for relative malleilactone, as described in Materials and Methods. Data shown are the growth-adjusted peak areas corresponding with malleilactone at 370 nm (the malleilactone λ_{max}). WT, Bp82; AHL$^-$, Bp82 with deletions in all three of the AHL synthase genes (*bpsI1 to* -3) (CM139); AHLs, 5 μM (each or individually, as indicated) C8-HSL, 3OHC8-HSL, and 3OHC10-HSL. AHL- MalR-, Bp82 with deletions of *bpsI1* to *-3* and *malR.* (B and C) AHL-dependent regulation of *malR* (B) and *malA* (C) transcription in Bp82 WT, AHL$^-$ cells, and AHL$^-$ cells with 5 μM 3OHC8-HSL added to the culture medium. Transcript abundance was normalized to the *rpoD* RNA polymerase sigma factor gene transcripts. In all cases, results are the means and standard errors of three independent experiments. *, statistical significance by *t* test compared with the wild type ($P \leq 0.05$).

hypothesized that AHLs regulate MalR indirectly by repressing *malR* expression. To test this hypothesis, we assessed *malR* expression in the triple AHL mutant and wild-type parent throughout growth. We also assessed *malR* expression in the AHL mutant with 3OHC8-HSL added to the culture medium. We sampled cells at three culture optical densities, namely, 2 (the transition between logarithmic and stationary phase), 4 (stationary phase), and 6 (stationary phase). For all three strains, *malR* expression was relatively low until the culture reached an optical density of 6. At this density, *malR* levels were almost 2-fold higher in the AHL mutant compared with those of the wild type, and more than 3-fold higher in the AHL mutant compared with those of the mutant grown with AHLs ($P < 0.05$) (**Fig. 2.5-B**). We also assessed *malA* expression in these cells. Our results showed that the pattern of *malA* expression was similar to that of *malR,* with maximal induction at a culture optical density of 6 (**Fig. 2.5-C**). These results are consistent with the idea that *malR* transcription is induced in the AHL mutant, causing subsequent induction of the malleilactone biosynthesis genes. Our results suggest that *malR* expression is repressed by AHLs very late in growth. It is possible other mechanisms repress *malR* at lower culture densities.

Malleilactone production is repressed by a quorum sensing-activated regulator, ScmR.

The *B. pseudomallei* AHL-responsive regulators BpsR1, BpsR2, and BpsR3 typically function as gene promoter activators (27-30); thus, we hypothesized that quorum sensing represses *malR* indirectly through another regulator. A likely candidate is the putative transcriptional regulator ScmR. In *B. thailandensis,* ScmR is a quorum sensing-activated repressor of malleilactone production and other secondary metabolites (31). The *B. pseudomallei* and *B. thailandensis* ScmR proteins are 99% identical. To test the role of *B. pseudomallei* ScmR in malleilactone production, we deleted *scmR* in Bp82 and compared malleilactone produced by the *scmR* mutant to that of the parent. Our results showed that deleting *scmR* increased malleilactone production almost 4-fold (**Fig. 2.6-A**, $P < 0.01$). We were able to restore malleilactone production in the *scmR* mutant to that of wild type by expressing *scmR* from the IPTG-inducible P*lac* promoter (**Fig. 2.6-A**). To test whether *B. pseudomallei* quorum sensing activates

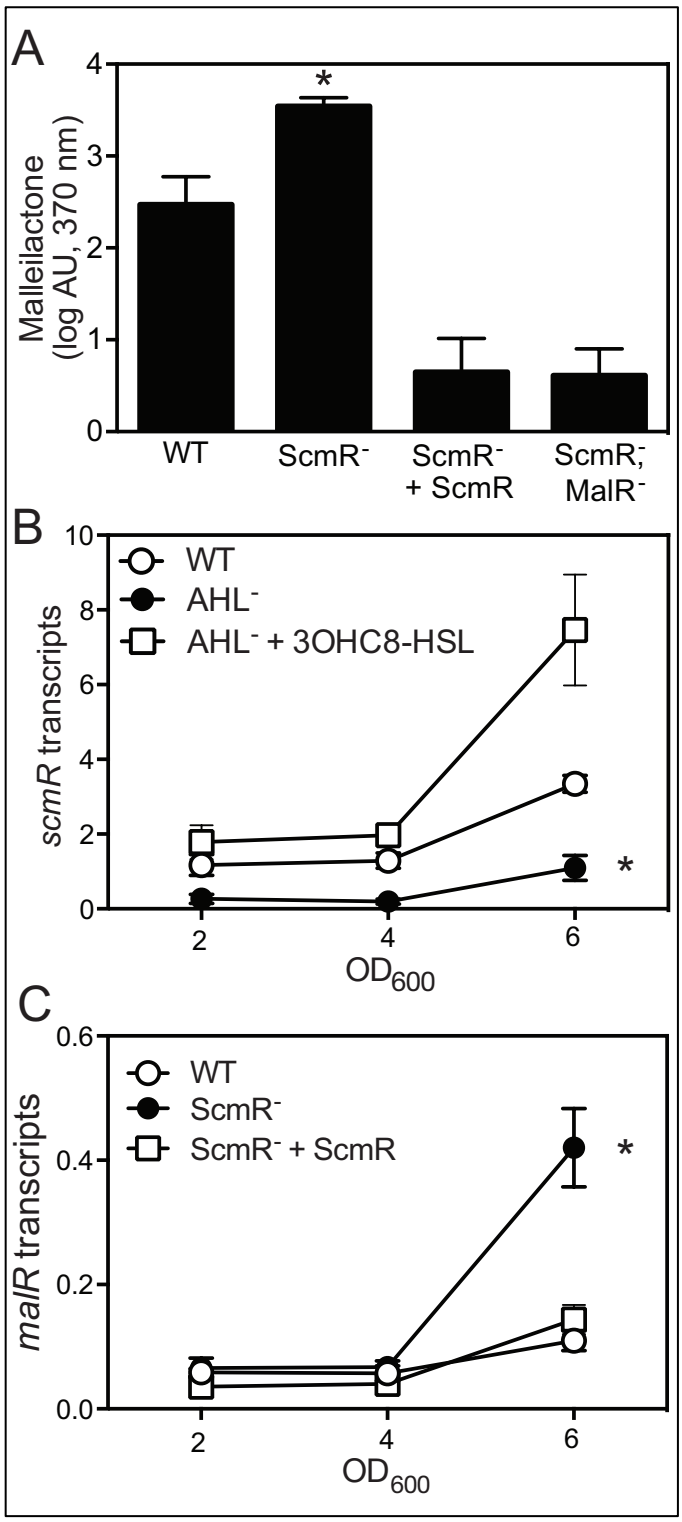

Figure 2.6. Regulation and activity of *B. pseudomallei* ScmR. (A) Cultures were collected in stationary phase (24 h), extracted with ethyl acetate, and assessed for relative malleilactone as described in Materials and Methods. Data shown are the growth-adjusted peak areas corresponding with malleilactone at 370 nm (the malleilactone λ_{max}). WT, Bp82 with the P*lac* cassette inserted into the *glmS3* site in the genome; ScmR$^-$, Bp82 *glmS3::*P*lac* with a deletion in *scmR;* ScmR$^-$ + ScmR, Bp82 with a deletion in *scmR* and P*lac-scmR* inserted into *glmS3;* ScmR,$^-$ MalR$^-$, Bp82 *glmS3::*P*lac* with deletions in *scmR* and *malR.* (B) AHL-dependent regulation of *scmR* transcription. WT, Bp82; AHL-, Bp82 with deletions in all three of the AHL synthase genes (*bpsI1* to *-3*) (CM139); AHL- + 3OHC8-HSL, CM139 with 5 μM 3OHC8-HSL added to the culture medium. (C) ScmR-dependent regulation of *malR* transcription. Strains are as described in the panel A legend. Transcript abundance (B and C) was normalized to the *rpoD* RNA polymerase sigma factor gene transcripts. Strains in panels A and C were grown with 1 mM IPTG. In all cases, results are the means and standard errors from three independent experiments. *, statistical significance by *t* test compared with wild type ($P \leq 0.05$).

scmR transcription, we measured *scmR* transcripts in our triple AHL mutant, the wild type parent, and the AHL mutant supplemented with 3OHC8-HSL. We found that *scmR* transcripts were 3-fold lower in the

AHL mutant than in wild-type cells ($P < 0.01$) (**Fig. 2.6-B**), suggesting that *B. pseudomallei scmR* transcription is controlled by quorum sensing. We also assessed the importance of MalR in ScmR-dependent regulation of malleilactone production. MalR is required for induction of malleilactone in the *scmR* mutant, because deleting *malR* in the *scmR* mutant nearly abolished malleilactone production (**Fig. 2.6-A**). We hypothesized that ScmR might repress malleilactone production by decreasing *malR* transcription. To test this hypothesis, we measured *malR* transcripts in an *scmR* mutant and compared these with those of the wild type at culture optical densities of 2, 4, and 6. In support of our hypothesis, *malR* transcripts were 2-fold higher in the *scmR* mutant compared with those of identically-grown wild-type cells during later growth ($P < 0.05$) (**Fig. 2.6-C**), a pattern consistent with that of *malR* expression in the AHL synthase mutant (**Fig. 2.5-B**). Together, our results support the idea that malleilactone production is controlled by quorum sensing indirectly through ScmR, and that ScmR acts by repressing transcription of *malR*, thereby explaining why little to no malleilactone is produced under standard laboratory conditions.

DISCUSSION

The *mal* gene cluster is well conserved in *B. thailandensis, B. pseudomallei,* and also *B. mallei* (~80% identity). These three species also share a high degree of genetic similarity. Yet, they each have a distinctly different lifestyle. *B. thailandensis* is a saprophyte, *B. pseudomallei* is an opportunistic pathogen, and *B. mallei* is a host-restricted pathogen that causes a disease called glanders. We are interested in studying this group because it provides a unique opportunity to understand how homologous systems adapt to different lifestyles. The finding that the malleilactone biosynthesis cluster is conserved in all three species suggests that it is important for diverse lifestyles. In a saprophytic lifestyle, malleilactone might be important for competition with other strains or species of bacteria. Malleilactone is also important for virulence in an animal host (**Fig. 2.2**) (8). There is evidence from recent transposon sequencing studies that malleilactone contributes to pathogenesis in mouse models of melioidosis (32, 33). These studies use pools of *B. pseudomallei* transposon mutant populations to infect the lungs of mice, and in these studies, insertions in *malR, malA* and some of the other *mal* biosynthetic genes had reduced fitness in the mouse lung and spleen (*e.g., malA* mutants were 3-fold and 39-fold reduced in the mouse lungs and spleen, respectively) (32, 33). The exact role of malleilactone in *B. pseudomallei* fitness during infections *in vivo* remains to be determined.

The regulatory circuits controlling malleilactone production appear to be well conserved in *B. pseudomallei* and *B. thailandensis.* The *B. pseudomallei mal* genes are induced by at least some of the same antibiotics as the *B. thailandensis mal* genes, such as trimethoprim, piperacillin, ceftazidime, and ciprofloxacin (15, 20) (**Table 2.1**). Further, the *mal* genes in both species are not induced by kanamycin (15, 20) (**Table 2.1**). These results suggest that the pathway of antibiotic-dependent regulation of the *mal* genes might be conserved in these two species. Quorum-sensing repression of *mal* gene expression is also similar in *B. thailandensis* and *B. pseudomallei.* In *B. pseudomallei,* malleilactone production is repressed by 3OHC8-HSL and 3OHC10-HSL (**Fig. 2.5-A**). These AHLs are specific to the BpsR2-I2 system (27). This system is conserved in *B. thailandensis,* where it also represses malleilactone production (31).

However, this system is missing from the *B. mallei* genome. Instead, in *B. mallei* the *mal* genes appear to be controlled by the C8-HSL-responsive system BmaR1-I1 (homologous to BpsR1-I1) (17). Despite the potential variation in which system controls malleilactone production, the conservation of quorum control of malleilactone production across these three species suggests an important association with cell density that is broadly beneficial in this group.

Our results show that ScmR represses malleilactone production in *B. pseudomallei.* They support a model whereby BpsR2-I2 activates production of the ScmR repressor during later stages of growth, and ScmR decreases malleilactone production by repressing transcription of *malR* (**Fig. 2.6**). ScmR also represses malleilactone production in *B. thailandensis;* however, in *B. thailandensis* ScmR was not shown to repress *malR* during late-log phase (31). It is possible that *malR* repression also occurs in *B. thailandensis* but only in late stationary phase, as it does in *B. pseudomallei* (**Fig. 2.6**). Alternatively, this result might represent a difference in the regulatory circuits of *B. thailandensis* and *B. pseudomallei.* The finding that ScmR represses malleilactone in *B. pseudomallei* suggests that ScmR might function as a global repressor of *B. pseudomallei* secondary metabolism, as it does in *B. thailandensis.* ScmR is also conserved in *B. mallei*, the causative agent of the disease glanders, and might be a useful target for eliciting production of other secondary metabolites in the *B. pseudomallei*-group pathogens. As some ScmR-dependent secondary metabolites are implicated in virulence (31), ScmR might also serve as a target for development of novel antivirulence therapeutics to treat melioidosis and glanders.

Our results show that *B. pseudomallei* malleilactone is structurally identical to that of *B. thailandensis* and corroborate previous studies showing that malleilactone is cytotoxic to both cultured mammalian cells and several kinds of Gram-positive bacteria. In our experiments, *B. thailandensis* and *B. pseudomallei* were relatively insensitive to malleilactone (MIC > 200 μg/mL) (see **Table S2.1** in supporting information). Previously, we showed *B. thailandensis* growth is slowed by about 50% when 10 to 15 μg/mL malleilactone is added to culture flasks (20). These results suggest that *B. thailandensis,* and possibly other bacterial species, is sensitive to malleilactone under certain conditions. In addition to cytotoxicity, malleilactone could also have another role as an iron-chelating molecule that binds or

possibly imports iron. The butyrolactone core of malleilactone has the potential to coordinate metal ions, and malleilactone has been shown to weakly interact with iron (8). Further, the *mal* genes are transcriptionally induced during growth in low iron (34), suggesting a possible link to extracellular iron levels (35).

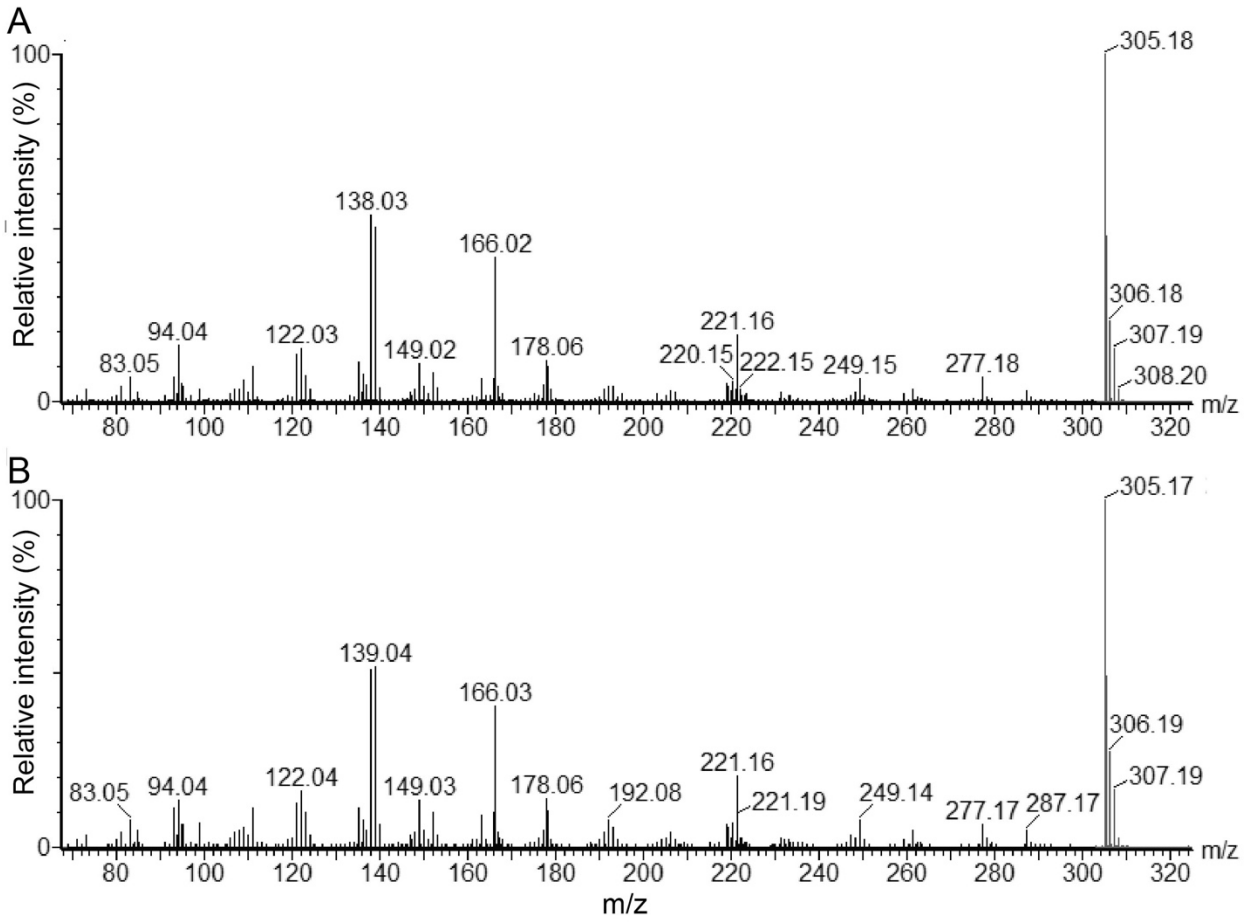

Figure S2.1. MS/MS spectral analysis of malleilactone from culture extracts. (A) *B. pseudomallei* Bp82 culture extracts. (B) *B. thailandensis* E264 culture extracts. For each, the product ions were of the same mass to 2 mmu and the fragment relative abundances were the same to better than 5%.

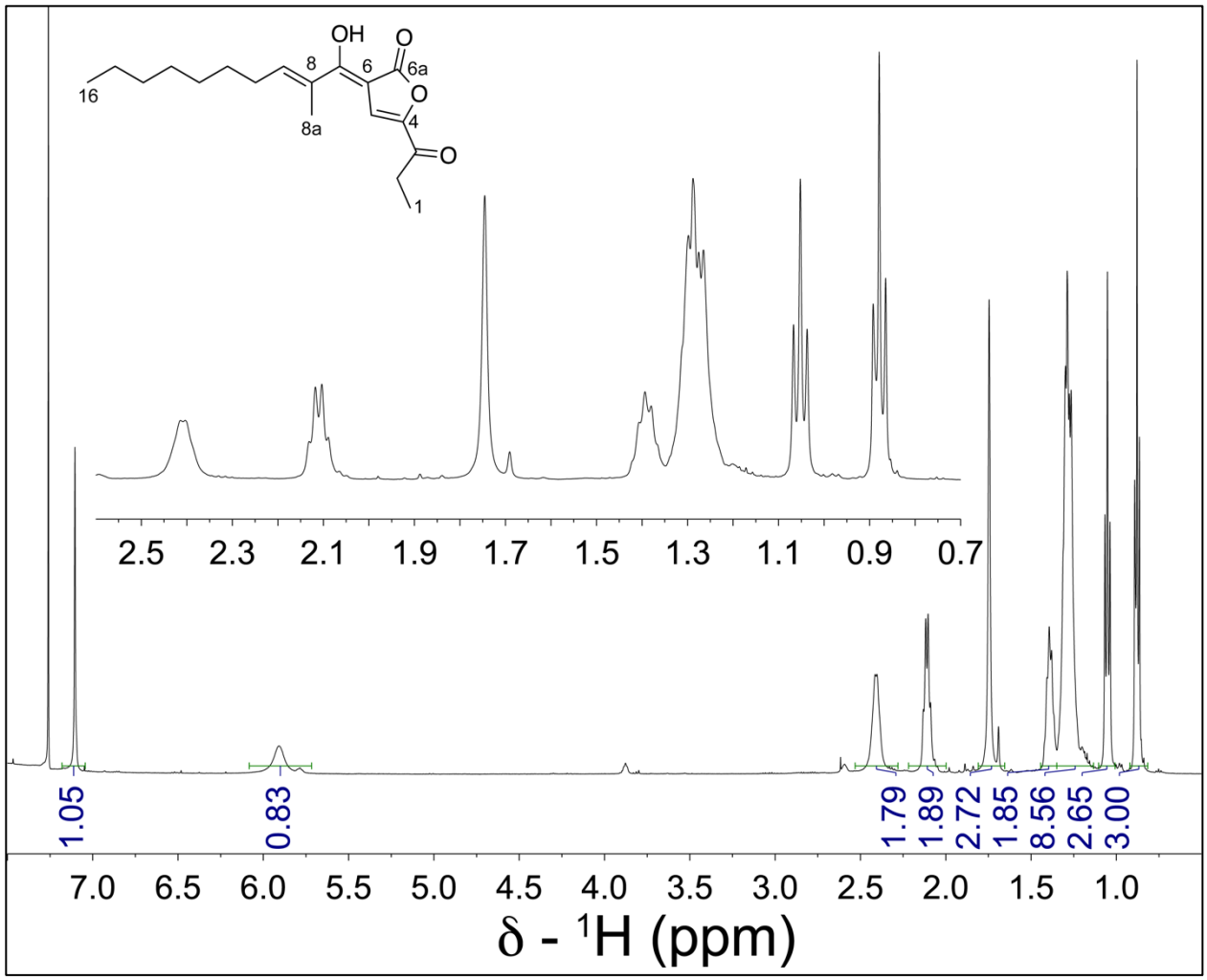

Figure S2.2. *B. pseudomallei* malleilactone 1D ^{1}H NMR, 500 MHz in $CDCl_3$. See **Table S2** for assignments.

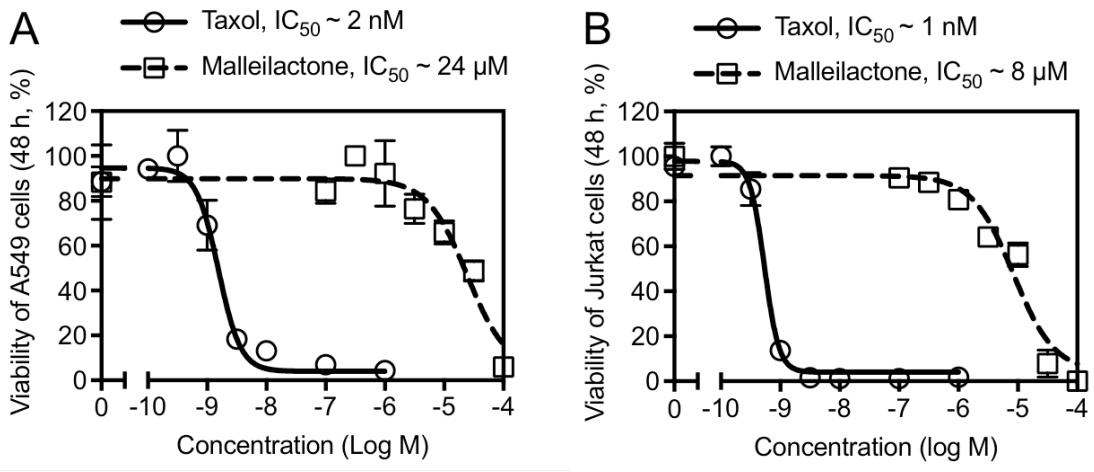

Figure S2.3. Cytotoxicity assays in cultured A549 (A) and Jurkat (B) cells. Cells were exposed to a range of concentrations of malleilactone, and to taxol as a positive control, and viability was measured using a propidium iodide uptake assay as described in Materials and Methods. IC_{50} values for taxol were 1–2 nM, similar to that reported previously (42).

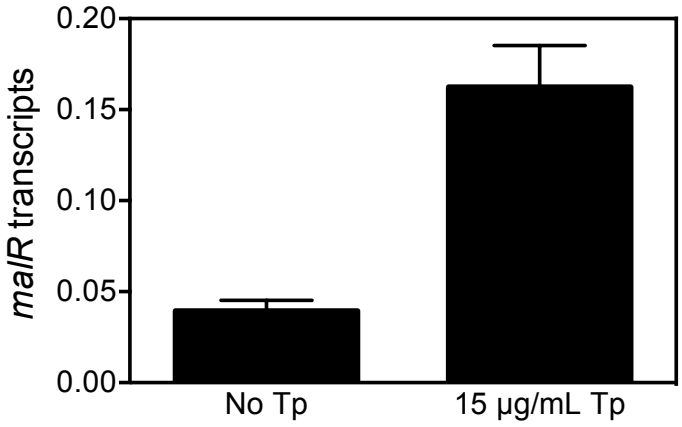

Figure S2.4. The effect of trimethoprim on *malR* expression. Droplet digital PCR was used to measure *malR* transcript abundance in wild-type *B. pseudomallei*. Logarithmic-phase cells were diluted to an OD_{600} of 0.05 and grown for 6 h without trimethoprim or with 15 µg/mL trimethoprim before collecting cells and isolating RNA. *malR* transcript abundance was normalized to the *gapA* RNA polymerase sigma factor gene transcripts. Values represent the mean and standard deviation of three independent experiments, and the difference is significant by *t*-test ($P = 0.0008$).

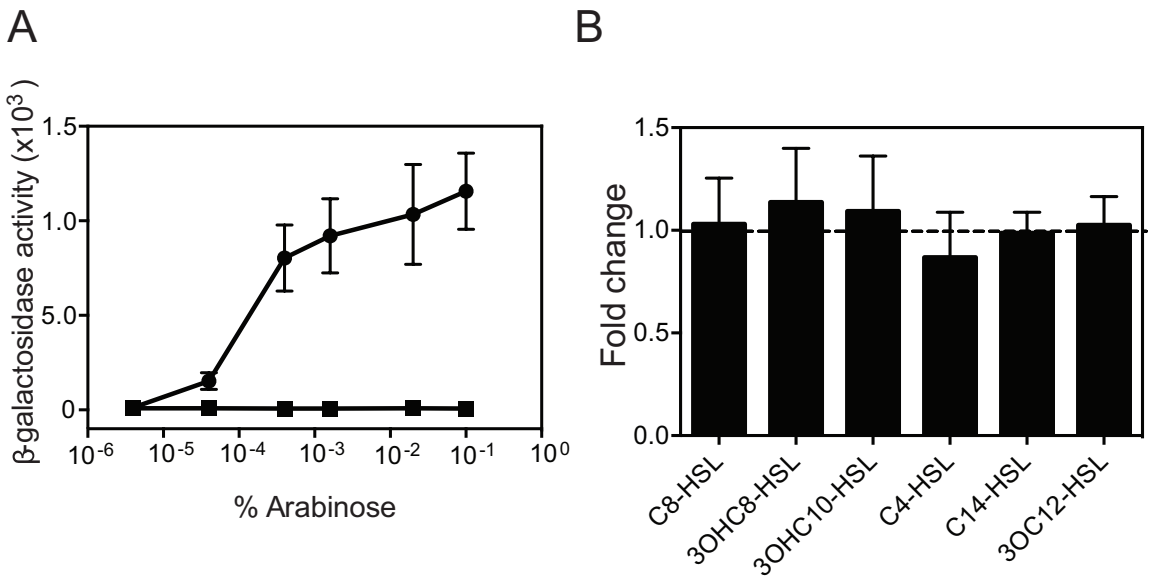

Figure S2.5. Activity of *B. pseudomallei* MalR in recombinant *E. coli.* (A) Activation of the *malA* promoter in *E. coli* BW27783 containing either an arabinose-inducible *malR* expression vector (pJN105 P_{BAD}-*malR*, circles) or vector control (pJN105, squares) and a *lacZ* reporter with the *B. pseudomallei malA* promoter (pQF50 P*malA-lacZ*) grown with the indicated arabinose concentrations. (B) *E. coli* BW27783 containing pJN105 P_{BAD}-*malR* and pQF50 P*malA-lacZ* grown with 0.1% arabinose and no AHLs or 5 μM C8-HSL, 3OHC8-HSL, 3OHC10-HSL (the *B. pseudomallei* AHLs), C4-HSL, C14-HSL, or 3-oxo-C12-HSL. Data shown are of the growth-adjusted fold change of AHL treatment condition compared with no AHLs. Results are the average fold changes and standard deviation of at least 7 independent experiments.

Table S2.1. Malleilactone antimicrobial activity.

Strain	MIC (μg per mL)[a]
Bacterial strain	
Bacillus subtilis 168	19 (6)
Staphylococcus aureus Newman	13
Enterococcus faecalis OG1RF	6
Escherichia coli JM109	>100
Pseudomonas aeruginosa PA14	>100
Burkholderia multivorans ATCC17616	>100
Burkholderia cenocepacia K56-2	>100
Burkholderia pseudomallei Bp82	>200
Burkholderia thailandensis E264	>200

[a]MICs of malleilactone were determined from two independent experiments with the range indicated in parentheses except when both experimental results were identical.

Table S2.2. Malleilactone NMR assignment table[a], in $CDCl_3$.

Atom number	δ – ^{1}H (ppm)	J	δ – ^{1}C (ppm)	Notes
1	1.06	t, 7.5 Hz	9.7	broad
2	2.41	br q, 7.9 Hz	29.4	
3	-	-	186.3	
4	-	-	136.0	
5	7.10	s	ND[b]	
6	-	-	99.6	
6a	-	-	170.6	
7	-	-	ND	
7-OH	ND	-	-	
8	-	-	ND	
8a	1.75	s	13.5	
9	5.91	br s	137	broad
10	2.11	q, 7.4 Hz	28.5	
11	1.39	m	29.2	
12[c]	1.29	m	32	
13[c]	1.29	m	29.7	
14[c]	1.29	m	29.7	
15[c]	1.29	m	22.8	
16	0.88	m	22.8	

[a]NMR assignments based on 1D ^{1}H NMR spectra from Fig. S2.

[b]ND, not determined.

[c]Interchangeable.

Table S2.3. Bacterial strains used in this study.

Strain	Relevant properties	Reference or source
Burkholderia pseudomallei		
Bp82	Δ*purM* mutant of strain 1026b; wild-type strain	(4)
BpΔ*malR*	Bp82 with a deletion of *malR*	This study
BpΔ*malF*	Bp82 with a deletion of *malF*	This study
BpΔ*scmR*	Bp82 with a deletion of *scmR*	This study
CM139	Bp82 with a deletion of *bspI1,* Δ*bpsI2,* Δ*bpsI3*	(17)
BpΔ*malR*Δ*scmR*	BpΔ*malR* with a deletion of *scmR*	This study
BpΔ*bspI1-3*Δ*malR*	CM139 with a deletion of *malR*	This study
Bp P*malA-lux*	Bp82 *glmS3 attn7::malA-lux* reporter; Zeo^R	This study
BpΔ*malR* P*malA-lux*	BpΔ*malR glmS3 attn7::malR-lux* reporter; Zeo^R	This study
Bp82 P*malA-lacZ*	Bp82 *glmS3 attn7::malA-lacZ* reporter; Zeo^R	This study
Bp82 P*lac-malR*	Bp82 *glmS3 attn7::*P*lac-malR*; Km^R	This study
Bp82 P*lac*	Bp82 *glmS3 attn7::*P*lac*; Km^R	This study
BpΔ*malR* P*lac-malR*	BpΔ*malR glmS3 attn7::*P*lac-malR*; Km^R	This study
BpΔ*malR* P*lac*	BpΔ*malR glmS3 attn7::*P*lac*; Km^R	This study
BpΔ*malR*Δ*scmR* P*lac*	BpΔ*malR*Δ*scmR glmS3 attn7::*P*lac*; Km^R	This study
BpΔ*scmR* P*lac*-scm*R*	BpΔ*scmR glmS3 attn7::*P*lac-scmR*; Km^R	This study
BpΔ*scmR* P*lac*	BpΔ*scmR glmS3 attn7::*P*lac*; Km^R	This study
Escherichia coli		
DH5α	F^- Φ80*lacZ* Δ*M15* Δ(*lacZYA-argF*) *U169 hsdR17*(r_K^- m_K^+) *recA1 endA1 phoA supE44 thi-1 gyrA96 relA1* λ^-	Invitrogen
DH10B	F^-*mcr*A Δ(*mrr-hsd*RMS-*mcr*BC) Φ80*lac*ZΔM15 Δ*lac*X74 *rec*A1 *end*A1 *ara*D139Δ(*ara*, *leu*)7697 *gal*U *gal*K λ^-*rps*L *nup*G	Invitrogen
OP50	*C. elegans* lab husbandry strain	(44)
JM109	(traD36, pro AB + lac Iq, lacZ M15) end A1 recA1 hsdR17(rk^-, mk^+) mcrA supE44 λ^- gyrA96 relA1 (lac^- proAB)	(45)
BW27783	Constitutive arabinose transporter expression strain; *Δ(araD-araB)567*, *ΔlacZ4787*(::rrnB-3), *λ*$^-$, *Δ(araH-araF)570(::FRT)*, *ΔaraEp-532::FRT*, *φ*P_{cp8}*araE535*, *rph-1*, *Δ(rhaD-rhaB)568*, *hsdR514*	(36),Yale GCSC
Burkholderia thailandensis E264	Wild-type strain	(46)
Bacillus subtilis 168	Wild-type strain	(47)
Enterococcus faecalis OG1RF	Wild-type strain	(48)
Burkholderia multivorans ATCC17616	Wild-type strain	ATCC
Burkholderia cenocepacia K56-2	Wild-type strain	(49)
Staphylococcus aureus Newman	Wild-type strain	(50)
Pseudomonas aeruginosa PA14	Wild-type strain	(51)

Table S2.4. Bacterial plasmids used in this study.

Plasmid	Relevant properties	Reference or source
pEX18km-*pheS*	Plasmid used to make unmarked, non-polar deletions in *B. pseudomallei;* Km^R	(52)
pEX18km-*pheS*-Δ*malR*	pEX18km-*pheS* plasmid used to make *malR* deletion; Km^R	This study
pEX18km-*pheS*-Δ*malF*	pEX18km-*pheS* plasmid used to make *malF* deletion; Km^R	This study
pEX18km-*pheS*-Δ*scmR*	pEX18km-*pheS* plasmid used to make *scmR* deletion; Km^R	This study
pTNS3	Tn7 transposase-expressing helper plasmid; Amp^R	(38)
pCM53	Mobilizable mini-Tn7 vector with a promoterless *luxCDABE*; Zeo^R, Ap^R	(39)
pUC18-mini-Tn7T-P*malA-lux*	pCM53 containing the *malA* promoter; Zeo^R, Amp^R	This study
pUC18-mini-Tn7T-P*malA-lacZ*	pUC18miniTn7T-P*malA-lux* containing the *lacZ* reporter in place of the *lux* reporter; Zeo^R, Amp^R	This study
pUC18-mini-Tn7T-Gm-*lacZ*	Mobilizable mini-Tn7 vector with a promoterless *lacZ*; Gm^R, Amp^R	(53)
pUC18-mini-Tn7T-Kan-GFP	Mobilizable mini-Tn7 vector with a promoterless *gfp*; Km^R, Amp^R	(40)
pUC18-mini-Tn7T-P*malA*-GFP	pUC18-mini-Tn7T-Kan-GFP containing the *malA* promoter; Km^R, Amp^R	This study
pUC18-mini-Tn7T-LAC-Tp	Mobilizable mini-Tn7 vector with the *lac* promoter (P*lac*) for IPTG-inducible gene expression; Tp^R, Ap^R	(20)
pUC18-mini-Tn7T-LAC-Km	pUC18miniTn7T-LAC-Tp with the kanamycin resistance gene; Km^R, Ap^R	This study
pUC18-mini-Tn7T-P*lac-malR*	pUC18miniTn7T-LAC-Km containing the *malR* gene; Km^R, Ap^R	This study
pUC18-mini-Tn7T-P*lac-scmR*	pUC18miniTn7T-LAC-Km containing the *scmR* gene; Km^R, Ap^R	This study
pQF50	Broad-host-range *lacZ* fusion vector; Ap^R	(54)
pQF50 P*malA-lacZ*	pQF50 containing the *malA* promoter; Ap^R	This study
pJN105	*araC*-P*araBAD* cloned into pBBR1MCS-5; Gm^R	(55)
pJN105 P_{BAD}-*malR*	pJN105 containing the *malR* gene; Gm^R	This study

Table S2.5. Primers used in this study.

Primer name	Sequence
Primers for cloning	
ScmR-HindIII-D1-F	TAATAAAAGCTTGATCGACATACGCGTCGGGTG
ScmR-D2-R	CTGGAGCCCGGTGACGGTCTGGATTTGGTTCATAGCTTTCGTTG
ScmR-D3-F	ATGAACCAAATCCAGACCGTCACCGGGCTCCAGTGA
ScmR-XbaI-D4-R	TAATAATCTAGAGCGTCGATCATGTGATGGGTCG
EcoRI-malR-F	ATTATTGAATTCATGTTCGAAGGCTTGTCCATTGGT
malR-XmaI-R	ATTATTCCCGGGTCAGATCAACCCGCGCG
Fwd_Compl_malR_SacI	ATTGGAGCTCATGTTCGAAGGCTTGTC
Rev_Compl_malR_HindIII	ATTGAAGCTTTCAGATCAACCCGCG
EcoRI-scmR-ORF-F	AATAATGAATTCATGAACCAAATCCAGACCATGCGTG
scmR-HindIII-ORF-R	AATAATAAGCTTTCACTGGAGCCCGGTGACG
BamHI-malAprom-F	ATTATTGGATCCAAACGAACCAATGGACAAGCCTTC
malAprom-PstI-R	ATTATTCTGCAGGAGAACCACTCCGAATGACCGG
5`PstISalI-GFP	TAATAACTGCAGGTCGACATGAGTAAAGGAGAAGAACTTTTCACTGGAG
3`GFP-SpeI	ACTAGTAGTCATTTATTTGTATAGTTCATCCATGCCATGTGTAATCCCAGC
5`SpeI-ZeoProm	TAATAAACTAGTTTGACAATTAATCATCGGCATAGTATATCGGC
3`outsideZeo gene	TGGCCTGCAAGGCCTTC
Primers for droplet digital PCR	
rpoD-2-F	GGCAAGCAGTTCGACGTCACG
rpoD-2-R	GTTCCCCTCGAGGAACGACTTC
malA-1-F	CACGTTTCGCCGCAACAC
malA-1-R	GGACGAAGGGTCGAGAAAATAGAAGTG
malR-2-F	CTGAACGCGACTTGCAAGAA
malR-2-R	GCCCAGTTGGCGAACGT
scmR-3-F	GGACCACTTCACGCATGTCGTC
scmR-3-R	GATGTAGCTCTCCGGCAGCAC

[a]Underlined sequences indicate added restriction enzyme sequences

REFERENCES

1. Limmathurotsakul D, Golding N, Dance DAB, Messina JP, Pigott DM, Moyes CL, Rolim DB, Bertherat E, Day NPJ, Peacock SJ, Hay SI. 2016. Predicted global distribution of *Burkholderia pseudomallei* and burden of melioidosis. Nature Microbiology 1.

2. Kim HS, Schell MA, Yu Y, Ulrich RL, Sarria SH, Nierman WC, DeShazer D. 2005. Bacterial genome adaptation to niches: divergence of the potential virulence genes in three *Burkholderia* species of different survival strategies. BMC Genomics 6:174.

3. Yu Y, Kim HS, Chua HH, Lin CH, Sim SH, Lin D, Derr A, Engels R, DeShazer D, Birren B, Nierman WC, Tan P. 2006. Genomic patterns of pathogen evolution revealed by comparison of *Burkholderia pseudomallei*, the causative agent of melioidosis, to avirulent *Burkholderia thailandensis*. BMC Microbiol 6:46.

4. Propst KL, Mima T, Choi KH, Dow SW, Schweizer HP. 2010. A *Burkholderia pseudomallei* Δ*purM* mutant is avirulent in immunocompetent and immunodeficient animals: candidate strain for exclusion from select-agent lists. Infect Immun 78:3136-43.

5. Norris MH, Propst KL, Kang Y, Dow SW, Schweizer HP, Hoang TT. 2011. The *Burkholderia pseudomallei* Δ*asd* mutant exhibits attenuated intracellular infectivity and imparts protection against acute inhalation melioidosis in mice. Infect Immun 79:4010-8.

6. Biggins JB, Kang HS, Ternei MA, DeShazer D, Brady SF. 2014. The chemical arsenal of *Burkholderia pseudomallei* is essential for pathogenicity. J Am Chem Soc 136:9484-90.

7. Cruz-Migoni A, Hautbergue GM, Artymiuk PJ, Baker PJ, Bokori-Brown M, Chang CT, Dickman MJ, Essex-Lopresti A, Harding SV, Mahadi NM, Marshall LE, Mobbs GW, Mohamed R, Nathan S, Ngugi SA, Ong C, Ooi WF, Partridge LJ, Phillips HL, Raih MF, Ruzheinikov S, Sarkar-Tyson M, Sedelnikova SE, Smither SJ, Tan P, Titball RW, Wilson SA, Rice DW. 2011. A *Burkholderia pseudomallei* toxin inhibits helicase activity of translation factor eIF4A. Science 334:821-4.

8. Biggins JB, Ternei MA, Brady SF. 2012. Malleilactone, a polyketide synthase-derived virulence factor encoded by the cryptic secondary metabolome of *Burkholderia pseudomallei* group pathogens. J Am Chem Soc 134:13192-5.

9. Seyedsayamdost MR, Chandler JR, Blodgett JA, Lima PS, Duerkop BA, Oinuma K, Greenberg EP, Clardy J. 2010. Quorum-sensing-regulated bactobolin production by *Burkholderia thailandensis* E264. Org Lett 12:716-9.

10. Biggins JB, Gleber CD, Brady SF. 2011. Acyldepsipeptide HDAC inhibitor production induced in *Burkholderia thailandensis*. Org Lett 13:1536-9.

11. Wong RR, Kong C, Lee SH, Nathan S. 2016. Detection of *Burkholderia pseudomallei* toxin-mediated inhibition of protein synthesis using a *Caenorhabditis elegans ugt-29* biosensor. Sci Rep 6:27475.

12. Alice AF, Lopez CS, Lowe CA, Ledesma MA, Crosa JH. 2006. Genetic and transcriptional analysis of the siderophore malleobactin biosynthesis and transport genes in the human pathogen *Burkholderia pseudomallei* K96243. J Bacteriol 188:1551-66.

13. Biggins JB, Liu X, Feng Z, Brady SF. 2011. Metabolites from the induced expression of cryptic single operons found in the genome of *Burkholderia pseudomallei*. J Am Chem Soc 133:1638-41.

14. Franke J, Ishida K, Hertweck C. 2012. Genomics-driven discovery of burkholderic acid, a noncanonical, cryptic polyketide from human pathogenic *Burkholderia* species. Angew Chem Int Ed Engl 51:11611-5.

15. Seyedsayamdost MR. 2014. High-throughput platform for the discovery of elicitors of silent bacterial gene clusters. Proc Natl Acad Sci U S A 111:7266-71.

16. Majerczyk C, Brittnacher M, Jacobs M, Armour CD, Radey M, Schneider E, Phattarasokul S, Bunt R, Greenberg EP. 2014. Global analysis of the *Burkholderia thailandensis* quorum sensing-controlled regulon. J Bacteriol 196:1412-24.

17. Majerczyk CD, Brittnacher MJ, Jacobs MA, Armour CD, Radey MC, Bunt R, Hayden HS, Bydalek R, Greenberg EP. 2014. Cross-species comparison of the *Burkholderia pseudomallei*, *Burkholderia thailandensis*, and *Burkholderia mallei* quorum-sensing regulons. J Bacteriol 196:3862-71.

18. Fuqua C. 2006. The QscR quorum-sensing regulon of *Pseudomonas aeruginosa*: an orphan claims its identity. J Bacteriol 188:3169-71.

19. Patel HK, Suarez-Moreno ZR, Degrassi G, Subramoni S, Gonzalez JF, Venturi V. 2013. Bacterial LuxR solos have evolved to respond to different molecules including signals from plants. Front Plant Sci 4:447.

20. Truong TT, Seyedsayamdost M, Greenberg EP, Chandler JR. 2015. A *Burkholderia thailandensis* Acyl-Homoserine Lactone-Independent Orphan LuxR Homolog That Activates Production of the Cytotoxin Malleilactone. J Bacteriol 197:3456-62.

21. Poulter S, Carlton TM, Spring DR, Salmond GP. 2011. The *Serratia* LuxR family regulator CarR 39006 activates transcription independently of cognate quorum sensing signals. Mol Microbiol 80:1120-31.

22. Kohanski MA, Dwyer DJ, Hayete B, Lawrence CA, Collins JJ. 2007. A common mechanism of cellular death induced by bactericidal antibiotics. Cell 130:797-810.

23. Ooi SK, Lim TY, Lee SH, Nathan S. 2012. *Burkholderia pseudomallei* kills *Caenorhabditis elegans* through virulence mechanisms distinct from intestinal lumen colonization. Virulence 3:485-96.

24. Gan YH, Chua KL, Chua HH, Liu B, Hii CS, Chong HL, Tan P. 2002. Characterization of *Burkholderia pseudomallei* infection and identification of novel virulence factors using a *Caenorhabditis elegans* host system. Mol Microbiol 44:1185-97.

25. Lee SH, Ooi SK, Mahadi NM, Tan MW, Nathan S. 2011. Complete killing of *Caenorhabditis elegans* by *Burkholderia pseudomallei* is dependent on prolonged direct association with the viable pathogen. PLoS One 6:e16707.

26. O'Quinn AL, Wiegand EM, Jeddeloh JA. 2001. *Burkholderia pseudomallei* kills the nematode *Caenorhabditis elegans* using an endotoxin-mediated paralysis. Cell Microbiol 3:381-93.

27. Gamage AM, Shui G, Wenk MR, Chua KL. 2011. N-Octanoylhomoserine lactone signalling mediated by the BpsI-BpsR quorum sensing system plays a major role in biofilm formation of *Burkholderia pseudomallei*. Microbiology 157:1176-86.

28. Lumjiaktase P, Diggle SP, Loprasert S, Tungpradabkul S, Daykin M, Camara M, Williams P, Kunakorn M. 2006. Quorum sensing regulates dpsA and the oxidative stress response in *Burkholderia pseudomallei*. Microbiology 152:3651-9.

29. Kiratisin P, Sanmee S. 2008. Roles and interactions of *Burkholderia pseudomallei* BpsIR quorum-sensing system determinants. J Bacteriol 190:7291-7.

30. Le Guillouzer S, Groleau MC, Deziel E. 2017. The Complex Quorum Sensing Circuitry of *Burkholderia thailandensis* Is Both Hierarchically and Homeostatically Organized. mBio 8.

31. Mao D, Bushin LB, Moon K, Wu Y, Seyedsayamdost MR. 2017. Discovery of *scmR* as a global regulator of secondary metabolism and virulence in *Burkholderia thailandensis* E264. Proc Natl Acad Sci U S A doi:10.1073/pnas.1619529114.

32. Moule MG, Spink N, Willcocks S, Lim J, Guerra-Assuncao JA, Cia F, Champion OL, Senior NJ, Atkins HS, Clark T, Bancroft GJ, Cuccui J, Wren BW. 2015. Characterization of New Virulence Factors Involved in the Intracellular Growth and Survival of *Burkholderia pseudomallei*. Infect Immun 84:701-10.

33. Gutierrez MG, Yoder-Himes DR, Warawa JM. 2015. Comprehensive identification of virulence factors required for respiratory melioidosis using Tn-seq mutagenesis. Front Cell Infect Microbiol 5:78.

34. Tuanyok A, Kim HS, Nierman WC, Yu Y, Dunbar J, Moore RA, Baker P, Tom M, Ling JM, Woods DE. 2005. Genome-wide expression analysis of iron regulation in *Burkholderia pseudomallei* and *Burkholderia mallei* using DNA microarrays. FEMS Microbiol Lett 252:327-35.

35. Kvitko BH, Goodyear A, Propst KL, Dow SW, Schweizer HP. 2012. *Burkholderia pseudomallei* known siderophores and hemin uptake are dispensable for lethal murine melioidosis. PLoS Negl Trop Dis 6:e1715.

36. Khlebnikov A, Keasling JD. 2002. Effect of *lacY* expression on homogeneity of induction from the P(tac) and P(trc) promoters by natural and synthetic inducers. Biotechnol Prog 18:672-4.

37. Chandler JR, Duerkop BA, Hinz A, West TE, Herman JP, Churchill ME, Skerrett SJ, Greenberg EP. 2009. Mutational analysis of *Burkholderia thailandensis* quorum sensing and self-aggregation. J Bacteriol 191:5901-9.

38. Choi KH, Mima T, Casart Y, Rholl D, Kumar A, Beacham IR, Schweizer HP. 2008. Genetic tools for select-agent-compliant manipulation of *Burkholderia pseudomallei*. Appl Environ Microbiol 74:1064-75.

39. Majerczyk C, Kinman L, Han T, Bunt R, Greenberg EP. 2013. Virulence of *Burkholderia mallei* quorum-sensing mutants. Infect Immun 81:1471-8.

40. Norris MH, Kang Y, Wilcox B, Hoang TT. 2010. Stable, site-specific fluorescent tagging constructs optimized for *Burkholderia* species. Appl Environ Microbiol 76:7635-40.

41. Choi KH, DeShazer D, Schweizer HP. 2006. mini-Tn7 insertion in bacteria with multiple glmS-linked attTn7 sites: example *Burkholderia mallei* ATCC 23344. Nat Protoc 1:162-9.

42. Lee MM, Gao Z, Peterson BR. 2017. Synthesis of a Fluorescent Analogue of Paclitaxel That Selectively Binds Microtubules and Sensitively Detects Efflux by P-Glycoprotein. Angew Chem Int Ed Engl 56:6927-6931.

43. Chugani S, Greenberg EP. 2010. LuxR homolog-independent gene regulation by acyl-homoserine lactones in *Pseudomonas aeruginosa*. Proc Natl Acad Sci U S A 107:10673-8.

44. Brenner S. 1974. The genetics of Caenorhabditis elegans. Genetics 77:71-94.

45. Yanisch-Perron C, Vieira J, Messing J. 1985. Improved M13 phage cloning vectors and host strains: nucleotide sequences of the M13mp18 and pUC19 vectors. Gene 33:103-19.

46. Brett PJ, DeShazer D, Woods DE. 1998. *Burkholderia thailandensis* sp. nov., a *Burkholderia pseudomallei*-like species. Int J Syst Bacteriol 48 Pt 1:317-20.

47. Burkholder PR, Giles NH, Jr. 1947. Induced biochemical mutations in Bacillus subtilis. Am J Bot 34:345-8.

48. Dunny GM, Brown BL, Clewell DB. 1978. Induced cell aggregation and mating in *Streptococcus faecalis*: evidence for a bacterial sex pheromone. Proc Natl Acad Sci U S A 75:3479-83.

49. Mahenthiralingam E, Coenye T, Chung JW, Speert DP, Govan JR, Taylor P, Vandamme P. 2000. Diagnostically and experimentally useful panel of strains from the *Burkholderia cepacia* complex. J Clin Microbiol 38:910-3.

50. Duthie ES, Lorenz LL. 1952. *Staphylococcal* coagulase; mode of action and antigenicity. J Gen Microbiol 6:95-107.

51. Rahme LG, Stevens EJ, Wolfort SF, Shao J, Tompkins RG, Ausubel FM. 1995. Common virulence factors for bacterial pathogenicity in plants and animals. Science 268:1899-902.

52. Barrett AR, Kang Y, Inamasu KS, Son MS, Vukovich JM, Hoang TT. 2008. Genetic tools for allelic replacement in *Burkholderia* species. Appl Environ Microbiol 74:4498-508.

53. Choi KH, Schweizer HP. 2006. mini-Tn7 insertion in bacteria with single attTn7 sites: example *Pseudomonas aeruginosa*. Nat Protoc 1:153-61.

54. Farinha MA, Kropinski AM. 1990. Construction of broad-host-range plasmid vectors for easy visible selection and analysis of promoters. J Bacteriol 172:3496-9.

55. Newman JR, Fuqua C. 1999. Broad-host-range expression vectors that carry the L-arabinose-inducible Escherichia coli araBAD promoter and the *araC* regulator. Gene 227:197-203.

Chapter 3: *Burkholderia thailandensis* methylated hydroxy-alkylquinolines: biosynthesis and antimicrobial activity in co-cultures

This chapter is written as per:

Jennifer R. Klaus*, Charlotte Majerczyk*, Stephanie Moon, Natalie A. Eppler, Sierra Smith, Emily Tuma, Patrick Ball, Marie-Christine Groleau, Kyle L. Asfahl, Nicole E. Smalley, Hillary Hayden, Marianne Piochon, Ajai A. Dandekar, Charles Gauthier, Eric Déziel, and Josephine R. Chandler. *Burkholderia thailandensis* methylated hydroxy-alkylquinolines: biosynthesis and antimicrobial activity in co-cultures 2020. BioRxiv doi:10.1101/2020.05.27.120295 (*submitted to Applied and Environmental Microbiology*, *equal contributions by JRK and CM)

COLLABORATIONS AND WORKLOAD ALLOCATIONS:

Charlotte Majerczyk, Stephanie Moon, Sierra Smith, Emily Tuma, and Patrick Ball performed the transposon mutagenesis, and the preliminary mutant screening, identification, and characterization. Kyle L. Asfahl, Nicole E. Smalley, Hillary Hayden, and Ajai A. Dandekar performed and analyzed whole-genome sequencing. Jennifer R. Klaus, Natalie E. Eppler, and Josephine R. Chandler performed the liquid and outgrowth diffusion assay co-cultures, the *B. thailandensis* and *E. coli* genetic manipulations, the sample preparation for chemical analysis, and the minimum inhibitory concentration assays. Marie-Christine Groleau, Marianne Piochon, Charles Gauthier, and Eric Déziel performed the *B. ambifaria* genetics, chemical analyses, and synthetic chemistry. Jennifer R. Klaus, Charlotte Majerczyk, and Josephine R. Chandler wrote the manuscript.

ABSTRACT

The bacterium *Burkholderia thailandensis* produces an arsenal of secondary metabolites that have diverse structures and roles in the ecology of this soil-dwelling bacterium. In liquid co-culture experiments, *B. thailandensis* secretes an antimicrobial that nearly eliminates another soil bacterium, *Bacillus subtilis*. To identify the antimicrobial, we used a transposon mutagenesis approach. This screen identified antimicrobial-defective mutants with insertions in the *hmqA, hmqC,* and *hmqF* genes involved in biosynthesis of a family of 2-alkyl-4(1*H*)-quinolones called 4-hydroxy-3-methyl-2-alkenylquinolines (HMAQs), which are closely related to the *Pseudomonas aeruginosa* 4-hydroxy-2-alkylquinolines (HAQs). Insertions also occurred in the previously uncharacterized gene BTH_II1576 ("*hmqL*"). Results confirm that BTH_II1576 is involved in generating *N*-oxide derivatives of HMAQs (HMAQ-NO) in *B. thailandensis* and that HMAQ-NOs are sufficient to eliminate *B. subtilis* in co-cultures. Moreover, synthetic HMAQ-NO is ~50-fold more active than HMAQ. Both the methyl group and the length of the carbon side chain account for high activity of HMAQ-NO against *B. subtilis.* The results provide new information on the biosynthesis and activities of HMAQs and reveal new insight into how these molecules might be important for the ecology of *B. thailandensis.*

IMPORTANCE

The soil bacterium *Burkholderia thailandensis* produces 2-alkyl-4(1*H*)-quinolones, mostly methylated 4-hydroxy-alkenylquinolines, a family of relatively unstudied metabolites similar to molecules also synthesized by *Pseudomonas aeruginosa.* Several of the methylated 4-hydroxy-alkenylquinolines have antimicrobial activity against other species. We show that *N*-oxidated methyl-alkenylquinolines are particularly antimicrobial and sufficient to kill *Bacillus subtilis* in co-cultures. We confirmed their biosynthesis requires the previously unstudied protein HmqL. These results provide new information about the biology of 2-alkyl-4(1*H*)-quinolones, particularly the methylated 4-hydroxy-alkenylquinolines, which are unique to *B. thailandensis.* This study also has importance for understanding *B. thailandensis* secondary metabolites and has implications for potential therapeutic development.

INTRODUCTION

The saprophytic β-Proteobacteria *Burkholderia thailandensis* is closely related to two pathogens, *B. pseudomallei* and *B. mallei,* which are the causative agents of melioidosis and glanders, respectively (3, 4). *B. pseudomallei* is also a saprophyte and causes respiratory or skin infections in humans following exposure to organisms in the environment, such as through skin contact with soil (5). *B. mallei* is a host-adapted pathogen and is spread to humans from horses and other ungulates, in which it is endemic in some regions (6). Because *B. pseudomallei* and *B. mallei* are Tier 1 Select Agents and require handling in BSL-3-level laboratory conditions, *B. thailandensis* is often used as a surrogate to study biology and virulence mechanisms of these pathogens (7). The development of versatile genetic techniques (8-11) and improvements in mouse models of melioidosis (12) have greatly improved the ability to study the biology of this relatively understudied group.

There has been much interest in elucidating the arsenal of small molecules produced by *B. thailandensis,* where there are at least 13 polyketide synthesis (PKS) gene clusters, with many of them conserved in *B. mallei* and/or *B. pseudomallei*. Although many of these metabolites have now been identified, only a few have been studied in much detail. One of the best studied is bactobolin (2, 13), which blocks translation by binding to a unique site in the 50S ribosomal subunit (14). Another PKS antibiotic is malleilactone (15, 16), and malleicyprol, a more toxic product of the malleilactone biosynthetic gene cluster (17), which contribute to virulence of *B. pseudomallei* (18). *B. thailandensis* also produces thailandenes, a group of polyenes with activity against Gram-positive bacteria (19). As with many bacterial natural products, malleilactone and thailandenes are not produced under standard laboratory conditions (15, 16, 19). Studies of these molecules were possible through genetic (15, 16) or chemical (20) elicitation of the gene clusters or through phenotype-based screening approaches (19).

Most of the PKS gene clusters are unique to this group of *Burkholderia.* A few of them have analogous biosynthesis pathways in other *Burkholderia* species or even beyond the *Burkholderia*. For example, the *hmqABCDEFG* operon coding for enzymes responsible for the biosynthesis of a family of 2-

alkyl-4(1*H*)-quinolones named 4-hydroxy-3-methyl-2-alkenylquinolines (HMAQs) are found in *B. thailandensis, B. pseudomallei* and other members of the *Burkholderia* genus such as *Burkholderia ambifaria* (21). The products made by the HmqABCDEFG enzymes have varying carbon chain lengths and saturation, and presence of substitutions on the quinolone ring such as methylation and oxidation. The relative abundance of these various congeners differs between species (1). The *hmq* operon is homologous to the *pqs* operon found in *P. aeruginosa* (1, 22). The molecules produced by *Burkholderia* also differ from that of *P. aeruginosa* in that most bear a methyl group at the 3' position and possess an unsaturated aliphatic side chain, which are linked to the presence of the additional *hmqG* and *hmqF* genes, respectively (1). The main product of the *P. aeruginosa pqs* operon, 4-hydroxy-2-heptylquinoline (HHQ), is converted to 3,4-dihydroxy-2-heptylquinoline (*Pseudomonas* Quinolone Signal; PQS) by the enzyme PqsH (23, 24). Both are involved in quorum sensing in *P. aeruginosa* and are detected by the MvfR regulator (25-27). No homologs of the *pqsH* and *mvfR* genes have been found in *Burkholderia* (1).

We are interested in the small molecule repertoire of *B. thailandensis* as an avenue to better understand its biology and make new discoveries on natural product biosynthesis. We observed that *B. thailandensis* culture fluid has significant antimicrobial activity that is not due to bactobolin, the only other known antimicrobial produced in these conditions. This bactobolin-independent activity was isolated to the *hmq* gene cluster using an approach involving transposon mutagenesis and screening for mutants exhibiting reduced antimicrobial activity. Purified and synthetic hydroxy-alkylquinoline derivatives were assessed for their antimicrobial properties of several biosynthetic products of the *hmq* genes, including HMAQ congeners and *N*-oxide derivatives (HMAQ-NO) with various alkenyl side chain lengths. We also confirmed the involvement of *hmqL* in the biosynthesis of HMAQ-NO compounds. Our results provide new information on the biosynthesis and activities of the methylated hydroxy-alkenylquinolines produced by *Burkholderia.*

MATERIALS & METHODS

Bacterial culture conditions and reagents

Bacteria were grown in Lysogeny broth (LB) (10 g tryptone, 5 g yeast extract, and 5 g NaCl per liter) supplemented with 50 mM morpholinepropanesulfonic acid (MOPS) where indicated, in M9 minimal medium supplemented with 0.4% D-glucose and 10 mM *para*-chloro-phenylalanine (*p*-Cl-Phe; Sigma) for *B. thailandensis* counterselection during mutant construction, or using DM media (0.25X M63 salts, 1 mM $MgSO_4$, 0.4% glycerol, 0.2% glucose, 1 μg/mL thiamine, and 40 μg/mL each of leucine, isoleucine, valine, tryptophan, glutamic acid, and glutamine) for transformation of PCR-generated products. For liquid co-cultures, *B. subtilis* and *B. thailandensis* growth was at 37°C. For all other experiments *B. thailandensis* growth was at 30 °C, and all *E. coli* and *B. ambifaria* growth was at 37°C. 4-Hydroxy-2-heptylquinoline (HHQ) was purchased from Sigma (cat. SML0747). 4-Hydroxy-2-heptylquinoline *N*-oxide (HQNO) was purchased from Cayman Chemicals (cat. 15159). 4-Hydroxy-3-methyl-2-nonenylquinoline (HMNQ) was purified from *B. thailandensis* E264 cultures as described previously (1). The other hydroxy-alkenylquinolines were synthesized as described below. For selection, trimethoprim was used at 100 μg/mL, gentamicin was used at 100 μg/mL, kanamycin was used at 500 μg/mL (*B. thailandensis*) or 50 μg/mL (*E. coli*), tetracycline was used at 225 μg/mL (*B. ambifaria*), and NaCl was used at 5% (for inhibiting *B. thailandensis* in co-culture enumerations). Isopropyl β-D-1-thiogalactopyranoside (IPTG) was added at 1 mM final concentration to cultures and plates, when appropriate. Genomic DNA, PCR and DNA fragments, and plasmid DNA were purified using a Puregene Core A kit, plasmid purification miniprep kit, or PCR cleanup/gel extraction kits (Qiagen or IBI-MidSci) according to the manufacturer's protocol.

Synthesis of *N*-oxides of hydroxy-alkenylquinolines

HMAQ-NOs were synthesized as previously described (28) from corresponding HMAQs in which the quinolone scaffold was built *via* the Conrad-Limpach approach (29). Briefly, aniline was condensed

with diethyl 2-methyl-3-oxosuccinate and the resulting diester was cyclized under acidic conditions. Reduction of the quinolone ester followed by halogen substitution led to 2-chloromethyl-3-methylquinolin-4(1*H*)-ones, which were subjected to Suzuki-Miyaura cross-coupling (30) with commercially available alkenylboronic acid pinacol esters to provide HMAQs. Then, they were converted into corresponding ethyl carbonates, oxidized with *m*CPBA, and deprotected to yield HMAQNOs (31). The structure of HMAQ-NOs were confirmed by HRMS as well as 1D and 2D NMR analysis.

Genetic manipulations

All bacterial strains, plasmids, and primers used in this study are listed in **Tables S3.1-S3.2**. We used wild type and mutant derivatives of *B. thailandensis* strain E264 (7). We used *B. ambifaria* strain HSJ1 (1), and *E. coli* strain DH5α for genetic manipulations (Invitrogen). The *B. thailandensis* bactobolin-defective mutant BD20 has a deletion of the bactobolin biosynthesis gene *btaK* as described previously (2). The *B. thailandensis hmqA* mutant was constructed using allelic exchange using methods described previously (8) and plasmid pMCG19. pMCG19 was constructed by first amplifying *hmqA* from the *B. thailandensis* E264 genome using primers hmqAfor and hmqArev containing HindIII and KpnI cleavage sites, respectively. The PCR product was digested with HindIII and KpnI and ligated to HindIII-KpnI-cut pEX18Tp-PheS (11). The chloramphenicol resistance cassette was amplified from pACYC184 (32) using primers CmFPstI and CmRPstI each containing the PstI cleavage site and ligated to the PstI site inside the *hmqA* gene in pEX18Tp-PheS-*hmqA* to make pMCG19.

B. thailandensis BTH_II1576 (*hmqL*) mutants were made by transforming a PCR-amplified BTH_II1576::*dhfr* allele from transposon mutant #56 into the genome of strain BD20 using PCR transformation using a modified protocol similar to Thongdee *et al.* (33). Briefly, shaking *B. thailandensis* cultures were grown at 37˚C to an optical density at 600 nm (OD_{600}) of 0.5, concentrated 20-fold, and distributed to five aliquots of 50 µL. Each aliquot was mixed with 5 µL of gel-extracted *hmqL::dhfR* PCR product (amplified using hmqL-Tn-for2 and hmqL-Tn-rev2 primers). The cell-DNA mixture was spotted onto solid DM media (DM liquid media with 1.5% agar) and incubated at 37 ˚C for

48 h. The DM plate growth was scraped up and collected, washed twice with DM, suspended in 200 μL DM, and spread onto LB agar containing trimethoprim. Mutant strains were verified by PCR-amplifying the mutated region and sequencing the PCR product.

For ectopic expression of *hmqL* in *B. thailandensis,* this gene was placed under control of the IPTG-inducible *lac* promoter in pUC18miniTn7T-LAC-Km (34). To construct this plasmid, we amplified *hmqL* from the *B. thailandensis* E264 genome using primers hmqL-ORF-F-SacI and hmqL-ORF-R-HindIII that incorporated the SacI and HindIII restriction enzyme sites, respectively, into the product. The amplicon was cut with SacI and HindIII and ligated to SacI- and HindIII-digested pUC18miniTn7T-Kan-P*lac-malR* (34) to make pUC18miniTn7T-P*lac-hmqL* (entirely removing the *malR* gene). This plasmid was used to transform competent *B. thailandensis* with the helper plasmid pTNS2 as described previously (35). We used PCR to verify insertion of the P*lac-hmqL* cassette into the *attn7* site near *glmS1*.

We used plasmid pME6010 (36) for expressing the *hmqL* gene from *B. thailandensis* in *B. ambifaria.* The *hmqL* (BTH_II1576) gene was amplified from the *B. thailandensis* E264 genome using primers hmqL-F and hmqL-R that incorporated the BglII and KpnI sites into the amplicon. The product was cut with BglII and KpnI and ligated to BglII- and KpnI-digested pME6010 to make pMCG17. *B. ambifaria* strains with pME6010 plasmids were constructed by electroporation as previously described for *B. thailandensis* (8).

Liquid co-cultures

Logarithmic-phase overnight starter cultures (OD_{600} between 0.5 and 1.5) of *B. subtilis* and *B. thailandensis* were diluted to an OD_{600} of 0.05 and combined at a starting ratio of 1:1 in a 10 mL volume of LB in 125 mL baffled flasks. The flasks were incubated with shaking at 250 rpm at 37˚C for 24 h before serially diluting and plating on LB agar plates containing gentamicin (to inhibit *B. subtilis*) or 5% NaCl (to inhibit *B. thailandensis*) and IPTG as appropriate to enumerate bacterial colony forming units (CFU).

Antimicrobial activity assays

Antimicrobial activities of *B. thailandensis* culture fluid were assayed using disc diffusion (for filtered fluid) or outgrowth diffusion (for unclarified fluid) methods. For both methods, inocula for each of the *B. thailandensis* strains and *B. subtilis* were prepared by suspending a colony from an LB agar plate into LB broth and growing overnight at 30˚C with shaking. *B. subtilis* overnight culture (100 µL) diluted 1:100 was spread onto an LB agar plate and allowed to dry. A filter disc was placed on the *B. subtilis* lawn and saturated with *B. thailandensis* cultures that were either centrifuged and filter sterilized through a 0.2 µm membrane (for disc diffusion) or spotted directly onto the *B. subtilis* lawns (for outgrowth diffusion). The plates were incubated at 30˚C for 24 h before observing zones of clearing of the *B. subtilis* lawns. The outgrowth assays were also conducted similarly on LB agar plates containing 5% NaCl, which inhibits growth of the *B. thailandensis* strains.

The antimicrobial activities of purified, commercial, or synthesized hydroxy-alkylquinoline compounds were assessed using a minimum inhibitory concentration (MIC) assay according to a modified protocol from the 2018 guidelines of the Clinical and Laboratory Standards Institute (CLSI). Inocula for each test organism were prepared by suspending a colony from an LB agar plate into Tryptic Soy Broth (TSB) and growing for 3-5 h at 37°C with shaking, then adjusting the culture turbidity in TSB to an OD_{600} of 0.25, roughly the equivalent of a 1.0 McFarland Standard (3×10^8 CFU per mL). These cell suspensions were used as inocula for microtiter MIC assays. A 2.5 µL inoculum, which corresponded to $1x10^6$ cells, was added to a 100 µL well containing diluted in cation-adjusted Mueller-Hinton II broth, and these were incubated with shaking for 24 h at 37°C. The MIC was defined as the lowest concentration of compound (µg/mL) in which bacterial growth in the well was not visible.

Transposon mutagenesis and screen

Transposon mutagenesis was performed using the EZ-Tn5™ <DHFR-1>Tnp Transposome™ Kit (Epicentre), according to manufacturer's specifications. Briefly, electrocompetent cells of the *B. thailandensis* bactobolin-defective mutant BD20 were generated by growing cultures to mid-exponential

phase (OD_{600} = 0.5-0.7), collecting with centrifugation, washing the cell pellet three times in ice-cold 0.5 M sucrose (using 25% the volume of the original culture), and then resuspending the cell pellet in 100 μL ice-cold 0.5 M sucrose. Immediately, 1 μL transposome was added to 50 μL electrocompetent cells in a 0.2 mm electroporation cuvette. This was electroporated with the Bio-Rad Gene Pulser II (settings 25 μF, 200 Ω, 2.5 kV), and the cells were immediately recovered in 1 mL LB broth with shaking at 37°C for 1 h. At the end of the recovery, the culture was diluted 1:25, and 100 μL samples were plated on 20 LB plates with trimethoprim selection (100 μg/mL). The plates were incubated overnight at 37°C. The following day, single colonies were patched onto plates prepared with *B. subtilis* to screen for antimicrobial activity. Due to the scale required for the screen, we added *B. subtilis* directly to molten agar used to pour plates, as opposed to spreading *B. subtilis* lawns after pouring. To prepare the *B. subtilis*-agar media, we added 1.43 mL of a stationary phase *B. subtilis* culture (overnight growth) to 1 L of cooled but molten LB agar media (55-60°C), mixed gently and poured. After a brief period to solidify and dry, plates were used to patch colonies isolated from the EZ-Tn5™ <DHFR-1> transposon mutagenesis. Patched plates were incubated overnight at 30°C prior to identifying mutants defective for antimicrobial activity, as determined by reduced zones of *B. subtilis* growth inhibition compared with the *B. thailandensis* parent. Identified candidates were streaked for single *B. thailandensis* colonies on LB with gentamicin to prevent *B. subtilis* growth, and re-tested in our assay to confirm the phenotype. Confirmed mutants with no apparent growth defects were subjected to whole genome sequencing.

Identification of transposon insertion sites

The transposon insertion locations of five transposon mutants (#7, 14, 31, 32, and 56) were determined by whole-genome re-sequencing. DNA isolated from the transposon mutant strains was used to make sequencing libraries with 300-bp inserts. The libraries were sequenced on an Illumina MiSeq System using the NEBNext Ultra II kit, generating approximately one million 200-bp paired-end reads per sample. The paired-end reads were assembled *de novo* into draft genomes using the SPAdes

assembler with standard settings (37). For each *de novo* assembly, the contig with Tn5 transposon sequence was located using a nucleotide search in the BLAST+ command line suite with individual blast databases for each transposon mutant (38). Clustal Omega was then used to precisely locate the sequence context of Tn5 insertion in each contig of interest (39). Genomic context for individual transposon insertions was then determined by blasting up- and down-stream sequences against a database of all *B. thailandensis* E264 gene sequences to identify specific loci interrupted by Tn5 insertion. Finally, the raw reads were aligned to the *B. thailandensis* E264 ATCC700388 reference genome (NC_007650, NC_007651 downloaded from burkholderia.com) using Strand NGS (Bangalore, India) software v 3.1.1 to confirm the insertion locus in each mutant. The remaining four transposon mutants (#9, 27 63, and 68) were assessed by PCR amplifying regions of the *hmq* locus (primers given in **Table S3.2**). Mutations identified by either method were verified by Sanger sequencing of PCR-amplified products. (**Table 3.1**).

Table 3.1. Location of transposon insertions

			Transposon insertion information	Location
Mutant	Locus	Gene	Predicted function	(bp in gene)
14	BTH_II1935	*hmqA*	2-aminobenzoate-CoA ligase	1231
27	BTH_II1935	*hmqA*	2-aminobenzoate-CoA ligase	1513
31	BTH_II1935	*hmqA*	2-aminobenzoate-CoA ligase	1478
68	BTH_II1933	*hmqC*	Unknown	783
7	BTH_II1930	*hmqF*	Polyketide synthase	163
9	BTH_II1930	*hmqF*	Polyketide synthase	2524
63	BTH_II1930	*hmqF*	Polyketide synthase	2872
32	BTH_II1576	*"hmqL"*	Putative monooxygenase	226
56	BTH_II1576	*"hmqL"*	Putative monooxygenase	998

HMAQ and HMAQ-NO measurements from bacterial cultures

To measure the production of HMAQ and HMAQ-NO in *B. thailandensis* cultures, samples were prepared by diluting stationary-phase *B. thailandensis* cultures to an OD_{600} of 0.05 into 5 mL of LB in 18 mm culture tubes and growing the cultures for 18 h with shaking at 250 rpm at 30˚C or as otherwise described. Where necessary, 1 mM IPTG was added to the LB at the beginning of the growth experiment. At 18 h, sample preparation and liquid chromatography-tandem mass spectrometry (LC-MS/MS)

analyses were performed as described by Lépine *et al.* (40), with minor modifications. Briefly, for each sample, 300 µL of grown culture was mixed with 300 µL of HPLC-grade methanol containing 4 ppm of 5,6,7,8-tetradeutero-4-hydroxy-2-heptylquinoline (HHQ-d_4) as an internal standard, vortexed and centrifuged for 5 min at maximum speed in a microfuge. The supernatant/methanol solution was carefully recovered for analysis. Samples were analyzed by high-performance liquid chromatograph (HPLC; Waters 2795, Mississauga, ON, Canada) equipped with a C8 reverse-phase column (Eclipse XDB-C8, Agilent Technologies, Mississauga, ON, Canada), and the detector was a tandem quadrupole mass spectrometer (Quattro Premier XE, Waters). Analyses were carried out in the positive electrospray ionization (ESI+) mode.

RESULTS

Antimicrobial activity of *B. thailandensis* bactobolin-null mutants

Initial liquid co-culture experiments with *B. thailandensis* and *B. subtilis* showed that *B. thailandensis* has a strong growth advantage over *B. subtilis*. The growth advantage was so substantial that after overnight liquid co-culture with *B. thailandensis*, *B. subtilis* decreased from a density of 10^6 cells per mL to below the limit of detection ($<10^2$ cells per mL). This result was not attributed to bactobolin, as a bactobolin-null mutant (BD20) also had the same growth advantage over *B. subtilis* (**Fig. 3.1-A**). This observation led to the hypothesis that *B. thailandensis* has a previously uncharacterized antimicrobial activity against *B. subtilis* that is not mediated by bactobolin. To further explore this hypothesis, culture fluids of several *B. thailandensis* strains were harvested and tested for antimicrobial activity **(Fig. 3.1-B)**. As previously observed (2), filter-sterilized culture fluids of wild-type *B. thailandensis* saturated to a paper filter disc placed on a lawn of *B. subtilis* caused a zone of growth inhibition around the filter disc, whereas there was no growth inhibition observed with the bactobolin-null BD20 strain **(Fig. 3.1-B,** top panel**)**. However, unprocessed culture fluid of both strains (wild-type and BD20), which had not gone through the filter sterilization process, demonstrated antimicrobial activity **(Fig. 3.1-B,** middle and bottom panels). This observation (i.e. that only unprocessed culture fluid had bactobolin-independent antimicrobial activity) could be explained by several possible hypotheses: first, that the filter sterilization process removes or inactivates antimicrobial activity; and second, that antimicrobial activity requires live cells. In support of the first hypothesis, the antimicrobial activity was observed in the absence of viable *B. thailandensis* bactobolin mutant cells; unprocessed *B. thailandensis* BD20 culture fluids had activity against *B. subtilis* when added directly to high-salt LB agar plates, which are conditions that do not allow for *B. thailandensis* growth (**Fig. 3.1-B, bottom panel**). Ethyl acetate extracts of *B. thailandensis* cultures also had activity against *B. subtilis* (**Fig. S3.1**). Together, these results suggest that *B. thailandensis* produces an antimicrobial other than bactobolin, which is eliminated by filter sterilization.

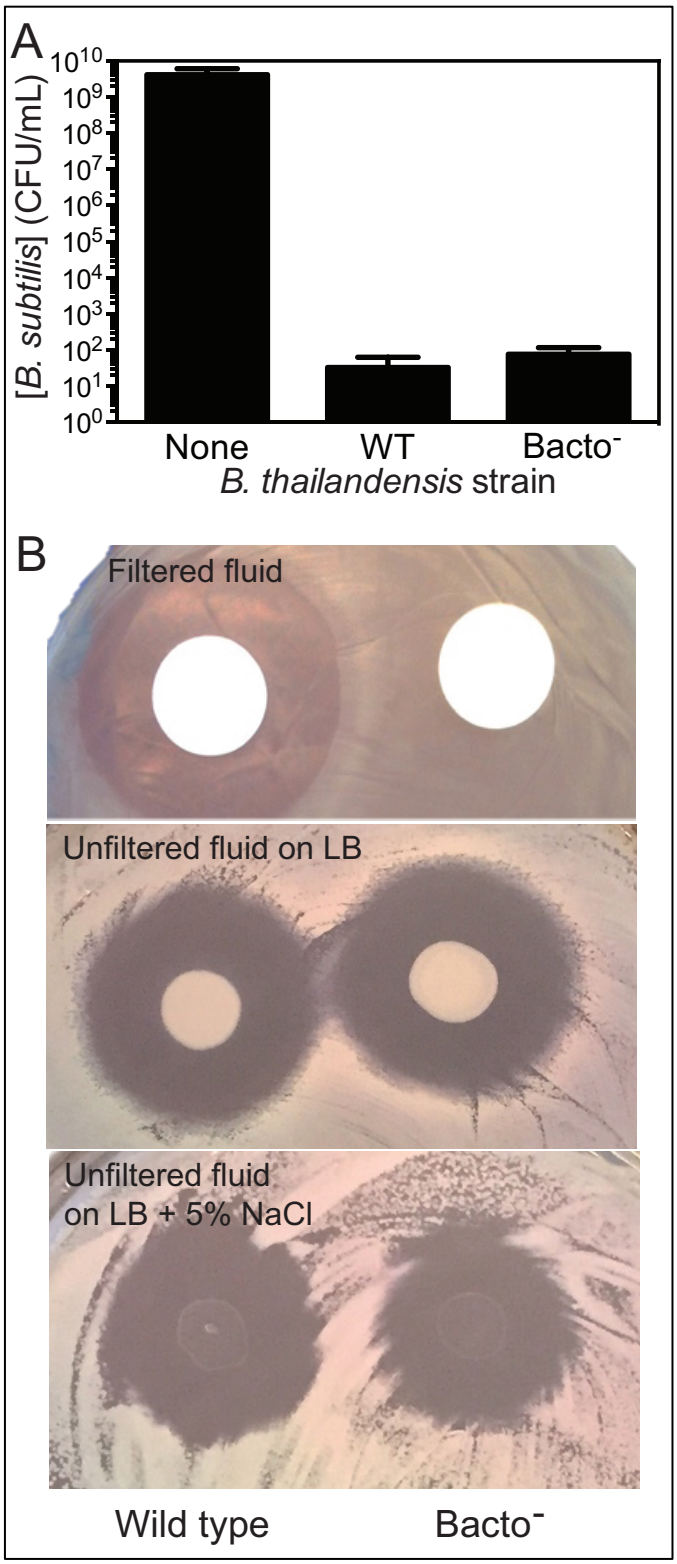

Figure 3.1. Sensitivity of *Bacillus subtilis* to a substance produced by *Burkholderia thailandensis.* **(**A) For liquid co-culture growth, *B. subtilis* was combined in a 1:1 ratio with either *Burkholderia thailandensis* E264 (WT) or bactobolin-deficient *Burkholderia thailandensis* (Bacto$^-$, strain BD20) in LB broth and grown for 24 h at 37 ˚C prior to plating to determine surviving colony forming units as described in Materials and Methods. Data are representative of three biological replicates. (B) On plates, *B. subtilis* growth inhibition following treatment with cultures or culture fluid from *B. thailandensis* after 18 h of growth. *B. thailandensis* wild type (E264) or the bactobolin-defective mutant (Bacto$^-$, strain BD20) were applied to a lawn of freshly plated *B. subtilis* and plates were incubated at 30ºC prior to imaging. **Top panel:** *B. thailandensis* culture fluid was filtered and used to saturate paper diffusion discs applied to the *B. subtilis* lawn. A zone of clearing around a diffusion disc indicates the region where *B. subtilis* growth was inhibited. Results are similar to those previously reported (2). **Middle panel:** Unfiltered *B. thailandensis* fluid (10 µL) was spotted directly onto *B. subtilis.* **Bottom panel:** Unfiltered *B. thailandensis* fluid as in the middle panel was spotted onto a lawn of *B. subtilis* on media containing 5% NaCl, which inhibits *B. thailandensis* growth.

Identification and isolation of antimicrobial-deficient transposon mutants

To identify the genes required for the observed antimicrobial activity, we used a mutagenesis and screening approach. First, we randomly mutagenized the *B. thailandensis* bactobolin-null mutant BD20 with a transposon containing the trimethoprim resistance gene *dhfR* (Tn5::*dhfR*). Next, we screened the mutants (~10,000) using a high-throughput method to assess antimicrobial activity (for experiment overview, see **Fig. S3.2**). Briefly, we added *B. subtilis* cells to cooled molten agar and mixed gently before pouring into plates. After the media solidified, single isolated colonies (i.e., *B. thailandensis* transposon mutants) were patched onto the plates. The next day, plates were assessed for zones of inhibition. *B. thailandensis* patches demonstrating reduced zones of inhibition compared with the *B. thailandensis* bactobolin-defective parent were re-isolated for further study. We initially identified 60 antimicrobial-defective candidates. Of those, 9 were confirmed to have reduced antimicrobial activity

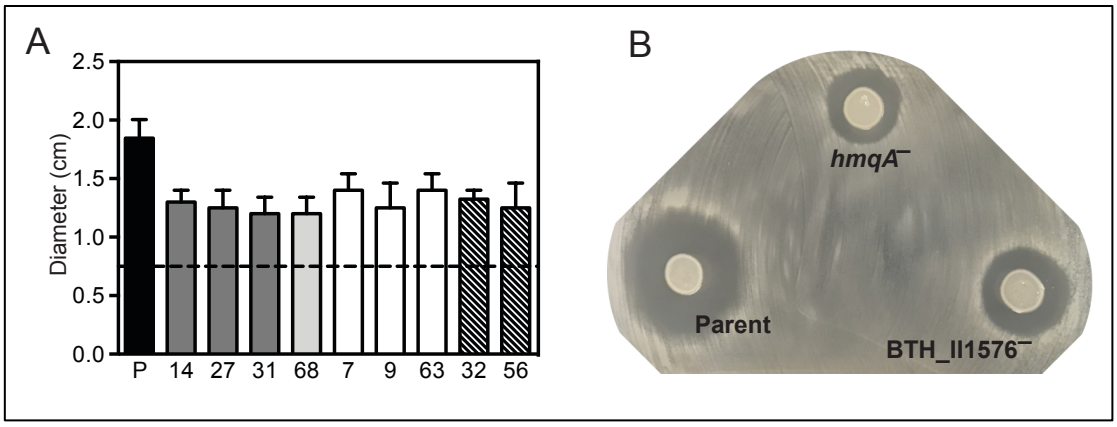

Figure 3.2. *B. thailandensis* transposon mutants with reduced *Bacillus subtilis* killing. (A) Unfiltered fluid (5 µL) from *B. thailandensis* stationary-phase cultures was spotted onto a lawn of freshly plated *B. subtilis* and incubated overnight at 30˚C. Results are shown as the diameter of the zones of inhibition. The black dashed line indicates the diameter of the spot of *B. thailandensis* culture. Transposon mutant numbers correspond with mutant locations in **Table 3.1** and are shaded by gene. Dark grey, *hmqA* disruption; light grey, *hmqC* disruption; white, *hmqF* disruption; hatched, BTH_II1576 disruption. P (parent), the *B. thailandensis* bactobolin-deficient mutant BD20 used for transposon mutagenesis. Data are the average of two biological replicates. B) Images of *B. subtilis* lawns spotted with 5 µL unfiltered fluid from cultures of the *B. thailandensis* bactobolin-deficient strain BD20 or BD20 with disruptions in *hmqA* or BTH_II1576 introduced by homologous recombination.

against *B. subtilis* (**Fig. 3.2A**) with no observable growth defects (**Table S3.3**). These were mutants 7, 9, 14, 27, 31, 32, 56, 63, and 68.

To identify the location of the transposon mutations, we performed whole-genome sequencing using an Illumina platform, followed by PCR amplification and Sanger sequencing to verify mutations in both the Illumina-sequenced isolates and the un-sequenced isolates. Of the nine mutants identified in our screen, seven had insertions in the *hmqABCDEFG* operon (BTH_II1929 - 1935, **Table 3.1).** The other two mutants had disruptions in a previously unstudied gene, BTH_II1576, which is predicted to encode a monooxygenase. To verify that the *hmq* locus and BTH_II1576 contribute to the antimicrobial defects observed for the transposon mutants, we disrupted *hmqA* or BTH_II1576 in the bactobolin-defective BD20 strain using homologous recombination. Both gene disruptions caused a similar defect in *B. subtilis* growth inhibition as observed with the transposon mutants (**Fig. 3.2-B**), supporting that the *hmq* genes and BTH_II1576 are important for the bactobolin-independent antimicrobial activity of *B. thailandensis*.

Identification and activities of *hmq* gene products

Both the *pqs* and *hmq* gene products use anthranilic acid and fatty acid precursors to generate H(M)AQs through the pathway illustrated in **Fig. 3.3**. The result of biosynthesis includes molecules with unsaturated or saturated side chains and *N*-oxide derivatives. The most abundant HMAQ in *B. thailandensis* E264 cultures is a congener with an unsaturated C_9 side chain, 4-hydroxy-3-methyl-2-nonenylquinoline referred to as HMNQ or HMAQ-C_9:2'(1). To test whether production of HMAQ-C_9:2' is absent in our transposon mutants, we measured this HMAQ in culture fluid using a LC-MS/MS method to find a product with the expected *m/z* of 284. Consistent with previous results (1, 41), transposon mutants with insertions in *hmqA* and *hmqF* had no HMAQ-C_9:2' (<0.05 μg/mL, the limit of detection). We also detected no HMAQ-C_9:2' in *hmqC* mutants, consistent with the proposed role of HmqC in HMAQ biosynthesis (**Fig. 3.3**). The BD20 parent strain and BTH_II1576 transposon mutants both readily produced this HMAQ congener (measured at 5-8 μg/mL).

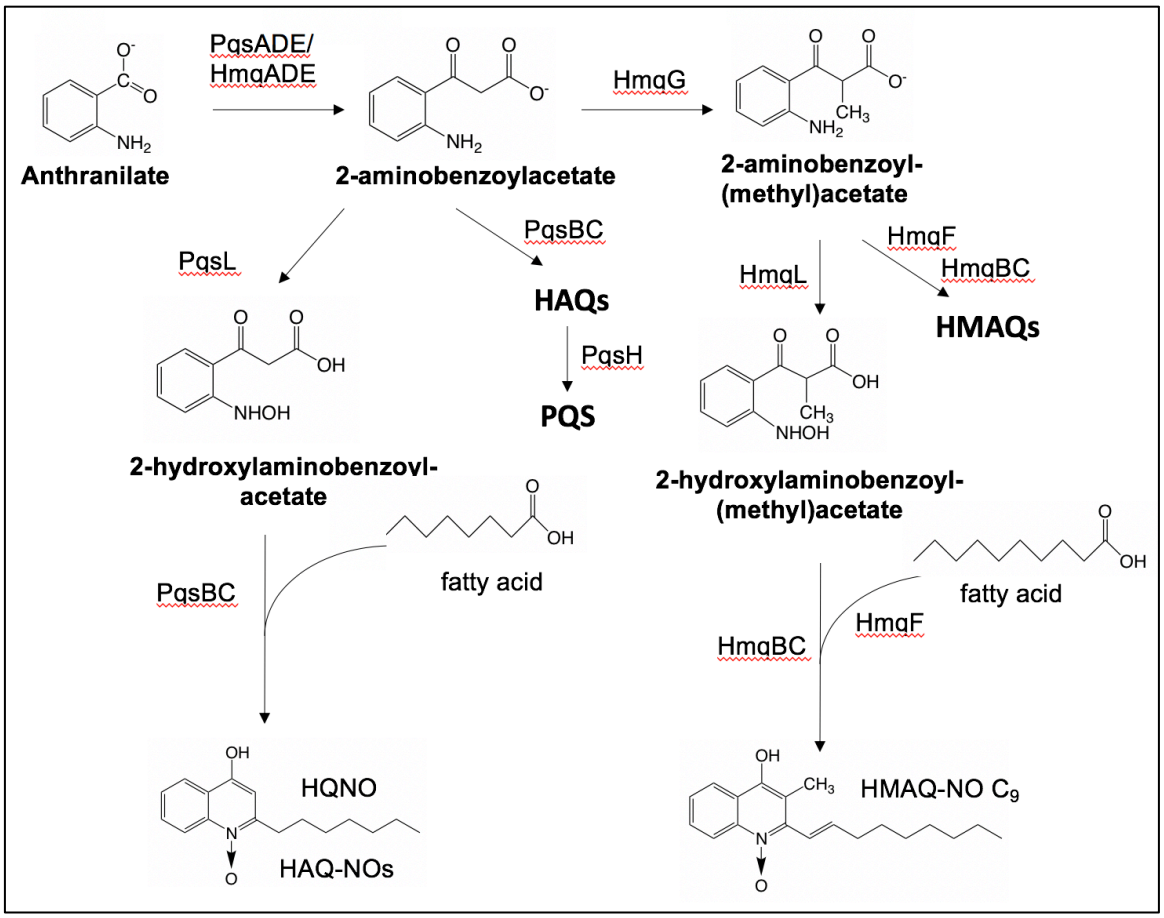

Figure 3.3. Biosynthesis of hydroxy-alkylquinolones. *Burkholderia thailandensis* uses the *hmq* gene products to synthesize hydroxy-alkylquinolones, including HMAQ and HMAQ-NO. In *Pseudomonas aeruginosa,* the analogous *pqs* gene products synthesize the related compounds HAQ, HAQ-NO, and PQS. Shown are the *N*-oxidated species referred to in the text, HQNO and HMAQ-NO-C_9 with a double bond at the 1'-2' position added by HmqF. The *B. thailandensis* compounds are methylated by HmqG, which does not have a homolog in *P. aeruginosa.* PqsH is needed for production of PQS, which is specific to *P. aeruginosa*.

We tested the activity of HMAQ-C_9:2' directly against *B. subtilis* using a standard minimum inhibitory concentration (MIC) assay. The MIC of purified HMAQ-C_9:2' against *B. subtilis* was 50 µg/mL (**Table 3.2).** HMAQ-C_9:2' also inhibited *Staphylococcus aureus* growth (MIC 25 µg/mL). We did not detect any antimicrobial activity of HMAQ-C_9:2' against *Escherichia coli* or *Pseudomonas aeruginosa* (MIC >200 µg/mL). Of note, the concentration of HMAQ-C_9:2' in *B. thailandensis* cultures (5-8 µg/mL) is ~5-fold lower than needed to inhibit *B. subtilis* growth (50 µg/mL), suggesting that HMAQ-C_9:2' alone is not sufficient for killing *B. subtilis* in our co-culture experiments. Instead, we hypothesized that the killing activity involves another product of the *hmq* genes.

Table 3.2. Antimicrobial activities of quinolone analogs.

			Minimum Inhibitory Concentration[b, c]	
Quinolone family[a]	Carbon chain	$[M+H]^+$	*B. subtilis*	*S. aureus*
HMAQ	C_9	284	50	25
HMAQ-NO	C_9	300	0.75	25
HAQ (HHQ)	C_7	242	>200	>200
HAQ-NO (HQNO)	C_7	259	25	25
HMAQ-NO	C_8	286	1.5	6.25
HMAQ-NO	C_7	272	6.25	12.5

[a]All quinolones had unsaturated carbon chains of the length indicated. HMAQ with a C_9 carbon chain (HMAQ-C9:2') was purified as described in (1). HMAQ-NO congeners were synthesized as described in Materials and Methods and Piochon et al. (28). HAQ-NO with a C_7 carbon chain (HQNO) and HAQ with a C_7 carbon chain (HHQ) were commercially purchased (Cayman Chemicals and Sigma Aldrich, respectively).
[b]Results are the averages of three independent experiments. In all cases the range was <5%.
[c]No activity of any of the compounds was observed up to 200 μg/mL against *Pseudomonas aeruginosa* strain PA14 and *Escherichia coli* strain JM109

Biosynthesis and antimicrobial activity of HMAQ-NO

The protein product of BTH_II1576 shares 52% amino acid sequence identity to that of the *P. aeruginosa* PqsL protein involved in HAQ biosynthesis. PqsL synthesizes 2-hydroxylaminobenzoyl-acetate (2-HABA) from 2-aminobenzoylacetate (2-ABA) as a step in the pathway to make *N*-oxide derivatives (HAQ-NO) (42, 43) (**Fig. 3.3**, left column). We hypothesized that BTH_II1576 is similarly involved in biosynthesis of *N*-oxide HMAQ (HMAQ-NO) in *B. thailandensis* (**Fig. 3.3**, right column). To test this hypothesis, we used LC-MS/MS to measure HMAQ-NO in the BTH_II1576 transposon mutants. We measured HMAQ-NO with an unsaturated C_9 or C_7 side chain, which are two abundant congeners in *B. thailandensis* E264. Both of the BTH_II1576 mutants and our constructed BD20 BTH_II1576 mutant had undetectable HMAQ-NO-C_9 (<0.05 μg/mL), whereas the BD20 parent had detectable levels (1.5 ± 0.5 μg/mL). We also ectopically expressed BTH_II1576 from an IPTG-inducible *lac* promoter from the neutral *glmS1* site in the engineered BTH_II1576 mutant genome, and we compared HMAQ-NO-C_9 and antimicrobial activities in this strain with an empty *lac* promoter-containing mutant or BD20 parent (**Fig. 3.4**). IPTG induction of BTH_II1576 in the mutant restored production of HMAQ-NO (**Fig. 3.4-A**) and increased the zone of inhibition of *B. subtilis* in colony outgrowth experiments (**Fig. 3.4-B**), supporting that BTH_II1576 is important for each of these processes. Further, BTH_II1576 induction significantly decreased HMAQs, supporting that the product of BTH_II1576 uses HMAQ as the substrate to generate

HMAQ-NO. Together, our results confirm that the BTH_II1576 product is analogous to PqsL in HAQ-NO biosynthesis and is appropriately named *hmqL*, as previously proposed (22).

Because HmqL generates HMAQ-NO and is important for antimicrobial activity observed in *B. thailandensis* cultures, we tested the hypothesis that HMAQ-NO has antimicrobial activity against *B. subtilis* (**Table 3.2**). We assessed the sensitivity of *B. subtilis* to the most abundant HMAQ-NO produced by *B. thailandensis* (1), synthetic HMAQ-NO-C_9:2' (28). The MIC of HMAQ-NO-C_9:2' was 0.75 μg/mL against *B. subtilis*. This MIC is below the measured concentration of HMAQ-NO-C_9:2' in *B. thailandensis* cell cultures (1.5 ± 0.5 μg/mL), supporting the idea that HMAQ-NOs are primarily responsible for the observed antimicrobial activity against *B. subtilis* in co-cultures with *B. thailandensis*. Interestingly, there was no difference in activity between the C_9 congeners of HMAQ-NO and HMAQ against *S. aureus* (MIC 25 μg/mL). Differences in diffusion or target site availability could explain the differences in relative activities of these two molecules in each species.

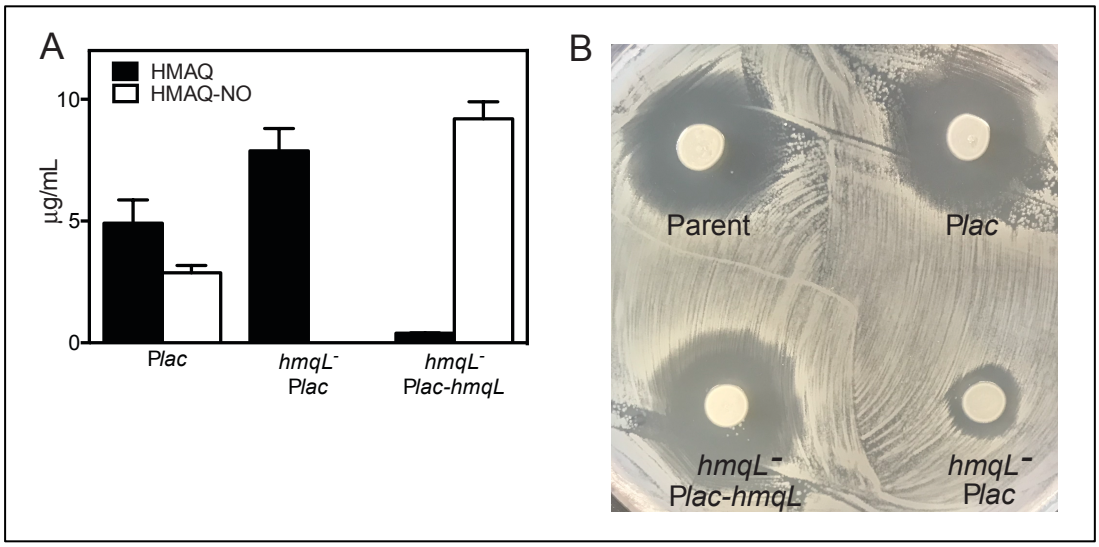

Figure 3.4. BTH_II1576 (*hmqL*) involvement in HMAQ-NO production and *B. subtilis* killing. (A) HMAQ-NO (C_9) was quantified in stationary-phase *B. thailandensis* strains using LC-MS/MS and methods described previously (1). (B) Antimicrobial activity of unfiltered *B. thailandensis* fluid (5 μL) on a lawn of freshly plated *B. subtilis* on plates containing 1 mM IPTG. Strains tested were the *B. thailandensis* bactobolin-deficient BD20 with the IPTG-inducible P*lac* expression cassette inserted into the neutral *glmS1* site in the genome (BD20 P*lac*), the constructed BD20 BTH_II1576 (*hmqL*) mutant with the P*lac* cassette in *glmS1* (*hmqL*$^-$ P*lac*), or the BD20 *hmqL* mutant with P*lac-hmqL* in *glmS1* (*hmqL*$^-$ P*lac-hmqL*).

Antimicrobial activities of structurally related hydroxy-alkylquinolines

We found it intriguing that the C_7 HAQ (HHQ) and its *N*-oxide derivative HAQ-NO-C_7 (HQNO) were much less active against *B. subtilis* than the respective C_9 HMAQ and HMAQ-NO molecules (**Table 3.2**). The difference in activity could be due to the difference in alkyl chain lengths or saturation level. Alternatively, the presence of the methyl group in HMAQs could also affect the activity. To address the first possibility, we tested synthetic HMAQ-NO congeners with a C_7 and C_8 unsaturated alkyl side chain against *B. subtilis*. Our results showed that the C_8 and C_7 HMAQ-NO molecules were 2- and 8-fold more active, respectively, against *B. subtilis* than the C_9 congener (**Table 3.2**). These results suggest that the longer carbon chain length has higher activity of HMAQ-NO against *B. subtilis*. The C_7 HMAQ-NO was also more active than HQNO (HAQ-NO-C_7) by about 2-fold against *S. aureus* and 4-fold against *B. subtilis* (**Table 3.2**). HQNO differs from C_7 HMAQ-NO in that it is unmethylated and has a saturated side chain. Thus, either methylation or saturation of the side chain also play a role in activity.

HMAQ-NO promotes competition in liquid co-cultures

Results of our transposon mutant analysis suggest that *hmqL* and HMAQ-NO-C_9 are important for the initial observation that *B. thailandensis* eliminates *B. subtilis* from liquid co-cultures. To test this hypothesis, we competed *B. subtilis* with a *B. thailandensis* bactobolin-deficient BD20 strain containing either a single *hmqA* or *hmqL* mutation or a *hmqA-hmqL* mutation in liquid co-culture experiments. Singly disrupting *hmqA* or *hmqL* nearly abolished the ability of *B. thailandensis* to kill *B. subtilis* (**Fig. 3.5-A**). Further, a strain disrupted for both *hmqL* and *hmqA* showed killing defects similar to that of either single mutant, supporting that *hmqL* and *hmqA* are in the same biosynthetic pathway. The results also support that the HMAQ-NO molecules, or HMAQ-NO together with other products of this pathway, are key for killing in liquid co-cultures.

Our initial observations suggested that the antimicrobial in *B. thailandensis* cultures was sensitive to filtration; thus, we also sought to test the sensitivities of HMAQ and HMAQ-NO to filtration. We measured concentrations of each of these molecules in unfiltered and filtered fluid from cell-free *B. thailandensis* cultures. We also determined the concentrations of these molecules in pelleted cells to determine if they are primarily associated with the cell, similar to HAQs in *P. aeruginosa* (26, 44). We found that the percent of HMAQs and HMAQ-NOs in the cell fraction was 91 ± 2 and 71 ± 3, respectively. Thus, these molecules are highly cell-associated. Furthermore, filtration further depletes molecules remaining in culture fluid to nearly undetectable levels (**Fig. 3.5-B**). These results are consistent with the idea that HMAQs and HMAQ-NOs are removed by separation of the cells and filtration of the remaining fluid, providing an explanation as to how the activity of these molecules have been missed in prior experiments.

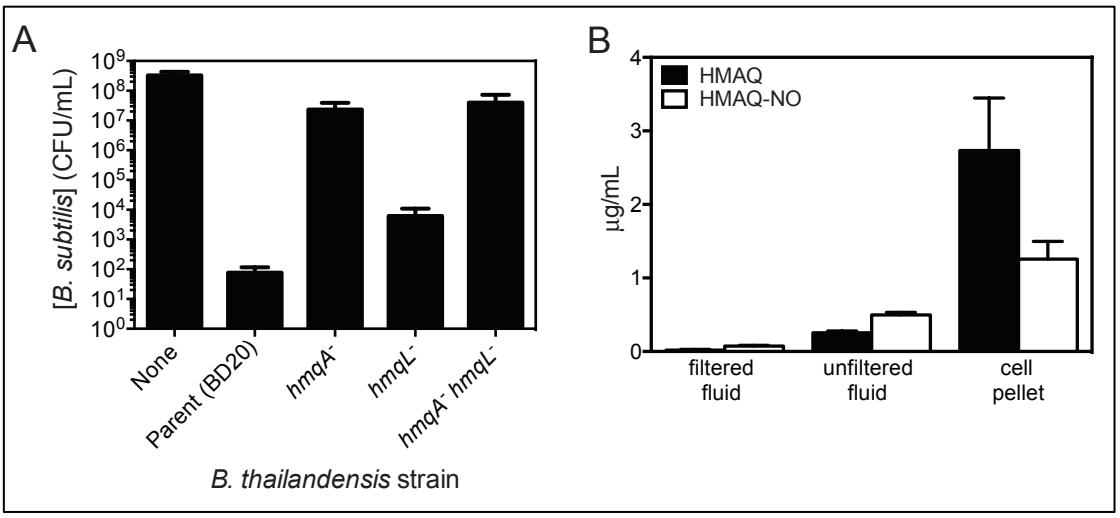

Figure 3.5. Involvement of BTH_II1576 (*hmqL*) in *B. subtilis* killing in liquid co-cultures and its cell pellet fraction localization. (A) Results of co-cultures of *B subtilis* combined in a 1:1 ratio with bactobolin-deficient *B. thailandensis* (Bacto$^-$) parent strain or the parent strain bearing a constructed deletion in *hmqA, hmqL,* or both in LB broth and grown for 24 h at 37˚C. Surviving colony forming units (CFU) were enumerated by serial dilution and plating on LB agar containing, for *B. subtilis,* 5% NaCl (non-permissive for *B. thailandensis* growth) and for *B. thailandensis,* 100 µg/mL gentamicin (non-permissive for *B. subtilis*). Data are representative of three biological replicates. (B) C_9 congeners of HMAQ and HMAQ-NO were quantified in unfiltered and filtered fluid from cell-free *B. thailandensis* cultures as well as in pelleted cells using LC-MS/MS and methods described previously (1).

HMAQ biosynthesis in *B. ambifaria*

The *Burkholderia ambifaria* genome encodes an *hmq* operon homologous to that of *Burkholderia thailandensis* (1). However, *B. ambifaria* does not produce HMAQ-NOs (1), presumably because it does not have a homolog of *hmqL/pqsL*. We predicted that introducing the *B. thailandensis hmqL* to *B. ambifaria* would enable production of HMAQ-NO. To test this prediction, we introduced the *hmqL* gene to *B. ambifaria* on plasmid pME6010 (36). Because HMAQ biosynthesis is less well characterized in this species, we used combined measurements of all three C_7, C_8, and C_9 congeners of HMAQs for our analysis. We observed that *B. ambifaria* (pME6010) had no detectable HMAQ-NO, as previously reported (1). However, *B. ambifaria* with pME6010-*hmqL* produced measurable levels of HMAQ-NO (**Fig. 3.6-A**), which is consistent with the idea that HmqL is the only missing enzyme and permits the production of HMAQ-NO production in *B. ambifaria.* This strain also had 100-fold less HMAQ than the empty plasmid-only strain (**Fig. 3.6-A**), suggesting strong competition for the HMAQ precursor, likely 2-aminobenzoyl(methyl)acetate (43) (the product of HmqADEG) (**Fig 3.3**). We also tested whether the expression of HmqL caused *B. ambifaria* to inhibit *B. subtilis* growth. We spotted unfiltered culture fluid from *B. ambifaria* with pME6010 or pME6010-*hmqL* onto a lawn of *B. subtilis.* Only cultures of the

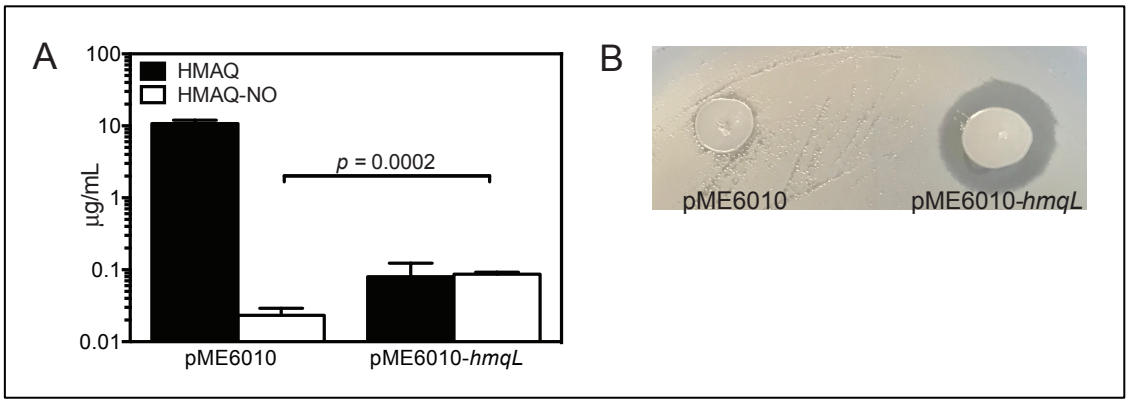

Figure 3.6. Heterologous expression of *hmqL* in *Burkholderia ambifaria*. (A) HMAQ and HMAQ-NO in cultures of *B. ambifaria* HSJ1 cells containing either pME6010 or pME6010-*hmqL.* Results are the average of three biological replicates and represent the sum of the C_7, C_8, and C_9 congeners of each molecule. (B) Antimicrobial activity of unfiltered fluid (5 µL) from cultures of *Burkholderia ambifaria* HSJ1 containing pME6010 or pME6010-*hmqL* spotted onto a freshly spread lawn of *B. subtilis* on plates containing 1 mM IPTG. Plates were imaged after 24 h of incubation at 37˚C.

strain expressing *hmqL* could inhibit *B. subtilis* growth (**Fig. 3.6B**). Together, the results provide further support that HmqL is crucial for production of the HMAQ-NO antimicrobials.

DISCUSSION

The antimicrobial properties of HAQs date back to 1945, when an "antibiotic metabolite" was described in *P. aeruginosa* (45). Although the biosynthesis steps and biology of the HAQs in *P. aeruginosa* have since been studied in detail, much less is known of those in *B. thailandensis* (1, 28, 46). Results of this study add new information to the known steps of biosynthesis of *B. thailandensis* HMAQs. Previous studies showed that enzymes analogous to PqsA-D in *P. aeruginosa* are involved in the synthesis of *B. thailandensis* HMAQ from anthranilate (**Fig. 3.3**, right side). In *P. aeruginosa,* the enzyme PqsL catalyzes an essential step in the synthesis of HAQ *N*-oxides (42, 43). *B. thailandensis* has no PqsH enzyme homolog and does not make 3-hydroxylated HAQs; a methyl is instead present as a substitution at that position. *B. thailandensis* is also missing a homolog of the HHQ/PQS receptor gene, *mvfR.* Our study validates the involvement on HmqL in *N*-oxide HMAQs biosynthesis and shows how the HMAQ family of molecules contribute to the arsenal of compounds used by *B. thailandensis* to compete with other species. The findings also provide new insight into the activities of specific *B. thailandensis* HMAQ family congeners against other bacteria.

Like many toxins, H(M)AQs have several known functions. In *P. aeruginosa,* where these molecules are best studied, the *N*-oxide congeners are potent antimicrobials that inhibit Gram-positive bacteria (24, 47, 48), and several of the HAQs are important for interspecies competition (49-51). Other *B. thailandensis* antimicrobials include bactobolin (13), malleilactone (15, 16), and thailandenes (19). This suite of diverse antimicrobials might be important for surviving competition with other microbes when space or other resources become limited. The loss of the *hmq* biosynthesis genes from the genome of the closely related host-adapted pathogen *B. mallei* supports a role of these genes in the saprophytic lifestyle of *B. thailandensis.* The current study demonstrates the *N*-oxide HMAQs are important for killing other species in several laboratory co-culture conditions, similar to *P. aeruginosa* HQNO. HQNO also has other known effects such as enhancing biofilm formation (52, 53) or increasing resistance to antimicrobials (54, 55) and it remains to be seen if HMAQ-NO is similar in these other ways.

A particularly interesting discovery in this work was that *B. thailandensis* HMAQ-NO-C_9:2' is much more active (33-fold) than *P. aeruginosa* HQNO (HAQ-NO-C_7) against *B. subtilis* (**Table 3.2**). Thus, the *B. thailandensis* HMAQ-NO has a particularly lethal structure compared with the related *P. aeruginosa* HQNO molecule. Results with synthetic HMAQ-NO molecules with shorter carbon side chains indicate the heightened activity is due to both side chain length and possibly methylation (or saturation). It remains to be seen whether the structural moieties important for this lethality alter the target site of this molecule, the ability to penetrate *B. subtilis* cells, or some other aspect of this molecule. In addition to the *N*-oxide congeners, *B. thailandensis* produces a variety of HMAQs with side chains of varying length and saturation (1, 26). Although these other molecules had less potent antimicrobial activities (**Table 3.2**), it is possible they contribute to competition in other ways. A previous study showed that different variations of HAQs used in combination can have synergistic antimicrobial effects on other bacteria by acting on distinctly different cellular targets (56). Thus, the diversity of H(M)AQs produced by *B. thailandensis* might serve to enhance killing during competition or could be important for averting development of antibiotic resistance in competitors.

We find it interesting that the *Burkholderias* do not have the enzyme responsible for generating PQS (PqsH, see **Fig. 3.3**). PQS has a variety of known functions such as immune modulation (57), cell density-dependent gene regulation (24, 58) and iron sequestration (26). *B. thailandensis* might have lost the ability to synthesize PQS because these functions are not needed, or because there is existing functional redundancy with other molecules or pathways. For example, the small-molecule malleilactone might have similar biophysical properties and also sequester iron (15). It is also interesting that *B. ambifaria* lacks the HmqL enzyme responsible for generating *N*-oxide HMAQs, which are the most antimicrobial members of this family. The lack of PQS or any *N*-oxide analog in *B. ambifaria* strongly supports that other products of this pathway have important functions that contribute to the survival of this species, although the biology of the other products of the Hmq system are not well understood.

SUPPORTING INFORMATION

Fig. S3.1. Activity of *B. thailandensis* BD20 ethyl acetate extracts against *B. subtilis.* Stationary phase *B. thailandensis* cultures grown in LB were ethyl acetate-extracted and 100 µL of the ethyl acetate fraction (left) or an ethyl acetate control was spotted onto a freshly spread lawn of *B. subtilis* on an LB agar plate and incubated at 30 ºC overnight prior to imaging. A zone of clearing around a diffusion disc indicates the region where *B. subtilis* growth was inhibited.

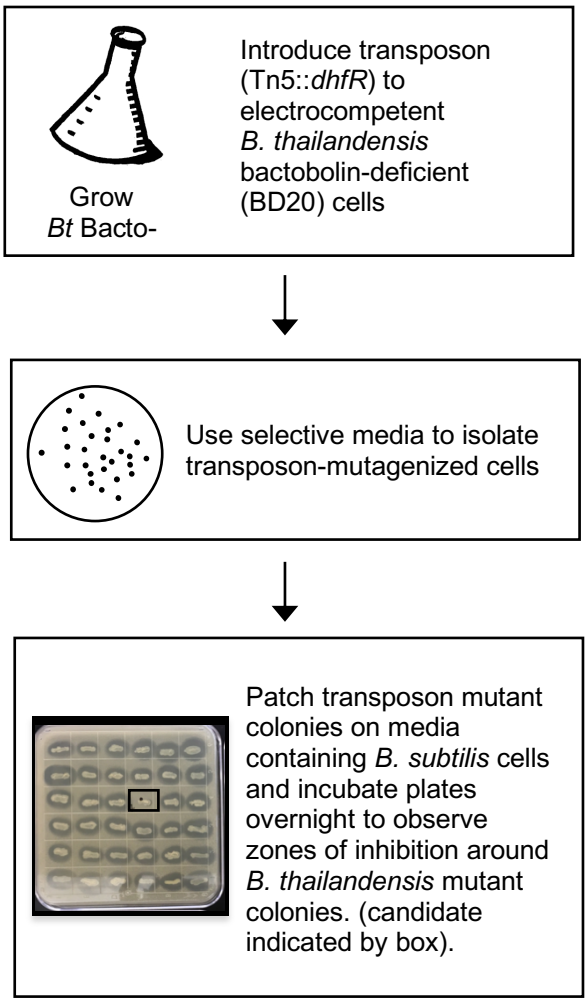

Figure S3.2. Overview of screen for antimicrobial-defective transposon mutants

Table S3.1. Bacterial strains and plasmids used in this study.

Strain or plasmid	Relevant properties	Reference or source
Burkholderia thailandensis		
E264	Wild-type strain	(7)
BD20	E264 with deletion of *btaK*	(2)
JRK100	E264 *hmqA::cm*	This study
JRK101	E264 BTH_II1576::FRT-*tmp*	This study
JRK102	BD20 *hmqA::cm*	This study
JRK103	BD20 BTH_II1576::FRT-*tmp*	This study
JRK104	BD20 *glmS1 attn7::*P*lac*; Km^R	This study
JRK105	JRK103 *glmS1 attn7::*P*lac*; Km^R	This study
JRK106	JRK103 *glmS1 attn7::*P*lac-hmqL,* Km^R	This study
Escherichia coli		
DH5α	F^- Φ80*lacZ* Δ*M15* Δ(*lacZYA-argF*) *U169 hsdR17*(r_K^- m_K^+) *recA1 endA1 phoA supE44 thi-1 gyrA96 relA1* λ^-	Invitrogen
JM109	(traD36, pro AB + *lac Iq*, *lacZ* M15) *endA1 recA1* hsdR17(rk^-, mk^+) *mcrA supE*44 λ^- *gyrA*96 *relA1* (*lac*$^-$ *proAB*)	(59)
Other strains		
Bacillus subtilis 168	Wild-type strain	(60)
Staphylococcus aureus Newman	Wild-type strain	(61)
Pseudomonas aeruginosa PA14	Wild-type strain	(62)
Burkholderia ambifaria HSJ1	Wild type strain	(1)
Plasmids		
pEX18Tp-pheS	Suicide plasmid; Tp^R	(11)
pMCG19	pEX18Tp-PheS with a *hmqA* disrupted by a chloramphenicol resistance cassette (*hmqA::cm*)	This study
pTNS2	Tn7 transposase-expressing helper plasmid; Amp^R	(63)
pUC18-mini-Tn7T-P*lac-malR*	Mobilizable mini-Tn7 vector with the *lac* promoter (P*lac*) for IPTG-inducible *malR* expression (used to Construct pUC18-mini-Tn7T-P*lac-malR*); Km^R, Ap^R	(34)
pUC18-mini-Tn7T-P*lac-hmqL*	pUC18miniTn7T-LAC-Km containing the BTH_II1576 gene (*hmqL*); Km^R, Ap^R	This study
pME6010	pVS1-p15A shuttle vector; Tc^R	(36)
pMCG17	pME6010 with the *B. thailandensis* BTH_II1576 (*hmqL*) gene	This study

Table S3.2. Primers used in this study.

Primer	Sequence (5` to 3`)
Primers for Tn5 mutant identification	
hmqA F-1	GATCTGCCATTGCTTTCCGCAACACG
hmqA R-1	TCAGGCCGCTTGCACGTCG
hmqF F-1	GCTGCATCTGAAGAGCATGGAGC
hmqF R-1	CGTGCTCTCTTCGTGATATCCCATCC
hmqC F-1	TCGGCAATGTGCGAAGCAAGGTC
hmqC R-1	GAGCGGATTGTCGGCAACGAC
hmqL-Tn5-Tp-F2	CGTCATGCCCAATGTGCGCTTG
hmqL-Tn5-Tp-R2	GTTGGTTGACGACTGCGCGAAC
Primers for constructing pUC18-mini-Tn7T-P*lac-hmqL* (BTH_II1576)	
hmqL-ORF-F-SacI	ATATTAGAGCTCATGAAAAACAACCAAGTCGATG
hmqL-ORF-R-HindIII	ATATTAAAGCTTATTCCCGCTTCGTCCGCCAGC
Primers for constructing pMCG19 (*hmqA::cm*)	
hmqAfor	ACGAAGCTTCATCTCTTGCCGCAGCTTGAA
hmqArev	ACGGTACCGATCATCAGCCTCGGCTACAC
CmFPstI	AAAACTGCAGGTGACGGAAGATCACTTCGCA
CmRPstI	AAAACTGCAGGCGTTTAAGGTCAACAATAACTGC
Primers for constructing pME6010 *hmqL*	
hmqL-F	CCGAGATCTACCCAATTCATAGACCAGCGTTGC
hmqL-R	CCGGGTACCTCATGATGCGTACCTCCGTCGATT
Primers for constructing the *hmqL::dhfr* mutant by natural transformation	
hmqL-Tn-for2	CGTCATGCCCAATGTGCGCTTG
hmqL-Tn-rev2	GTTGGTTGACGACTGCGCGAAC

Underlined sequences indicate restriction enzyme sites

Table S3.3. Growth rate measurements of *B. thailandensis* mutants[a]

	Doubling Time
Strain Name	Median (SD), minutes
BD20 (Bt Bacto$^-$	60.00 (0.52)
Bt Bacto$^-$ Tn5::*tmp* #7	57.51 (0.47)
Bt Bacto$^-$ Tn5::*tmp* #9	59.74 (1.03)
Bt Bacto$^-$ Tn5::*tmp* #14	62.56 (3.98)
Bt Bacto$^-$ Tn5::*tmp* #27	60.52 (0.53)
Bt Bacto$^-$ Tn5::*tmp* #31	59.23 (0.00)
Bt Bacto$^-$ Tn5::*tmp* #32	62.15 (0.56)
Bt Bacto$^-$ Tn5::*tmp* #56	59.49 (0.51)
Bt Bacto$^-$ Tn5::*tmp* #63	63.00 (0.00)
Bt Bacto$^-$ Tn5::*tmp* #68	62.73 (1.70)

[a]The values are the means of three independent experiments with the standard deviation in parentheses, determined from at least three hourly measurements of the optical density at 600 nm of logarithmic-stage cultures grown with shaking in LB-MOPS.

REFERENCES

1. Vial L, Lepine F, Milot S, Groleau MC, Dekimpe V, Woods DE, Deziel E. 2008. *Burkholderia pseudomallei*, *B. thailandensis*, and *B. ambifaria* produce 4-hydroxy-2-alkylquinoline analogues with a methyl group at the 3 position that is required for quorum-sensing regulation. J Bacteriol 190:5339-52.

2. Duerkop BA, Varga J, Chandler JR, Peterson SB, Herman JP, Churchill ME, Parsek MR, Nierman WC, Greenberg EP. 2009. Quorum-sensing control of antibiotic synthesis in *Burkholderia thailandensis*. J Bacteriol 191:3909-18.

3. Cheng AC, Currie BJ. 2005. Melioidosis: epidemiology, pathophysiology, and management. Clin Microbiol Rev 18:383-416.

4. Whitlock GC, Estes DM, Torres AG. 2007. Glanders: off to the races with *Burkholderia mallei*. FEMS Microbiol Lett 277:115-22.

5. Dance DA. 2000. Ecology of *Burkholderia pseudomallei* and the interactions between environmental *Burkholderia* spp. and human-animal hosts. Acta Trop 74:159-68.

6. Van Zandt KE, Greer MT, Gelhaus HC. 2013. Glanders: an overview of infection in humans. Orphanet J Rare Dis 8:131.

7. Brett PJ, DeShazer D, Woods DE. 1998. *Burkholderia thailandensis* sp. nov., a *Burkholderia pseudomallei*-like species. Int J Syst Bacteriol 48 Pt 1:317-20.

8. Chandler JR, Duerkop BA, Hinz A, West TE, Herman JP, Churchill ME, Skerrett SJ, Greenberg EP. 2009. Mutational analysis of *Burkholderia thailandensis* quorum sensing and self-aggregation. J Bacteriol 191:5901-9.

9. Choi KH, DeShazer D, Schweizer HP. 2006. mini-Tn7 insertion in bacteria with multiple glmS-linked attTn7 sites: example *Burkholderia mallei* ATCC 23344. Nat Protoc 1:162-9.

10. Lopez CM, Rholl DA, Trunck LA, Schweizer HP. 2009. Versatile dual-technology system for markerless allele replacement in *Burkholderia pseudomallei*. Appl Environ Microbiol 75:6496-503.

11. Barrett AR, Kang Y, Inamasu KS, Son MS, Vukovich JM, Hoang TT. 2008. Genetic tools for allelic replacement in *Burkholderia* species. Appl Environ Microbiol 74:4498-508.

12. Lawrenz MB, Fodah RA, Gutierrez MG, Warawa J. 2014. Intubation-mediated intratracheal (IMIT) instillation: a noninvasive, lung-specific delivery system. J Vis Exp doi:10.3791/52261:e52261.

13. Seyedsayamdost MR, Chandler JR, Blodgett JA, Lima PS, Duerkop BA, Oinuma K, Greenberg EP, Clardy J. 2010. Quorum-sensing-regulated bactobolin production by *Burkholderia thailandensis* E264. Org Lett 12:716-9.

14. Amunts A, Fiedorczuk K, Truong TT, Chandler J, Peter Greenberg E, Ramakrishnan V. 2015. Bactobolin A binds to a site on the 70S ribosome distinct from previously seen antibiotics. J Mol Biol 427:753-5.

15. Biggins JB, Ternei MA, Brady SF. 2012. Malleilactone, a polyketide synthase-derived virulence factor encoded by the cryptic secondary metabolome of *Burkholderia pseudomallei* group pathogens. J Am Chem Soc 134:13192-5.

16. Franke J, Ishida K, Hertweck C. 2012. Genomics-driven discovery of burkholderic acid, a noncanonical, cryptic polyketide from human pathogenic *Burkholderia* species. Angew Chem Int Ed Engl 51:11611-5.

17. Trottmann F, Franke J, Richter I, Ishida K, Cyrulies M, Dahse HM, Regestein L, Hertweck C. 2019. Cyclopropanol warhead in malleicyprol confers virulence of human- and animal-pathogenic *Burkholderia* species. Angew Chem Int Ed Engl 58:14129-14133.

18. Moule MG, Spink N, Willcocks S, Lim J, Guerra-Assuncao JA, Cia F, Champion OL, Senior NJ, Atkins HS, Clark T, Bancroft GJ, Cuccui J, Wren BW. 2015. Characterization of New Virulence Factors Involved in the Intracellular Growth and Survival of *Burkholderia pseudomallei*. Infect Immun 84:701-10.

19. Park JD, Moon K, Miller C, Rose J, Xu F, Ebmeier CC, Jacobsen JR, Mao D, Old WM, DeShazer D, Seyedsayamdost MR. 2020. Thailandenes, cryptic polyene natural products isolated from *Burkholderia thailandensis* using phenotype-guided transposon mutagenesis. ACS Chem Biol doi:10.1021/acschembio.9b00883.

20. Seyedsayamdost MR. 2014. High-throughput platform for the discovery of elicitors of silent bacterial gene clusters. Proc Natl Acad Sci U S A 111:7266-71.

21. Coulon PML, Groleau MC, Deziel E. 2019. Potential of the *Burkholderia cepacia* Complex to Produce 4-Hydroxy-3-Methyl-2-Alkyquinolines. Front Cell Infect Microbiol 9:33.

22. Diggle SP, Winzer K, Chhabra SR, Worrall KE, Camara M, Williams P. 2003. The *Pseudomonas aeruginosa* quinolone signal molecule overcomes the cell density-dependency of the quorum sensing hierarchy, regulates rhl-dependent genes at the onset of stationary phase and can be produced in the absence of LasR. Mol Microbiol 50:29-43.

23. Gallagher LA, McKnight SL, Kuznetsova MS, Pesci EC, Manoil C. 2002. Functions required for extracellular quinolone signaling by *Pseudomonas aeruginosa*. J Bacteriol 184:6472-80.

24. Deziel E, Lepine F, Milot S, He J, Mindrinos MN, Tompkins RG, Rahme LG. 2004. Analysis of *Pseudomonas aeruginosa* 4-hydroxy-2-alkylquinolines (HAQs) reveals a role for 4-hydroxy-2-heptylquinoline in cell-to-cell communication. Proc Natl Acad Sci U S A 101:1339-44.

25. Pesci EC, Milbank JB, Pearson JP, McKnight S, Kende AS, Greenberg EP, Iglewski BH. 1999. Quinolone signaling in the cell-to-cell communication system of *Pseudomonas aeruginosa*. Proc Natl Acad Sci U S A 96:11229-34.

26. Diggle SP, Matthijs S, Wright VJ, Fletcher MP, Chhabra SR, Lamont IL, Kong X, Hider RC, Cornelis P, Camara M, Williams P. 2007. The *Pseudomonas aeruginosa* 4-quinolone signal molecules HHQ and PQS play multifunctional roles in quorum sensing and iron entrapment. Chem Biol 14:87-96.

27. Xiao G, Deziel E, He J, Lepine F, Lesic B, Castonguay MH, Milot S, Tampakaki AP, Stachel SE, Rahme LG. 2006. MvfR, a key *Pseudomonas aeruginosa* pathogenicity LTTR-class regulatory protein, has dual ligands. Mol Microbiol 62:1689-99.

28. Piochon M, Coulon PML, Caulet A, Groleau M-C, Déziel E, Gauthier C. 2020. Synthesis and antimicrobial activity of *Burkholderia*-related 4-hydroxy-3-methyl-2-alkenylquinolones (HMAQs) and their *N*-oxide counterparts doi:10.26434/chemrxiv.11859144.v1.

29. Conrad M, Limpach L. 1887. "Syntheses of quinoline derivatives using acetoacetic ester". Reports of the German Chemical Society 20:944-948.

30. Salvaggio F, Hodgkinson JT, Carro L, Geddis SM, Galloway WRJD, Welch M, Spring DR. 2016. The synthesis of quinolone natural products from *Pseudonocardia* sp. European Journal of Organic Chemistry 2016:434-437.

31. Woschek A, Mahout M, Mereiter K, Hammerschmidt F. 2007. Synthesis of 2-Heptyl-1-hydroxy-4(1H)-quinolone - Unexpected Rearrangement of 4-(Alkoxycarbonyloxy)quinoline N-Oxides to 1-(Alkoxycarbonyloxy)-4(1H)-quinolones. Synthesis 2007:1517-1522.

32. Chang AC, Cohen SN. 1978. Construction and characterization of amplifiable multicopy DNA cloning vehicles derived from the P15A cryptic miniplasmid. J Bacteriol 134:1141-56.

33. Thongdee M, Gallagher LA, Schell M, Dharakul T, Songsivilai S, Manoil C. 2008. Targeted mutagenesis of *Burkholderia thailandensis* and *Burkholderia pseudomallei* through natural transformation of PCR fragments. Appl Environ Microbiol 74:2985-9.

34. Klaus JR, Deay J, Neuenswander B, Hursh W, Gao Z, Bouddhara T, Williams TD, Douglas J, Monize K, Martins P, Majerczyk C, Seyedsayamdost MR, Peterson BR, Rivera M, Chandler JR. 2018. Malleilactone Is a *Burkholderia pseudomallei* Virulence Factor Regulated by Antibiotics and Quorum Sensing. J Bacteriol 200.

35. Choi KH, Mima T, Casart Y, Rholl D, Kumar A, Beacham IR, Schweizer HP. 2008. Genetic tools for select-agent-compliant manipulation of *Burkholderia pseudomallei*. Appl Environ Microbiol 74:1064-75.

36. Heeb S, Itoh Y, Nishijyo T, Schnider U, Keel C, Wade J, Walsh U, O'Gara F, Haas D. 2000. Small, stable shuttle vectors based on the minimal pVS1 replicon for use in gram-negative, plant-associated bacteria. Mol Plant Microbe Interact 13:232-7.

37. Bankevich A, Nurk S, Antipov D, Gurevich AA, Dvorkin M, Kulikov AS, Lesin VM, Nikolenko SI, Pham S, Prjibelski AD, Pyshkin AV, Sirotkin AV, Vyahhi N, Tesler G, Alekseyev MA, Pevzner PA. 2012. SPAdes: a new genome assembly algorithm and its applications to single-cell sequencing. J Comput Biol 19:455-77.

38. Camacho C, Coulouris G, Avagyan V, Ma N, Papadopoulos J, Bealer K, Madden TL. 2009. BLAST+: architecture and applications. BMC Bioinformatics 10:421.

39. Sievers F, Wilm A, Dineen D, Gibson TJ, Karplus K, Li W, Lopez R, McWilliam H, Remmert M, Soding J, Thompson JD, Higgins DG. 2011. Fast, scalable generation of high-quality protein multiple sequence alignments using Clustal Omega. Mol Syst Biol 7:539.

40. Lepine F, Milot S, Groleau MC, Deziel E. 2018. Liquid chromatography/mass spectrometry (LC/MS) for the detection and quantification of N-acyl-L-homoserine lactones (AHLs) and 4-hydroxy-2-alkylquinolines (HAQs). Methods Mol Biol 1673:49-59.

41. Agarwal A, Kahyaoglu C, Hansen DB. 2012. Characterization of HmqF, a protein involved in the biosynthesis of unsaturated quinolones produced by *Burkholderia thailandensis*. Biochemistry 51:1648-57.

42. Lepine F, Milot S, Deziel E, He J, Rahme LG. 2004. Electrospray/mass spectrometric identification and analysis of 4-hydroxy-2-alkylquinolines (HAQs) produced by *Pseudomonas aeruginosa*. J Am Soc Mass Spectrom 15:862-9.

43. Drees SL, Ernst S, Belviso BD, Jagmann N, Hennecke U, Fetzner S. 2018. PqsL uses reduced flavin to produce 2-hydroxylaminobenzoylacetate, a preferred PqsBC substrate in alkyl quinolone biosynthesis in *Pseudomonas aeruginosa*. J Biol Chem 293:9345-9357.

44. Lepine F, Deziel E, Milot S, Rahme LG. 2003. A stable isotope dilution assay for the quantification of the *Pseudomonas* quinolone signal in *Pseudomonas aeruginosa* cultures. Biochim Biophys Acta 1622:36-41.

45. Hays EE, Wells IC, Katzman PA, Cain CK, Jacobs FA, Thayer SA, Doisy EA, Gaby WL, Roberts EC, Muir RD, Carroll CJ, Jones LR, Wade NJ. 1945. Antibiotic substances produced by *Pseudomonas aeruginosa*. Biological Chemistry 159:725-50.

46. Diggle SP, Lumjiaktase P, Dipilato F, Winzer K, Kunakorn M, Barrett DA, Chhabra SR, Camara M, Williams P. 2006. Functional genetic analysis reveals a 2-Alkyl-4-quinolone signaling system in the human pathogen *Burkholderia pseudomallei* and related bacteria. Chem Biol 13:701-10.

47. Machan ZA, Taylor GW, Pitt TL, Cole PJ, Wilson R. 1992. 2-Heptyl-4-hydroxyquinoline N-oxide, an antistaphylococcal agent produced by *Pseudomonas aeruginosa*. J Antimicrob Chemother 30:615-23.

48. Smirnova IA, Hagerhall C, Konstantinov AA, Hederstedt L. 1995. HOQNO interaction with cytochrome b in succinate:menaquinone oxidoreductase from Bacillus subtilis. FEBS Lett 359:23-6.

49. Nguyen AT, Jones JW, Ruge MA, Kane MA, Oglesby-Sherrouse AG. 2015. Iron depletion enhances production of antimicrobials by *Pseudomonas aeruginosa*. J Bacteriol 197:2265-75.

50. Mashburn LM, Jett AM, Akins DR, Whiteley M. 2005. *Staphylococcus aureus* serves as an iron source for *Pseudomonas aeruginosa* during *in vivo* coculture. J Bacteriol 187:554-66.

51. Korgaonkar A, Trivedi U, Rumbaugh KP, Whiteley M. 2013. Community surveillance enhances *Pseudomonas aeruginosa* virulence during polymicrobial infection. Proc Natl Acad Sci U S A 110:1059-64.

52. Mitchell G, Seguin DL, Asselin AE, Deziel E, Cantin AM, Frost EH, Michaud S, Malouin F. 2010. Staphylococcus aureus sigma B-dependent emergence of small-colony variants and biofilm production following exposure to Pseudomonas aeruginosa 4-hydroxy-2-heptylquinoline-N-oxide. BMC Microbiol 10:33.

53. Fugere A, Lalonde Seguin D, Mitchell G, Deziel E, Dekimpe V, Cantin AM, Frost E, Malouin F. 2014. Interspecific small molecule interactions between clinical isolates of Pseudomonas aeruginosa and Staphylococcus aureus from adult cystic fibrosis patients. PLoS One 9:e86705.

54. Hoffman LR, Deziel E, D'Argenio DA, Lepine F, Emerson J, McNamara S, Gibson RL, Ramsey BW, Miller SI. 2006. Selection for *Staphylococcus aureus* small-colony variants due to growth in the presence of *Pseudomonas aeruginosa*. Proc Natl Acad Sci U S A 103:19890-5.

55. Lightbown JW. 1954. An antagonist of streptomycin and dihydrostreptomycin produced by Pseudomonas aeruginosa. J Gen Microbiol 11:477-92.

56. Wu Y, Seyedsayamdost MR. 2017. Synergy and Target Promiscuity Drive Structural Divergence in Bacterial Alkylquinolone Biosynthesis. Cell Chem Biol 24:1437-1444 e3.

57. Hooi DS, Bycroft BW, Chhabra SR, Williams P, Pritchard DI. 2004. Differential immune modulatory activity of *Pseudomonas aeruginosa* quorum-sensing signal molecules. Infect Immun 72:6463-70.

58. Bredenbruch F, Geffers R, Nimtz M, Buer J, Haussler S. 2006. The *Pseudomonas aeruginosa* quinolone signal (PQS) has an iron-chelating activity. Environ Microbiol 8:1318-29.

59. Yanisch-Perron C, Vieira J, Messing J. 1985. Improved M13 phage cloning vectors and host strains: nucleotide sequences of the M13mp18 and pUC19 vectors. Gene 33:103-19.

60. Burkholder PR, Giles NH, Jr. 1947. Induced biochemical mutations in Bacillus subtilis. Am J Bot 34:345-8.

61. Duthie ES, Lorenz LL. 1952. *Staphylococcal* coagulase; mode of action and antigenicity. J Gen Microbiol 6:95-107.

62. Rahme LG, Stevens EJ, Wolfort SF, Shao J, Tompkins RG, Ausubel FM. 1995. Common virulence factors for bacterial pathogenicity in plants and animals. Science 268:1899-902.

63. Choi KH, Gaynor JB, White KG, Lopez C, Bosio CM, Karkhoff-Schweizer RR, Schweizer HP. 2005. A Tn7-based broad-range bacterial cloning and expression system. Nat Methods 2:443-8.

Chapter 4: Efflux pumps alleviate self-toxicity of the *Burkholderia pseudomallei* cytotoxin malleilactone

COLLABORATIONS AND WORKLOAD ALLOCATIONS:

Jennifer R. Klaus did the cloning and genetic manipulations, performed growth yield experiments and minimum inhibitory concentration assays (assisted by Alicia Brown), and performed transcriptional reporter assays. Jennifer R. Klaus, Alicia Brown, and Wyatt Hursh optimized and performed sample preparation for UV-Vis and mass spectrometry (MS) analysis. Benjamin Neuenswander performed malleilactone UV-Vis/MS analyses and assisted Jennifer R. Klaus in data interpretation. Benjamin Neuenswander purified malleilactone. Todd D. Williams performed malleicyprol MS analysis. Jennifer R. Klaus and Josephine R. Chandler managed project conceptualization and experimental design.

ABSTRACT

Burkholderia pseudomallei is an opportunistic human pathogen which can cause the potentially-fatal disease melioidosis. In addition to other known pathogenesis mechanisms, *B. pseudomallei* can utilize the production of secondary metabolites to enhance its survival within a host. Despite their role in pathogenicity, secondary metabolite biology is not fully understood. Further, some such metabolites can be self-toxic, and even less is known about how these products are detoxified by the cell. Thus, secondary metabolite biosynthesis and associated resistance mechanisms could be a promising route toward establishing new therapeutic targets. Here, we show that the *B. pseudomallei* secondary metabolite malleilactone, which is encoded by the *mal* gene cluster, exhibits more robust toxicity against efflux-deficient *E. coli* relative to wild-type. *B. pseudomallei* encodes an antibiotic efflux pump BpeEF-OprC adjacent to the *mal* biosynthetic genes. We used mass spectrometry to show this pump is involved in the export of malleilactone into culture supernatants. We observed modest malleilactone self-toxicity under paraquat-induced cellular stress conditions in BpeEF-OprC efflux-deficient *B. pseudomallei*, which was more severe in conditions shown in the related species *B. thailandensis* to promote the formation of more cytotoxic malleilactone isomers, the recently discovered malleicyprol-family molecules. Known transcriptional activators of *bpeEF-oprC* have modest effects on *mal* cluster regulation, effects that are less robust than caused by the antibiotic trimethoprim, a well-known *mal* cluster activator as well as a substrate of BpeEF-OprC. Thus, a primary role of BpeEF-OprC might be to moderate the concentrations of endogenous *mal* products, which could explain the partial overlaps in their regulatory elements. Our findings suggest that the BpeEF-OprC efflux pump is important for malleilactone export and preventing self-toxicity and that targeting *mal* product efflux pumps could be a promising therapeutic strategy for melioidosis treatment.

INTRODUCTION

Burkholderia pseudomallei, B. thailandensis, and *B. mallei* are a closely related clade of Gram-negative bacteria with diverse ecological niches. *B. mallei* is the pathogenic agent that causes glanders in equines and is host restricted (2, 3). The other two species are soil-dwellers: *B. thailandensis* is a saprophyte that is not pathogenic to humans (4, 5), and *B. pseudomallei* is the opportunistic etiological agent of the protean and difficult-to-treat human disease melioidosis (6, 7). Most often manifesting as pneumonia and tissue abscesses, melioidosis is a disease with multifaceted symptoms that requires intense antimicrobial therapies for resolution (for reviews, see (8-10)). Estimates place the melioidosis global annual death toll at or above those due to leptospirosis, dengue fever, and measles (11). The pathogens *B. mallei* and *B. pseudomallei* have biosafety level 3 (BSL3) classification due to their Tier 1 Select Agent status (https://www.selectagents.gov/SelectAgentsandToxinsList.html), so until the advent of attenuated BSL2-safe strains of each nearly a decade ago (12-16), *B. thailandensis* served as a study surrogate to understand the often-multifaceted roles of virulence factors and metabolites in pathogenesis of the two other strains. The genomes of this *Burkholderia* group encode many secondary metabolite biosynthetic gene clusters that are predicted to be important in bacterial survival or virulence toward a host.

Some of the products of these secondary metabolite gene clusters are antimicrobial, such as bactobolin (17-19) and malleilactone (20, 21). In such cases, these toxic products may benefit producing cells by providing a competitive advantage during interspecies competition as does bactobolin (22, 23) or by causing toxicity to eukaryotic host cells during infection. Some of these toxic metabolites can also cause self-poisoning under some conditions. In a few cases, mechanisms to avert self-poisoning by these metabolites have been studied, though generally, such mechanisms are not well understood. In one example, in the Actinobacteria *Streptomyces lusitanus* NRRL 8034, the secreted oxidoreductase NapU activates the *S. lusitanus*-produced antimicrobial/antitumor molecule napthyridinomycin (NDM) once it is safely outside of the cell, preventing self-toxicity in the cytoplasm; further, NapU can also inactivate

NDM to prevent self-toxicity that could result from prolonged proximity of active NDM to producer cells (24). Understanding producer cell resistance to such toxins/factors is of interest because it is an essential process in many bacteria. Such knowledge could also aid our ability to combat microbial pathogenesis, such as by eliminating the producer's ability to resist toxicity and thereby render it susceptible to its own toxins.

In the human pathogen *B. pseudomallei,* we are broadly interested in understanding the characteristics, function(s), and regulation of secondary metabolites in order to understand the biology of this pathogen, and also so we can exploit these metabolites to develop novel therapeutics for *B. pseudomallei* infections. Here, we focus on malleilactone, the product of the highly conserved *mal* biosynthetic gene cluster, which was among 'cryptic' metabolites discovered and characterized first in *B.*

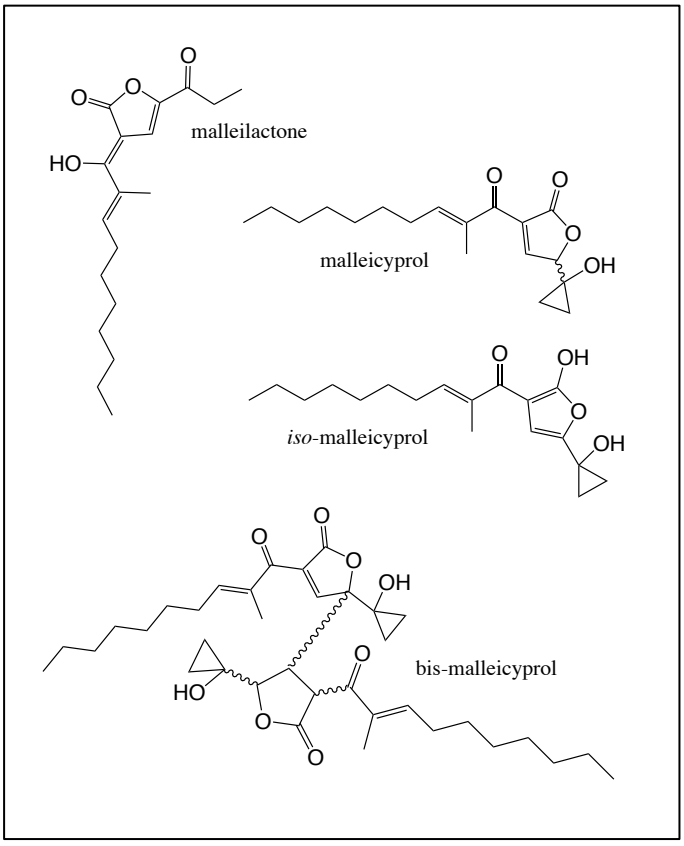

Figure 4.1. Chemical structures of malleilactone and as per Trottmann et al. (1), the proposed malleilactone biosynthetic precursor molecules malleicyprol, its isomer *iso*-malleicyprol, and the adduct of the two, bis-malleicyprol.

thailandensis (21, 25). Malleilactone has been shown to contribute to bacterial pathogenesis in the soil nematode *Caenorhabditis elegans* (20, 21) and the social amoeba *Dictyostelium discoidium* (21), and when purified, it exhibits cytotoxicity toward a variety of eukaryotic cell lines and Gram-positive bacteria (20, 21).

We previously reported that purified malleilactone in sufficiently high concentrations is toxic to *B. thailandensis,* causing ~50% growth inhibition of batch cultures at 15 μg/mL (26). However, using malleilactone purified at a different institution, we did not observe a similar exogenous self-toxicity (minimum inhibitory concentration (MIC) > 200 μg/mL for both *B. thailandensis* strain E264 and *B. pseudomallei* strain Bp82) (20). Notably, a 2019 study (1) characterized precursor molecules in the malleilactone biosynthetic pathway and demonstrated that these other molecules are around 100 times more cytotoxic than malleilactone. These newly described structural isomers are malleicyprol molecules, and they differ from malleilactone by the presence of a cyclopropanol ring substitution off the core γ-lactone ring (**Fig. 4.1**). Thus, additional components of the malleilactone biosynthetic pathway could also be important for full cytotoxicity. Therefore, we sought to further address the questions: Can *mal* cluster products cause self-toxicity to producing cells, and if so, what are the resistance mechanisms that can mitigate that toxicity?

MATERIALS AND METHODS

Bacterial strains, culture conditions, and reagents

All bacterial strains and plasmids used in this study are listed in **Table 4.1**. We used the select agent-excluded Bp82 strain (12), an attenuated, adenine and thiamine auxotrophic mutant of the BSL3 *B. pseudomallei* strain 1026b. Genetic manipulations of plasmids were carried out in *E. coli* strain DH5α (Invitrogen).

Bacteria were grown in Luria-Bertani (LB) broth (10 g tryptone, 5 g yeast extract, and 5 g NaCl per liter) supplemented with 50 mM morpholinepropanesulfonic acid (MOPS) pH=7.0 (or at the concentration and pH indicated), or on YTSX counterselection media (10 g yeast extract, 10 g tryptone, 15% w/v sucrose, and 50 μg/mL of the blue/white indicator 5-bromo-4-chloro-3-indoxyl-beta-D-glucuronide (X-gluc; Gold Biotechnology, St. Louis, MO)) for *B. pseudomallei* counterselection during mutant construction. With the exception of agar plates, all *B. pseudomallei* growth media was supplemented with 1.6 mM adenine hemisulfate and 0.005% thiamine HCl. Growth was at 37˚C with shaking at either 250 rpm or 150 pm as indicated. The inducer molecule isopropyl-β-D-thiogalactopyranoside (IPTG) was used at 1 mM as indicated. Where appropriate, the following antibiotics were used (per mL): 50 μg (*E. coli*) and 1 mg (*B. pseudomallei*) kanamycin, 100 μg (*E. coli*) ampicillin, 15 μg (*E. coli*) and 2 mg (*B. pseudomallei*) gentamicin, and 25 μg (*E. coli*) and 2 mg (*B. pseudomallei*) zeocin. Paraquat (methyl viologen; 1,1'-dimethyl-4,4'-bipyridinium dichloride), which generates reactive superoxides and as a result, cellular oxidative stress, was used as indicated at concentrations that resulted in ~50% growth inhibition after 24 hrs of growth relative to when left untreated.

Genomic DNA, plasmid DNA, and PCR and DNA fragments were obtained using the Qiagen Puregene Core A kit, miniprep plasmid purification kit, or gel-extraction/PCR clean-up kits (IBI/MidSci or Qiagen), respectively, according to manufacturers' protocols.

Table 4.1. Plasmids and bacterial strains used in this study and relevant biological properties.

Plasmid	Relevant properties	Reference
pPS2591	pEXkm5 Δ*bpeEFoprC*	(27)
pPS2647	pEXkm5-Δ*bpeT*	(28)
pPS3177	pEXkm5-*bpeT* C310R	(28)
pPS3190	pEXkm5-*bpeS* K267T	(28)
pPS3158	pEXGm5B-ΔbpeS::*Frt-Km-Frt*	(28)
pUC18miniTn7T-Kan-P*lac*	IPTG-inducible vector plasmid	(20)
pUC18miniTn7T-Kan-P*lac-malR*	IPTG-inducible *malR* for *mal* cluster overexpression	(20)
pUC18miniTn7T-Zeo-P*malA-lacZ*	*mal* gene cluster β-galactosidase reporter	(20)
pTNS3	Transposase-expressing suicide helper plasmid	(29)
Bacterial strain	**Relevant properties**	**Reference**
E. coli DH5α	For genetic manipulations	Invitrogen
E. coli BW25113	Parent strain of the *E. coli* Keio collection	(30)
E. coli BW25113 Δ*tolC*	Δ*tolC* efflux-deficient strain	(31)
B. pseudomallei Bp82	Δ*purM* mutant of strain 1026b	(12)
Bp82 *glmS3::*P*lac-malR*		(20)
Bp82 *glmS3::*P*lac* (empty vector)		(20)
Bp82 *bpeT* C310R	Bp82 with *bpeT* C310R mutation	This study
Bp82 *bpeT* C310R *glmS3::*P*malA-lacZ*		This study
Bp82 *bpeS* K267T	Bp82 with *bpeS* K267T mutation	This study
Bp82 *bpeS* K267T *glmS3::*P*malA-lacZ*		This study
Bp82 Δ*bpeT*	Bp82 with deletion in *bpeT*	This study
Bp82 Δ*bpeT glmS3::*P*malA-lacZ*		This study
Bp82 Δ*bpeS*::Km	Bp82 with deletion in *bpeS*	This study
Bp82 Δ*bpeS*::Km *glmS3::*P*malA-lacZ*		This study
Bp82 Δ*bpeT* Δ*bpeS*::Km	Bp82 with deletion in *bpeT* and *bpeS*	This study
Bp82 Δ*bpeT* Δ*bpeS*::Km *glmS3::*P*malA-lacZ*		This study
Bp82 Δ*bpeEFoprC*	Bp82 with deletion in *bpeEF-oprC*	This study
Bp82 Δ*bpeEFoprC glmS3::*P*lac-malR*		This study
Bp82 Δ*bpeEFoprC glmS3::*P*lac* (empty vector)		This study
Bp82 Δ*bpeEFoprC bpeT* C310R	Bp82 with deletion in *bpeEF-oprC* and *bpeT* C301R mutation	This study
Bp82 Δ*bpeEFoprC bpeS* K267T	Bp82 with deletion in *bpeEF-oprC* and *bpeS* K267T mutation	This study

LacZ reporter assays

β-galactosidase activity was assayed using the Tropix Galacto-Light Plus chemiluminescence kit (Applied Biosystems) according to the manufacturer's protocol. Luminescence output was measured using a BioTek Synergy 2 plate reader and Gen5 software. In all cases, the β-galactosidase activity is reported as light units relative to the optical density at wavelength 600 nm (OD_{600}) of the bacterial culture sample.

Genetic manipulations

We used our own Bp82 strain to construct in-frame, unmarked deletion alleles of the *bpeEF-oprC, bpeT,* and *bpeS* genes, or single nucleotide polymorphism (SNP) mutated alleles of the *bpeT* and *bpeS* genes as described previously (28). Briefly, the appropriate pEXkm5 or pEXGm5b plasmid (**Table 4.1**) was electroporated into Bp82, and transformants were selected using kanamycin (which was a cleaner selection and lower concentrations were needed than for gentamicin). Resulting merodiploid clones were subjected to 4 rounds of counterselection on YTSX sucrose media, selecting white colonies (indicating loss of plasmid) for further purification. Clones were then verified for kanamycin or gentamicin sensitivity and by PCR-amplifying and sequencing across the gene deletion regions. As previously reported (28), the *bpeT* and *bpeS* SNP mutants were also screened for increased trimethoprim minimum inhibitory concentration (MIC) phenotypes relative to wild type.

We constructed Bp82 strains containing either a P*malA-lacZ* reporter, IPTG-inducible *malR* (P*lac-malR*), or a vector control (P*lac* empty vector) as follows. The relevant plasmids (**Table 4.1**) were introduced along with the transposase-expressing helper plasmid pTNS3 by electroporation into Bp82 strains. PCR was used as previously described (29) to confirm insertion of the plasmid-borne transposable element regions into the neutral *attTn7* site in the Bp82 genome near the *glmS3* gene in all cases.

Malleilactone UV-VIS/MS measurements

We assessed relative malleilactone in strains grown as indicated for 24 hrs. Analytical ultraviolet-visible spectroscopy (UV/VIS) and mass spectrometry analysis was performed on ethyl acetate extracts similar to (20) for malleilactone. Briefly, the organic phase of the extracts was dried under nitrogen gas and suspended in 300 µL dimethyl sulfoxide (DMSO) plus 1300 µL acetonitrile (with additional acetonitrile dilutions as needed). 2 µL sample injections were made on an Acquity ultraperformance liquid chromatography (UPLC) system (Waters) with a wash of acetonitrile and water/methanol (1:1) between each injection. The UPLC system was coupled to a photodiode array detector and an LCT Premier TOF mass spectrometer (Waters), and the system was fitted with an Acquity C_{18} ethylene bridged

hybrid (BEH) column (2.1 x 50 mm, 1.7 μm; Waters). The chromatography was developed using an aqueous mobile phase with NH_4OH at pH 9.8 and an acetonitrile organic phase increased by gradient of 5% to 99% over 2.7 min and then held at 99% for 0.4 min (flow rate was 0.6 mL per min). Relative malleilactone was reported as the total area under the 370 nm peak corresponding with malleilactone (malleilactone λ_{max} is 373 nm) adjusted by the culture OD_{600}, and technical triplicate injections were performed for each sample. Fragments were monitored using mass spectrometry to validate the molecular weight of malleilactone in the expected peak.

RESULTS

Efflux pumps increase resistance to purified malleilactone in *E. coli*

Efflux pumps are membrane-associated exporters of various cytoplasmic or periplasmic molecules to the extracellular space, and they are well-characterized antibiotic resistance mechanisms used by many bacteria. Resistance nodulation cell division (RND)-family efflux pumps, including the Mex systems in *P. aeruginosa* and the well-studied AcrAB-TolC system in *E. coli*, are structurally comprised of three protein components: a periplasmic membrane fusion protein (i.e. AcrA), a cytoplasmic/inner membrane transport protein (i.e. AcrB), and an outer membrane lipoprotein (i.e TolC) which forms a porin (for an extensive review of efflux pump families, see (32)). Previously, we showed that purified malleilactone was generally not cytotoxic to *E. coli* (20)(MIC > 100 μg/mL). However, we sought to test whether disrupting efflux pumps might increase malleilactone susceptibility. We similarly tested malleilactone toxicity against an *E. coli* strain disrupted for TolC. In *E. coli,* TolC can associate with multiple inner membrane porin-membrane fusion protein complexes to form functional pumps (33, 34) which confer resistance to a wide variety of compounds such as antibiotics, ethidium bromide, bile salts, short-chain fatty acids, and even mammalian steroids (35). Specifically, *E. coli* TolC can associate with AcrA-AcrB and export multiple families of antimicrobials and other compounds (36, 37), with HlyB-HlyD to export the protein toxin α-hemolysin (38, 39), and with CvaA-CvaB to export the antimicrobial peptide colicin V (40, 41). As the primary outer membrane protein of *E. coli* efflux pump systems, TolC disruption effectively disables all efflux (33, 42, 43). We found that while the parent *E. coli* strain BW25113 was not susceptible to malleilactone, as we previously reported for *E. coli* strain JM109 (20), we observed an MIC of 12.5 μg/mL against the BW25113 Δ*tolC* strain. Our finding that disrupting efflux in *E. coli* increased susceptibility to malleilactone supports the idea that efflux pumps might be important for malleilactone resistance.

The *B. pseudomallei* BpeEF-OprC pump exports malleilactone from the cell

The idea that efflux pumps can export endogenous toxins from the cell to increase self-resistance is not new (44-46). For example, in *Pseudomonas aeruginosa,* a highly reactive intermediate called 5-methylphenazine-1-carboxylic acid (5-Me-PCA) is produced by the phenazine biosynthetic pathway and is targeted for export by the MexGHI-OpmD efflux pump, thereby preventing intracellular accumulation and subsequent self-toxicity (47). Guided by the findings that efflux pumps can be used to prevent malleilactone cytotoxicity in *E. coli*, we sought to determine if this was true for *B. pseudomallei* as well. The *B. pseudomallei* genome contains around 10 multidrug resistance efflux pumps (48, 49), at least 3 of which have been characterized as RND-family efflux pumps; these are AmrAB-OprA, BpeAB-OprB, and BpeEF-OprC. The first RND efflux pump discovered in *B. pseudomallei,* AmrAB-OprA, is responsible for broad-spectrum aminoglycoside and macrolide resistance (50, 51), and it is known to be constitutively expressed at least somewhat highly (52, 53) in the *B. pseudomallei* strain 1026b (isolated from a patient in Thailand and the parent of the attenuated Bp82 strain (12)). Seemingly the least clinically relevant, BpeAB-OprB can confer resistance to macrolides, fluoroquinolones, and tetracycline (49, 54). However, BpeAB-OprB is not highly active in strain 1026b (53), nor is it involved with quorum-sensing and virulence-related phenotypes like siderophore export and motility (54) to which it contributes in the *B. pseudomallei* strain KHW (isolated from a patient in Singapore) (55, 56). The BpeEF-OprC pump is also not as highly active as the AmrAB-OprA pump, but it confers strong resistance to antibiotics that inhibit the tetrahydrofolate synthesis pathway (trimethoprim and sulfamethoxazole) and to fluoroquinolone drugs (ciprofloxacin), among others (27, 28, 57, 58). Notably, the BpeEF-OprC pump genes (*llpE-bpeE-bpeF-oprC* and a LysR-family regulator gene *bpeT*) are located only 4 genes downstream of the *mal* biosynthetic operon. Because of this genetic linkage, we explore here our hypothesis that there could be an evolutionarily conserved association between BpeEF-OprC and the malleilactone biosynthetic pathway, namely: that efflux could be important for export of malleilactone-family molecules and thereby aid in self-resistance.

We sought to test this malleilactone export hypothesis directly using analytical chemistry. Of note, the BpeEF-OprC efflux pump is not very active in wild-type cells under typical laboratory culture conditions (28). Therefore, we constructed strains in which the BpeEF-OprC pump is constitutively produced through previously characterized mutations in the genes encoding the LysR-family BpeT and BpeS activators of the *bpeEF-oprC* gene cluster (28). These were *bpeT* C310R (encoded on chromosome II divergently and adjacent to the *bpeEF-oprC* gene cluster) and *bpeS* K267T (encoded on chromosome I). These *bpeT* and *bpeS* SNP mutations increase resistance to the BpeEF-OprC substrate trimethoprim by 5-fold and over 30-fold, respectively. (28). Whole-volume extracts of 50 mL cultures were examined, and to focus on exported material specifically, we also measured malleilactone in the centrifugation-separated supernatant fractions of 100 mL batches of grown cultures. Samples were extracted with ethyl acetate and then analyzed. Consistent with a lack of BpeEF-OprC activity, we saw no difference in malleilactone levels detected by UV-vis and mass spectrometry (MS) analysis in 50 mL culture extracts of wild-type and Δ*bpeEF-oprC* strains (**Fig. 4.2-A**). We observed strong increases in malleilactone levels, at least 10-fold in extracted whole-volume cultures and 5- to 10-fold in extracted culture supernatants of the *bpeT* and *bpeS* SNP mutant strains (designated *bpeT** and *bpeS**) compared with identically prepared wild-type samples (**Fig. 4.2-B and 4.2-C**). Importantly, these increases occurred in a *bpeEF-oprC* efflux pump-dependent manner for both the *bpeT** and *bpeS** mutants, demonstrating that BpeEF-OprC is involved in malleilactone export into the culture supernatant (**Fig. 4.2-B and 4.2-C**).

In a complementary approach, we also measured malleilactone in the cell pellet fractions of wild type Bp82 and of a mutant lacking the BpeEF-OprC pump. Because malleilactone production is very low or off in standard laboratory conditions (20, 21, 25, 26, 59), we genetically induced malleilactone production using our IPTG-inducible P*lac-malR* cassette integrated into the chromosomes of Bp82 and Bp82 Δ*bpeEF-oprC*, and we increased the culture volumes to 200 mL. In this experiment, we observed that around 25-fold more malleilactone was retained in the cell pellets of the efflux pump-deficient strain than

in wild-type cell pellets, further supporting the idea that BpeEF-OprC can readily export malleilactone from the cell (**Fig. 4.2-D**).

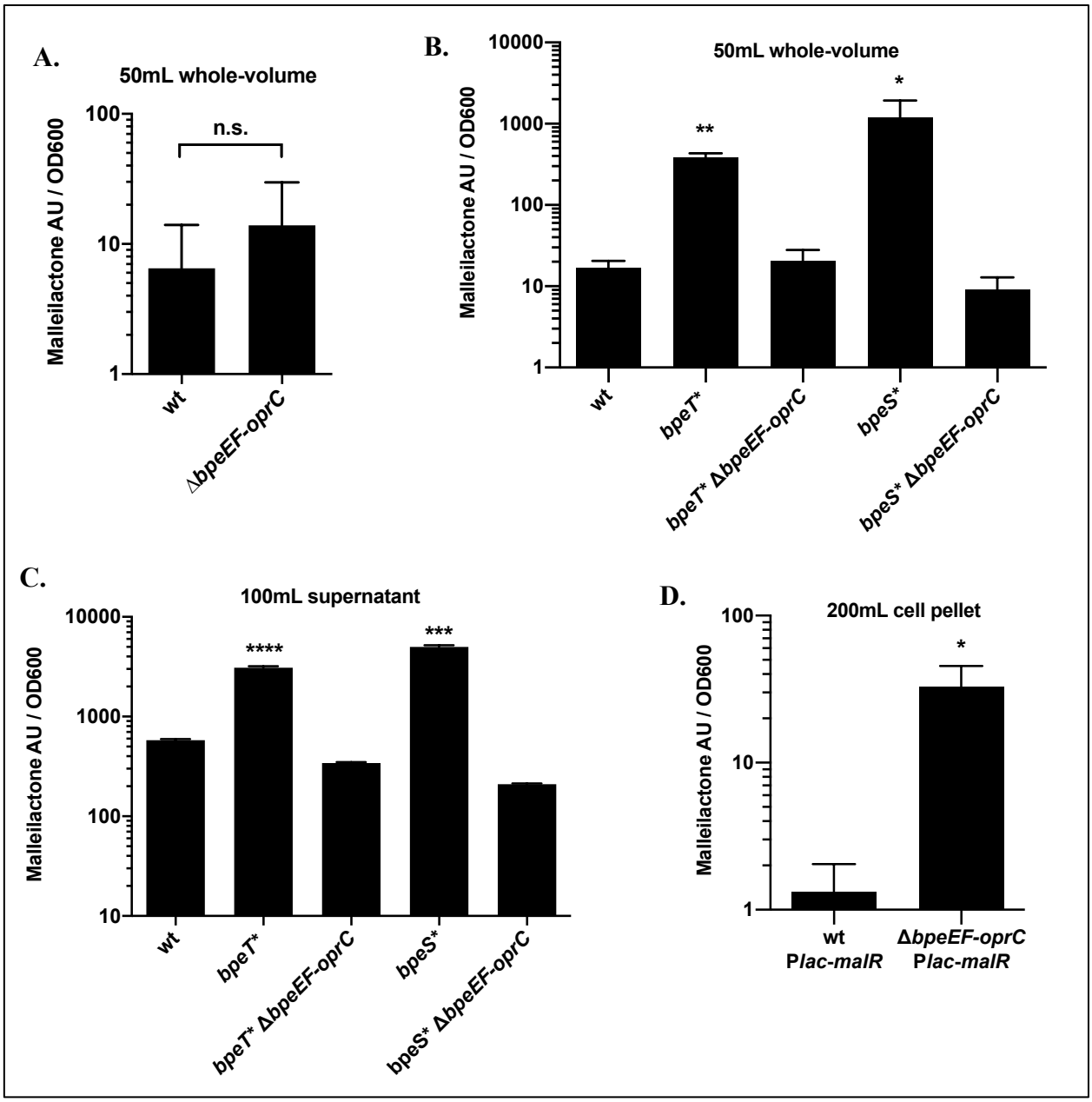

Figure 4.2. Relative malleilactone UV-Vis/mass spectrometry analysis of ethyl acetate extractions of (A) and (B) 50mL whole-volume cultures, (C) 100 mL culture supernatants, and (D) 200mL culture cell pellets from the indicated Bp82 strains. Malleilactone AU: area under the curve at 370 nm, the λ_{max} of malleilactone, reported relative to OD_{600}: culture optical density at 600 nm.; wt: wild type; *bpeT**: *bpeT* C310R; *bpeS**: *bpeS* K267T; P*lac-malR*: IPTG-inducible *malR* cassette integrated at the *glmS3* site in the genome. Results are the averages and standard deviations of (A), (C), and (D) four biological replicates, and (B) three technical replicates, which are representative of the trends of additional biological replicate experiments. Statistical significance is indicated relative to the wild-type strain in each case using student's T-test in (A) and (D) and repeated-measures one-way ANOVA and Tukey's multiple comparisons tests in (B) and (C), 'n.s.' = not significant, *p > 0.05, **p > 0.005, ***p = 0.0003, ****p < 0.0001.

The malleilactone biosynthetic products cause self-poisoning in the absence of BpeEF-OprC

Because the BpeEF-OprC efflux pump is involved in export of malleilactone in *B. pseudomallei,* we asked whether these endogenous products might be toxic to the producing cells during growth and cause self-poisoning in cultures, and whether efflux is important in preventing any self-poisoning. To test this idea, we grew strain Bp82 with the P*lac-malR* cassette in our standard LB media buffered with 50 mM pH 7.0 MOPS with and without the inducer IPTG to increase *mal* gene cluster expression and determined the final growth yield by plating after 24 hours. We similarly tested a Bp82 Δ*bpeEF-oprC* P*lac-malR* strain to assess the importance of export in alleviating potential self-poisoning. In our initial experiments, we observed that there were no growth defects caused by inducing the *mal* genes (data not shown). When cultures were treated with growth-inhibitory concentrations of paraquat, which generates toxic reactive oxygen species (60, 61), to cause cellular stress, we observed a modest but insignificant reduction in growth of the *bpeEF-oprC* mutant that was overexpressing the *mal* genes (**Fig. 4.3-A**). Based on the very recent work in (1) characterizing the more cytotoxic malleicyprol-family precursor molecules in the malleilactone biosynthetic pathway (**Fig. 4.1**), we hypothesized that the lack of observable fitness defects in efflux-deficient cells could be because these conditions were not well-suited for malleicyprol production or activity. Mimicking the more acidic growth conditions used in (1) under which the malleicyprol isomers were characterized, we grew strain Bp82 with the P*lac-malR* cassette at 150 rpm with 200 mM MOPS buffer at pH 6.5. Again, we observed no growth differences (**Fig. 4.3-B**). However, active *mal* cluster biosynthesis significantly decreased growth in the *bpeEF-oprC* mutant when cultures were treated with paraquat to cause cellular stress (**Fig. 4.3-C**). Notably in these conditions, no growth decreases were observed in controls consisting of either wild-type or *bpeEF-oprC*-deficient strains with a chromosomally-integrated P*lac-malR* cassette grown without IPTG (no expression of the malleilactone biosynthesis genes). We also used two other controls: each strain with the P*lac* empty vector cassette grown with IPTG, or containing a deletion of the critical malleilactone biosynthesis gene *malF* and with the P*lac-malR* cassette grown with IPTG. Together, these results support that the toxicity we observed is

due to products of the malleilactone biosynthesis genes. This might be malleicyprol or other products that were stabilized by our altered growing conditions.

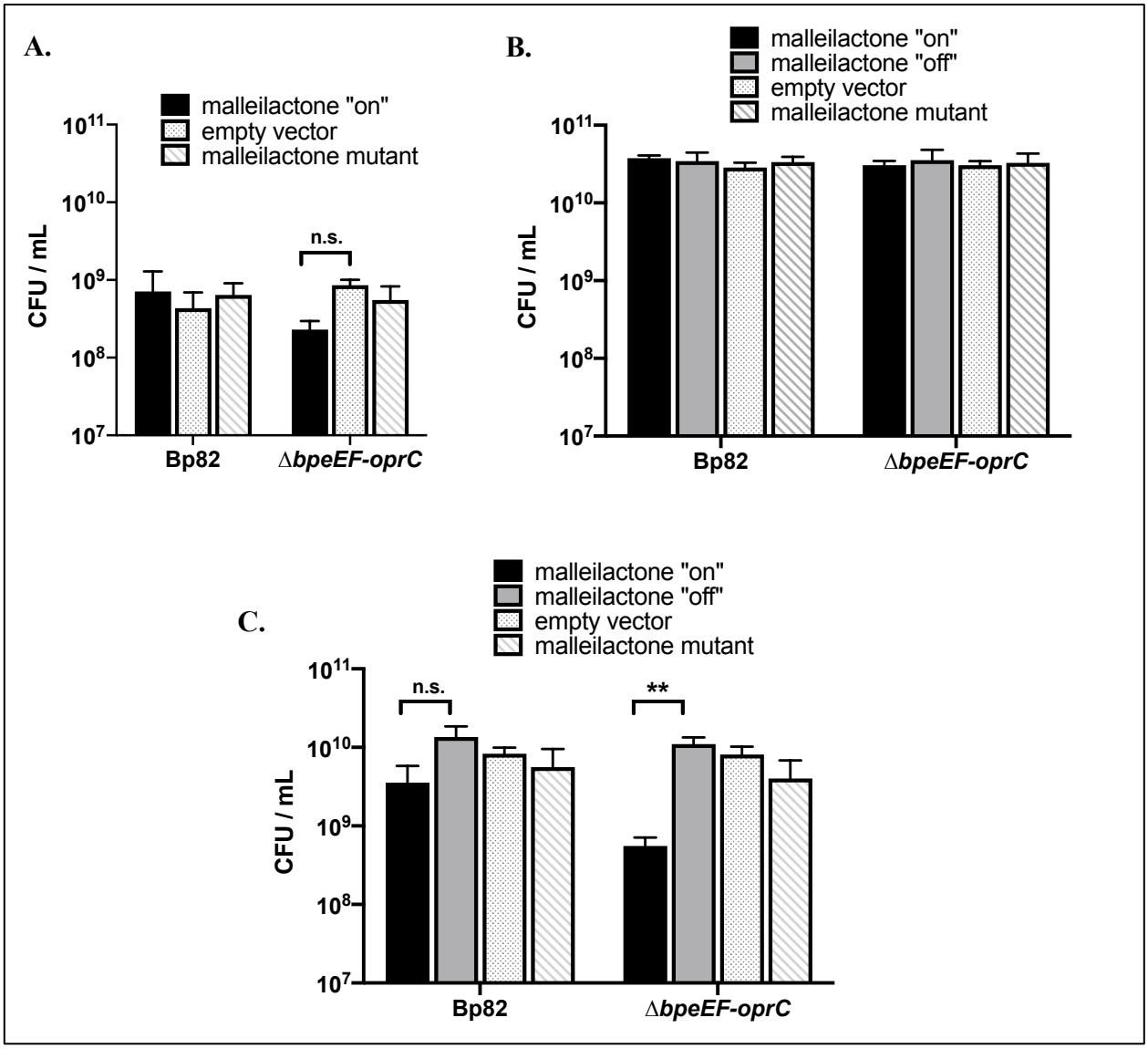

Figure 4.3. Fitness of Bp82 strains grown in (A) pH 7.0-buffered media that was supplemented with 750 µM paraquat and in (B) pH 6.5-buffered media that was unsupplemented and (C) supplemented with 1800 µM paraquat. Paraquat concentrations inhibited growth ~50% relative to untreated in both cases. All Bp82 strains had the IPTG-inducible *mal* cluster genetic element P*lac-malR* chromosomally integrated, except those indicated as 'empty vector' which contained the empty vector IPTG-inducible genetic element. Malleilactone "on": media supplemented with 1 mM IPTG inducer; malleilactone off: no IPTG added; malleilactone mutant: strains with P*lac-malR* chromosomally integrated into a Δ*malF* deletion mutant of the indicated background strain. Results are colony-forming units (CFU) per mL of culture and are the averages and standard deviations of at least three biological replicates. Statistical significance using repeated measures one-way ANOVA and Tukey's multiple comparisons test: 'n.s.' indicates not significant, **$p < 0.005$.

Examination of regulatory networks of the *bpeEF-oprC* and *mal* gene clusters.

Our findings support that the BpeEF-OprC efflux pump is involved in exporting *mal* products. Efflux or other self-resistance mechanisms can be linked to the various metabolites to which they offer producer cells resistance (62, 63), suggestive of some overlap in regulation of both elements. Substrate presence often promotes efflux pump expression (64, 65) by substrate or resulting effector binding to and altering the activity of local or global regulators. The current understanding is that *bpeEF-oprC* is activated similarly through either effector-bound BpeT and BpeS binding to possibly the same site in the promoter region, or through constitutively activating mutations (such as *bpeT* C310R and *bpeS* K267T in the predicted co-inducer binding domains) that relieve the need for effector binding to modulate function (28, 66). Because BpeT and BpeS regulate the BpeEF-OprC pump, we thought these regulators might also be involved in regulating the nearby *mal* genes. To test this hypothesis, we used a chromosomally integrated P*malA-lacZ* reporter cassette (20) with the *lacZ* reporter fused to the promoter of the first gene in the *mal* cluster, *malA*. We examined strains deficient in *bpeS* or *bpeT* or both, or with the *bpeS** or *bpeT** SNP mutation that cause constitutive activation of the *bpeEF-oprC* target genes. We assayed P*malA-lacZ* activity in cultures grown for 24 hrs in our standard LB media conditions and then adjusted the activity output by the OD_{600} of the cultures. The growth-adjusted *mal* expression in a *bpeT* mutant was slightly higher (~1.6-fold) than that of wild type (**Fig. 4.4-A**), suggesting that BpeT could play a role in regulating expression of the malleilactone biosynthetic genes. However, no changes in P*malA-lacZ* activity were observed in the *bpeT** mutant (**Fig. 4.4-A**). Strains disrupted in *bpeS*, either in the Bp82 parent or in the *bpeT*-disrupted strain, had *mal* expression that was not different from wild-type levels, although the constitutively active *bpeS** mutant also had ~1.6-fold higher activity than that of wild type (**Fig. 4.4-A**). In comparison, P*malA-lacZ* levels were ~8-fold higher in cells treated with trimethoprim at levels that reduce growth by 50-70%, as previously reported (see "wt" column in **Fig. 4.4-B** and (20)). Thus, BpeS may play a small role in activating the *mal* genes under these conditions, while BpeT may play a small role in *mal* repression, but neither regulator had an effect comparable to that of treating cells with trimethoprim.

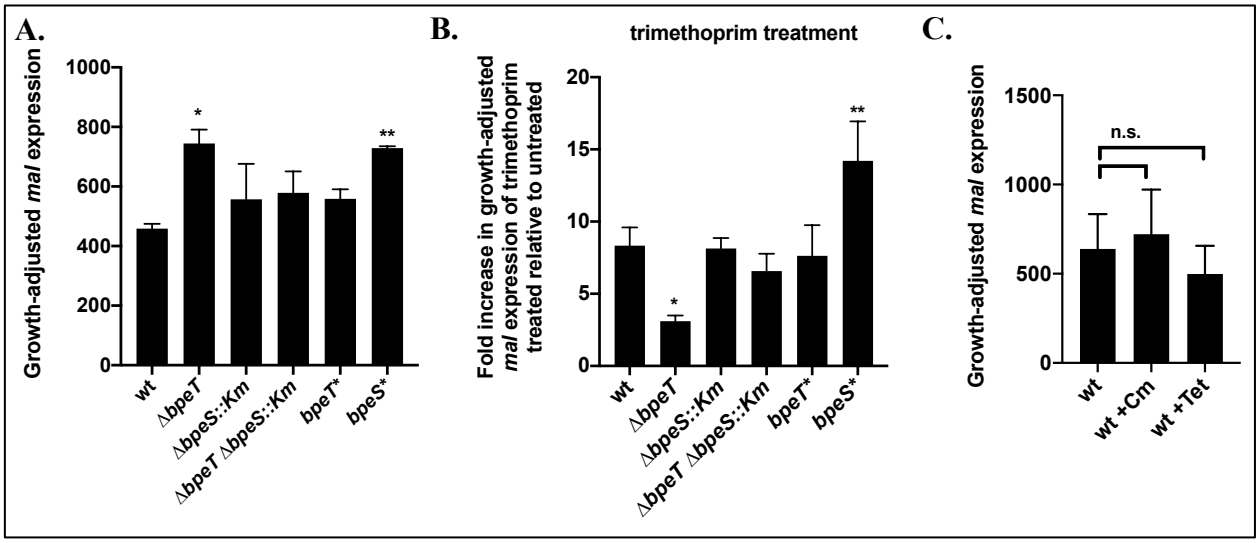

Figure 4.4. Levels of *mal* gene cluster expression in Bp82 strains grown in (A) un-supplemented media and in media supplemented with (B) trimethoprim and with (C) chloramphenicol and tetracycline at concentrations that inhibited growth ~50 to 70% at 24 hrs relative to untreated. All Bp82 strains had the P*malA-lacZ* genetic reporter element chromosomally integrated at the neutral *glmS3* site. Strains and trimethoprim concentrations used (μg/mL): 'wild-type' wt, 15; '*bpeT**' *bpeT* C310R, 75; '*bpeS**' *bpeS* K267T, 150; Δ*bpeT*, 3; Δ*bpeS*::*Km*, 15; Δ*bpeT* Δ*bpeS*::*Km*, 3. Chloramphenicol 'Cm' was used at 20 μg/mL and tetracycline 'Tet' was used at 0.8 μg/mL. Results are the average of the relative light units (the output of enzymatic cleavage of the Tropix kit β-galactosidase substrate) from technical triplicate luminescence readings divided by the OD_{600} of each culture sample (growth-adjusted *mal* expression) and are the averages and standard deviations of at least three independent biological replicates. In (B) for each strain, results are reported as average of the growth-adjusted *mal* expression of the trimethoprim-treated sample divided by the growth-adjusted *mal* expression of the untreated sample. Statistical significance is indicated relative to the Bp82 parent strain using repeated measures (A) or ordinary (B, C) one-way ANOVA and Tukey's multiple comparisons tests: 'n.s.' indicates not significant, *$p < 0.05$ and **$p < 0.008$.

Because trimethoprim is also a substrate of the BpeEF-OprC pump, we sought to ask whether the ability of trimethoprim to activate expression of the *mal* genes (20, 26, 59) requires BpeS or BpeT. To address this possibility, we assessed activation of the P*malA-lacZ* reporter in cells treated with ~50-70% growth-inhibiting trimethoprim concentrations in each of the same *bpeT* and *bpeS* single and double deletion and constitutively activated mutant strains. In trimethoprim-treated cells, the deletion of *bpeT* resulted in less than half the wild-type level of trimethoprim induction, suggesting that BpeT does contribute somewhat toward the activation of P*malA-lacZ* by trimethoprim. Interestingly, cells with the *bpeS** allele showed about 75% stronger *mal* cluster induction when treated with trimethoprim than did wild type. All other alleles and combinations were dispensable for trimethoprim-dependent *mal* cluster expression increases (**Fig. 4.4-B**). While the constitutively active *bpeS** mutant might have a slightly

stronger *mal* induction response to trimethoprim than the wild-type *bpeS,* and the trimethoprim *mal* cluster induction is less robust in the absence of *bpeT*, these data generally support that the trimethoprim induction of the *mal* genes occurs largely independently of the BpeT and BpeS regulators. Further, two additional antibiotic substrates of the BpeEF-OprC efflux pump that were not previously examined in (20), tetracycline and chloramphenicol, did not show *mal* cluster-inducing activity (**Fig. 4.4-C**).

DISCUSSION

Here, we examined the role of the BpeEF-OprC efflux pump in malleilactone export and in mitigating self-toxicity. Our results demonstrate that BpeEF-OprC is important for exporting malleilactone and that this pump contributes to *B. pseudomallei* resistance to endogenous malleilactone pathway biosynthesis products, thereby enabling aversion of self-poisoning by these molecules. The genomic localization of resistance factor genes near the genetic elements responsible for toxin/metabolite biosynthesis has been reported elsewhere (47). Guided by our observation that efflux-deficient *E. coli* Δ*tolC* was at least ~10-fold more susceptible to our purified *B. pseudomallei* malleilactone than efflux-intact *E. coli*, we hypothesized that the close proximity of the BpeEF-OprC efflux pump-encoding genes to the *mal* cluster in *B. pseudomallei* could be indicative of a similar arrangement of a possible resistance mechanism genetically linked to toxin synthesis. The *bpeT* gene and the *llpE-bpeE-bpeF-oprC* gene cluster are conserved across the *B. pseudomallei-thailandensis-mallei* group of *Burkholderia* species (including the *llpE* gene, which doesn't appear to have any structural/functional role in the export process (66) despite being the first gene in the operon), and though its antibiotic substrate profile is known (27, 28, 57, 58), the involvement of BpeEF-OprC in export of natively-produced secondary metabolite substrates had not yet been examined before this study. By measuring malleilactone in cultures and supernatants, we showed that its production is significantly increased in the constitutive *bpeEF-oprC*-activating *bpeT** and *bpeS** SNP mutant strains in an efflux-dependent manner (**Fig. 4.2-B and 4.2-C**). The increase in malleilactone retained in the cell pellet fraction of Δ*bpeEF-oprC* relative to wild-type (**Fig. 4.2-D**), taken together with the malleilactone susceptibility of efflux-deficient *E. coli,* demonstrates that malleilactone efflux is a viable resistance mechanism.

Originally, we were stymied by the very small but not significant self-toxicity effects of inducing malleilactone production in the Δ*bpeEF-oprC* mutant. However, we observed robust and reproducible effects by adjusting our culturing conditions to those thought to stabilize malleicyprol (**Fig. 4.1**) in *B. thailandensis* as per (1). Malleicyprol is a highly reactive cyclopropanol-containing malleilactone

precursor molecule that is believed to exist in a tautomeric mixture of malleicyprol and *iso*-malleicyprol, which can interconvert between those forms and the dimeric/adduct form bis-malleicyprol (**Fig. 4.1**). The purified mixture the authors in (1) obtained of bis-malleicyprol and malleicyprol/*iso*-malleicyprol had increased cytotoxicity over malleilactone toward *C. elegans* in both agar and liquid assays, and it had two-log increased molar antiproliferative activity against human leukemia (K-562) and umbilical endothelial (HUVEC) cells. Further, it was demonstrated *in vitro* that malleicyprol readily converts to malleilactone under basic conditions (1), so we similarly cultured our strains in LB strongly buffered with more acidic pH 6.5 MOPS to favor the malleicyprol isomers. Though we have not yet investigated the malleicyprol-family molecules fully in our lab, our preliminary analytical mass spectrometry observations showed that we could detect both malleilactone (and possibly malleicyprol and/or *iso*-malleicyprol, as all three have identical mass and are thus indistinguishable by this type of chemical analysis) and bis-malleicyprol in wild-type Bp82 cultures and neither of them in *mal* cluster-disrupted Δ*malF* mutant cultures grown under these adjusted conditions (**Table 4.2**). Presumably this Δ*bpeEF-oprC*-dependent growth disadvantage phenotype (**Fig. 4.3-C**) is due to the lack of ability to export the toxic *mal* products, among which could be malleicyprol-family molecules (though additional study is needed to confirm this).

Crude Culture Extracts	Malleilactone (or *iso*-malleicyprol or malleicyprol; *m/z*=305.1) present?	bis-malleicyprol (*m/z*=611.3589) present?
Bp82 P*lac-malR*	Yes	Yes
Bp82 Δ*malF* P*lac-malR*	No	No

Table 4.2. Mass spectrometry (negative ion mode) analysis examining the presence of malleilactone-family molecules in ethyl acetate extracts of cultures of Bp82 and Bp82 Δ*malF* strains.

Our observation that malleilactone causes self-toxicity was dependent on the addition of paraquat to the growth medium. Paraquat generates oxygen radicals, thereby causing cellular stress. It is possible that causing cellular stress in this way could in itself increase susceptibility to the toxic malleilactone biosynthesis products. Alternatively, it is possible that paraquat further increases malleilactone production in the cell, though this possibility is unlikely as we have previously determined that *mal* expression is

unaffected by paraquat treatment (20). We do note that it has been shown that paraquat can activate the AcrAB-TolC efflux pump in *Salmonella enterica* serovar Typhimurium (67) in a manner dependent upon the superoxide-responsive AraC-family transcriptional activator SoxS. BpeEF-OprC efflux could be similarly more active in cells treated with paraquat, and though this has not yet been tested in *B. pseudomallei*, RNA sequencing showed that transcripts of the *llpE-bpeE-bpeF-oprC* genes were elevated ~7 to 10-fold under trimethoprim treatment in *B. thailandensis* (68). Paraquat activation of the BpeEF-OprC pump could potentially enhance the protective effects we observed in our growth experiments.

Our findings suggest that BpeEF-OprC might have primary functions of exporting malleilactone or other products made by the *mal* biosynthetic gene cluster and mitigating associated self-toxicity. This efflux pump was previously studied for its role in trimethoprim resistance, though it also has specificity for additional antibiotics such as fluoroquinolones, chloramphenicol, and tetracyclines (49). The presence of efflux pump substrates is sometimes the primary activation efflux mechanism. Some BpeEF-OprC antibiotic substrates (i.e. trimethoprim, sulfamethoxazole, ciprofloxacin) are also able to elicit *mal* cluster expression and malleilactone biosynthesis in both *B. pseudomallei* and *B. thailandensis* (20, 26), though treatment with 50-70% growth-inhibiting concentrations of chloramphenicol and tetracycline did not (**Fig. 4.4-C**). Work by others showed that short-term doxycycline (a tetracycline antibiotic) and chloramphenicol exposure caused dose-dependent *bpeF* efflux gene expression increases in Bp82 even in the absence of *bpeT* and *bpeS*, suggesting that these regulators are dispensable for doxycycline- and chloramphenicol-induced efflux expression (28, 69). Authors in (27, 70) showed that short-term 32 μg/mL trimethoprim exposure did not appreciably induce *bpeF* in strain 1026b (the Bp82 parent strain), and though it did in some highly trimethoprim-resistant *B. pseudomallei* environmental and clinical isolates, that high-trimethoprim *bpeF* induction occurred independently of BpeT. Conversely, BpeT is somewhat responsible for lower-dose trimethoprim induction of *bpeEF-oprC* , as short-term 1 μg/mL exposure increased *bpeF* ~3-fold in Bp82 but reduced *bpeF* in the absence of *bpeT*; however, *bpeF* expression was unchanged in the absence of BpeS singly or with Δ*bpeT* (28, 69). Thus, we were interested in understanding any possible cross-regulation of the *mal* gene cluster and the efflux pump

gene cluster by the BpeT or BpeS regulators or trimethoprim. Our relative *mal* expression data (**Fig. 4.4**), which was obtained under the growth-slowing concentration of 3 μg/mL for Δ*bpeT*, tracks well with the previous data showing that deleting *bpeT* makes the trimethoprim response less robust. Notably, we had to use 150 μg/mL trimethoprim for *bpeS** to achieve inhibition to the same degree, and that led to increased P*malA-lacZ* expression in both treated and untreated cells. Altogether, these data suggest that BpeT and BpeS appear to have at least minor roles in modulating malleilactone gene expression, but that they are not fully required for the phenotype of increased *mal* expression in the presence of growth-inhibiting concentrations of trimethoprim.

It is still unclear precisely how trimethoprim is sensed by cells and thus acts to modulate BpeEF-OprC activity in response. However, more is known regarding trimethoprim upregulation of the *mal* genes. Trimethoprim increases expression of the positive *mal* regulator MalR (20), which is important for the subsequent increase in *mal* expression. Recent work (68) in *B. thailandensis* showed that sublethal trimethoprim, by inhibition of dihydrofolate reductase, causes accumulation of the methionine precursor homoserine, which promotes robust malleilactone production in a *malR*-dependent manner. The sensing of similar (but yet unknown) pathway intermediates, substrates, or byproducts by BpeT, BpeS, or another regulator might be an important mechanism for *bpeEF-oprC* regulation, though it remains unclear exactly how the regulation of these activities might be purposefully linked toward moderating self-toxicity. It is possible that BpeEF-OprC evolved primarily to export endogenous products like malleilactone but has since adapted roles in broad-spectrum export of various antibiotic substrates encountered in the environmental reservoir. The relative genetic silence of the *mal* and *bpeEF-oprC* operons in typical laboratory conditions and the increases of each in response to cellular stressors like trimethoprim (and of efflux perhaps by paraquat) could indicate a more careful mechanism of activity control for both that is restricted to conditions when each function will be either most useful or least energetically costly to cells, or both. This idea is supported by our previous work showing that the quorum sensing-activated regulator ScmR represses malleilactone production in high-density late growth stages by reducing *malR* expression, suggesting that *mal* products are no longer needed in such conditions and are therefore decreased. The

fact that cells are not completely killed when *mal* is overproduced, when they are under cellular stress, and when efflux is deficient indicate that there likely are yet other mechanisms which can assist in malleilactone self-toxicity prevention, such as a reverse chemical shift along the *mal* biosynthetic pathway or additional enzymatic inactivation of the bioactive forms of the *mal* products, in addition to the role played by quorum sensing-mediated repression. A more thorough understanding of how *mal* self-toxicity is managed by cells could be exploited as a therapeutic approach to treating *B. pseudomallei* infections by disabling its toxicity management system and thereby promoting *mal*-mediated self-destruction of infecting cells. Ultimately, this work provides multiple lines of evidence to support the reduction of self-harmful effects of cytotoxic *mal* gene cluster products by export via the genetically adjacent BpeEF-OprC efflux pump.

REFERENCES

1. Trottmann F, Franke J, Richter I, Ishida K, Cyrulies M, Dahse HM, Regestein L, Hertweck C. 2019. Cyclopropanol Warhead in Malleicyprol Confers Virulence of Human- and Animal-Pathogenic *Burkholderia* Species. Angew Chem Int Ed Engl doi:10.1002/anie.201907324.

2. Wilkinson L. 1981. Glanders: medicine and veterinary medicine in common pursuit of a contagious disease. Med Hist 25:363-84.

3. Van Zandt KE, Greer MT, Gelhaus HC. 2013. Glanders: an overview of infection in humans. Orphanet J Rare Dis 8:131.

4. Brett PJ, DeShazer D, Woods DE. 1998. *Burkholderia thailandensis* sp. nov., a *Burkholderia pseudomallei*-like species. Int J Syst Bacteriol 48 Pt 1:317-20.

5. Brett PJ, Deshazer D, Woods DE. 1997. Characterization of *Burkholderia pseudomallei* and *Burkholderia pseudomallei*-like strains. Epidemiol Infect 118:137-48.

6. White NJ. 2003. Melioidosis. The Lancet 361:1715-1722.

7. Wuthiekanun V SM, Dance DAB, White NJ. 1995. The isolation of *Pseudomonas pseudomallei* from soil in Northeastern Thailand. Transactions of the Royal Society of Tropical Medicine and Hygiene 89:41-43.

8. Wiersinga WJ, Currie BJ, Peacock SJ. 2012. Melioidosis. N Engl J Med 367:1035-44.

9. Cheng AC, Currie BJ. 2005. Melioidosis: epidemiology, pathophysiology, and management. Clin Microbiol Rev 18:383-416.

10. Currie BJ. 2015. Melioidosis: evolving concepts in epidemiology, pathogenesis, and treatment. Semin Respir Crit Care Med 36:111-25.

11. Limmathurotsakul D, Golding N, Dance DAB, Messina JP, Pigott DM, Moyes CL, Rolim DB, Bertherat E, Day NPJ, Peacock SJ, Hay SI. 2016. Predicted global distribution of *Burkholderia pseudomallei* and burden of melioidosis. Nature Microbiology 1.

12. Propst KL, Mima T, Choi KH, Dow SW, Schweizer HP. 2010. A *Burkholderia pseudomallei* Δ*purM* mutant is avirulent in immunocompetent and immunodeficient animals: candidate strain for exclusion from select-agent lists. Infect Immun 78:3136-43.

13. Norris MH, Propst KL, Kang Y, Dow SW, Schweizer HP, Hoang TT. 2011. The *Burkholderia pseudomallei* Δ*asd* mutant exhibits attenuated intracellular infectivity and imparts protection against acute inhalation melioidosis in mice. Infect Immun 79:4010-8.

14. Gutierrez MG, Warawa JM. 2016. Attenuation of a select agent-excluded *Burkholderia pseudomallei* capsule mutant in hamsters. Acta Trop 157:68-72.

15. Warawa JM, Long D, Rosenke R, Gardner D, Gherardini FC. 2009. Role for the *Burkholderia pseudomallei* capsular polysaccharide encoded by the *wcb* operon in acute disseminated melioidosis. Infect Immun 77:5252-61.

16. Norris MH, Kang Y, Lu D, Wilcox BA, Hoang TT. 2009. Glyphosate resistance as a novel select-agent-compliant, non-antibiotic-selectable marker in chromosomal mutagenesis of the essential genes asd and *dapB* of *Burkholderia pseudomallei*. Appl Environ Microbiol 75:6062-75.

17. Seyedsayamdost MR, Chandler JR, Blodgett JA, Lima PS, Duerkop BA, Oinuma K, Greenberg EP, Clardy J. 2010. Quorum-sensing-regulated bactobolin production by *Burkholderia thailandensis* E264. Org Lett 12:716-9.

18. Amunts A, Fiedorczuk K, Truong TT, Chandler J, Greenberg EP, Ramakrishnan V. 2015. Bactobolin A binds to a site on the 70S ribosome distinct from previously seen antibiotics. J Mol Biol 427:753-755.

19. Chandler JR, Truong TT, Silva PM, Seyedsayamdost MR, Carr G, Radey M, Jacobs MA, Sims EH, Clardy J, Greenberg EP. 2012. Bactobolin resistance is conferred by mutations in the L2 ribosomal protein. mBio 3.

20. Klaus JR, Deay J, Neuenswander B, Hursh W, Gao Z, Bouddhara T, Williams TD, Douglas J, Monize K, Martins P, Majerczyk C, Seyedsayamdost MR, Peterson BR, Rivera M, Chandler JR. 2018. Malleilactone Is a *Burkholderia pseudomallei* Virulence Factor Regulated by Antibiotics and Quorum Sensing. J Bacteriol 200.

21. Biggins JB, Ternei MA, Brady SF. 2012. Malleilactone, a polyketide synthase-derived virulence factor encoded by the cryptic secondary metabolome of *Burkholderia pseudomallei* group pathogens. J Am Chem Soc 134:13192-5.

22. Chandler JR, Heilmann S, Mittler JE, Greenberg EP. 2012. Acyl-homoserine lactone-dependent eavesdropping promotes competition in a laboratory co-culture model. ISME J 6:2219-28.

23. Evans KC, Benomar S, Camuy-Velez LA, Nasseri EB, Wang X, Neuenswander B, Chandler JR. 2018. Quorum-sensing control of antibiotic resistance stabilizes cooperation in *Chromobacterium violaceum*. ISME J 12:1263-1272.

24. Zhang Y, Wen WH, Pu JY, Tang MC, Zhang L, Peng C, Xu Y, Tang GL. 2018. Extracellularly oxidative activation and inactivation of matured prodrug for cryptic self-resistance in naphthyridinomycin biosynthesis. Proc Natl Acad Sci U S A 115:11232-11237.

25. Franke J, Ishida K, Hertweck C. 2012. Genomics-driven discovery of burkholderic acid, a noncanonical, cryptic polyketide from human pathogenic *Burkholderia* species. Angew Chem Int Ed Engl 51:11611-5.

26. Truong TT, Seyedsayamdost M, Greenberg EP, Chandler JR. 2015. A *Burkholderia thailandensis* Acyl-Homoserine Lactone-Independent Orphan LuxR Homolog That Activates Production of the Cytotoxin Malleilactone. J Bacteriol 197:3456-62.

27. Podnecky NL, Wuthiekanun V, Peacock SJ, Schweizer HP. 2013. The BpeEF-OprC efflux pump is responsible for widespread trimethoprim resistance in clinical and environmental *Burkholderia pseudomallei* isolates. Antimicrob Agents Chemother 57:4381-6.

28. Podnecky NL, Rhodes KA, Mima T, Drew HR, Chirakul S, Wuthiekanun V, Schupp JM, Sarovich DS, Currie BJ, Keim P, Schweizer HP. 2017. Mechanisms of Resistance to Folate Pathway Inhibitors in *Burkholderia pseudomallei*: Deviation from the Norm. MBio 8.

29. Choi KH, Mima T, Casart Y, Rholl D, Kumar A, Beacham IR, Schweizer HP. 2008. Genetic tools for select-agent-compliant manipulation of *Burkholderia pseudomallei*. Appl Environ Microbiol 74:1064-75.

30. Datsenko KA, Wanner BL. 2000. One-step inactivation of chromosomal genes in *Escherichia coli* K-12 using PCR products. Proc Natl Acad Sci U S A 97:6640-5.

31. Baba T, Ara T, Hasegawa M, Takai Y, Okumura Y, Baba M, Datsenko KA, Tomita M, Wanner BL, Mori H. 2006. Construction of *Escherichia coli* K-12 in-frame, single-gene knockout mutants: the Keio collection. Molecular Systems Biology 2:2006.0008.

32. Li XZ, Plesiat P, Nikaido H. 2015. The challenge of efflux-mediated antibiotic resistance in Gram-negative bacteria. Clin Microbiol Rev 28:337-418.

33. Zgurskaya HI, Krishnamoorthy G, Ntreh A, Lu S. 2011. Mechanism and Function of the Outer Membrane Channel TolC in Multidrug Resistance and Physiology of Enterobacteria. Front Microbiol 2:189.

34. Koronakis V, Eswaran J, Hughes C. 2004. Structure and function of TolC: the bacterial exit duct for proteins and drugs. Annu Rev Biochem 73:467-89.

35. Elkins CA, Mullis LB. 2006. Mammalian steroid hormones are substrates for the major RND- and MFS-type tripartite multidrug efflux pumps of *Escherichia coli*. J Bacteriol 188:1191-5.

36. Tikhonova EB, Zgurskaya HI. 2004. AcrA, AcrB, and TolC of *Escherichia coli* Form a Stable Intermembrane Multidrug Efflux Complex. J Biol Chem 279:32116-24.

37. Anes J, McCusker MP, Fanning S, Martins M. 2015. The ins and outs of RND efflux pumps in *Escherichia coli*. Front Microbiol 6:587.

38. Thanabalu T, Koronakis E, Hughes C, Koronakis V. 1998. Substrate-induced assembly of a contiguous channel for protein export from *E. coli*: reversible bridging of an inner-membrane translocase to an outer membrane exit pore. EMBO J 17:6487-96.

39. Wandersman C, Delepelaire P. 1990. TolC, an *Escherichia coli* outer membrane protein required for hemolysin secretion. Proc Natl Acad Sci U S A 87:4776-80.

40. Hwang J, Zhong X, Tai PC. 1997. Interactions of dedicated export membrane proteins of the colicin V secretion system: CvaA, a member of the membrane fusion protein family, interacts with CvaB and TolC. J Bacteriol 179:6264-70.

41. Gilson L, Mahanty HK, Kolter R. 1990. Genetic analysis of an MDR-like export system: the secretion of colicin V. The EMBO Journal 9:3875-3884.

42. Sulavik MC, Houseweart C, Cramer C, Jiwani N, Murgolo N, Greene J, DiDomenico B, Shaw KJ, Miller GH, Hare R, Shimer G. 2001. Antibiotic susceptibility profiles of *Escherichia coli* strains lacking multidrug efflux pump genes. Antimicrob Agents Chemother 45:1126-36.

43. Piddock LJ. 2006. Multidrug-resistance efflux pumps - not just for resistance. Nat Rev Microbiol 4:629-36.

44. Hopwood DA. 2007. How do antibiotic-producing bacteria ensure their self-resistance before antibiotic biosynthesis incapacitates them? Mol Microbiol 63:937-40.

45. Almabruk KH, Dinh LK, Philmus B. 2018. Self-Resistance of Natural Product Producers: Past, Present, and Future Focusing on Self-Resistant Protein Variants. ACS Chem Biol 13:1426-1437.

46. Ogawara H. 2018. Comparison of Strategies to Overcome Drug Resistance: Learning from Various Kingdoms. Molecules 23.

47. Sakhtah H, Koyama L, Zhang Y, Morales DK, Fields BL, Price-Whelan A, Hogan DA, Shepard K, Dietrich LE. 2016. The *Pseudomonas aeruginosa* efflux pump MexGHI-OpmD transports a natural phenazine that controls gene expression and biofilm development. Proc Natl Acad Sci U S A 113:E3538-47.

48. Holden MT, Titball RW, Peacock SJ, Cerdeno-Tarraga AM, Atkins T, Crossman LC, Pitt T, Churcher C, Mungall K, Bentley SD, Sebaihia M, Thomson NR, Bason N, Beacham IR, Brooks K, Brown KA, Brown NF, Challis GL, Cherevach I, Chillingworth T, Cronin A, Crossett B, Davis P, DeShazer D, Feltwell T, Fraser A, Hance Z, Hauser H, Holroyd S, Jagels K, Keith KE, Maddison M, Moule S, Price C, Quail MA, Rabbinowitsch E, Rutherford K, Sanders M, Simmonds M, Songsivilai S, Stevens K, Tumapa S, Vesaratchavest M, Whitehead S, Yeats C, Barrell BG, Oyston PC, Parkhill J. 2004. Genomic plasticity of the causative agent of melioidosis, *Burkholderia pseudomallei*. Proc Natl Acad Sci U S A 101:14240-5.

49. Podnecky NL, Rhodes KA, Schweizer HP. 2015. Efflux pump-mediated drug resistance in *Burkholderia*. Front Microbiol 6:305.

50. Moore RA, DeShazer D, Reckseidler S, Weissman A, Woods DE. 1999. Efflux-Mediated Aminoglycoside and Macrolide Resistance in *Burkholderia pseudomallei*. Antimicrobial Agents and Chemotherapy 43:465-470.

51. Viktorov DV, Zakharova IB, Podshivalova MV, Kalinkina EV, Merinova OA, Ageeva NP, Antonov VA, Merinova LK, Alekseev VV. 2008. High-level resistance to fluoroquinolones and cephalosporins in *Burkholderia pseudomallei* and closely related species. Transactions of the Royal Society of Tropical Medicine and Hygiene 102:S103-S110.

52. Mima T, Schweizer HP, Xu ZQ. 2011. *In vitro* activity of cethromycin against *Burkholderia pseudomallei* and investigation of mechanism of resistance. J Antimicrob Chemother 66:73-8.

53. Trunck LA, Propst KL, Wuthiekanun V, Tuanyok A, Beckstrom-Sternberg SM, Beckstrom-Sternberg JS, Peacock SJ, Keim P, Dow SW, Schweizer HP. 2009. Molecular basis of rare aminoglycoside susceptibility and pathogenesis of *Burkholderia pseudomallei* clinical isolates from Thailand. PLoS Negl Trop Dis 3:e519.

54. Mima T, Schweizer HP. 2010. The BpeAB-OprB efflux pump of *Burkholderia pseudomallei* 1026b does not play a role in quorum sensing, virulence factor production, or extrusion of aminoglycosides but is a broad-spectrum drug efflux system. Antimicrob Agents Chemother 54:3113-20.

55. Chan YY, Bian HS, Tan TM, Mattmann ME, Geske GD, Igarashi J, Hatano T, Suga H, Blackwell HE, Chua KL. 2007. Control of quorum sensing by a *Burkholderia pseudomallei* multidrug efflux pump. J Bacteriol 189:4320-4.

56. Chan YY, Chua KL. 2005. The *Burkholderia pseudomallei* BpeAB-OprB efflux pump: expression and impact on quorum sensing and virulence. J Bacteriol 187:4707-19.

57. Kumar A, Chua KL, Schweizer HP. 2006. Method for regulated expression of single-copy efflux pump genes in a surrogate *Pseudomonas aeruginosa* strain: identification of the BpeEF-OprC chloramphenicol and trimethoprim efflux pump of *Burkholderia pseudomallei* 1026b. Antimicrob Agents Chemother 50:3460-3.

58. Randall LB, Georgi E, Genzel GH, Schweizer HP. 2017. Finafloxacin overcomes *Burkholderia pseudomallei* efflux-mediated fluoroquinolone resistance. J Antimicrob Chemother 72:1258-1260.

59. Seyedsayamdost MR. 2014. High-throughput platform for the discovery of elicitors of silent bacterial gene clusters. Proc Natl Acad Sci U S A 111:7266-71.

60. Hassan H.M. FI. 1979. Paraquat and *Escherichia coli*: Mechanism of production of extracellular superoxide radical. Journal of Biological Chemistry 254:10846-10852.

61. Scott MD, Meshnick SR, Eaton JW. 1987. Superoxide Dismutase-rich Bacteria. Journal of Biological Chemistry 262:3640-2645.

62. Mak S, Xu Y, Nodwell JR. 2014. The expression of antibiotic resistance genes in antibiotic-producing bacteria. Mol Microbiol 93:391-402.

63. Peterson E, Kaur P. 2018. Antibiotic Resistance Mechanisms in Bacteria: Relationships Between Resistance Determinants of Antibiotic Producers, Environmental Bacteria, and Clinical Pathogens. Front Microbiol 9:2928.

64. Alcalde-Rico M, Hernando-Amado S, Blanco P, Martinez JL. 2016. Multidrug Efflux Pumps at the Crossroad between Antibiotic Resistance and Bacterial Virulence. Front Microbiol 7:1483.

65. Blanco P, Hernando-Amado S, Reales-Calderon JA, Corona F, Lira F, Alcalde-Rico M, Bernardini A, Sanchez MB, Martinez JL. 2016. Bacterial Multidrug Efflux Pumps: Much More Than Antibiotic Resistance Determinants. Microorganisms 4.

66. Rhodes KA, Somprasong N, Podnecky NL, Mima T, Chirakul S, Schweizer HP. 2018. Molecular determinants of *Burkholderia pseudomallei* BpeEF-OprC efflux pump expression. Microbiology 164:1156-1167.

67. Nikaido E, Shirosaka I, Yamaguchi A, Nishino K. 2011. Regulation of the AcrAB multidrug efflux pump in *Salmonella enterica* serovar Typhimurium in response to indole and paraquat. Microbiology 157:648-655.

68. Li A, Mao D, Yoshimura A, Rosen PC, Martin WL, Gallant E, Wuhr M, Seyedsayamdost MR. 2020. Multi-Omic Analyses Provide Links between Low-Dose Antibiotic Treatment and Induction of Secondary Metabolism in *Burkholderia thailandensis*. mBio 11.

69. Rhodes KA. 2016. Complex Regulation of BpeEF-OprC Mediated Drug Efflux in *Burkholderia pseudomallei*. Dissertation Department of Microbiology, Immunology, and Pathology, Colorado State University, Fort Collins, Colorado.

70. Podnecky NL. 2013. Folate Pathway Inhibitor Resistance Mechanisms in *Burkholderia pseudomallei*. Dissertation Department of Microbiology, Immunology, and Pathology, Colorado State University, Fort Collins, Colorado.

Chapter 5: The potential role of the cytotoxic polyketide malleilactone in *Burkholderia pseudomallei* iron acquisition

COLLABORATIONS AND WORKLOAD ALLOCATIONS:

Jennifer R. Klaus did the cloning and genetic manipulations, performed *lacZ* transcriptional reporter assays (with optimization by Catherine Kerr), and performed growth yield experiments. Jennifer R. Klaus and Wyatt Hursh optimized and performed sample preparation for UV-Vis and mass spectrometry (MS) analysis. Benjamin Neuenswander performed UV-Vis/MS analyses and assisted Jennifer R. Klaus in data interpretation. Benjamin Neuenswander purified malleilactone. Iron binding spectophotometric assays were performed by Anabel Soldano and Mario Rivera. Mohammad R. Seyedsayamdost and Mario Rivera provided conceptual project discussions and experimental design input. Jennifer R. Klaus and Josephine R. Chandler managed overall project conceptualization and experimental design.

ABSTRACT

Infections by the antibiotic-resistant opportunistic bacterial pathogen *Burkholderia pseudomallei*, termed melioidosis, are difficult to treat and can be fatal up to 40% of the time. Thus, studies of its virulence factors and elements of its biology that can be exploited as druggable targets are important for the future of successfully managing infections. *B. pseudomallei* encodes many secondary metabolites that have contributions to its pathogenicity. One such secondary metabolite is malleilactone, a small molecule cytotoxin that is important for *B. pseudomallei* virulence in various infection models. Here, we show that malleilactone appears to play a role in the ability of *B. pseudomallei* to survive severe limitation of iron. Iron is a required growth nutrient for bacteria (1), and it is of especially low bioavailability within eukaryotic hosts (2, 3). First, we demonstrate that expression of the *mal* gene cluster, which encodes the proteins that synthesize malleilactone, is increased in iron starvation conditions relative to iron-replete media. Our studies show that the genetically linked malleilactone activator MalR is important for the iron starvation-induced *mal* expression increase in *B. pseudomallei*. The host-responsive transcriptional regulators Fur and HrpB, as well as acyl-homoserine lactone quorum sensing and malleilactone itself do not modulate *mal* expression in low iron, though the secondary metabolite regulator ScmR has a suppressive effect. We used chemical titration experiments to demonstrate that culture-purified malleilactone is able to coordinate with ferric iron. Finally, we show that a malleilactone-deficient strain has a growth defect compared to the malleilactone-producing wild-type under iron starvation, though this occurs in a manner dependent on the presence of bacterially-produced iron chelating siderophores, suggesting that malleilactone might assist siderophores Altogether, our data support the idea that malleilactone is a previously unrecognized player in the important process of acquiring iron from limited-resource environments, such as within a host. Thus, malleilactone might contribute to the virulence of *B. pseudomallei* by aiding in iron acquisition during host infections.

INTRODUCTION

Melioidosis is an often-fatal, difficult-to-treat infection caused by the intrinsically antibiotic-resistant opportunistic pathogen *Burkholderia pseudomallei* (4-6). This disease is most prevalent in semi-tropical regions such as Vietnam, Thailand, and northern Australia, causing an ~40% case mortality rate depending on the severity of infection and availability of treatment, with an estimated 89,000 annual deaths (7). The soils and water of such regions are known environmental reservoirs of *B. pseudomallei*, which infect humans through inhalation of aerosolized bacteria (especially during the rainy season) or through exposure to open wounds or breaks in the skin. Most often presenting as deep-lung pneumonia, melioidosis can also cause abscesses, abdominal pain, organ failure, and sepsis. Treatment consists of a multi-week acute phase of intravenous antibiotics followed by a multi-month eradication phase of oral antibiotic therapy in order to ensure clearance (4, 8). Melioidosis relapse has also been observed (9-12). Thus, as a dangerous bacterial pathogen with a low infective dose, strong innate antibiotic resistance, and high aerosolization potential, *B. pseudomallei* is classified as a Centers for Disease Control (CDC) tier 1 select agent (https://www.selectagents.gov/SelectAgentsandToxinsList.html), and its study is restricted to biosafety level 3 (BSL3) facilities with the exception of a handful of attenuated, BSL2-safe mutant strains generated in the past decade. While some virulence factors have been characterized (13-16), much remains to be understood about the mechanisms by which *B. pseudomallei* causes disease.

Secondary metabolite small molecules could play yet-uncharacterized important roles in *B. pseudomallei* virulence (17), especially in bacterial infections manifesting in such a wide array of symptoms as melioidosis. One such small molecule is malleilactone, which is encoded by the *malA-malM* gene cluster. First described in 2012 (18, 19) in the soil saprophyte *B. thailandensis*, a non-pathogenic close relative of *B. pseudomallei*, it has been previously shown to be important for virulence of both species in *Caenorhabditis elegans* nematodes (18, 20) and of *B. thailandensis* to the social amoeba *Dictyostelium discoideum* (18). Additionally, two different transposon sequencing (Tn-seq) studies have

demonstrated using mouse melioidosis models that some transposon-disrupted *mal* genes showed reduced fitness by 3- to 7-fold in the mouse lung and that a *malA* disruption had a ~40-fold fitness reduction in the mouse spleen (14, 15). This body of evidence suggests that malleilactone contributes to *B. pseudomallei* pathogenesis in a variety of hosts, though our mechanistic understanding of this is still in its infancy. One mechanism of virulence could be through its cytotoxicity, which was demonstrated using purified malleilactone against eukaryotic cells and select Gram-positive bacteria (18, 20). Another possible role of malleilactone in pathogenesis is in iron acquisition.

Iron is a critical nutrient for bacteria, serving as an enzyme co-factor for a variety of vital processes, including respiration, DNA replication, and nitrogen fixation (1, 21). The environmental bioavailability of iron is vanishingly low, as vertebrate hosts have evolved intracellular iron storage mechanisms such as heme and transferrin (3) to keep essential iron sequestered away from bacterial pathogens. One mechanism that pathogens have evolved to reacquire that tightly-bound host iron is the use of siderophores, which are potent chelators. Siderophores are exported, they scavenge iron from host protein-iron complexes, and then they are reimported and shuttle their bound iron to be used in various enzymatic pathways or stored until needed in proteins such as ferritin and bacterioferritin (22). Pyochelin and malleobactin are examples of siderophores produced and utilized by *B. pseudomallei* (23-25). However, even in the absence of these major *B. pseudomallei* siderophores malleobactin and pyochelin, some residual siderophore-like iron binding activity is detectable using a chrome azurol S (CAS) chelation plate assay (26). These results suggest that *B. pseudomallei* produces factors other than pyochelin and malleobactin that are involved in transporting iron.

Several lines of evidence suggest malleilactone could be important for transporting iron. First, a key malleilactone positive regulator, MalR (20, 27), is transcriptionally upregulated in low-iron growth conditions relative to iron-replete conditions, ~25% more highly in microarrays of cultures grown in Chelex-100 resin-chelated tryptic soy broth. Because many factors involved in iron transport are upregulated during growth in low iron, these findings support the idea that malleilactone has a similar role

in iron transport. Additionally, the Biggins group, one of the first to characterize the malleilactone molecule, demonstrated using a chromogenic liquid CAS assay that their *B. thailandensis* purified malleilactone is able to bind to iron (18). They proposed that based on its structure, malleilactone could coordinate with ferric iron molecules using a mechanism similar to that of two other known families of molecules with iron-binding properties: tetronic acids and tetramic acids. Tetramic acids (see (28) for an extensive historical review) contain derivatives of a common 2,4-pyrrolidinedione ring structural unit that is present in natural products from a wide variety of biological sources, and they have diverse biological functions such as antiviral, anticancer, and antimicrobial activities. In *Pseudomonas aeruginosa,* C_{12}-tetramic acid, derived from the 3-oxo-C_{12}-homoserine lactone (HSL) quorum-sensing (QS) molecule, can dissipate the membrane potential and pH gradients of some Gram-positive bacteria (29). Importantly, tetramic acids and tetronic acids (4-hydroxy-[5H] furan-2-ones) both have known potent metal binding capabilities, including to iron (30, 31).

Here, we investigate the idea that malleilactone binds iron and is important for transporting iron into the cell. We show that purified malleilactone does bind iron. We also show that malleilactone provides a fitness benefit to *B. pseudomallei* in iron-liming conditions. We posit that malleilactone could be involved in transporting iron through an iron-binding or chelation mechanism related to that of siderophores, or as an accessory to existing iron acquisition systems.

MATERIALS AND METHODS

Bacterial strains, culture conditions, and reagents.

All bacterial strains and plasmids used in this study are listed in **Table 5.1**. All experiments with *B. pseudomallei* used the select agent-excluded strain Bp82 (32), an adenine and thiamine auxotrophic mutant of the BSL3-restricted strain 1026b. Genetic manipulations were carried out in either *E. coli* strain DH5α (Invitrogen) or strain DH10B (Invitrogen). Bacteria were grown in Luria-Bertani (LB) broth (10g tryptone, 5g yeast extract, and 5g NaCl per liter) supplemented with 50 mM morpholinopropanesulfonic acid (MOPS) pH=7.0, or in M9 minimal media supplemented with 0.4% glucose and 10 mM *para*-chloro-phenylalanine (*p*-Cl-Phe; Sigma) for *B. pseudomallei* counterselection during mutant construction. With the exception of LB agar plates, all *B. pseudomallei* growth media was supplemented with 1.6 mM adenine hemisulfate and 0.005% thiamine HCl. Growth was at 37˚C with shaking at 250 rpm. The inducer molecule isopropyl-β-D-thiogalactopyranoside (IPTG) was used at 1 mM as indicated. Where appropriate, the following antibiotics were used (per mL): 50 μg (*E. coli*) and 1 mg (*B. pseudomallei*) kanamycin, 100 μg (*E. coli*) ampicillin, and 25 μg (*E. coli*) and 2 mg (*B. pseudomallei*) zeocin. For iron growth experiments, the defined minimal media protocol for low-iron conditions as per (33) was used with minor modifications (supplemented with 20% glucose, 1.6 mM adenine hemisulfate, and 0.005% thiamine HCl). Overnight starter cultures in the same media were back-diluted to an OD_{600} of 0.05 in 4mL volumes in 14 mL plastic culture tubes for growth experiments (**Fig. 5.3**) and in 10 mL volumes in "iron-stripped" 125 mL flat-bottom Bellco Erlenmeyer flasks that were soaked overnight with 10% TraceSelect nitric acid (Sigma), rinsed with milliQ deionized water, soaked for 2-3 hours with ~0.05M ethylenediaminetetraacetid acid (EDTA), and again rinsed with milliQ deionized water before sterilization for LacZ assays (**Fig. 5.1-C**). All samples were incubated for 24 hours before analysis.

Genomic DNA, plasmid DNA, and PCR and DNA fragments were obtained using the Qiagen Puregene Core A kit, miniprep plasmid purification kit, or gel-extraction/PCR clean-up kits (IBI or Qiagen), respectively, according to the manufacturers' protocols.

Table 5.1 Plasmids and bacterial strains used in this study and relevant biological properties.

Plasmid	Relevant properties	Reference
pEX18km-*pheS*	Plasmid used to make unmarked, non-polar deletions in *B. pseudomallei;* Km^R	(34)
pEX18km-*pheS*-Δ*hrpB*	pEX18km-*pheS* plasmid used to make *hrpB* deletion	This study
pEX18km-*pheS*-Δ*mbaJ*	pEX18km-*pheS* plasmid used to make *mbaJ* deletion	This study
pEX18km-*pheS*-Δ*pchAB*	pEX18km-*pheS* plasmid used to make *pchAB* deletion	This study
pUC18miniTn7T-P*malA-lacZ*	LacZ reporter driven by the *malA* promoter	(20)
pUC18miniTn7T-Kan-P*lac*	IPTG-inducible empty expression vector	(20)
pUC18miniTn7T-Kan-P*lac-malR*	IPTG-inducible *malR* for *mal* cluster overexpression	(20)
pUC18miniTn7T-Kan-P*lac-hrpB*	IPTG-inducible *hrpB* for *mal* cluster overexpression	This study
pTNS3	Transposase-expressing suicide helper plasmid	(35)
Bacterial strain	**Relevant properties**	**Reference**
E. coli DH5α	Genetic manipulations	Invitrogen
E. coli DH10B	Genetic manipulations	Invitrogen
Burkholderia pseudomallei Bp82	Δ*purM* mutant of strain 1026b	(32)
Bp82 *glmS3*::P*malA-lacZ*		(20)
Bp82 Δ*pchAB*Δ*mbaJ*	Bp82 with deletions in *pchAB* and *mbaJ*	This study
Bp82 Δ*malF* Δ*pchAB*Δ*mbaJ*	Bp82 with deletions in *malF, pchAB* and *mbaJ*	This study
Bp82 Δ*malR*	Bp82 with deletion in *malR*	(20)
Bp82 Δ*malF*	Bp82 with deletion in *malF*	(20)
Bp82 Δ*hrpB*	Bp82 with deletion in *hrpB*	This study
Bp82 Δ*scmR*	Bp82 with deletion in *scmR*	(20)
CM139 aka Bp82 Δ*bpsI1*Δ*bpsI2*Δ*bpsI3*	Acyl-homoserine lactone-deficient, AHL^-	(36)
Bp82 *glmS3*::P*lac-malR*		(20)
Bp82 *glmS3*::P*lac* (empty vector)		(20)
Bp82 *glmS3*::P*lac-hrpB*		This study
Bp82 Δ*malR glmS3*::P*lac-hrpB*		This study
Burkholderia pseudomallei JW270	Δ*wcb* mutant of strain DD503 (37) derived from 1026b	(38)
JW270 Δ*fur*	Δ*fur* mutant of strain JW270	J. Warawa, unpublished
JW270 *glmS3*::P*malA-lacZ*		This study
JW270 Δ*fur glmS3*::P*malA-lacZ*		This study

LacZ reporter assays.

β-galactosidase activity was assayed using the Tropix Galacto-Light Plus chemiluminescence kit (Applied Biosystems) according to the manufacturer's protocol. Luminescence output was measured

using a BioTek Synergy 2 plate reader and Gen5 software. In all cases, the β-galactosidase activity is reported as light units relative to the CFU (colony-forming units) per mL of the bacterial culture sample. For this CFU standardization, 500 µL of each culture sample was added to a ~100 µL -equivalent of 0.2 mm stainless steel beads in a 1.5 mL Eppendorf microtube and placed in a bead mill homogenizer (Bullet Blender, Next Advance) on high for 1 min three times to disrupt any cell clumping before serially diluting and plating.

Genetic manipulations

To genetically inactivate the malleobactin and pyochelin siderophores, in-frame, unmarked deletions of *mbaJ* and *pchAB* genes were generated using methods previously described (39). Briefly, the DNA regions ~460-480 base pairs (bp) upstream and downstream of the *mbaJ* and *pchAB* open reading frames (ORFs), as well as the first and last 3-7 amino acids, were synthesized (GenScript, New Jersey) with incorporated HindIII and XbaI restriction digest sites. These regions were connected together, the resulting fragment was digested with HindIII and XbaI, and ligated into HindIII- and XbaI-cut pEX18km-*pheS* vector. In the same manner, to generate an in-frame, unmarked deletion of the positive *mal* regulator HrpB, the DNA regions ~815bp upstream and ~700bp downstream of the *hrpB* ORF, as well as the first and last 7 amino acids, were PCR-amplified with incorporated XbaI and HindIII sites, joined together by a second round of PCR, digested with HindIII and XbaI, and ligated into HindIII- and XbaI-cut pEX18km-*pheS* vector. The resulting pEX18km-*pheS* deletion plasmids were electroporated into Bp82 with kanamycin selection. Resulting merodiploid colonies were subjected to 4 rounds of counterselection on M9 minimal media containing *p*-Cl-Phe. Mutants were then screened for susceptibility to kanamycin and verified by PCR-amplifying and sequencing across the gene deletion regions.

To make the P*lac-hrpB* expression cassette, we PCR-amplified *hrpB* from the Bp82 genome using primers that incorporated restriction sites (SacI and KpnI) into the product. The amplicon was cut with

SacI and KpnI and ligated into SacI- and KpnI-digested pUC18-mini-Tn7T-Km-P*lac* to generate pUC18-mini-Tn7T-Km-P*lac-hrpB*.

The malleilactone gene cluster β-galactosidase reporter P*malA-lacZ* (20) was introduced along with the transposase-expressing helper plasmid pTNS3 by electroporation into Bp82 strains. PCR was used as previously described (35) to confirm integration of the plasmid-borne reporter elements into the neutral chromosomal *attTn7* site near the *glmS3* gene.

Malleilactone purification

Malleilactone was purified from 5.2 L cultures of Bp82 *glmS3*::P*lac-malR* grown for 24 hours in LB supplemented with MOPS, adenine, thiamine, and with 1 mM IPTG to induce production of malleilactone, as per (20). Briefly, samples were extracted with ethyl acetate, treated with sodium sulfate anhydrous, evaporated at 35°C in a Genevac rotovap, and reconstituted in 10 mL acetonitrile. For malleilactone purification, two separate rounds of chromatography were performed on a Waters autopurification system equipped with a Waters 996 photodiode array, a 2525 binary pump, a 2767 sample manager, a Waters ZQ single quad mass spectrometer, and a Waters XBridge C_{18} column (5 µm, 19 by 150 mm). For round one, 1,200 µL injections were made using an aqueous mobile phase with NH_4OH at pH 9.8 and an organic phase of acetonitrile which increased by gradient from 25% to 45% over 4 min, followed by a 2-min hold at 100%; the flow rate was 20 µL/min. The fractions were pooled, evaporated at 35°C in a Genevac rotovap, and the residue was reconstituted in 10 mL of acetonitrile. For round two, 1200 µL injections were made using an aqueous mobile phase with 20 mM NH_4COO at pH 7.0, and an organic mobile phase of acetonitrile with a gradient of 35% to 55% over 4 min followed by a 2-min hold at 100%. Fractions were triggered by UV absorption at 370 nm and mass at 305 *m/z* with a mass spectrometer set to negative ionization mode (capillary at 2.9 kV, source at 100°C, and cone at 50 V). All final fractions were combined, evaporated under a stream of N_2 gas, and stored fully dry at -20˚C.

Malleilactone-iron titrations

The dried sample of malleilactone (2.2 mg) was dissolved in methanol to get a stock solution of 1 mg/mL. The binding of iron to malleilactone was monitored spectrophotometrically by titrating small increments (5 μL) of $FeCl_3$ (10 mM in 50% methanol) into a solution (2 mL) of purified malleilactone (39 μM in methanol) and following the optical absorbance changes between 200 and 800 nm with the aid of a Cary UV-60 spectrophotometer. To calculate the malleilactone concentration, the extinction coefficient at 376 nm was utilized (ε_{376} = 24,612 M^{-1} cm^{-1}). The titration was carried out at room temperature in a cuvette with 1.0 cm path length under constant stirring. After addition of each $FeCl_3$ aliquot, 5 μL of 10 mM NaOH in water was added to the cuvette to neutralize the H^+ released from malleilactone upon coordinating iron; the solution was equilibrated for 5 min, and the spectrum was recorded. The concentration of iron during the titration changed from 10 to 110 μM while maintaining the malleilactone concentration at 39 μM. Control spectral changes curves were recorded by titrating $FeCl_3$ (10 to 110 μM) into methanol (data not shown).

RESULTS

Regulation of the *mal* gene cluster during iron starvation

To test whether transcription of the malleilactone biosynthesis genes is induced under iron starvation conditions, we used a chromosomally-integrated P*malA-lacZ* reporter, wherein ß-galactosidase activity is a measure of activity at the *malA* promoter, the first gene in the *mal* operon. We grew *B. pseudomallei* strain Bp82 with P*malA-lacZ* in defined minimal media both with 50 μM iron ($(NH_4)_2Fe(SO_4)_2$) and without added iron for 24 hours, and we measured ß-galactosidase activity. Relative to the iron-supplemented media, Bp82 had ~125-fold greater CFU-adjusted ß-galactosidase activity when grown in the absence of added iron ("wt" in **Fig. 5.1-A, B**). These results support the idea that malleilactone is important during conditions of iron starvation.

In attempts to understand more about the how regulation of the *mal* genes occurs during iron starvation conditions, we first tested some of the known *mal* regulators for a role in this process, chief among them being the LuxR-family transcriptional activator MalR, which is encoded just upstream of the malleilactone cluster. Notably, the *mal* cluster can also be induced by growth-inhibiting concentrations of some antibiotics such as the tetrahydrofolate (THF) synthesis pathway inhibitor trimethoprim (20, 27, 40, 41). MalR is somehow activated by the homoserine intermediates that build up due to the THF synthesis disruption and subsequently activates expression of the malleilactone biosynthesis genes (20, 27, 42). We tested the role of MalR in activating the *mal* genes in iron-limited growth medium using a *malR*-deficient strain ("Δ*malR"* in **Fig. 5.1-A**). With Δ*malR,* we did not detect any ß-galactosidase activity in either the presence or absence of iron, supporting the idea that MalR is important for activating the *mal* biosynthesis genes in this media and under iron-limited conditions.

It is possible that malleilactone or another product of the *mal* genes can induce *mal* cluster expression in a type of positive feedback mechanism, as is true of various other bacterially-produced small molecules such as acyl-homoserine lactones (AHLs) (43, 44). Thus, we tested induction of the P*malA-lacZ* reporter

in a strain disrupted for malleilactone biosynthesis through deletion of a key biosynthesis gene, one of two large polyketide synthases *malF* ("Δ*malF"* in **Fig. 5.1-A**)(18-20). We observed that this malleilactone-deficient strain still showed an iron depletion-dependent ~130-fold increase in CFU-adjusted *mal* expression, suggesting that malleilactone does not regulate its own expression through a feedback loop under iron starvation.

When bacteria enter a vertebrate host where free iron is effectively unavailable, they initially encounter a situation of nutritional starvation, and they have evolved systems to recognize this lack of essential nutrients and respond by increasing the transcription of genes important in acquisition (3). The ferric uptake repressor (Fur) system is a well-known iron-responsive regulator in many bacterial species that is important for turning on iron acquisition genes upon sensing iron starvation in the host (21, 22, 45). Our attempts to generate a *fur*-deficient or *fur*-inactivated strain of Bp82 have thus far been unsuccessful, though we were able to obtain a *fur*-inactivated mutant of a different BSL2-safe attenuated strain of *B. pseudomallei* 1026b called JW270 (38). We observed a much more modest increase in JW270 P*malA-lacZ* expression under iron starvation conditions than we saw with in Bp82 (**Fig. 5.1-C**). However, the increase occurred independently of a *fur*-inactivating mutation (*fur** in **Fig. 5.1-C**), suggesting that Fur does not influence the malleilactone response under iron starvation, at least in strain JW270.

Another known host-responsive regulator, the AraC-family transcriptional regulator protein HrpB, moderates the type-3 secretion system (T3SS) virulence gene cluster upon plant cell contact in the plant pathogen *Ralstonia solanacearum* (46). A closely related HrpB ortholog is encoded in *B. pseudomallei*. Previously, it was demonstrated that expressing HrpB from an inducible synthetic promoter increases *malR* transcription (47); thus, we examined the role of HrpB in regulating malleilactone production. We observed that inducing HrpB expression strongly activates malleilactone production in a MalR-dependent manner (**Fig. 5.1-D**). We also observed that HrpB is not required for trimethoprim-dependent activation of malleilactone (**Fig. 5.1-E**). Together, these results show that HrpB induces malleilactone through MalR, and that HrpB is not involved in trimethoprim-dependent malleilactone induction. We also tested if

HrpB is involved in activating transcription of the *mal* genes in iron-deficient conditions (**Fig. 5.1-A**). In the Δ*hrpB* mutant, P*malA-lacZ* induction in low-iron growth media was equivalent to that of wild-type

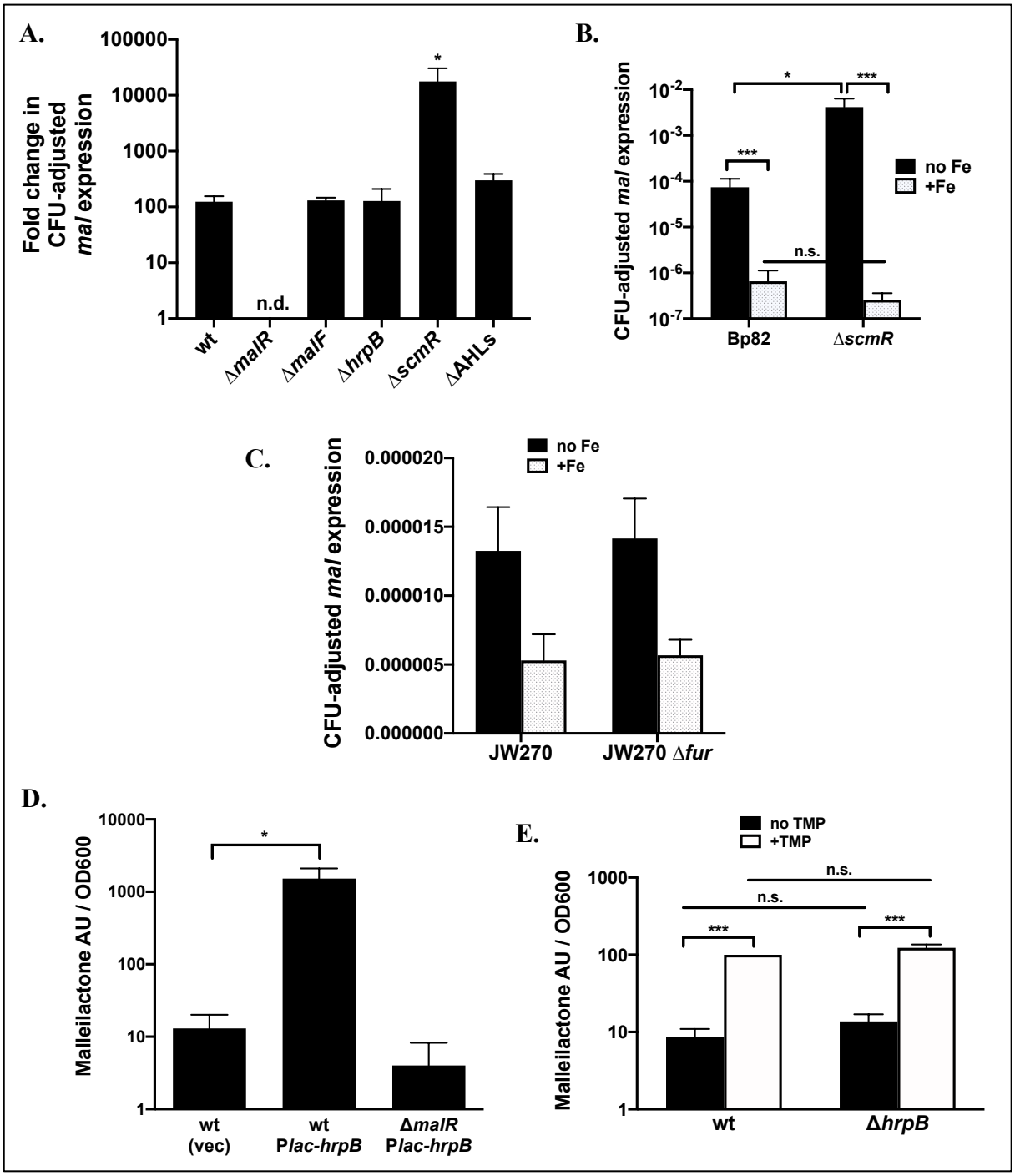

Figure 5.1. Levels of *mal* gene cluster expression in Bp82 strains (A, B) or JW270 strains (C) grown for 24 hrs in defined minimal media either un-supplemented or supplemented with 50 μM Fe^{2+} ferrous ammonium sulfate. Relative malleilactone UV-Vis/mass spectrometry analysis of ethyl acetate extractions of 50mL whole-volume cultures grown for 24 hrs in LB supplemented with IPTG (D) or with 4.5 μg/mL of trimethoprim (E) from indicated Bp82 strains. Malleilactone AU: area under the curve at 370 nm, the λ_{max} of malleilactone, reported relative to OD_{600}: culture optical density at 600 nm. Strains had an IPTG-inducible P*lac* empty vector 'vec' or P*lac-hrpB* element in (D) and the P*malA-lacZ* genetic reporter element in (A, B, C) chromosomally integrated at the neutral *glmS3* site. Bp82 strains used: 'wild-type' wt, Δ indicates unmarked deletion in *malR, malF, hrpB, scmR,* or in the case of ΔAHLs, of all three of the LuxI-family acyl-homoserine lactone (AHL) synthase genes *bpsI1, bpsI2,* and *bpsI3.* JW270 strains used were the parent or had an unmarked deletion in the *fur* gene. For each strain, results in (A) are reported as average of the growth-adjusted *mal* expression (the average of the relative light units, the output of enzymatic cleavage of the Tropix kit β-galactosidase substrate, from technical triplicate luminescence readings divided by the CFU per mL counts of each sample) of the no-iron media sample divided by that of the iron-supplemented sample. 'n.d.': no LacZ activity detected. Results in (B, C) are average growth-adjusted *mal* expression. Depicted are the averages and standard deviations of two (C, D, E) or three (A, B) independent biological replicate experiments. Statistical significance is indicated relative to the 'wt' parent strain using ordinary one-way (D), two-way (E), or repeated-measures one-way ANOVA (A, B) and Tukey's multiple comparisons tests: 'n.s.' = not significant, *p > 0.05, ***p > 0.001.

Bp82. Our results support the conclusion that HrpB is an important *mal* gene regulator, but that it plays no role in regulating the *mal* genes in response to low iron.

Finally, we had previously shown that the *B. pseudomallei* AHL quorum sensing (QS) systems (BpsI1-R1, BpsI2-R2, and BpsI3-R3) repress expression of the *mal* genes, likely through the global secondary metabolite regulator ScmR (48, 49) and MalR (20). Thus, we tested whether quorum sensing or ScmR play a role in inducing the *mal* biosynthesis genes using a strain where all three AHL synthase genes are deleted (*bpsI1, bpsI2,* and *bpsI3,* the 'ΔAHLs' strain), or an *scmR* deletion mutant. In the ΔAHL strain, there was no difference in the induction of the *mal* genes in low iron growth media relative to that of wild-type (**Fig. 5.1-A**), suggesting that the AHL-dependent QS signaling circuitry is not important for the induction of the *mal* genes during iron starvation. However, when we deleted the malleilactone repressor ScmR, we saw a statistically significant increase in the magnitude of the low-iron *mal* expression response relative to that in iron supplemented media (**Fig. 5.1-A**). Notably, the *mal* response in Δs*cmR* in the presence of iron is not statistically significantly different from that of wild-type in plentiful iron (**Fig. 5.1-B**). This result indicates that ScmR likely plays some role in the regulation of the *mal* genes in response to iron limitation. ScmR appears to normally act as an iron-responsive repressor of *mal* gene

cluster expression during iron-starvation conditions, though control of this specific type of conditional repression is likely mediated by some mechanism other than AHL QS.

Purified malleilactone can coordinate with iron

We were interested in understanding more about the ability of malleilactone to bind to iron to better appreciate its potential role as a siderophore or siderophore helper. In collaboration with Dr. Mario Rivera's lab at Louisiana State University (formerly of the University of Kansas Department of Chemistry), we performed iron titration experiments with *B. pseudomallei* culture-purified malleilactone.

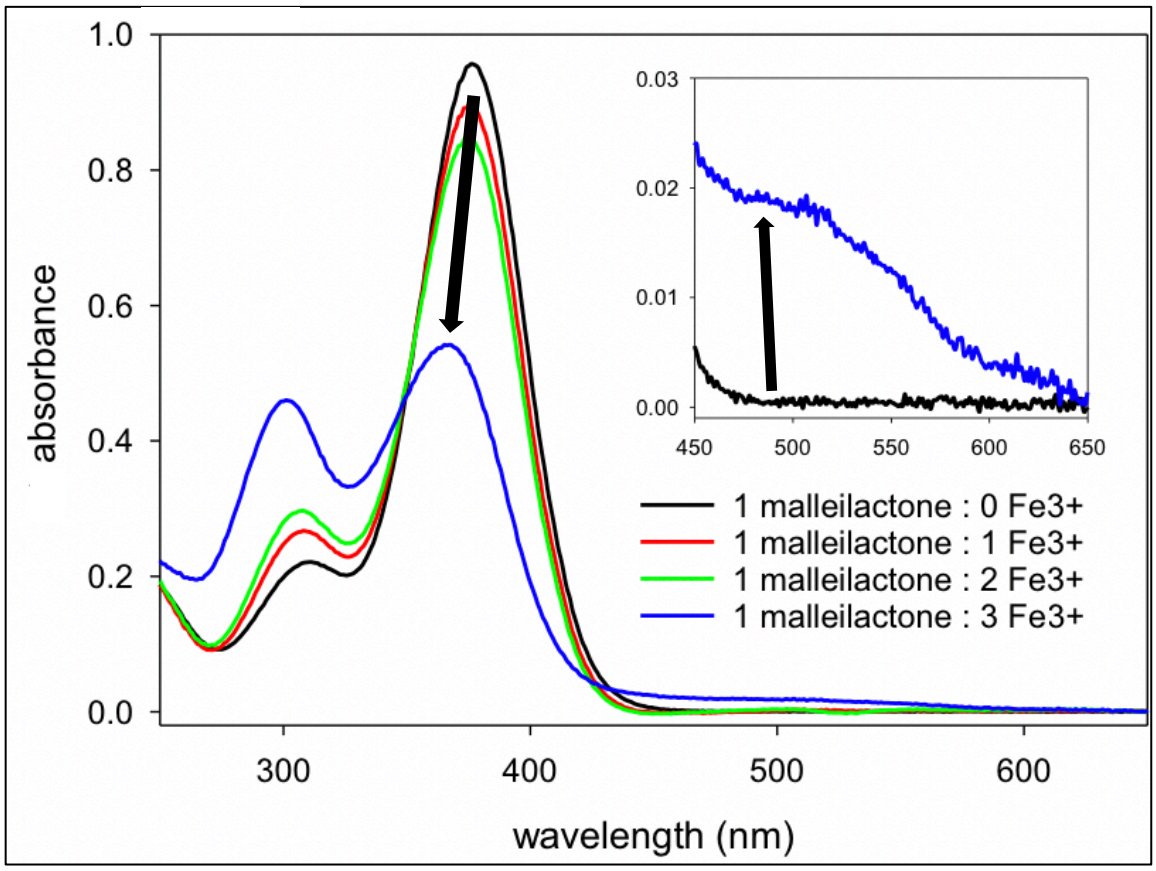

Figure 5.2. Purified malleilactone binds to iron. UV-vis spectrophotometric analysis of purified malleilactone titrated with $FeCl_3$. The inset is a closer view of the section spanning 450 to 650 nm. Arrows indicate notable peak shifting. This graph is one representative of multiple titration experiments.

We purified malleilactone from large batch cultures of our *malR*-expressing Bp82 strain as per (20). The binding of Fe^{3+} to purified malleilactone was determined by absorption spectrophotometry. Incremental addition of Fe^{3+} to malleilactone allows visualization of a shift in the malleilactone-only spectra (black trace) from its peak at ~376 nm to ~365 nm (**Fig. 5.2**). Additional shifting in absorbance of the malleilactone-only spectra was observed with increased iron (blue trace) with a charge transfer band appearing in the inset region over the range of 400 to 600 nm (inset, **Fig. 5.2**), which indicates charge transfer or differential electron sharing. These spectrophotometric observations support the coordination or binding of ferric iron by malleilactone.

Malleilactone deficiency results in poorer low-iron growth in a siderophore-dependent manner

To assess the contribution of malleilactone to fitness under iron starvation, we cultured both malleilactone-intact (wild-type, $MalF^{+}$) and malleilactone-deficient (Δ*malF*, $MalF^{-}$) strains of the parent Bp82 and of Bp82 with deletions in the two well-characterized *B. pseudomallei* siderophores malleobactin and pyochelin (Δ*pchAB*Δ*mbaJ*). All strains had identical growth yields averaging around $5x10^9$ to $7x10^9$ CFU per mL in the presence of 50 μM Fe^{2+} in our defined minimal media (**Fig. 5.3-A**). In the defined minimal media with no added iron, the growth yield of wild-type Bp82 was over 3-fold lower than when wild-type was grown in iron-supplemented media. However, under the no-iron conditions, we observed that the growth yield of the malleilactone-deficient strain was about 2.2-fold less than that of the wild type, which supports the notion of malleilactone providing some type of fitness advantage under iron starvation conditions (**Fig. 5.3-B**). However, this difference was not observed in the strain defective for production of malleobactin and pyochelin (**Fig. 5.3-B**). These results indicate that any benefit of malleilactone occurs in a siderophore-dependent manner. We posit that malleilactone might provide some assistance to malleobactin or pyochelin (or both), an idea that will be explored in future studies.

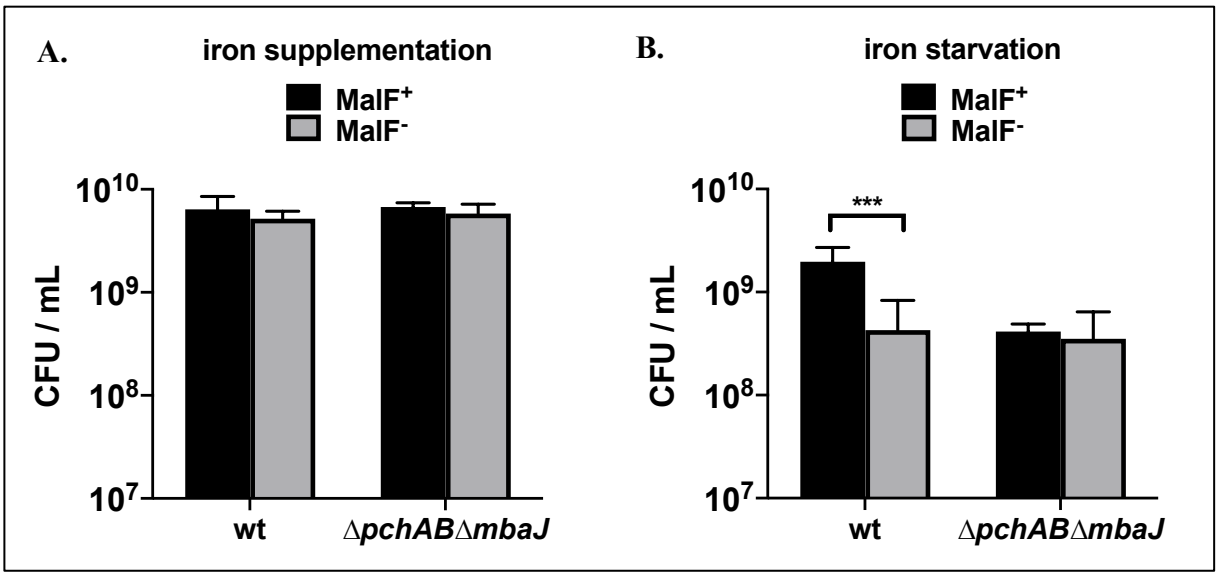

Figure 5.3. Fitness of Bp82 strains grown under defined minimal media conditions with 50μM Fe^{2+} iron supplementation (A) and under iron starvation (B). Wild-type ('$MalF^{+}$') strains and mutants deficient in malleilactone production (Δ*malF*, '$MalF^{-}$') were examined in both the wild-type Bp82 and siderophore mutant (Δ*pchAB*Δ*mbaJ*) backgrounds. Growth yield results are colony-forming units (CFU) per mL of culture and are the averages and standard deviations of at least four biological replicates. Statistical significance using ordinary one-way ANOVA and Dunnett's multiple comparisons test, ***$p < 0.001$.

DISCUSSION

Results of previous studies suggest that in addition to acting as a cytotoxin, malleilactone might play a role in transporting iron for use by the cell (18, 50, 51). Here, we offer additional support of this idea. We show that transcription of the malleilactone gene cluster is increased under iron starvation conditions, purified malleilactone chelates iron, and the malleilactone biosynthetic genes are important for growth in low-iron conditions.

Our results lend some insight into how low iron regulation overlaps with known regulators of the malleilactone biosynthesis genes. MalR is required for *mal* expression in our defined minimal media and in low iron conditions, but another positive *mal* regulator HrpB is dispensable for the low iron-dependent activation of *mal* transcription. Further, regulation by low iron does not seem to occur through a feedback loop. However, as noted by many in the field, malleilactone bears a notable structural similarity to AHL signaling molecules, and thus it could play a yet uncharacterized role in directly or indirectly signaling transcription of additional genes, an idea that has not been formally ruled out. Quorum sensing (QS) is also dispensable for activation of the *mal* cluster by low iron, though the QS-activated *mal* repressor ScmR does appear to repress these genes under low iron conditions. ScmR is known to repress production of malleilactone and many secondary metabolite compounds in *B. thailandensis* and *B. pseudomallei*, especially in later growth stages when cell density is high (20, 49, 52). Our data suggest that ScmR acts an iron-responsive repressor through an as yet-unknown QS-independent mechanism, as the iron response in the QS-deficient strain was not different from that of wild-type. Preliminary studies with the *B. pseudomallei* JW270 strain (a capsule mutant whose parent is an *amrAB-oprA*-deficient derivative of the common 1026b parent) suggest that Fur is uninvolved in *mal* regulation in iron-depleted conditions. Notably, there are multiple genetic differences between JW270 and Bp82, and we have not yet been able to assess the possible role of Fur in regulating malleilactone in our Bp82 strain.

Our spectral data provide strong support of the idea that malleilactone can chelate iron. These data suggest that three equivalents of iron relative to malleilactone promoted the greatest peak shifts, though that is in disagreement based on the preliminary model of tetramic and tetronic acid-like malleilactone coordination with iron proposed by (18), which suggests that as many as three malleilactone molecules would be needed to coordinate a single Fe^{3+} ion. This discrepancy suggests that there might be substructures or molecular forms of malleilactone or reaction condition variation with which we are yet unfamiliar that could influence how malleilactone interacts with iron atoms. One possibility is that malleilactone forms micelles and that iron coordinates to micellar malleilactone. Other similar hydrophobic small molecules have been shown to form micelles and other various supramolecular self-assembly structures (53). Hence, it is possible that malleilactone molecules behave in the same manner under these conditions. These ideas will be addressed in future experimentation.

Our data that malleilactone might not be a full siderophore is in line with the theory that multiple siderophores with varied polarities and structures can provide alternate routes for securing iron and thereby enable bacterial pathogens to better avoid host defense mechanisms that target and neutralize siderophores with conserved structures (22). Previous results showed that purified malleilactone had a less robust CAS assay response than the chelating reagent EDTA (18), which is a less potent iron binder than common siderophores, though malleilactone could still serve as a lower-affinity accessory to existing iron acquisition processes. Additionally, full virulence of the clinical isolate *B. pseudomallei* strain 1710b was observed using a murine acute infection model even in the absence of malleobactin, pyochelin, and two different hemin uptake systems (26). Those authors posit that the lack of virulence could be associated with the known predominant intracellular portions of the *B. pseudomallei* infection lifestyle (4, 54) wherein iron could be more readily acquired in siderophore-independent manners, as siderophores seem to be more beneficial to extracellular or free-living bacteria. Consistent with this idea, the pyochelin locus is absent in the host-restricted pathogenic relative *B. mallei,* which causes glanders in horses and has no known free-living environmental niche (55). Additionally, it appears that while useful to *B.*

pseudomallei, siderophores and iron uptake systems contribute only partially to virulence overall (26, 56) or perhaps only at certain stages during infection, though much remains to be identified and understood about which iron acquisition elements are important, how so, and under what conditions.

Alternatively, malleilactone could somehow upregulate other siderophores or acquisition elements, or it could assist the functions of existing iron acquisition systems or cellular iron use. An example of a type of siderophore helper is mycobactin, a molecule with plentiful iron coordination groups and a hydrophobic tail which is produced by the pathogen *Mycobacterium tuberculosis,* the causative agent of tuberculosis. The current understanding of mycobactins is that they aid in iron import. Fe^{3+}-bound extracellular carboxymycobactin siderophores are brought into the bacterial cell through specific transport proteins in the outer membranes, and then it is believed that mycobactins in the periplasmic space help shuttle the iron to another TonB-like transporter across the inner membrane, where it gets stored and utilized by cytoplasmic proteins (57). Notably, the anti-tuberculosis drug *p*-aminosalicylate acts by targeting the conversion of salicylate to mycobactin and carboxymycobactin (58). It is possible that malleilactone, which has a similar hydrophobic component like mycobactins, might also function to help shuttle iron in *B. pseudomallei*, and if so, this process could be a potential drug target. Furthering our knowledge of how and under what conditions malleilactone is called to action to benefit by producing cells will help us better understand its function toward the goal of exploiting the biology of malleilactone biosynthesis in melioidosis therapeutic approaches.

REFERENCES

1. Andrews SC, Robinson AK, Rodríguez-Quiñones F. 2003. Bacterial iron homeostasis. FEMS Microbiology Reviews 27:215-237.

2. Dlouhy AC, Outten CE. 2013. The iron metallome in eukaryotic organisms. Met Ions Life Sci 12:241-78.

3. Skaar EP. 2010. The battle for iron between bacterial pathogens and their vertebrate hosts. PLoS Pathog 6:e1000949.

4. Wiersinga WJ, Currie BJ, Peacock SJ. 2012. Melioidosis. N Engl J Med 367:1035-44.

5. Wuthiekanun V SM, Dance DAB, White NJ. 1995. The isolation of *Pseudomonas pseudomallei* from soil in Northeastern Thailand. Transactions of the Royal Society of Tropical Medicine and Hygiene 89:41-43.

6. Cheng AC, Currie BJ. 2005. Melioidosis: epidemiology, pathophysiology, and management. Clin Microbiol Rev 18:383-416.

7. Limmathurotsakul D, Golding N, Dance DAB, Messina JP, Pigott DM, Moyes CL, Rolim DB, Bertherat E, Day NPJ, Peacock SJ, Hay SI. 2016. Predicted global distribution of *Burkholderia pseudomallei* and burden of melioidosis. Nature Microbiology 1.

8. Dance D. 2014. Treatment and prophylaxis of melioidosis. Int J Antimicrob Agents 43:310-8.

9. Limmathurotsakul D, Chaowagul W, Day NP, Peacock SJ. 2009. Patterns of organ involvement in recurrent melioidosis. Am J Trop Med Hyg 81:335-7.

10. Maharjan B, Chantratita N, Vesaratchavest M, Cheng A, Wuthiekanun V, Chierakul W, Chaowagul W, Day NP, Peacock SJ. 2005. Recurrent melioidosis in patients in northeast Thailand is frequently due to reinfection rather than relapse. J Clin Microbiol 43:6032-4.

11. Chaowagul W, Suputtamongkol Y, Dance D, Rajchanuvong A, Pattaraarechachai J, White NJ. 1993. Relapse in Melioidosis: Incidence and Risk Factors. Journal of Infectious Diseases 168:1181-1185.

12. Currie BJ, Fisher DA, Anstey NM, Jacups SP. 2000. Melioidosis: acute and chronic disease, relapse and re-activation. Transactions of the Royal Society of Tropical Medicine and Hygiene 94:301-304.

13. French CT, Bulterys PL, Woodward CL, Tatters AO, Ng KR, Miller JF. 2020. Virulence from the rhizosphere: ecology and evolution of *Burkholderia pseudomallei*-complex species. Curr Opin Microbiol 54:18-32.

14. Gutierrez MG, Yoder-Himes DR, Warawa JM. 2015. Comprehensive identification of virulence factors required for respiratory melioidosis using Tn-seq mutagenesis. Front Cell Infect Microbiol 5:78.

15. Moule MG, Spink N, Willcocks S, Lim J, Guerra-Assuncao JA, Cia F, Champion OL, Senior NJ, Atkins HS, Clark T, Bancroft GJ, Cuccui J, Wren BW. 2015. Characterization of New Virulence Factors Involved in the Intracellular Growth and Survival of *Burkholderia pseudomallei*. Infect Immun 84:701-10.

16. Sarovich DS, Price EP, Webb JR, Ward LM, Voutsinos MY, Tuanyok A, Mayo M, Kaestli M, Currie BJ. 2014. Variable virulence factors in *Burkholderia pseudomallei* (melioidosis) associated with human disease. PLoS One 9:e91682.

17. Biggins JB, Kang HS, Ternei MA, DeShazer D, Brady SF. 2014. The chemical arsenal of *Burkholderia pseudomallei* is essential for pathogenicity. J Am Chem Soc 136:9484-90.

18. Biggins JB, Ternei MA, Brady SF. 2012. Malleilactone, a polyketide synthase-derived virulence factor encoded by the cryptic secondary metabolome of *Burkholderia pseudomallei* group pathogens. J Am Chem Soc 134:13192-5.

19. Franke J, Ishida K, Hertweck C. 2012. Genomics-driven discovery of burkholderic acid, a noncanonical, cryptic polyketide from human pathogenic *Burkholderia* species. Angew Chem Int Ed Engl 51:11611-5.

20. Klaus JR, Deay J, Neuenswander B, Hursh W, Gao Z, Bouddhara T, Williams TD, Douglas J, Monize K, Martins P, Majerczyk C, Seyedsayamdost MR, Peterson BR, Rivera M, Chandler JR. 2018. Malleilactone Is a *Burkholderia pseudomallei* Virulence Factor Regulated by Antibiotics and Quorum Sensing. J Bacteriol 200.

21. Dauros-Singorenko P, Swift S. 2014. The transition from iron starvation to iron sufficiency as an important step in the progression of infection. Sci Prog 97:371-82.

22. Miethke M, Marahiel MA. 2007. Siderophore-based iron acquisition and pathogen control. Microbiol Mol Biol Rev 71:413-51.

23. Alice AF, Lopez CS, Lowe CA, Ledesma MA, Crosa JH. 2006. Genetic and transcriptional analysis of the siderophore malleobactin biosynthesis and transport genes in the human pathogen *Burkholderia pseudomallei* K96243. J Bacteriol 188:1551-66.

24. Gupta A, Bedre R, Thapa SS, Sabrin A, Wang G, Dassanayake M, Grove A. 2017. Global Awakening of Cryptic Biosynthetic Gene Clusters in *Burkholderia thailandensis*. ACS Chem Biol 12:3012-3021.

25. Franke J, Ishida K, Ishida-Ito M, Hertweck C. 2013. Nitro versus hydroxamate in siderophores of pathogenic bacteria: effect of missing hydroxylamine protection in malleobactin biosynthesis. Angew Chem Int Ed Engl 52:8271-5.

26. Kvitko BH, Goodyear A, Propst KL, Dow SW, Schweizer HP. 2012. *Burkholderia pseudomallei* known siderophores and hemin uptake are dispensable for lethal murine melioidosis. PLoS Negl Trop Dis 6:e1715.

27. Truong TT, Seyedsayamdost M, Greenberg EP, Chandler JR. 2015. A *Burkholderia thailandensis* Acyl-Homoserine Lactone-Independent Orphan LuxR Homolog That Activates Production of the Cytotoxin Malleilactone. J Bacteriol 197:3456-62.

28. Royles BJL. 1995. Naturally Occurring Tetramic Acids: Structure, Isolation, and Synthesis. Chemical Reviews 95:1981-2001.

29. Lowery CA, Park J, Gloeckner C, Meijler MM, Mueller RS, Boshoff HI, Ulrich RL, Barry CE, 3rd, Bartlett DH, Kravchenko VV, Kaufmann GF, Janda KD. 2009. Defining the mode of action of tetramic acid antibacterials derived from *Pseudomonas aeruginosa* quorum sensing signals. J Am Chem Soc 131:14473-9.

30. Zaghouani M, Nay B. 2016. 3-Acylated tetramic and tetronic acids as natural metal binders: myth or reality? Nat Prod Rep 33:540-8.

31. Athanasellis G, Igglessi-Markopoulou O, Markopoulos J. 2010. Tetramic and tetronic acids as scaffolds in bioinorganic and bioorganic chemistry. Bioinorg Chem Appl doi:10.1155/2010/315056:315056.

32. Propst KL, Mima T, Choi KH, Dow SW, Schweizer HP. 2010. A *Burkholderia pseudomallei* Δ*purM* mutant is avirulent in immunocompetent and immunodeficient animals: candidate strain for exclusion from select-agent lists. Infect Immun 78:3136-43.

33. Eshelman K, Yao H, Punchi Hewage AND, Deay JJ, Chandler JR, Rivera M. 2017. Inhibiting the BfrB:Bfd interaction in *Pseudomonas aeruginosa* causes irreversible iron accumulation in bacterioferritin and iron deficiency in the bacterial cytosol. Metallomics 9:646-659.

34. Barrett AR, Kang Y, Inamasu KS, Son MS, Vukovich JM, Hoang TT. 2008. Genetic tools for allelic replacement in *Burkholderia* species. Appl Environ Microbiol 74:4498-508.

35. Choi KH, Mima T, Casart Y, Rholl D, Kumar A, Beacham IR, Schweizer HP. 2008. Genetic tools for select-agent-compliant manipulation of *Burkholderia pseudomallei*. Appl Environ Microbiol 74:1064-75.

36. Majerczyk CD, Brittnacher MJ, Jacobs MA, Armour CD, Radey MC, Bunt R, Hayden HS, Bydalek R, Greenberg EP. 2014. Cross-species comparison of the *Burkholderia pseudomallei*, *Burkholderia thailandensis*, and *Burkholderia mallei* quorum-sensing regulons. J Bacteriol 196:3862-71.

37. Moore RA, DeShazer D, Reckseidler S, Weissman A, Woods DE. 1999. Efflux-Mediated Aminoglycoside and Macrolide Resistance in *Burkholderia pseudomallei*. Antimicrobial Agents and Chemotherapy 43:465-470.

38. Warawa JM, Long D, Rosenke R, Gardner D, Gherardini FC. 2009. Role for the *Burkholderia pseudomallei* capsular polysaccharide encoded by the *wcb* operon in acute disseminated melioidosis. Infect Immun 77:5252-61.

39. Chandler JR, Duerkop BA, Hinz A, West TE, Herman JP, Churchill ME, Skerrett SJ, Greenberg EP. 2009. Mutational analysis of *Burkholderia thailandensis* quorum sensing and self-aggregation. J Bacteriol 191:5901-9.

40. Seyedsayamdost MR. 2014. High-throughput platform for the discovery of elicitors of silent bacterial gene clusters. Proc Natl Acad Sci U S A 111:7266-71.

41. Okada BK, Wu Y, Mao D, Bushin LB, Seyedsayamdost MR. 2016. Mapping the Trimethoprim-Induced Secondary Metabolome of *Burkholderia thailandensis*. ACS Chem Biol 11:2124-30.

42. Li A, Mao D, Yoshimura A, Rosen PC, Martin WL, Gallant E, Wuhr M, Seyedsayamdost MR. 2020. Multi-Omic Analyses Provide Links between Low-Dose Antibiotic Treatment and Induction of Secondary Metabolism in *Burkholderia thailandensis*. mBio 11.

43. Engebrecht J, Nealson K, Silverman M. 1983. Bacterial bioluminescence: Isolation and genetic analysis of functions from *Vibrio fischeri*. Cell 32:773-781.

44. Abisado RG, Benomar S, Klaus JR, Dandekar AA, Chandler JR. 2018. Bacterial Quorum Sensing and Microbial Community Interactions. MBio 9.

45. Troxell B, Hassan HM. 2013. Transcriptional regulation by Ferric Uptake Regulator (Fur) in pathogenic bacteria. Front Cell Infect Microbiol 3:59.

46. Marenda M, Brito B, Callard D, Genin S, Barberis P, Boucher C, Arlat M. 1998. PrhA controls a novel regulatory pathway required for the specific induction of *Ralstonia solanacearum hrp* genes in the presence of plant cells. Mol Microbiol 27:437-53.

47. Lipscomb L, Schell MA. 2011. Elucidation of the regulon and *cis*-acting regulatory element of HrpB, the AraC-type regulator of a plant pathogen-like type III secretion system in *Burkholderia pseudomallei*. J Bacteriol 193:1991-2001.

48. Le Guillouzer S, Groleau MC, Mauffrey F, Deziel E. 2020. ScmR, a global regulator of gene expression, quorum sensing, pH homeostasis, and virulence in *Burkholderia thailandensis*. J Bacteriol doi:10.1128/JB.00776-19.

49. Mao D, Bushin LB, Moon K, Wu Y, Seyedsayamdost MR. 2017. Discovery of *scmR* as a global regulator of secondary metabolism and virulence in *Burkholderia thailandensis* E264. Proc Natl Acad Sci U S A 114:E2920-E2928.

50. Ooi WF, Ong C, Nandi T, Kreisberg JF, Chua HH, Sun G, Chen Y, Mueller C, Conejero L, Eshaghi M, Ang RM, Liu J, Sobral BW, Korbsrisate S, Gan YH, Titball RW, Bancroft GJ, Valade E, Tan P. 2013. The condition-dependent transcriptional landscape of *Burkholderia pseudomallei*. PLoS Genet 9:e1003795.

51. Tuanyok A, Kim HS, Nierman WC, Yu Y, Dunbar J, Moore RA, Baker P, Tom M, Ling JM, Woods DE. 2005. Genome-wide expression analysis of iron regulation in *Burkholderia pseudomallei* and *Burkholderia mallei* using DNA microarrays. FEMS Microbiol Lett 252:327-35.

52. Thapa SS, Grove A. 2019. Do Global Regulators Hold the Key to Production of Bacterial Secondary Metabolites? Antibiotics (Basel) 8.

53. Sarkar S, Choudhury P, Dinda S, Das PK. 2018. Tailor-Made Self-Assemblies from Functionalized Amphiphiles: Diversity and Applications. Langmuir 34:10449-10468.

54. Stone JK, DeShazer D, Brett PJ, Burtnick MN. 2014. Melioidosis: molecular aspects of pathogenesis. Expert Rev Anti Infect Ther 12:1487-99.

55. Khan I, Wieler LH, Melzer F, Elschner MC, Muhammad G, Ali S, Sprague LD, Neubauer H, Saqib M. 2013. Glanders in animals: a review on epidemiology, clinical presentation, diagnosis and countermeasures. Transbound Emerg Dis 60:204-21.

56. Butt AT, Thomas MS. 2017. Iron Acquisition Mechanisms and Their Role in the Virulence of *Burkholderia* Species. Front Cell Infect Microbiol 7:460.

57. Sritharan M. 2016. Iron Homeostasis in *Mycobacterium tuberculosis*: Mechanistic Insights into Siderophore-Mediated Iron Uptake. J Bacteriol 198:2399-409.

58. Nagachar N, Ratledge C. 2010. Knocking out salicylate biosynthesis genes in *Mycobacterium smegmatis* induces hypersensitivity to *p*-aminosalicylate (PAS). FEMS Microbiol Lett 311:193-9.

Chapter 6: Discussion

SUMMARY OF FINDINGS

This body of work was primarily focused on the opportunistic pathogen *Burkholderia pseudomallei* and its close non-pathogenic relative, *Burkholderia thailandensis. B. pseudomallei* is an antibiotic-resistant pathogenic agent of the sometimes-fatal, multifarious human disease melioidosis. Although many aspects of *B. pseudomallei* biology remain unknown, this species has been receiving increased research attention into its many diverse virulence mechanisms. Secondary metabolite products are often underappreciated contributors to pathogenesis (1, 2) and are the focus of this research. The research goal of this body of work was to further our understanding of two families of antimicrobial secondary metabolites produced by the species *B. pseudomallei* and *B. thailandensis*: malleilactone, produced by the *mal* cluster gene products, and 2-hydroxy-3-methyl-4-alkylquinolones (HMAQs), produced by the *hmq* cluster gene products.

My work was focused on malleilactone in *B. pseudomallei,* and it complements and extends work published by other groups on malleilactone in *B. thailandensis.* First, I performed a basic characterization of malleilactone in *B. pseudomallei* (highlighted in Chapter 2), showing that malleilactone contributes to *B. pseudomallei* virulence in *C. elegans* nematodes, is structurally identical to that of *B. thailandensis,* and is similarly regulated by antibiotics and a global repressor, ScmR. In other work highlighted in Chapter 4, I showed that malleilactone is exported by the efflux pump BpeEF-OprC and that efflux is a viable mechanism by which *B. pseudomallei* abrogates malleilactone self-toxicity under conditions when it is highly expressed. In Chapter 5, I provide evidence supporting the idea that malleilactone is involved

in iron acquisition, which was weakly supported by results of studies by another group (3). Altogether, results of my work provide new and expanded information about malleilactone biology. We hypothesize that malleilactone might promote *B. pseudomallei* survival during infections based on our iron, cytotoxicity, and *C. elegans* virulence studies, or that malleilactone could promote survival within the polymicrobial communities of the soil, based on its responsiveness to various antibiotics, two hypotheses that are not mutually exclusive.

HMAQs are relatively under-studied in the *Burkholderia* genus, and my work on *B. thailandensis* HMAQs highlighted in Chapter 3 suggest that these molecules could be important for competition with other species in soil communities where this organism is found. HMAQs are antimicrobial in nature, especially against Gram-positive bacteria. The methylated analogs produced by *B. thailandensis* are less well characterized than the related hydroxy-alkylquinolines produced in other species (*P. aeruginosa*, etc.). In addition, my work showed that the methylated compounds appear to have, in some cases, more potent activity. We verify that the product of the *hmqL* gene is responsible for generating the *N*-oxide derivative of HMAQ compounds. Such derivatization increases antimicrobial activity relative to the HMAQ parent. In further support of this idea, heterologous expression of *hmqL* in *Burkholderia ambifaria* (which does not encode a homologous gene) confers upon it the ability to kill *Bacillus subtilis* that it normally lacks. This work provides additional characterization for the *Burkholderia* HMAQ family of compounds and their roles in interspecies competition.

DISCUSSION AND SIGNIFICANCE

As this body of work further supports, secondary metabolites are important for increasing survival in certain contexts, such as during infections of animal hosts or in competition with other bacterial species. They differ notably from primary metabolites in that they are more often silent or conditionally expressed and tend to have functions extracellularly of the producer cells (4). Malleilactone provides a good example of conditional expression, as this product is not detectable in *B. thailandensis* and barely

detectable in *B. pseudomallei* grown in standard laboratory conditions (3, 5-8). This indicates that its production might be especially carefully regulated, conditionally induced, or both; this is in further keeping with its classification as a secondary metabolite (compounds which could be too energetically costly or harmful to fitness if not carefully controlled or expressed under inappropriate conditions).

Secondary metabolite pathways can be highly divergent, resulting in many possible deviations on the parent structure of the metabolite product. Possible explanations for the biosynthesis of divergent products could be a less stringent requirement for precise metabolic pathway outcomes of secondary metabolites as compared with vital primary metabolism. Another possible explanation is that the diversity of product formed by a single secondary metabolite pathway contributes to bacterial fitness (9). In fact, multiple types of small-molecule virulence factors, many of which are a family of related compounds rather than single end products, have been shown to be indispensable for *B. pseudomallei* pathogenicity in mice (2). This metabolite diversity phenotype is evident among both the products of the *mal* gene pathway and the HMAQs, as highlighted by my work.

Previously unknown until recent work by Trottmann et al. (10), the malleicyprol-family isomeric products provide an example of diversity that exists in the malleilactone biosynthetic pathway. The malleicyprol compounds appear to be favored in acidic conditions and have increased cytotoxicity compared with malleilactone. While much of their preliminary work done with purified malleicyprol was performed *in vitro*, our evidence that malleicyprol can be self-toxic under certain conditions in live bacterial cultures supports that this compound could potentially be cytotoxic in other conditions such as in *in vivo* infections. More careful studies are needed to solidify the role of malleicyprol vs. malleilactone, either separately or in combination, in virulence of *B. pseudomallei*. Discovery of more details of the malleicyprol biosynthesis pathway, including recent studies showing the involvement of the methyltransferase MalB and the decarboxylase MalI in formation of the malleicyprol molecules (11), will be helpful to such future work.

Our results showing that HMAQ diversity allows for differential activity against different species also supports the idea that such diversity could confer survival advantages within a multispecies

community. The *hmq* biosynthesis pathway produces a variety of analogs with different acyl chain lengths, degree of saturation, or *N*-oxidation substitution. These vary in their activities against different bacteria (Chapter 3) and might also have different cellular targets. In fact, two different but structurally-similar hydroxy-alkylquinolone products were shown to have different mechanisms of action and to synergistically inhibit *E. coli* growth (12). In this case, metabolite diversity might contribute to competition by providing a "bet hedging" approach of producing a variety of molecules to increase the chance that one of them is effective. Synergistic activity also enhances their potency. Multiple molecules with different cellular targets can block the ability of a competitor to overcome their activity through genetic mutation, because it takes more than one mutation to become resistant to the whole family of molecules.

The diversity of and within secondary metabolite families provides a wealth of opportunities for new natural product discoveries. For example, understanding the diversity of molecules produced by a particular pathway can give insight into which molecules might serve as potential lead compounds in drug and therapeutic development. Numerous examples of microbial natural products that have led to clinically useful drugs include colistins and viridicatumtoxins, which have served as key scaffolds for next-generation polymixins and tetracyclines, respectively, and others reviewed in (13). As reviewed in (14), the *Burkholderia* genus is incredibly rich in natural products. Some of these products have even begun clinical trials, such as the antimitotic compound rhizoxin. In addition to taking advantage of their potential clinical usefulness, secondary metabolite biology could also be exploited to prevent virulence of producer cells, either as independent therapies or to act synergistically in a combinatorial treatment cocktail. Because secondary metabolites are, by definition, not strictly required for survival, using them as anti-virulence targets could lessen the opportunity for the quick evolution of resistance to antibacterial drugs that attack or inhibit essential bacterial processes. Thus, secondary metabolites are also good options for druggable targets that specifically hinder virulence aspects of bacteria and not necessarily their survival. For instance, our new understanding of efflux mitigation of self-toxicity could support the design and use of efflux pump inhibitors in combination with existing therapies or with molecules that

increase production of self-toxic *mal* metabolites as a strategy to reduce the virulence of *B. pseudomallei* by promoting its self-destruction.

FUTURE DIRECTIONS

Much remains to be understood about the malleilactone biosynthetic pathway. As has been revealed through recent work in *B. thailandensis* (10, 11), more products result from this pathway than originally known, depending on the pH and possibly other aspects of the growing conditions. The first question to be answered is whether *B. pseudomallei* produces malleicyprol compounds similar to *B. thailandensis*. Our lab has made early strides with utilizing analytical chemistry to detect the higher molecular-weight bis-malleicyprol isomer in ethyl acetate-extracted *B. pseudomallei* cultures (Klaus, Hursh, Brown, Bouddhara, and Chandler, unpublished); however, much more work is needed to isolate and verify the molecular structure of this compound. The malleicyprol-family compounds appear to have greatly reduced chemical stability relative to malleilactone and thus will likely require very careful assay conditions and optimization work, especially so for studies involving attempts to purify them. Analytical chemistry will also be used to understand the environmental conditions that give rise to malleicyprol derivatives in *B. pseudomallei,* in which they have not yet been carefully studied aside from our preliminary chemical analysis.

We also aim to follow up on the iron-binding ability of purified *B. thailandensis* malleilactone observed by chrome azurol S assay (3) and on our observation of *B. pseudomallei* malleilactone coordination with iron by titration assays to more accurately determine the binding affinities and kinetics of this interaction. For instance, our current iron binding assays support a result whereby malleilactone interacts with ferric iron at a 3:1 ratio, which is the opposite of the ratio in the model put forth by Biggins et al. (3) based on malleilactone's structural similarity to known iron-binding tetramic and tetronic acids. Therefore, something about the conditions in which we are performing our *in vitro* titration assays appears to alter how malleilactone behaves toward iron relative to the model's expectations. The very

hydrophobic tail of the core lactone structure could support the formation of more complex assemblies of malleilactone molecules such as micelles, which could alter the apparent ratio of malleilactone to iron. Malleilactone might also form outer membrane vesicles (OMVs) similar to the *Pseudomonas* quinolone signal PQS, which is somewhat like malleilactone with a substituted ring structure bearing a saturated alkyl chain tail. OMVs form in producing *Pseudomonas aeruginosa* cells by first integrating PQS into lipid bilayers (15, 16). PQS is also able to bind to iron, and OMVs containing iron-bound PQS are targeted by effector proteins for delivery to siderophore receptors on iron-starved cells (17). Malleilactone could behave similar to PQS in OMVs; our evidence suggests that while efflux is a means by which malleilactone is able to exit the cell, diffusion or the activation of other similar export mechanisms to OMV formation are possible. Further, it remains unknown if malleicyprol-family isomers are also able to bind to iron in the same manner as malleilactone, though we hypothesize that they could, given that the structure of malleicyprol still maintains the Biggins et al. (3) group's proposed iron coordination functional groups in the same relative position in which they occur within the malleilactone molecule.

Micelle formation has not been reported before for malleilactone-family molecules, nor have any careful localization studies yet been carried out, but it is likely that we could look for these molecular structures by using a variety of analytical techniques such as UV/vis spectrophotometry, dynamic light scattering, or by other critical micelle concentration determinants, and with fractionation experiments, respectively. Conditions under which micelles or other molecular assemblies form and their properties could offer valuable insight into the function, localization, and transport of malleilactone. Moreover, our iron starvation growth data showed that the low-iron-dependent helpful effects of malleilactone occur in a siderophore-dependent manner, which could further indicate that malleilactone is some type of helper or accessory to existing iron acquisition systems (18) rather than a siderophore itself, in a manner similar to the *Mycobacterium tuberculosis* mycobactins, which are periplasmic molecules that aid in iron import by shuttling iron brought to the cell membrane by siderophores through an inner membrane transporter to the cytoplasm (19). Thus, we will also assess the potential of malleilactone to have a supporting role in the function of two known siderophores malleobactin and pyochelin (20, 21).

We aim to use exogenous purified malleilactone and malleicyprol to corroborate the established role of efflux of endogenous *mal* products by the BpeEF-OprC efflux pump. Our work thus far is the first example of efflux serving in both active malleilactone export and as a self-resistance mechanism. We aim to further characterize the likely overlap in regulation of the *mal* and *bpeEF-oprC* gene clusters. Substrate activation of antibiotic efflux pumps is well-documented (22-24), and while we do not yet know an exact mechanism, it is possible that the known BpeT and BpeS efflux transcriptional activators are able to somehow sense critical concentrations of *mal* pathway products, intermediates, or precursors within the cell and activate efflux in response. In future work, we will assess the ability of *mal* cluster products to induce efflux expression, and examine the potential influence on efflux pump expression of the known *mal* cluster regulators: antibiotics (5, 6, 8, 25), homoserine (26), ScmR (6, 27), HrpB, quorum sensing (6), and nutrient (iron) starvation. Complex, antibiotic substrate concentration-dependent crosstalk in the regulation of the three main RND-family efflux pumps AmrAB-OprA, BpeAB-OprB, and BpeEF-OprC has been shown in *B. thailandensis* (28), so it is possible that the *mal* and *bpeEF-oprC* regulatory networks in *B. pseudomallei* are similarly multifaceted and complicated. Further, evolved BpeT mutants have been isolated from later bacterial samples in recurrent melioidosis patients (29). This result suggests that high efflux expression might be selected for in *B. pseudomallei* over time within a human host, further underscoring the possible roles of active efflux in export of virulence factors, self-resistance to endogenous metabolites, or resistance to host immune factors and to clinical antibiotic drugs.

Ultimately, the primary research goal is to more fully elucidate the specific role that malleilactone plays in melioidosis pathology. Future experiments will include both single-strain and 1:1 wild-type to mutant competition challenge studies in mice using bacterial luminescence reporter strains and the intubation-mediated intratracheal delivery method developed by Warawa and colleagues (30), which closely mimics the deep lung symptoms of human pneumonic melioidosis, to directly assess the impact of the *mal* gene cluster products on infectivity, bacterial burden, infection localization, and systemic spread. These would be the first of such studies to measure the virulence aspects of malleilactone-family molecules in an animal model system in a straightforward approach, as all previous mouse work

implicating virulence roles of *mal* genes was done using large transposon mutant libraries which can be subject to data-skewing bottlenecking and interlibrary mutant competition. Further, we would like to understand the role of efflux in preventing malleilactone self-toxicity *in vivo*, as we have some preliminary evidence that malleilactone expression might be detrimental to bacterial survival in mice when efflux is absent (Chandler lab, unpublished results). We are also interested in assessing more precisely the cytotoxic mechanism of action of malleilactone against both bacterial and eukaryotic cells to better understand its biological activity. Preliminary evidence suggests that cytochromes may be malleilactone targets in other bacteria (Chandler lab, unpublished results), but its specific toxicity effects on eukaryotic cells remains unknown. Appreciating how malleilactone-family compounds function in mammalian hosts is vital knowledge that would guide melioidosis therapeutic approaches aimed at targeting malleilactone or various aspects of its biology in a specific way.

The HAQ-family of molecules have been studied for a number of years, but we could still learn more about their structural diversity, how that begets their specificity of function, and the full breadth of their potency and mechanisms of action. Further, HMAQs produced by *B. thailandensis* and related bacteria are very poorly described. Our work showed that *N*-oxide derivatives of the HMAQ parent molecules appear to increase the *B. thailandensis* antimicrobial activity to *B. subtilis*, in a manner that increases as the carbon length of the alkyl side chain increases, though careful analysis of the *B. thailandensis* HMAQ and HMAQ-NO molecular mechanism(s) of action have yet to be characterized. Our new understanding of the increased HMAQ-NO forms and the influence of the alkyl chain length on activity could inform future work focused on adapting the scaffolds of existing bacterial metabolites for alternative functions, for increased or decreased toxicity, and for clinical therapeutic potential.

REFERENCES

1. Sarovich DS, Price EP, Webb JR, Ward LM, Voutsinos MY, Tuanyok A, Mayo M, Kaestli M, Currie BJ. 2014. Variable virulence factors in *Burkholderia pseudomallei* (melioidosis) associated with human disease. PLoS One 9:e91682.

2. Biggins JB, Kang HS, Ternei MA, DeShazer D, Brady SF. 2014. The chemical arsenal of *Burkholderia pseudomallei* is essential for pathogenicity. J Am Chem Soc 136:9484-90.

3. Biggins JB, Ternei MA, Brady SF. 2012. Malleilactone, a polyketide synthase-derived virulence factor encoded by the cryptic secondary metabolome of *Burkholderia pseudomallei* group pathogens. J Am Chem Soc 134:13192-5.

4. Seyedsayamdost MR. 2019. Toward a global picture of bacterial secondary metabolism. J Ind Microbiol Biotechnol 46:301-311.

5. Truong TT, Seyedsayamdost M, Greenberg EP, Chandler JR. 2015. A *Burkholderia thailandensis* Acyl-Homoserine Lactone-Independent Orphan LuxR Homolog That Activates Production of the Cytotoxin Malleilactone. J Bacteriol 197:3456-62.

6. Klaus JR, Deay J, Neuenswander B, Hursh W, Gao Z, Bouddhara T, Williams TD, Douglas J, Monize K, Martins P, Majerczyk C, Seyedsayamdost MR, Peterson BR, Rivera M, Chandler JR. 2018. Malleilactone Is a *Burkholderia pseudomallei* Virulence Factor Regulated by Antibiotics and Quorum Sensing. J Bacteriol 200.

7. Franke J, Ishida K, Hertweck C. 2012. Genomics-driven discovery of burkholderic acid, a noncanonical, cryptic polyketide from human pathogenic *Burkholderia* species. Angew Chem Int Ed Engl 51:11611-5.

8. Seyedsayamdost MR. 2014. High-throughput platform for the discovery of elicitors of silent bacterial gene clusters. Proc Natl Acad Sci U S A 111:7266-71.

9. Fischbach MA, Clardy J. 2007. One pathway, many products. Nat Chem Biol 3:353-5.

10. Trottmann F, Franke J, Richter I, Ishida K, Cyrulies M, Dahse HM, Regestein L, Hertweck C. 2019. Cyclopropanol Warhead in Malleicyprol Confers Virulence of Human- and Animal-Pathogenic *Burkholderia* Species. Angew Chem Int Ed Engl doi:10.1002/anie.201907324.

11. Trottmann F, Ishida K, Franke J, Stanisic A, Ishida-Ito M, Kries H, Pohnert G, Hertweck C. 2020. Sulfonium Acids Loaded onto an Unusual Thiotemplate Assembly Line Construct the Cyclopropanol Warhead of a *Burkholderia* Virulence Factor. Angew Chem Int Ed Engl doi:10.1002/anie.202003958.

12. Wu Y, Seyedsayamdost MR. 2017. Synergy and Target Promiscuity Drive Structural Divergence in Bacterial Alkylquinolone Biosynthesis. Cell Chem Biol 24:1437-1444 e3.

13. Moloney MG. 2016. Natural Products as a Source for Novel Antibiotics. Trends Pharmacol Sci 37:689-701.

14. Kunakom S, Eustaquio AS. 2019. *Burkholderia* as a Source of Natural Products. J Nat Prod 82:2018-2037.

15. Reen FJ, McGlacken GP, O'Gara F. 2018. The expanding horizon of alkyl quinolone signalling and communication in polycellular interactomes. FEMS Microbiol Lett 365.

16. Florez C, Raab JE, Cooke AC, Schertzer JW. 2017. Membrane Distribution of the *Pseudomonas* Quinolone Signal Modulates Outer Membrane Vesicle Production in *Pseudomonas aeruginosa*. mBio 8.

17. Lin J, Zhang W, Cheng J, Yang X, Zhu K, Wang Y, Wei G, Qian PY, Luo ZQ, Shen X. 2017. A *Pseudomonas* T6SS effector recruits PQS-containing outer membrane vesicles for iron acquisition. Nat Commun 8:14888.

18. Butt AT, Thomas MS. 2017. Iron Acquisition Mechanisms and Their Role in the Virulence of *Burkholderia* Species. Front Cell Infect Microbiol 7:460.

19. Sritharan M. 2016. Iron Homeostasis in *Mycobacterium tuberculosis*: Mechanistic Insights into Siderophore-Mediated Iron Uptake. J Bacteriol 198:2399-409.

20. Alice AF, Lopez CS, Lowe CA, Ledesma MA, Crosa JH. 2006. Genetic and transcriptional analysis of the siderophore malleobactin biosynthesis and transport genes in the human pathogen *Burkholderia pseudomallei* K96243. J Bacteriol 188:1551-66.

21. Kvitko BH, Goodyear A, Propst KL, Dow SW, Schweizer HP. 2012. *Burkholderia pseudomallei* known siderophores and hemin uptake are dispensable for lethal murine melioidosis. PLoS Negl Trop Dis 6:e1715.

22. Piddock LJ. 2006. Multidrug-resistance efflux pumps - not just for resistance. Nat Rev Microbiol 4:629-36.

23. Anes J, McCusker MP, Fanning S, Martins M. 2015. The ins and outs of RND efflux pumps in *Escherichia coli*. Front Microbiol 6:587.

24. Blanco P, Hernando-Amado S, Reales-Calderon JA, Corona F, Lira F, Alcalde-Rico M, Bernardini A, Sanchez MB, Martinez JL. 2016. Bacterial Multidrug Efflux Pumps: Much More Than Antibiotic Resistance Determinants. Microorganisms 4.

25. Okada BK, Wu Y, Mao D, Bushin LB, Seyedsayamdost MR. 2016. Mapping the Trimethoprim-Induced Secondary Metabolome of *Burkholderia thailandensis*. ACS Chem Biol 11:2124-30.

26. Li A, Mao D, Yoshimura A, Rosen PC, Martin WL, Gallant E, Wuhr M, Seyedsayamdost MR. 2020. Multi-Omic Analyses Provide Links between Low-Dose Antibiotic Treatment and Induction of Secondary Metabolism in *Burkholderia thailandensis*. mBio 11.

27. Mao D, Bushin LB, Moon K, Wu Y, Seyedsayamdost MR. 2017. Discovery of *scmR* as a global regulator of secondary metabolism and virulence in *Burkholderia thailandensis* E264. Proc Natl Acad Sci U S A 114:E2920-E2928.

28. Biot FV, Lopez MM, Poyot T, Neulat-Ripoll F, Lignon S, Caclard A, Thibault FM, Peinnequin A, Pages JM, Valade E. 2013. Interplay between three RND efflux pumps in doxycycline-selected strains of *Burkholderia thailandensis*. PLoS One 8:e84068.

29. Hayden HS, Lim R, Brittnacher MJ, Sims EH, Ramage ER, Fong C, Wu Z, Crist E, Chang J, Zhou Y, Radey M, Rohmer L, Haugen E, Gillett W, Wuthiekanun V, Peacock SJ, Kaul R, Miller SI, Manoil C, Jacobs MA. 2012. Evolution of *Burkholderia pseudomallei* in recurrent melioidosis. PLoS One 7:e36507.

30. Gutierrez MG, Yoder-Himes DR, Warawa JM. 2015. Comprehensive identification of virulence factors required for respiratory melioidosis using Tn-seq mutagenesis. Front Cell Infect Microbiol 5:78.